

**A NOVEL MECHANISM FOR INTESTINAL ABSORPTION OF THE  
TYPE II DIABETES DRUG METFORMIN: ROLE OF CATION-  
SELECTIVE APICAL TRANSPORTERS IN PARACELLULAR  
ABSORPTION**

**William Ross Proctor III**

A dissertation submitted to the faculty of the University of North Carolina at Chapel Hill in partial fulfillment of the requirements for the degree of Doctor of Philosophy in the School of Pharmacy.

Chapel Hill  
2010

Approved by

Advisor: Dhiren R. Thakker, Ph.D.

Chairperson: Moo J. Cho, Ph.D.

Reader: James M. Anderson, M.D., Ph.D.

Reader: Kim L.R. Brouwer, Pharm.D., Ph.D.

Reader: Joseph W. Polli, Ph.D.

Reader: Zhiyang Zhao, Ph.D.

© 2010  
William Ross Proctor III  
ALL RIGHTS RESERVED

## **ABSTRACT**

William Ross Proctor III: A Novel Mechanism for Intestinal Absorption of the  
Type II Diabetes Drug Metformin: Role of Cation-selective Apical  
Transporters in Paracellular Absorption  
(Under the direction of Dhiren R. Thakker, Ph.D.)

Metformin, a widely prescribed anti-hyperglycemic agent, is very hydrophilic with net positive charge at physiological pH, and thus should be poorly absorbed. Instead, the drug is well absorbed (oral bioavailability of 40-60%), although the absorption is dose-dependent and variable; the drug accumulates in enterocytes during oral absorption. To date, the transport processes associated with the intestinal absorption of metformin are poorly understood. This dissertation work describes an unusual and novel intestinal absorption mechanism for metformin. The absorption mechanism involves two-way transport of metformin across the apical membrane of enterocytes that is mediated by cation-selective transporters, and facilitated diffusion across the paracellular route, working in concert to yield high and sustained absorption

Metformin absorption was evaluated in the well established model for intestinal epithelium, Caco-2 cell monolayers. Metformin was efficiently transported across the apical membrane by bidirectional cation-selective transporters; however, the drug accumulated in the cells due to inefficient egress across the basolateral membrane. Consequently, the absorptive transport was almost exclusively through the paracellular route; however, the paracellular transport contained a distinct saturable component.

Evidence is presented to show that the mechanism responsible for the observed saturable paracellular transport involves electrostatic interactions between positively charged metformin and negatively charged amino acid residues on the pore-forming tight-junction protein, claudin-2. Treating Caco-2 cells with the active metabolite of vitamin D<sub>3</sub>, 1,25-dihydroxyvitamin D<sub>3</sub>, selectively induced claudin-2 in preference to other tight junction proteins, and concurrently increased paracellular transport of metformin. Overexpression of claudin-2 in renal epithelial cells, LLC-PK1, caused size-dependent increase in paracellular transport of small organic cations, further supporting the role of claudin-2 in facilitating paracellular transport of hydrophilic cationic compounds. By employing a novel chemical inhibition scheme, it was revealed that both the organic cation transporter 1 (hOCT1) and the plasma membrane monoamine transporter (PMAT) were involved in the apical uptake/efflux of metformin in Caco-2 cell monolayers.

Taken together, these results suggest a novel mechanism to explain how a hydrophilic cation like metformin is absorbed efficiently, though it uses the inefficient paracellular route for absorption. It is hypothesized that metformin is taken up into enterocytes via apical cation-selective transporters, hOCT1 and PMAT, and accumulates in the cells because of inefficient basolateral egress due to the lack of cation-selective efflux transporters. At each segment of the intestine, a small fraction of the metformin dose is absorbed via the paracellular route, facilitated by claudin-2, while a significant portion of the dose is taken up into the cells. Drug is then effluxed back into the lumen as the dose of the drug travels forward, taken up into distal enterocytes, or absorbed through the paracellular space. The apical transporters function to sequester the drug and allow for multiple opportunities to be absorbed by the paracellular route; thus, increasing the residence time in the intestine

enabling efficient absorption. This dissertation work provides novel insights into the mechanisms associated with intestinal absorption and accumulation of metformin. The absorption mechanism proposed can account for the sustained high exposure of metformin achieved in the primary pharmacological organ, the liver, via the portal circulation. Additionally, the mechanisms proposed here can account for the possible role of the intestine in the pharmacology, gastrointestinal side effects, and adverse events of metformin.

## **ACKNOWLEDGEMENTS**

I am incredibly grateful for my advisor Dr. Dhiren R. Thakker for his continued support, mentorship, patience, and friendship throughout my graduate training.

I am deeply indebted to all my committee members, Drs. James M. Anderson, Kim L.R. Brouwer, Moo J. Cho, Joseph W. Polli, and Zhiyang Zhao for their time, suggestions, and valuable insight. I would especially like to thank James M. Anderson for his expertise and generous resources regarding the claudin studies presented in this dissertation.

I would also like to acknowledge all of the faculty and students at the Eshelman School of Pharmacy for making my experience here memorable and rewarding. In particular I would like to thank Drs. Arlene Bridges, Mary F. Paine, and Craig Lee for opening up their laboratories and resources to me during my graduate training.

This dissertation work was possible by generous support from Amgen, Inc. and the PhRMA Foundation in the form of pre-doctoral fellowships.

I would like to express my deepest gratitude to my family and friends for helping me through this long journey. In particular I would like to thank my mother Alice C. Proctor for her unwavering love, support, and encouragement. Additionally, I would like to thank my brother and best friend, David Proctor, for always being there for me. I would like to acknowledge my sister Emily Kenning for keeping me grounded and for continually taking care of our family. I also would like to acknowledge my father Ross Proctor for encouraging me to explore and experience the world.

Lastly, I would like to thank my future wife, Julie M. Bessette, for her love, support, and understanding throughout this difficult time. I am extremely fortunate to have her in my life.

## TABLE OF CONTENTS

	Page
LIST OF TABLES .....	xi
LIST OF FIGURES .....	xii
LIST OF ABBREVIATIONS .....	xiv
Chapter	
1. INTRODUCTION .....	1
A. INTRODUCTION .....	2
B. PATHOLOGY AND PATHOGENESIS OF TYPE II DIABETES.....	3
C. METFORMIN PHARMACOLOGY .....	4
1. Clinical Effects.....	4
2. Insulin Sensitivity and Insulin Resistance .....	6
3. Inhibition of Hepatic Gluconeogenesis.....	7
4. Intestinal Glucose Utilization .....	7
5. Peripheral Glucose Uptake in Skeletal Muscle.....	8
6. Adipose Tissue and Insulin Resistance.....	9
7. Off-Label Indications and Emerging Therapeutic Areas.....	10
D. ACTIVATION OF AMP-ACTIVATED PROTEIN KINASE (AMPK) .....	11
1. Overview of AMPK.....	11
2. AMPK Activation and Downstream Events .....	13

3. Inhibition of Complex I of the Mitochondrial Respiratory Chain .....	16
E. METFORMIN PHARMACOKINETICS.....	18
1. Clinical Pharmacokinetics .....	18
a. Intravenous Administration .....	19
b. Peroral Administration.....	20
2. Intestinal Disposition and Absorption .....	21
3. Distribution .....	22
4. Elimination.....	24
a. Renal Clearance .....	24
b. Non-Renal Clearance .....	24
5. Clinically Observed Drug-Drug Interactions (DDIs) .....	26
6. Adverse Events and Toxicity .....	28
a. Gastrointestinal Side Effects.....	28
b. Metformin Associated Lactic Acidosis (MALA) .....	28
F. CATION-SELECTIVE TRANSPORTERS .....	29
1. Substrate Specificity .....	30
2. Hepatic Transporters Involved in Liver Accumulation .....	32
3. Transporters Involved in Active Renal Secretion.....	33
4. Transporters Involved in Absorptions and Intestinal Accumulation .....	36
5. Transporters in Peripheral Tissues.....	38
6. Pharmacogenomics of Metformin Transporters .....	39
a. hOCT1 Polymorphisms .....	39
b. hOCT2 Polymorphisms .....	41



c. MATE1 and MATE2K Polymorphisms .....	42
G. THE CACO-2 CELL MODEL OF INTESTINAL EPITHELIUM.....	43
1. Overview of Intestinal Absorption Processes .....	43
2. Overview of Caco-2 Cell Transwell™ Model.....	44
3. Cation-Selective Transporters Expressed in Caco-2 Cells .....	45
4. Metformin and Ranitidine Transport across Caco-2 Cell Monolayers .....	46
5. Paracellular Transport and Claudins .....	48
H. RATIONAL AND OVERVIEW OF PROPOSED RESEARCH.....	49
I. REFERENCES .....	59
2. MECHANISMS UNDERLYING THE SATURABLE ABSORPTION OF METFORMIN .....	78
A. ABSTRACT.....	79
B. INTRODUCTION .....	80
C. METHODS .....	83
D. RESULTS .....	92
E. DISCUSSION .....	101
F. REFERENCES .....	120
3. VITAMIN D <sub>3</sub> ENHANCES PARACELLULAR TRANSPORT OF METFORMIN ACROSS CACO-2 CELL MONOLAYERS VIA INDUCTION OF CLAUDIN-2.....	123
A. ABSTRACT.....	124
B. INTRODUCTION .....	125
C. RESULTS .....	129
D. DISCUSSION .....	138
E. MATERIALS AND METHODS.....	145

F. ACKNOWLEDGEMENTS.....	157
G. SUPPLEMENTAL MATERIAL.....	164
H. REFERENCES .....	166
4. CLAUDIN-2 FACILITATES PARACELLULAR TRANSPORT OF SMALL ORGANIC CATIONS ACROSS EPITHELIAL MONOLAYERS: A MOLECULAR MECHANISM FOR SATURABLE PARACELLULAR TRANSPORT OF METFORMIN AND OTHER ORGANIC CATIONS.....	172
A. ABSTRACT.....	173
B. INTRODUCTION .....	174
C. MATERIALS AND METHODS.....	177
D. RESULTS .....	187
E. DISCUSSION.....	193
F. ACKNOWLEDGMENTS .....	202
G. REFERENCES .....	210
5. CATION-SELECTIVE TRANSPORTERS INVOLVED IN APICAL UPTAKE AND ACCUMULATION OF METFORMIN IN CACO-2 CELLS AND INTESTINAL EPITHELIUM.....	215
A. ABSTRACT.....	216
B. INTRODUCTION .....	217
C. MATERIALS AND METHODS.....	220
D. RESULTS .....	229
E. DISCUSSION.....	235
F. ACKNOWLEDGMENTS .....	245
G. REFERENCES .....	255
6. CONCLUSIONS.....	261

## LIST OF TABLES

Table 1.1.	Pharmacokinetic parameters for orally administered metformin in humans ...	53
Table 2.1.	Estimated kinetic parameter for AP uptake, BL uptake, and absorptive (AP to BL) transport of metformin in Caco-2 cells .....	110
Table 2.2.	Effects of donor concentration and inhibition by quinidine on kinetic parameters for metformin transport and cellular accumulation in Caco-2 cells .....	111
Table 2.3.	Relative contribution of paracellular and transcellular transport to overall transport of metformin as a function of donor concentration in Caco-2 cells .....	112
Table 3.1.	Calculated molecular radius for hydrophilic organic solutes in relation to reported values .....	158
Table 3.S1.	List of primer sequences and amplified product size for TJ and cation-selective transporters gene products .....	164
Table 4.1.	Calculated molecular radius for hydrophilic organic solutes in relation to reported values .....	203
Table 5.1.	Chemical inhibitors of cation-selective candidate transporters .....	246
Table 5.2.	Experimental $IC_{50}$ values for chemical inhibitors on metformin uptake into CHO cells expressing hOCT1-3 and literature PMAT and MATE1 $IC_{50}$ values .....	247

## LIST OF FIGURES

Figure 1.1.	Structures of guanidine and biguanide compounds .....	54
Figure 1.2.	Organ specific and systemic pharmacologic effects of metformin.....	55
Figure 1.3.	Schematic diagram of metformin cellular pathways to elicit pharmacologic responses .....	56
Figure 1.4.	Cation-selective transporters implicated in metformin disposition in the intestine, liver, and kidney .....	57
Figure 1.5.	Diagrams of the Caco-2 Transwell™ model and the transporter expression and localization in Caco-2 cells.....	58
Figure 2.1.	Structure of metformin.....	113
Figure 2.2.	Schematic representation of the three-compartment model describing the transport of metformin across Caco-2 cell monolayers.....	114
Figure 2.3.	Concentration-dependent transport, apparent permeability, and AP uptake of metformin in Caco-2 cells.....	115
Figure 2.4.	Efflux of preloaded metformin across the AP and BL membranes of Caco-2 cells .....	116
Figure 2.5.	Relative rates and clearance values of transport (AP-BL) and BL efflux of metformin across Caco-2 cell monolayers.....	117
Figure 2.6.	Concentration dependence of metformin transport and cellular accumulation in Caco-2 cells .....	118
Figure 2.7.	Schematic of the proposed “sponge” hypothesis for dose-dependent absorption of metformin.....	119
Figure 3.1.	Vitamin D <sub>3</sub> -mediated induction of calcium transport across Caco-2 cell monolayers.....	159
Figure 3.2.	Effect of vitamin D <sub>3</sub> -treatment on absorptive transport of hydrophilic compounds across Caco-2 cell monolayers .....	160
Figure 3.3.	Transcellular transport of metformin is not affected by vitamin D <sub>3</sub> -treatment.....	161
Figure 3.4.	Effect of vitamin D <sub>3</sub> -treatment on tight-junction gene products and protein expression .....	162

Figure 3.5.	Schematic diagram of the effects of vitamin D <sub>3</sub> on the tight junctions in Caco-2 P27.7 cell monolayers .....	163
Figure 3.S1.	Gel electrophoresis of the reverse transcription-polymerase chain reaction (RT-PCR) primer products .....	165
Figure 4.1.	Space-filling structures for hydrophilic organic solutes guanidine, 1-methylguanidine, metformin, TEA, and D-mannitol .....	204
Figure 4.2.	LC-MS/MS chromatograms for 1-methylguanidine quantitative analysis ....	205
Figure 4.3.	Western blot analysis of claudin-2 expression in LLC-PK <sub>1</sub> parental and PT2:13 LLC-PK <sub>1</sub> cells with decreasing doxycycline concentrations .....	206
Figure 4.4.	The effect of claudin-2 expression on monolayer resistance (TEER) and paracellular transport of calcium and mannitol.....	207
Figure 4.5.	Claudin-2 dependent increase in paracellular transport of organic cations across LLC-PK <sub>1</sub> cell monolayers .....	208
Figure 4.6.	Polyethylene glycol (PEG) oligomer permeability as a function of hydrodynamic radius in un-induced PT2:13 LLC-PK <sub>1</sub> monolayers.....	209
Figure 5.1.	Time-course for uptake of metformin in CHO-hOCT1, CHO-hOCT2, CHO-hOCT3, CHO-hOCTN2, and mock CHO cells.....	248
Figure 5.2.	Concentration dependent uptake of metformin into CHO cells expressing hOCT1, hOCT2, and hOCT3 .....	249
Figure 5.3.	Concentration-dependent inhibition of hOCT1-, hOCT2-, and hOCT3-mediated metformin uptake by cation-selective inhibitors.....	250
Figure 5.4.	A novel chemical inhibition scheme to elucidate the contribution of candidate cation-selective transporters involved in metformin AP initial uptake in Caco-2 cells .....	251
Figure 5.5.	The contribution of candidate cation-selective transporters involved in metformin initial AP uptake in Caco-2 cells .....	252
Figure 5.6.	Effect of extracellular pH on metformin AP uptake in Caco-2 cells.....	253
Figure 5.7.	Relative mRNA expression of hOCT1, hOCT3, hOCTN2, and PMAT in Caco-2 (HTB-37) cells relative to GAPDH expression .....	254

## LIST OF ABBREVIATIONS

ACC	Acetyl-CoA Carboxylase
AICAR	5'-Aminoimidazole-4-Carboxamide Riboside
AMP	5'-Adenosine Monophosphate
AMPK	AMP-Activated Protein Kinase
ANOVA	Analysis of Variance
AP	Apical
ATP	5'-Adenosine Triphosphate
AUC	Area Under the Curve
BCA	Bicinchoninic acid
BL	Basolateral
$\beta$ -ME	$\beta$ -Mercaptoethanol
CBP	CREB Binding Protein
CHO	Chinese Hamster Ovary
CLDN	Claudin
CL	Clearance
CREB	cAMP Response Element-Binding
c-Src	Cellular Sarcoma
1,25-(OH) <sub>2</sub> D <sub>3</sub>	1,25-dihydroxyvitamin D <sub>3</sub>
DDI	Drug-Drug Interaction
DMSO	Dimethyl Sulfoxide
EDTA	Ethylenediaminetetraacetic Acid
EMEM	Eagle's Minimum Essential Medium

eNOS	Endothelial Nitric Oxide Synthase
FBS	Fetal Bovine Serum
FFA	Free Fatty Acid
FOXO1	Forkhead Box-Containing Protein O Subfamily 1
GCN5	General Control of Amino-Acid Synthesis 5
HBSS	Hank's Balanced Salt Solution
HEPES	N-(2-Hydroxyethyl)piperazine-N'-(2-ethanesulfonic acid)
HNF4 $\alpha$	Hepatocyte Nuclear Factor 4 $\alpha$
HPLC	High Pressure Liquid Chromatography
IBD	Inflammatory Bowel Disease
$J$	Flux
$J_{\max}$	Maximal Flux
$K_m$	Michaelis-Menten Constant
LDL	Low Density Lipoprotein
LKB1	Serine-threonine kinase 11
MALA	Metformin Associated Lactic Acidosis
MATE	Material and Toxin Extrusion
MDCK	Madin Darby Canine Kidney
MPP <sup>+</sup>	1-methyl-4-phenylpyridinium
NEAA	Non-Essential Amino Acids
1-NIC	1-Naphthylisocyanate
OCT	Organic Cation Transporter
OCTN	Novel Organic Cation Transporter

OGTT	Oral Glucose Tolerance Test
ONOO <sup>-</sup>	Peroxynitrite
P <sub>app</sub>	Apparent Permeability
PAGE	Polyacrylamide Gel Electrophoresis
PAMPA	Parallel Artificial Membrane Permeation Assay
PCOS	Polycystic Ovary Syndrome
PDPK-1	Phosphoinositide-Dependent Protein Kinase 1
PEG	Polyethylene glycol
PEPCK	Phosphoenolpyruvate carboxykinase
PGC-1 $\alpha$	Peroxisome Proliferator-Activated Receptor Gamma Coactivator-1 $\alpha$
P-gp	P-glycoprotein
PI3K	Phosphoinositide 3-Kinase
PKC	Protein Kinase C
PMAT	Plasma Membrane Monoamine Transporter
RNS	Reactive Nitrogen Species
ROS	Reactive Oxygen Species
RT-PCR	Reverse-Transcription Polymerase Chain Reaction
S.D.	Standard Deviation
SDS	Sodium-Dodecyl Sulfate
SIRT1	Sirtuin-1
SLC	Solute Carrier Family
SHP	Small Heterodimer Partner
SNP	Single-Nucleotide Polymorphism



SREBP-1	Sterol Regulatory Element Binding Protein-1
TEA	Tetraethylammonium
TEER	Transepithelial Electrical Resistance
TJ	Tight Junction
TORC2	CREB Regulated Transcription Coactivator 2
TRIS	Tris(hydroxymethyl)aminomethane
$V_D$	Volume of Distribution
$V_{\max}$	Maximal Velocity
ZO-1	Zonal Occludens 1

## **CHAPTER 1**

### **INTRODUCTION**

## 1.A. INTRODUCTION

Metformin, known by the brand name Glucophage™, is the front line therapy to treat adult onset non-insulin dependent diabetes mellitus (Type II). Metformin belongs to a class of anti-diabetic agents known as biguanides that also include buformin and phenformin (refer to Figure 1.1 for protonated structures of biguanide compounds). Buformin and phenformin were discontinued from use in the 1970s due to their increased incidences of toxicity, mainly surrounding occurrences of drug induced lactic acidosis (refer to Section 1.E.6) (Natrass and Alberti, 1978). Interest in biguanide compounds as potential anti-diabetic agents emerged after identification of the plant extract, galegine. Galegine, or isoamylene guanidine, was isolated from extracts of the European herbal medicine Goat's rue (*Galega officinalis*) (Bailey and Day, 1989). This plant, otherwise known as French lilac or Spanish sanfoin, contained high levels of guanidine and galegine, which was first proposed in the 17<sup>th</sup> century Europe to possess anti-diabetic properties (Bailey and Day, 2004).

Metformin, or 1,1,-dimethylbiguanide, was first synthesized by Werner and Bell in 1921 (Werner and Bell, 1921) and introduced into humans as an oral treatment for Type II diabetes by Dr. Jean Sterne in 1957 at the Hôpital de la Pitie in Paris, France (Bailey and Day, 1989). Commercial use of metformin first occurred in the United Kingdom (UK) in which the small French pharmaceutical company Aron and UK subsidiary Rona marketed metformin as an oral antihyperglycemic agent for treatment of mature onset diabetes in 1958 (Hadden, 2005). In Europe, metformin did not achieve widespread use until the late 1970s due to the market focus on the other more potent biguanides and insulin therapy (Bailey and Day, 2004). The drug was approved for use in Canada in 1972 (Lucis, 1983) and was introduced in the United States in December of 1994. In 2007, metformin therapy for

management of type II diabetes accounted for approximately 54% of the 34 million treatment visits that took place in the United States (Alexander et al., 2008).

The proposed mechanisms by which metformin exerts its pharmacological effect involve activation of AMP-activated protein kinase (AMPK) (Zhou et al., 2001). AMPK is a key regulator of energy balance in the body and activation of AMPK produces pharmacologic effects that are system dependent (e.g. dependent upon the cell, tissue, or organ) (Hardie, 2008). As a result, the distribution and disposition of metformin throughout the body drive its local and overall pharmacologic effects. However, metformin is a polar hydrophilic molecule (logD at pH7.4 of -6.13) that contains a net positively charge (pKa 12.4) at physiological pH (Saitoh et al., 2004). Consequently, metformin is unable to efficiently diffuse across biological membranes; thus, requiring carrier-mediated transport processes for efficient entry and exit from cells, tissues, or organs. Therefore, transport processes drive both the pharmacokinetics and pharmacodynamics of this drug.

## **1.B. PATHOLOGY AND PATHOGENESIS OF TYPE II DIABETES**

Non-insulin dependent diabetes mellitus (type II) can exist in patients for years in a pre-diabetic state and typically is not diagnosed in patients until complications appear (Codario, 2005). Common symptoms of hyperglycemia are polyurea, polydipsia, and unexplained weight loss (ADA, 2009). The hyperglycemia observed in the type II diabetic patient is often associated with other metabolic abnormalities such as obesity, hyperinsulinemia, hypertension, dyslipidemia, and impaired fibrinolysis (Henry, 1996). These factors potentiate progression of type II diabetes. In particular, obesity is the greatest risk factor for developing type II diabetes, where increased abdominal or visceral adipose

tissue alters free-fatty acid (FFA) metabolism, changes adipokine release, and increases fat accumulation in muscle, epicardial, and liver tissue (Despres and Lemieux, 2006). Even though there are significant non-obese populations that develop type II diabetes, 54% of the reported cases of type II diabetes over a three year prospective study (1999-2002) occurred in patients that were obese (e.g. body mass index greater than 30 kg/m<sup>2</sup>) (MMWR, 2004).

The prevailing phenotype associated with type II diabetes involves three major metabolic disturbances: increased hepatic gluconeogenesis, impaired insulin secretion, and peripheral insulin resistance (Henry, 1996). Of these three factors, insulin resistance plays a significant role in pre-diabetic state and progression to type II diabetes (Codario, 2005). Insulin resistance typically occurs 10-20 years prior to clinical diagnosis of type II diabetes (Warram et al., 1990). During this asymptomatic phase of the disease, insulin secretion by the pancreatic beta cells is increased to regulate glucose homeostasis. Progression to type II diabetes occurs when the beta cells exhaust their ability to increase insulin release, resulting in elevated plasma glucose levels. Insulin resistance is manifested by a myriad of causes including: genetics factors, elevated FFA concentrations, hyperglycemia, pregnancy, obesity, sedentary lifestyle, and aging (Codario, 2005). In particular, elevated serum FFA concentrations appear to be a main source for conferring insulin resistance (Dresner et al., 1999; Roden et al., 2000; Abdul-Ghani et al., 2008; Liu et al., 2009).

## **1.C. METFORMIN PHARMACOLOGY**

### **1.C.1. Clinical Effects**

The pharmacological effects of metformin are tissue and organ specific. Small intestine, liver, skeletal muscle, and adipose tissue each have distinct metformin

pharmacological effects that combine to reduce systemic glucose burden and increase insulin sensitivity (refer to Figure 1.2). Metformin reduces both basal (e.g. preprandial) and postprandial plasma glucose levels in type II diabetic patients (Lord et al., 1983; Jackson et al., 1987; Hermann et al., 1994; Sambol et al., 1996b). The greatest reduction in plasma glucose occurs postprandial (Bailey, 1992; Sambol et al., 1996b). Metformin glucose lowering effect on healthy patients was not significant (Sambol et al., 1996b) and treatment did not cause clinical hypoglycemia (Bailey et al., 1989). Even in cases where accidental or intentional metformin overdose occurred, patients were not clinically hypoglycemic (McLelland, 1985). Oral and intravenous glucose tolerance were improved with metformin treatment in type II diabetes patients (Lord et al., 1983; Jackson et al., 1987). This data taken together supports metformin to be an anti-hyperglycemic agent and potentially an insulin sensitizer rather than a hypoglycemic drug.

Long term treatment of metformin has been also been associated with weight loss in obese and non-obese type II diabetic patients (Clarke and Campbell, 1977; Hermann et al., 1994; Tuthill et al., 2008). Metformin-induced weight loss has been associated with reduced caloric intake and appetite suppression (Lee and Morley, 1998). However, there was no treatment effect on body weight in a 29 week study with metformin and placebo control in type II diabetic patients, although metformin treatment did not induce weight gain (DeFronzo and Goodman, 1995). The effect of metformin on reducing or maintaining body weight in type II diabetics directly contrasts the effects of sulphonyureas, which are known to significant increase body weight following long term treatment (Clarke and Campbell, 1977; Hermann et al., 1994).

Metformin significantly reduced total plasma cholesterol and plasma low density lipoprotein (LDL) cholesterol, while no significant changes were observed for plasma triglyceride levels (DeFronzo and Goodman, 1995). Obese type II diabetic patients treated with 2.5 g/day of metformin for 3 months had reduced plasma free fatty acid (FAA) concentrations, a significant reduction in plasma triglycerides, and a reduction in total plasma cholesterol and LDL cholesterol (DeFronzo et al., 1991). Another study in pre-diabetic obese patients, metformin induced significant weight loss and reduced total and LDL cholesterol, while not affecting blood pressure, triglycerides, and HDL cholesterol (Fontbonne et al., 1996). Of these effects, only a reduction in LDL cholesterol was attributed to the intrinsic effect of metformin and not due to its antihyperglycemic effects (Wulffele et al., 2004).

### **1.C.2. Insulin Sensitivity and Insulin Resistance**

The effect metformin treatment on blood glucose levels is not related to an increase in insulin levels (Lord et al., 1983; Jackson et al., 1987; Sambol et al., 1996b; Hundal et al., 2000), and in some cases a small (e.g. 15%) but significant reduction in plasma insulin levels were observed with 4 month metformin treatment (Stumvoll et al., 1995). In obese pre-diabetic patients, metformin treatment significantly reduced plasma glucose levels and fasting insulinemia (Fontbonne et al., 1996); supporting the role of metformin in increasing insulin sensitivity. Metformin did not significantly affect the basal release of insulin from pancreas or isolated islets of non-diabetic rats (Schatz et al., 1972) or plasma insulin levels in rats (Song et al., 2001). In isolated human pancreatic islets, metformin did not affect insulin release but conferred protection against glucose induced desensitization (Lupi et al., 1999). Additionally, a study by Fantus et al. (1986) showed that the glucose-lowering effect of

metformin was independent of basal (e.g. untreated) insulin binding status in type II diabetic patients (Fantus and Brosseau, 1986). However, short term treatment of metformin (e.g. 10 days) increased insulin sensitivity towards glucose following an oral glucose tolerance test (OGTT) (Iannello et al., 2004). In summary, metformin induced insulin sensitivity is independent of insulin receptors and is most likely dependent upon downstream post-receptor effects.

### **1.C.3. Inhibition of Hepatic Gluconeogenesis**

The liver is the major site of metformin action, where it inhibits hepatic gluconeogenesis. Metformin reduced hepatic glucose output and reduced lactate gluconeogenesis in patients with type II diabetes (Jackson et al., 1987; Stumvoll et al., 1995). Using  $^{13}\text{C}$  NMR spectroscopy and  $^2\text{H}_2\text{O}$  glucose labeling approaches, patients that had poorly controlled type II diabetes had increased glycogen cycling and reduced overall gluconeogenesis (Hundal et al., 2000). Metformin-treatment reduces key gluconeogenic enzyme expression levels and activities for hepatic fructose-1,5-biphosphate (FBPase), phosphoenolpyruvate carboxykinase (PEPCK), and glucose-6-phosphate (Song et al., 2001; Heishi et al., 2008; Caton et al., 2010). The molecular mechanism behind the inhibition of gluconeogenesis by metformin involves activation of AMPK pathway in the liver and will be discussed in detail in Section 1.D.

### **1.C.4. Intestinal Glucose Utilization**

The role of the intestine in metformin pharmacology is not well known or widely established. However, there are several reports over the past 20 years implicating the intestine in mediating a significant portion of the overall glucose lowering effects of metformin. Metformin has been shown to increase mucosal and serosal glucose transport in



the intestine (Wilcock and Bailey, 1991; Bailey et al., 1994), which has been attributed in part to activation of AMPK to recruit GLUT2 to the apical membrane of the intestinal enterocytes (Walker et al., 2005). Metformin-treatment increased the uptake of the intravenously administered positron emission tomography imaging agent,  $^{18}\text{F}$ -flourodeoxyglucose, in the small intestine and colon of healthy volunteers (Gontier et al., 2008). These observations support the role of metformin in increasing systemic glucose uptake in the intestine. Another intestinal related effect of metformin is its ability to increase intestinal anaerobic glucose metabolism by enhancing lactate production and secretion (Wilcock and Bailey, 1990; Bailey et al., 1992; Bailey et al., 2008). Taken together, metformin appears to increase glucose utilization in the intestine, decreasing overall systemic glucose burden (Figure 1.2). A study using different administration routes in streptozotocin-induced diabetic rats clearly demonstrated the importance of intestine in metformin pharmacology, where portal administration of metformin caused a significant reduction in overall blood glucose-lowering effects in relation to intraduodenal administration of the drug (Stepensky et al., 2002). In conclusion, the intestine appears to play a role in the pharmacology of metformin; yet these effects are often overlooked or underplayed.

#### **1.C.5. Peripheral Glucose Uptake in Skeletal Muscle**

Skeletal muscle is another major organ responsible for metformin-mediated glucose lowering effects. A mechanism of insulin resistance in type II diabetes involves a decrease in insulin stimulated recruitment of glucose transporters (in particular GLUT4) to the plasma membrane of skeletal muscle (Garvey et al., 1988; Garvey et al., 1998). Metformin treatment significantly increases glucose disposal, muscle glycogen concentrations, and lactate levels (Johnson et al., 1993; Musi et al., 2002). Activation of AMPK results in up-

regulation of GLUT4 expression (Zheng et al., 2001) and membrane trafficking (Kurth-Kraczek et al., 1999) in skeletal muscle. In addition, *in vitro* studies using L6 skeletal muscle cells revealed that metformin treatment activated AMPK which induced lipoprotein lipase expression and activity (Ohira et al., 2009), a protein involved in LDL catabolism. This observation presents a possible mechanism for the *in vivo* effect of metformin to reduce serum LDL levels (Wulffele et al., 2004).

#### **1.C.6. Adipose Tissue and Insulin Resistance**

The pharmacologic effects of metformin in adipocytes are not fully understood and are currently under active investigation (Palanivel and Sweeney, 2005; Ren et al., 2006; Bourron et al., 2010). Metformin treatment does not affect glucose transport and GLUT4 expression (Ciaraldi et al., 2002) nor does it affect the insulin binding and associated insulin effects (Pedersen et al., 1989) in adipocytes. The major action of metformin in adipocytes involves inhibition of lipolysis caused by activation of AMPK (Bourron et al., 2010) (Figure 1.2). Lipolysis of triglycerides in adipocytes provides the main source of FFA and glycerol release into systemic circulation (Despres and Lemieux, 2006), which have been associated with conferring insulin resistance (Boden and Shulman, 2002). Another mechanism of responsible for increasing insulin sensitivity in adipocytes by metformin involves adipocyte-specific hormone regulation, in particular the effect on resistin. Resistin is an adipocyte-specific hormone secreted exclusively by white adipocytes and causes systemic insulin resistance and reduces glucose uptake in adipocytes (Steppan et al., 2001). Resistin protein expression and activity was down-regulated by approximately 85% following 16 hour treatment with 0.1 mM metformin in 3T3-L1 adipocytes (Rea and Donnelly, 2006). This effect likely mediates insulin sensitivity in adipocytes and systemically, although further

studies are required to determine the exact mechanism and effects associated with metformin regulation of resistin.

#### **1.C.7. Off-Label Indications and Emerging Therapeutic Areas**

Therapeutic benefits of metformin have been identified for the endocrine disorder, polycystic ovary syndrome (PCOS), cardiovascular disease, and cancer chemotherapy. PCOS is the most common endocrine disorder in women of reproductive age with a prevalence of approximately 7% (Diamanti-Kandarakis et al.). The disease is characterized by infrequent menstruation and infertility due to anovulation. Metformin has proved to be effective in achieving ovulation, increasing pregnancy rates, reducing fasting insulin concentrations, reducing blood pressure, and reducing LDL cholesterol in women with PCOS (Lord et al., 2003).

There appear to be significant cardioprotective and cardiovascular benefits of metformin. Meta-analysis of 342 overweight diabetic patients treated with metformin had 39% reduced risk for myocardial infarction ( $p < 0.01$ ) (UKPDS, 1998). Furthermore, metformin has been shown in pre-clinical animal models to prevent the progression of heart failure by attenuating oxidative stress induced cardiomyocyte apoptosis (Sasaki et al., 2009). The mechanism behind this action appears to stem from metformin mediated activation of AMPK that regulates expression of the Bcl-2 family of proteins, Bad, which are responsible for initiating apoptosis-induced signaling (Kewalramani et al., 2009). Further clinical studies are required to determine the role of metformin treatment in preventing cardiomyocyte apoptosis in humans.

Population studies and meta-analysis have indicated that metformin treatment in type II diabetic patients have reduced incidences of cancer and improved rates of remission than

other type II diabetes therapies. Jijalerspong et al. (2009) surveyed 2,529 patients who underwent chemotherapy for early stage breast cancer between 1990 and 2007. It was found that diabetic patients receiving metformin had a 24% rate of complete remission, in relation to 8% for the diabetic patients not receiving metformin ( $p < 0.01$ ) (Jiralerspong et al., 2009). The increase in prolonged remission in breast cancer was postulated to involve the ability of metformin to starve or kill the drug-resistant progenitor cancer stem cells. Metformin inhibited cellular transformation and killed cancer stem cells from four genetically different types of breast cancer *in vitro* in a concentration dependent manner (Hirsch et al., 2009). Additionally, metformin significantly inhibited proliferation of chemo-resistant ovarian cancer cell lines through activation of AMPK and its downstream effector, acetyl-CoA carboxylase (ACC) (Rattan et al., 2009). In order for metformin to activate AMPK it requires entry into the cytosol, therefore characterizing the transport mechanisms in cancer cell lines may provide valuable insight into which cancer types are more susceptible to metformin treatment. Clearly, metformin treatment in cancer is promising.

## **1.D. ACTIVATION OF THE AMP-ACTIVATED PROTEIN KINASE (AMPK)**

### **1.D.1. Overview of AMPK**

The main cellular target of metformin is AMP-activated protein kinase (AMPK) (Zhou et al., 2001). AMPK regulates both cellular and whole body energy balance and is conserved across the majority of eukaryotes (McBride and Hardie, 2009). It has been implicated in the regulation of glucose and lipid homeostasis (Hardie, 2003) and remains an important target for treatment of type II diabetes (Towler and Hardie, 2007; Gugliucci, 2009). AMPK is activated in response to metabolic stresses that induce hypoxia such as

muscle contractions or exercise. Additionally, activation can occur due to several physiological stimuli such as hormones, cytokines, or exogenous stimuli such as metformin (Hardie, 2008). Activation of AMPK under normal cellular responses occurs in states of low energy and it function to trigger a metabolic switch from anaerobic state of energy [e.g. adenosine triphosphate (ATP)] depletion to a catabolic state of energy generation. Anaerobic metabolic states utilize ATP hydrolysis to synthesize and store glucose, glycogen, fatty acids, cholesterol, and triglycerides. AMPK activation switches this state to catabolic pathways that result in oxidation of glucose, fatty acids, and triglycerides to produce ATP. In other words, activation of AMPK reduces the levels of cellular glucose and lipid production and storage and increases consumption of glucose and oxidation of lipids (Hardie, 2008).

AMPK function as a heterotrimeric complex composed of  $\alpha$  subunit and regulatory  $\beta$  and  $\gamma$  subunits (Davies et al., 1994). As its namesake implies, it is a kinase that is activated by 5'-adenosine monophosphate (AMP). AMPK activation triggers several downstream effects, one of which is to phosphorylate and inactivate ACC and 3-hydroxy-3-methylglutaryl-CoA reductase (Carling et al., 1987), two enzymes responsible for lipid biosynthesis. AMP functions as a direct allosteric modulator of AMPK by binding to the  $\gamma$  subunit and also promotes phosphorylation at a critical threonine residue (Thr-172) of the  $\alpha$  subunit (Suter et al., 2006). The combined effects synergistically activate AMPK by 1000-fold in relation to the native kinase. Binding of AMP to AMPK does not affect the rate of phosphorylation by upstream kinases, rather it inhibits dephosphorylation by protein phosphatases (Suter et al., 2006). Therefore, a small increase in AMP causes a significant increase in overall kinase activity. High levels of ATP antagonize AMP binding and overall

AMPK activity (Corton et al., 1995); therefore regulating AMPK activity to states of low energy. This function is the driving force behind AMPK primary role as an energy sensor.

Activation of AMPK is dependent upon phosphorylation of  $\alpha$  subunit Thr-172 residue by upstream kinases, in particular the tumor suppressor serine-threonine kinase 11 (LKB1) (Woods et al., 2003). LKB1 requires complexation with two other accessory subunits, Ste20-related adaptor protein and mouse protein 25, to mediate phosphorylation of AMPK at Thr-172 (Hawley et al., 2003). The AMPK activator and 5'-AMP analogue, 5-aminoimidazole-4-carboxamide riboside (AICAR), did not affect LKB1 activity (Woods et al., 2003), supporting LKB1 activity on AMPK is independent of AMP binding. In conclusion, AMPK activation involves phosphorylation of the Thr-172 residue by LKB1, which is further potentiated by an increase in AMP/ATP ratio.

#### **1.D.2. AMPK Activation and Downstream Events**

Activation of AMPK by metformin was first proposed by Zhou et al. (2001), in which metformin treatment caused a significant increase in phosphorylated AMPK and a decrease in sterol regulatory element binding protein-1 (SREBP-1), a key lipogenic transcription factor (Zhou et al., 2001). Since then, AMPK activation by metformin has been implicated in most of metformin perceived therapeutic benefits. For example, AMPK activation by metformin in mouse jejunal tissue increased expression and activity of the lumen GLUT2 transporter (Walker et al., 2005). Metformin activation of AMPK caused a significant increase in phosphorylation of ACC (Cleasby et al., 2004; Zou et al., 2004), an increase in fatty acid oxidation (Zhou et al., 2001), a decrease in gluconeogenesis enzymes PEPCK and glucose-6-phosphatase (Kim et al., 2008; Ota et al., 2009), inhibition of cardiomyocyte apoptosis (Sasaki et al., 2009), inhibition of lipolysis in human adipocytes

(Bourron et al., 2010), and an increase in expression and activity of lipoprotein lipase responsible for LDL catabolism (Ohira et al., 2009). AMPK activation also results in up-regulation of GLUT4 expression (Zheng et al., 2001) and membrane trafficking (Kurth-Kraczek et al., 1999) in skeletal muscle. The diversity of functions of AMPK in different cell types and organs makes it an ideal target for treatment of type II diabetes and is responsible for the complex pattern of pharmacologic effects metformin exerts in the body.

The most studied AMPK activation event for metformin is the triggered reduction of expression and activity of gluconeogenic enzymes in the liver (refer to Figure 1.3). AMPK activation by metformin decreased expression of PEPCK and glucose-6-phosphatase (Kim et al., 2008), similarly to the effects exerted by AICAR activation (Lochhead et al., 2000). AMPK activation results in phosphorylation of the transcriptional co-activator, CREB regulated transcription coactivator 2 (TORC2), which is then translocated with the CREB binding protein (CBP) from the nucleus to the cytoplasm (Koo et al., 2005). Recent evidence demonstrated that AMPK does not directly phosphorylate TORC2, but activates the downstream atypical protein kinase C isoform  $\alpha/\lambda$  (aPKC $\alpha/\lambda$ ). PKC $\alpha/\lambda$  phosphorylates TORC2 at its Ser436 residue to disassociate the CREB-CBP-TORC2 complex and halt transcription of gluconeogenic genes (He et al., 2009).

There exist another redundant pathway by which metformin down-regulates PEPCK and glucose-6-phosphatase. This pathway involves the induced expression by metformin of both signaling proteins sirtuin-1 (SIRT1) and general control of amino-acid synthesis 5 (GCN5). SIRT1 is an NAD<sup>+</sup> dependent protein deacetylase, which inhibits gluconeogenesis through disrupting the TORC2 signaling pathway and the peroxisome proliferator-activated receptor gamma coactivator 1-alpha (PGC1 $\alpha$ ) pathway (Rodgers et al., 2005). SIRT1

deacetylates two targets with opposite effects. SIRT1 can deacetylate TORC2 causing it to be targeted for ubiquitin mediated degradation. SIRT1 can also deacetylate PGC1 $\alpha$ , allowing it to associate with its partner transcription factors in the nucleus to induce gluconeogenic gene expression. Furthermore, SIRT1 is independent of insulin and is activated based on changes in levels of pyruvate and NAD<sup>+</sup> (Rodgers et al., 2005). GNC5 is an acetyl transferase that acetylates PGC1 $\alpha$ , causing inhibition of its complexation with the transcription factor forkhead box-containing protein O subfamily 1 (FOXO1) and CPB, in turn inhibiting transcription of gluconeogenic genes (Lerin et al., 2006). Metformin treatment in db/db mice caused an increase in both SIRT1 and GNC5 protein expression, a decrease in both TORC2 and PGC1 $\alpha$  expression, a reduction in PEPCK expression, and a reduction of blood glucose (Caton et al., 2010). Up-regulation of GNC5 by metformin activation of AMPK is proposed to trump the effects of increased SIRT1 on deacetylating PGC1 $\alpha$ ; thus providing overall inhibition of gluconeogenesis. Surprisingly, inhibition by 6-[4-(2-piperidin-1-ylethoxy)-phenyl]-3-pyridin-4-yl-pyrazolo[1,5-a] pyrimidine (Compound C), a potent select inhibitor of AMPK pathway, did not affect the metformin induced increase in GCN5 and SIRT1 expression. Compound C did result in decreased the effect metformin treatment had on reducing PEPCK activity and overall glucose lowering (Caton et al., 2010). This suggests that up-regulation of SIRT1 and GCN5 is partially independent of AMPK pathway, although further studies are warranted to elucidate the mechanisms by which metformin affect SIRT1 and GCN5 expression.

Additionally, AMPK activated down-regulation of PEPCK and glucose-6-phosphatase appear to be related to the metformin-AMPK associated increase in the orphan nuclear receptor small heterodimer partner (SHP). Metformin caused a concentration-



dependent increase in SHP expression in rat hepatocytes which coincided with proportional decreases in PEPCK and glucose-6-phosphatase protein levels (Kim et al., 2008). SHP is an atypical orphan nuclear receptor capable of binding to several transcription factors and can regulate various genes responsible for bile acid, lipid, and glucose homeostasis (Boulias et al., 2005). SHP expression inhibits expression of gluconeogenic enzymes by displacing CPB from the transcription factors hepatocyte nuclear factor (HNF)-4 $\alpha$  and FOXO1, which are responsible for initiating transcription of PEPCK and glucose-6-phosphatase, respectively (Kim et al., 2004; Yamagata et al., 2004). This pathway appears to be independent of CREB-CBP-TORC2 complex, supporting redundant pathways in metabolic regulation in the liver by metformin-AMPK pathway. A schematic diagram depicting the metformin associated AMPK activation and downstream effects is depicted in Figure 1.3. In conclusion, metformin activation of AMPK results in various redundant cellular responses to halt gluconeogenesis.

#### **1.4.3. Inhibition of Complex I of the Mitochondrial Respiratory Chain**

Metformin can not directly activate AMPK in a manner similar to AMP or the AMP analogue, AICAR (Zhou et al., 2001; Hawley et al., 2002). Furthermore, metformin does not increase the activity of the AMPK upstream kinase, LKB1 (Woods et al., 2003). The prevailing mechanism for metformin associated AMPK activation involves inhibition complex I of the mitochondrial respiratory chain (El-Mir et al., 2000; Owen et al., 2000). Metformin inhibited mitochondrial oxygen consumption with complex I substrates glutamate and malate, but not with complex II or complex IV substrates in rat hepatocytes (El-Mir et al., 2000; Owen et al., 2000). Inhibition of complex I by metformin caused a time- and concentration-dependent decrease in gluconeogenesis in isolated rat hepatocytes and

decreased the ATP to ADP ratio in rat liver *in vivo* (Owen et al., 2000). In skeletal muscle, inhibition of complex I by metformin resulted in a concentration-dependent increase in lactate release and glucose transport and a decrease in glucose oxidation, glycogen synthesis, overall glycogen content, and carbon dioxide production (Brunmair et al., 2004). In adipocytes, metformin caused concentration dependent increase in mitochondrial fatty acid  $\beta$ -oxidation and ROS production and an overall reduction in adipocyte mass (Lenhard et al., 1997; Anedda et al., 2008). This data together supports the involvement of inhibition of mitochondrial respiration on metformin associated pharmacologic effects: decreased hepatic gluconeogenesis, increased peripheral glucose utilization, and increased lipid metabolism (refer to Figure 1.2 and 1.3). Interestingly, metformin inhibition of complex I of the respiratory chain occurred at physiological concentrations in intact cells and not in purified mitochondria (El-Mir et al., 2000; Owen et al., 2000), suggesting that carrier-mediated processes are required to accumulate metformin in the cytosol in order for it to exert its effect on the mitochondria.

Inhibition of complex I of the mitochondrial respiratory chain decreases ATP synthesis as well as increases production of ROS and RNS (Nishikawa et al., 2000), with the latter process directly involved in activating AMPK. Zou and colleagues in 2004 published a detailed and thorough report on the role mitochondrial ROS and RNS had on metformin activation of AMPK and subsequent downstream effects. By using combinations of chemical inhibitors, over-expressed cell lines, and transgenic mouse models, this group elegantly demonstrated that metformin activated AMPK through inhibition of complex I, resulting in mitochondrial superoxide formation, a subsequent increase in RNS, which activated a cellular sarcoma (c-Src) and phosphoinositide 3-kinase (PI3K) signaling event to

phosphorylate a 3-phosphoinositide-dependent protein kinase 1 (PDK-1), and ultimately activated AMPK (Zou et al., 2004) (Figure 1.3). Metformin AMPK activation was dependent upon nitric oxide (NO) production by endothelial nitric oxide synthase (eNOS) and mitochondrial superoxide to form a peroxynitrite (ONOO<sup>-</sup>) species, where AICAR activation of AMPK was independent of eNOS expression (Zou et al., 2004). Peroxynitrite is a potent oxidant formed by NO and superoxide at a diffusion-controlled rate that is known to activate AMPK via a c-Src-PI3K-dependent pathway that is not dependent upon the AMP to ATP ratio (Zou et al., 2003). This pathway is supported by previous data that metformin activation of AMPK was independent of AMP to ATP ratio in the cells (Hawley et al., 2002).

In conclusion, metformin mediates its pharmacologic action through indirect activation of AMPK. Metformin is transported across the cell membrane into the cytosol and binds to the mitochondria to inhibit complex I, producing ROS and ultimately peroxynitrite that causes a signal cascade to associate LKB1 with AMPK, resulting in phosphorylation and activation of downstream effectors (refer to Figure 1.3). It is possible that other cellular and mitochondrial effects, independent of AMPK activation, are responsible for metformin associated anti-hyperglycemic properties and increased insulin sensitivity.

## **1.E. METFORMIN PHARMACOKINETICS**

### **1.E.1. Clinical Pharmacokinetics**

Metformin is an orally administered anti-hyperglycemic agent that is dosed as immediate release formulations of 500, 850, and 1000 mg or extended release formulations of 500, 750, and 1000 mg tablets. Maximal daily doses for immediate and extended formulations are 2550 mg and 2000 mg, respectively. The pharmacokinetic properties of

metformin have been examined in both healthy and type II diabetic patients. The overall pharmacokinetics of metformin is not dependent upon disease state (Tucker et al., 1981; Sambol et al., 1996b); therefore description of the pharmacokinetic parameters here will involve data from both populations. The drug does not bind to plasma proteins *in vivo* or *in vitro* (Pentikainen et al., 1979; Tucker et al., 1981). Furthermore, metformin undergoes negligible metabolism (e.g. < 20%) and is excreted primarily unchanged. Small contributions of hepatic metabolism has been postulated to explain the less than 20% of the drug not accounted for following intravenous administration (Tucker et al., 1981). More detailed description of non-renal clearance mechanisms of metformin will be described below in Section 1.E.4b, although the contribution of this pathway to overall metformin clearance is negligible.

#### **1.E.1.a. Intravenous Administration**

Metformin administered as a bolus intravenous dose is rapidly cleared from the body with a intravenous plasma half-life ( $t_{1/2,P}$ ) of approximately 2 hours (Pentikainen et al., 1979). Intravenous plasma concentration data were fit to a two-compartment open model with one central compartment that is rapidly equilibrated and a second “deep” peripheral compartment that accumulates metformin (Noel, 1979; Pentikainen et al., 1979; Tucker et al., 1981). The rate of elimination from the peripheral deep compartment is significantly slower than elimination from the central compartment with a peripheral compartment half-life ranging between 12-20 hours (Pentikainen et al., 1979; Tucker et al., 1981). The proposed organs, tissues, or cells that make up this peripheral compartment will be discussed in later in the Section 1.E.3. Following intravenous administration, the majority of metformin was excreted in the urine unchanged with the percent of dose recovered ranging from 80-100%

(Pentikainen et al., 1979; Tucker et al., 1981). Renal clearance represented total clearance of metformin following intravenous administration and was approximately 5-fold higher than creatinine clearance (Pentikainen et al., 1979; Tucker et al., 1981); indicating active tubular secretion in its elimination.

#### **1.E.1.b. Peroral Administration**

Oral administration of single doses ranging from 0.25 to 1.5 g yielded non-compartmental and compartmental parameters outlined in Table 1.1. The maximal plasma concentration ( $C_{\max}$ ) of metformin was generally described by the dose input and for the most part was dose proportional with reported  $C_{\max}$  values for 0.25 g tablet and the 1.5 g tablet of  $0.59 \pm 0.24$  and  $3.10 \pm 0.93 \mu\text{g ml}^{-1}$  (Table 1.1) (Tucker et al., 1981; Somogyi et al., 1987). The oral plasma half life ( $t_{1/2,p}$ ) of metformin ranges between 2 and 6 hours (Table 1.1), with a mean half life of approximately 4 hours. Similar to the intravenous data, the plasma metformin pharmacokinetic profile was well described by a three-compartment open model with the gastrointestinal compartment providing input into the central compartment which can eliminate the drug into the urine or distribute the drug into the deep peripheral compartment (Pentikainen et al., 1979). Plasma metformin concentrations measured throughout two weeks of continuous oral dosing were accurately predicted from single dose data, although the trough levels of metformin were under predicted by the model (Tucker et al., 1981). This observation supports slow accumulation and elimination from a deep peripheral compartment. The absorptive half life ( $t_{1/2,abs}$ ) determined by deconvolution analysis for 0.5 g oral dose was significantly greater for the dose equivalent intravenous elimination half-life ( $t_{1/2,\beta}$ ) (Pentikainen et al., 1979); indicating that the elimination rate during oral administration likely represented the rate of absorption. In other words,

metformin undergoes “flip-flop” kinetics, where absorption is the rate-limiting step to its elimination following oral administration. Absolute oral bioavailability (F) of metformin ranges between 40-60% and appears to be dose-dependent (Noel, 1979; Pentikainen et al., 1979; Tucker et al., 1981; Karttunen et al., 1983; Pentikainen, 1986) (Table 1.1). The volume of distribution ( $V_D$ ) of metformin is relatively large considering the hydrophilicity of the drug, with reported values that are highly variable ranging between 60 and 280 L (Noel, 1979; Pentikainen et al., 1979; Tucker et al., 1981) (Table 1.1).

### **1.E.2. Intestinal Disposition and Absorption**

The gastrointestinal absorption of metformin is high considering its net positive charge and significant hydrophilicity at physiological pH values (refer to Figure 1.1 structure of metformin). The fraction of dose absorbed of metformin ranged between 80% and 65%, with 20 to 35% of the drug recovered in the feces (Tucker et al., 1981). No drug was detected in the feces following intravenous administration; therefore it was assumed that metformin present in the feces was unabsorbed drug (Tucker et al., 1981). Furthermore, metformin absorption was dose-dependent, with greater percent of the drug being absorbed at low dose in relation to high dose (Noel, 1979; Tucker et al., 1981; Sambol et al., 1996a; Sambol et al., 1996b). For example, the absolute bioavailability for 0.85 g dose was 14% lower than the bioavailability for 0.5 g dose in healthy volunteers (Sambol et al., 1996a). Intestinal perfusion experiments supported this observation in which metformin permeability across the rat duodenum decreased with increasing dose (Song et al., 2006). Another report in rats indicated that metformin gastrointestinal absorption was dose-independent and linear for the three doses selected: 50-, 100-, and 200-mg/kg (Choi et al., 2006). It should be noted that during this study the doses selected were relative high (e.g. 50 mg/kg is equivalent to 1 g

tablet) and therefore, the dose-independence observed likely represents post-saturable linear absorption.

A study in healthy volunteers using direct administration of metformin into the stomach, jejunum, and ileum revealed that metformin is poorly absorbed across the gastric mucosa ( $\leq 10\%$  over 4 hours) and that metformin treatment did not affect gastric emptying (Vidon et al., 1988). Approximately 20% of the dose was absorbed in the duodenum and the remaining 60% of the dose absorbed across the jejunum and ileum, with 20% of the 1-g dose ending up in the colon where it was not absorbed (Vidon et al., 1988); indicating that metformin requires the entire length of the intestine for absorption.

Metformin accumulates in the intestine following oral administration and likely mediates its slow rate of absorption. Human jejunum tissue biopsies taken from type II diabetic patients treated in the presence of metformin had between 30- and 300-fold higher metformin concentrations than observed plasma concentrations (Bailey et al., 2008). In a diabetic mouse model, the greatest accumulation of metformin following oral administration was in the small intestine with levels 50- to 100-fold higher than plasma concentrations 30 minutes post dose (Wilcock and Bailey, 1994). The drug remained accumulated in mouse small intestine 20-fold greater than plasma concentrations 8 hours following oral administration (Wilcock and Bailey, 1994). In conclusion, metformin intestinal absorption is slow and requires the entire length of the small intestine to be absorbed; yet it is relatively efficient and dose-dependent, supporting saturable transport processes are involved.

### **1.E.3. Distribution**

Metformin distribution in the body is rapid, but a slow transfer to a deep peripheral compartment was observed (Pentikainen et al., 1979; Tucker et al., 1981). In humans,

metformin accumulates in the small intestine (Bailey et al., 2008) and in the liver (Shu et al., 2008). In mice, metformin is known to accumulate mostly in the stomach, liver, small intestine, and kidneys and to a lesser extent the heart, skeletal muscle, and white adipose tissue (Wilcock et al., 1991; Wilcock and Bailey, 1994; Wang et al., 2002). Metformin was actively taken up into rat liver at levels greater than the vascular space, supporting hepatic intracellular accumulation of metformin (Chou, 2000). Cellular localization of metformin has been estimated in tissue and cells isolated from mice treated with [ $^{14}\text{C}$ ]metformin, in which the majority (approximately 75%) of metformin exists in the cytosolic compartment with the remaining found in the nuclear, mitochondrial, lysosomal, and membrane fractions (Wilcock et al., 1991).

As stated earlier, metformin does not bind to plasma proteins, although there appears to be a clinically relevant slow association/disassociation with erythrocytes (Tucker et al., 1981; Robert et al., 2003). A study in healthy subjects that received 0.85 g of orally administered metformin revealed that the drug accumulated in both plasma and erythrocytes *in vivo*. Maximal concentration of metformin was attained significantly later in erythrocytes than plasma, with  $T_{\text{max}}$  values of  $5.7 \pm 0.5$  and  $3.0 \pm 0.3$  h, respectively (Robert et al., 2003). Plasma  $C_{\text{max}}$  was 6-fold greater than the erythrocyte  $C_{\text{max}}$ , yet the overall metformin AUC for plasma and erythrocyte levels were not significantly different. This was due to the very slow dissociation rate from erythrocytes in relation to plasma, in which the elimination half-life was  $23.5 \pm 1.9$  and  $2.7 \pm 1.2$  h, respectively (Robert et al., 2003). The slow association and subsequent disassociation of metformin in erythrocytes provides insight into the potential “deep” peripheral compartment.



#### **1.E.4. Elimination**

##### **1.E.4.a. Renal Clearance**

Metformin is primarily excreted unchanged in the urine by active tubular secretion (Noel, 1979; Pentikainen et al., 1979; Tucker et al., 1981; Sambol et al., 1996b). Approximately 60% of the oral dose is recovered in the urine following oral administration (refer to Table 1.1). Renal function strongly correlated with the renal clearance rates observed with metformin treatment ( $r=0.88$ ,  $p<0.001$ ) (Tucker et al., 1981); therefore, adequate renal function is necessary to eliminate the drug. Additionally, metformin therapy must be temporarily discontinued in patients receiving intravenous radiographic contrast agents, which are known to inhibit renal filtration and secretion (Bailey and Turner, 1996). The mechanisms by which metformin is actively excreted in the urine is mediated by specific organic cation transporters and will be discussed in detail in Section 1.F.3.

##### **1.E.4.b. Non-Renal Clearance**

There is no direct evidence to support metformin is excreted in the bile, although recent studies in animal models suggest the drug may be excreted into the bile. No metformin was recovered in the feces following intravenously administered (Pentikainen et al., 1979; Tucker et al., 1981), which suggested biliary excretion was negligible. It should be noted that biliary excretion of metformin can not be rule out. Metformin accumulates in the liver (Wilcock and Bailey, 1994; Chou, 2000; Wang et al., 2002); yet how this drug exits the hepatocytes back into systemic circulation has yet to be determined. Recent study in healthy volunteers revealed that individuals who carried a variant allele for the organic cation transporter 1 (OCT1), an uptake transporter in the liver, had a decrease in total clearance that was not attributed to alterations in renal clearance (Shu et al., 2008). It was hypothesized

that the decrease in total clearance was due to the inability of individuals carrying the variant alleles to accumulate metformin in the liver and excrete it into the bile; therefore reducing the total clearance without affecting the renal clearance (Shu et al., 2008). It is possible that excreted metformin in the bile would be readily absorbed in the small intestine and would not result in a clinically observed “double-peak” due to the prolonged absorption and intestinal accumulation of metformin.

Metformin in humans is excreted primarily in the kidney unchanged, although there is approximately 20% of the dose that cannot be accounted for during mass balance studies (Tucker et al., 1981). Whether this percent of the dose was metabolized or if it remained bound is unknown. From a clinical standpoint, metformin is not considered to be metabolized, nor is there any evidence to support metformin induced drug-drug interactions related to metabolism (Scheen, 1996). However, there have been recent reports suggesting that metformin is cleared via hepatic metabolism. All of the data has been proposed by the same research group and performed in rats. The non-renal clearance in rats was approximately 30% of the total metformin clearance following intravenous administration of 100 mg/kg metformin, which was attributed to involve hepatic cytochrome P450 (CYP450) isoforms 2C11, 2D1, and 3A1/2 (Choi and Lee, 2006). The conclusion regarding involvement of CYP450s in non-renal clearance of metformin was based solely on the effects of chemical inhibitors and inducers of CYP450 enzymes treated prior to metformin intravenous administration. These chemicals affected both the estimated non-renal clearance and renal clearance (Choi and Lee, 2006). The effects on other physiological parameters and on cation-selective transporters were not addressed. No direct measurement of metabolites or structural information of the metabolites have been presented; yet there have been reports

on the effects of bacterial lipopolysaccharide (Cho et al., 2009), water-deprivation (Choi et al., 2007), acute renal failure (Choi et al., 2010), and a new electrogenic drug (Choi et al., 2008) on metformin metabolic clearance. Furthermore, no work has been done with human hepatocytes or microsomes to demonstrate that the effects observed in rats are applicable to humans. Without conclusive evidence of metabolite formation in both rats and humans, these reports at best provide no benefit and at worst confuse our understanding of metformin pharmacokinetics. In summary, there is no evidence to support metformin hepatic metabolism in humans and little conclusive evidence to support metabolic clearance in rats.

#### **1.E.6. Clinically Observed Drug-Drug Interactions (DDIs)**

Metformin is metabolically stable and not protein bound. These two factors limit the likelihood of pharmacokinetic drug-drug interactions. As a result, there are not many clinically documented pharmacokinetic related drug-drug interactions (DDIs) with metformin therapy (Scheen, 2005). The most characterized DDI involves inhibition of metformin renal clearance by cimetidine. A 0.4 g dose of cimetidine, a H<sub>2</sub>-receptor antagonist, caused a 50% increase in the AUC and a 27% reduction in the renal clearance of metformin (0.25 g dose) (Somogyi et al., 1987). Metformin was not capable of altering cimetidine pharmacokinetics. The effect of cimetidine has been attributed to inhibiting cation transporters responsible for metformin active tubular secretion in the kidney (Tsuda et al., 2009b). Another clinical example of a metformin drug-drug interaction involves co-administered cephalexin, a first generation cephalosporin antibiotic. Co-administering 0.5 g of metformin and cephalexin caused an increase in metformin plasma C<sub>max</sub> and AUC by an average of 34% and 24%, respectively, and reduced renal clearance by 14% (Jayasagar et al., 2002). Similar to cimetidine, metformin did not alter the pharmacokinetics of cephalexin. Renal organic cation

transporters share similar substrate specificity towards cephalexin and metformin (Tanihara et al., 2007); supporting the hypothesis that the DDI was due to inhibition of metformin active renal secretion.

There are two reports of non-renal drug-drug interactions with metformin and other co-administered drugs. The  $\alpha$ -glucosidase inhibitor acarbose has been shown to significantly reduce the bioavailability of metformin in normal subjects that was not related to alterations in metformin renal clearance (Scheen et al., 1994). Acarbose (0.1 g) and metformin (1.0 g) co-administration resulted in a significant reduction in early serum levels (e.g. first 3 hours) and reduced both the  $C_{\max}$  and  $AUC_{0-9h}$  of metformin by 35% ( $p < 0.05$ ), while not affecting 24 hour urinary excretion (Scheen et al., 1994). The exact mechanism of this drug-drug interaction remains unknown. Metformin also has been shown to decrease the pharmacologic action of the anticoagulant phenprocoumon by increasing its hepatic metabolic clearance (Ohnhaus et al., 1983). Phenprocoumon  $t_{1/2,p}$  and AUC were reduced by 31% ( $p < 0.01$ ) and 37% ( $p < 0.05$ ), respectively following 6-week treatment with metformin. Interestingly, microsomal metabolic activity on phenprocoumon was not affected by metformin treatment in both animal models or in humans (Ohnhaus et al., 1983). Metformin has been shown in rats to increase liver blood flow that was inhibited by co-treatment of the  $\beta$ -adrenergic antagonist propranolol (Ohnhaus et al., 1978); suggesting metformin increased liver blood flow via a selective  $\beta$ -adrenergic effect. The mechanism of this DDI is likely due to an increase in liver blood flow, thus increasing the metabolic clearance of the highly lipid soluble phenprocoumon. No other examples are present on the effects of metformin increased portal blood flow and metabolic clearance.

### **1.E.7. Adverse Events and Toxicity**

#### **1.E.7.a. Gastrointestinal Side Effects**

Oral administered metformin is generally well tolerated and safe, although there are side effects and adverse reactions that occur. Major side effects surround gastrointestinal symptoms of diarrhea, nausea, abdominal discomfort, and anorexia (Bailey and Nattrass, 1988). These symptoms are typically transient and subside after the patients have adjusted to metformin. Approximately 3% of patients treated with metformin discontinue due to intolerance surrounding the gastrointestinal side effects (Hermann and Melander, 1992). Administration of food with metformin has been shown to ameliorate the gastrointestinal side effects (Bailey and Turner, 1996). Other side effects have been reported to be metallic taste and altered absorption of vitamin B12 and folic acid (Bailey and Nattrass, 1988).

#### **1.E.6.b. Metformin Associated Lactic Acidosis (MALA)**

The major adverse event associated with metformin treatment is lactic acidosis. Metformin associated lactic acidosis (MALA) is rare (approximately 2-10 incidents per 100,000 patient years), although the mortality rate is approximately 50% (Brown et al., 1998; Misbin et al., 1998). MALA occurs in patients that intentionally or accidentally overdose on metformin or patients with significant renal impairment or acute renal failure (Assan et al., 1977). Even though other contraindications exist regarding lactic acidosis, elevated metformin accumulation in plasma highly correlates with incidences of MALA (Runge et al., 2008; Seidowsky et al., 2009). Metabolic pattern associated with MALA is characterized by severe metabolic acidosis (serum pH < 7.35), hyperlactataemia (serum lactate >5mM), and high serum lactate/pyruvate ratio (Assan et al., 1977; Seidowsky et al., 2009). MALA patients require immediate blood purification by hemodialysis with a bicarbonate-buffered

and high-sodium dialyzate to remove both metformin and circulating lactate and to increase blood volume and renal blood flow (Seidowsky et al., 2009).

Even though the exact mechanisms of leading to MALA are not fully understood, stimulated intestinal and liver lactate production by metformin accumulation likely plays the major role. Metformin accumulates significantly in intestinal mucosa, increased glucose uptake, and increased lactate production (Bailey et al., 2008). Accumulation in the liver of mice significantly increased the blood lactate concentration and reduced the oxygen consumption (Wang et al., 2003). In mice deficient in the murine organic cation transport 1 (Oct1) (Oct1(-/-)), the increase in blood lactate due to metformin treatment was abolished (Wang et al., 2003). Oct1 is present on the basolateral membrane of mouse liver and intestine (Wang et al., 2002). The conclusion from this work was that the liver is likely the major organ for metformin induced lactate production. However, knocking out Oct1 in the mouse may have decreased intestinal and liver metformin accumulation, in turn reducing stimulated lactate production in both organs. In summary, overdose or acute renal failure can cause severe metformin systemic accumulation leading to increases in anaerobic lactate production and ultimately metabolic acidosis.

## **1.F. CATION-SELECTIVE TRANSPORTERS**

Metformin requires carrier-mediated transporters to shuttle it across biological membranes due its net charge and hydrophilicity. There are three families of transporters that have been implicated in various transport processes of metformin. They include the members from the human organic cation transporters (hOCTs) (SLC22), material and toxin extrusion transporters (MATEs) (SLC47), and the equilibrative nucleoside transporters

(ENTs) (SLC29). Detailed description of the function and role of cation-selective transporters on metformin in each tissue or organ is presented below.

### **1.F.1. Substrate Specificity**

Metformin is a known substrate for several organic cation transporters and is generally considered a promiscuous substrate with modest affinity. It is a substrate for three hOCTs from the SLC22 gene family: hOCT1 (SLC22A1) (Kimura et al., 2005a), hOCT2 (SLC22A2) (Kimura et al., 2005b), and hOCT3 (SLC22A3) (Nies et al., 2009). The reported affinities (e.g. Michaelis-Menten apparent  $K_m$  values) of hOCT1 to transport metformin range from 0.9 to 2.5 mM (Kimura et al., 2005a; Shu et al., 2007; Nies et al., 2009; Sogame et al., 2009). Apparent  $K_m$  values of hOCT2 to transport metformin range between 0.3 to 1.0 mM (Kimura et al., 2005b; Song et al., 2008; Chen et al., 2009a). Recently, metformin was shown to be a substrate for hOCT3 with an apparent  $K_m$  of 2.3 mM (Nies et al., 2009). hOCT1-3 function as facilitative transporters that translocate organic cations in an electrogenic manner (e.g. dependent on membrane potential) and are capable of bidirectional functionality (Gorboulev et al., 1997; Zhang et al., 1997; Kekuda et al., 1998; Koepsell et al., 2007). The driving force for hOCT1, hOCT2, and hOCT3 function is not sodium dependent (Gorboulev et al., 1997). hOCT3 function is dependent upon extracellular pH and can function as proton-antiporter, in which increasing pH results in increased activity (Kekuda et al., 1998). Additionally, metformin was shown not to be transported by the active ATP-binding transporter, P-glycoprotein, in rats (Song et al., 2006) and likely is not a substrate for this efflux pump in humans.

Other SLC22 transporters, in particular the novel carnitine transporters hOCTN1 (SLC22A4) and hOCTN2 (SLC22A5), affinities towards metformin are not known.

hOCTN1 is a bidirectional cation and carnitine transporter that is pH dependent (e.g. acts as a proton antiporter) and the function appears to be independent of sodium (Tamai et al., 1997; Yabuuchi et al., 1999). hOCTN1 has greatest efficiency to transport the zwitterionic antioxidant ergothioneine (Grundemann et al., 2005). hOCTN1 is known to transport organic cations such as tetraethylammonium (TEA) (Tamai et al., 1997), verapamil, quinidine, and pyrilamine (Yabuuchi et al., 1999). hOCTN2 also functions in as a bidirectional carnitine and cation transporter dependent upon sodium to translocate carnitine (Tamai et al., 1998) and independent of sodium to transport organic cations (Wu et al., 1999). hOCTN2 is capable of transporting TEA, cephaloridine, choline, mildronate, and sulpiride (Wu et al., 1999; Ganapathy et al., 2000; Watanabe et al., 2002; Grigat et al., 2009). In summary, hOCTN1 and hOCTN2 are capable of transporting organic cations, although they lack the degree of polyspecificity observed with hOCT1-3.

Metformin is a known substrate of the newly cloned material and toxin extrusion transporters, MATE1 (SLC47A1) and MATE2K (SLC47A2) (Tanihara et al., 2007). Both isoforms function as bidirectional cation-selective transporters independent of sodium and membrane potential (Otsuka et al., 2005; Masuda et al., 2006). MATE transporter driving force is an oppositely directed proton gradient, indicating that these transporters function as proton antiporters. Human MATE1 and MATE2K have reported affinities (apparent  $K_m$  values) for transporting metformin of  $0.78 \pm 0.1$  and  $1.98 \pm 0.48$  mM, respectively (Tanihara et al., 2007).

Metformin has also been identified as a substrate for the newly cloned plasma membrane monoamine transporter, PMAT, which belongs to the equilibrative nucleoside transporter family (SLC29A4) (Zhou et al., 2007). PMAT functions as a bidirectional



transporter that functions independent of sodium and chloride, although it is dependent upon membrane potential and enhanced by an inward proton gradient (Engel et al., 2004). PMAT functions as a proton-symporter in which its uptake of metformin was increased 5-fold when the extracellular pH was changed from 7.4 to 6.6 (Zhou et al., 2007). PMAT has a reported affinity for metformin similar to the reported affinities for OCTs and MATEs, with an apparent  $K_m$  of 1.32 mM (Zhou et al., 2007).

### **1.F.2. Hepatic Transporters Involved in Liver Accumulation**

Accumulation of metformin in the liver, in particular the hepatocytes, is required for metformin to inhibit gluconeogenesis and increase fatty acid oxidation. Human liver has detectable mRNA of hOCT1-3, hOCTN1-2, and MATE1 (Zhang et al., 1997; Verhaagh et al., 1999; Otsuka et al., 2005; Lamhonwah and Tein, 2006; Hilgendorf et al., 2007). MATE2K is a kidney specific MATE isoform and is not present in the liver (Otsuka et al., 2005). Very weak mRNA expression of PMAT was detected in homogenate of human liver (Engel et al., 2004). Direct protein expression and localization of PMAT in human liver is unknown. hOCT1 and hOCT3 protein expression are localized exclusively to the basolateral membrane of hepatocytes (Nies et al., 2009), while hOCT2 protein was not detected in human liver (Nies et al., 2008). hOCT1 expression in the liver was significantly greater than hOCT3 expression (Hilgendorf et al., 2007; Nies et al., 2009), indicating that hOCT1 likely plays a major role in metformin liver accumulation in relation to hOCT3. hOCTN1 protein staining in human liver is not known, although there is evidence to support that it is localized to mitochondria in the human liver derived HepG2 cell line (Lamhonwah and Tein, 2006). hOCTN2 direct protein expression and localization in human liver has yet to be determined; however rat Octn2 protein was detected and localized to the basolateral membrane in rat

hepatocytes (Fujita et al., 2009). MATE1 protein expression in human liver was detected at the apical bile canalicular membrane (Otsuka et al., 2005).

Metformin uptake in human liver is believed to involve both hOCT1 and hOCT3 at the basolateral membrane (Nies et al., 2009). In Oct1(-/-) mice, metformin liver accumulation was significantly reduced following intravenous administration (Wang et al., 2002) and overall plasma metformin concentrations were elevated following oral administration (Shu et al., 2008) in relation to wild-type mice. Similar uptake kinetics of metformin were observed in primary human hepatocytes and hOCT1 expressing *Xenopus laevis* oocytes, with apparent  $K_m$  values of 0.91 and 0.93 mM, respectively (Sogame et al., 2009).

The role of MATE1 in excreting metformin into the bile remains unknown. Recent reports using transgenic mice deficient in MATE1 or mice treated with a select MATE1 inhibitor, pyrimethamine, indicated that metformin accumulated in the liver to a greater extent when MATE1 was not functionally active (Tsuda et al., 2009a; Ito et al., 2010). These reports suggest that MATE1 may play a role in biliary excretion of metformin, although more conclusive studies are needed. There is currently no evidence to support the involvement of hOCTN1, hOCTN2, and PMAT in transporting metformin in the liver. In summary, metformin appears to be taken up into hepatocytes by hOCT1 and to a lesser extent hOCT3 and then potentially is excreted in the bile by MATE1 or effluxed back into the blood by hOCT1 and/or hOCT3 (refer to Figure 1.4).

### **1.F.3. Transporters Involved in Active Renal Secretion**

The transport mechanisms of metformin in the kidney have been the most extensively studied due to its reliance on active secretion for elimination. Human kidneys have

detectable mRNA expression of hOCT1-3, hOCTN1-2, MATE1, MATE2K, and PMAT (Engel et al., 2004; Otsuka et al., 2005; Hilgendorf et al., 2007; Xia et al., 2007). In contrast to the liver, hOCT2 is highly expressed in human kidney in relation to hOCT1 and hOCT3 (Aoki et al., 2008). hOCT2 protein is expressed on the basolateral membrane of proximal tubule epithelial cells in humans (Nies et al., 2008). hOCT1 expression in the kidney is controversial. Contrary to the report by Nies et al. (2008) that failed to detect hOCT1 in the kidney, hOCT1 protein was detected and localized on the apical and subapical domains of both proximal and distal tubules in humans (Tzvetkov et al., 2009). hOCT1 protein was not detected in crude plasma membrane fractions from human kidney cortex (Motohashi et al., 2002). If hOCT1 is functionally active in the kidney, it may facilitate reabsorption and not excretion. These findings provide insight into organ/tissue specific localization of hOCT1 in humans; however whether hOCT1 is functionally active in the kidney remains to be determined.

hOCT3 protein expression in the kidney is less studied than hOCT1 and hOCT2. It has significantly higher (approximately 10-fold) expression than hOCT1 in human kidney, although 50-100-fold lower than OCT2 expression (Motohashi et al., 2002). One report indicated that hOCT3 protein was localized to the basolateral membrane of proximal tubule epithelial cells (Koepsell et al., 2007), although actual immunofluorescent staining images were not presented. Mouse Oct3 protein was detected in the proximal and distal convoluted tubules and within the Bowman's capsule, though membrane localization was not determined (Wu et al., 2000b). In the human derived proximal tubule cell model, Caki-1, hOCT3 is constitutively expressed and localized to the basolateral membrane (Glube and Langguth, 2008).

MATE1 and MATE2K protein is localized on the brush-border apical membrane of proximal tubule cells (Otsuka et al., 2005; Masuda et al., 2006). Identification of MATE1 and MATE2K provided evidence linking hOCT2 with an apical cation transporter to complete vectorial transport of metformin from the blood to the urine. Transport studies in double transfected MDCK cells with human OCT2 and MATE1 revealed efficient vectorial transport of metformin from the basolateral to apical compartment (Tsuda et al., 2009b). Using this *in vitro* model of proximal tubule cells, metformin secretory transport was highly sensitive to co-administered cimetidine. The results supported the hypothesis that the clinically observed DDI between cimetidine and metformin was due to cimetidine inhibition of MATE1 and not through inhibition of hOCT2 (Tsuda et al., 2009b). Renal secretion of metformin was markedly reduced in the transgenic mice deficient in *Mate1* (Tsuda et al., 2009a) or mice treated with the *Mate1* inhibitor pyrimethamine (Ito et al., 2010), further supporting the role of MATE1 in facilitating renal secretion of metformin.

Surprisingly, PMAT protein expression in human kidney was found to be exclusively in the glomerulus and more specifically on the membranes of podocytes (Xia et al., 2009). There was no expression in the nephron tubules suggesting that PMAT plays a different role in the kidney than other hOCT and MATE isoforms and is unlikely to be involved in tubular secretion of metformin. Whether PMAT functions to accumulate metformin in podocytes or to enhance/impede glomerular filtration remains unknown. hOCTN1 and hOCTN2 have been detected in human kidney and are expressed on the apical lumen membrane of proximal tubule cells (Tamai et al., 2004; Glube et al., 2007). There is no evidence to support that metformin is transported by either hOCTN1 or hOCTN2; consequently no functional evidence exists to implicate these transporters in the renal secretion or reabsorption of

metformin. In summary, renal secretion of metformin in humans is likely mediated by uptake across the basolateral membrane of proximal tubule cells by hOCT2 and is transported into the lumen by MATE1 and to a lesser extent MATE2K (Figure 1.4).

#### **1.F.4. Transporters Involved in Absorption and Intestinal Accumulation**

In humans, metformin has been shown to accumulate in intestinal enterocytes following oral administration (Bailey et al., 2008) and overall intestinal absorption was dose-dependent (Tucker et al., 1981; Sambol et al., 1996b). The role of transporters in metformin intestinal absorption remains largely unknown. Human small intestine contains detectable mRNA expression of hOCT1-3, hOCTN1-2, and PMAT (Muller et al., 2005; Englund et al., 2006; Kim et al., 2007; Meier et al., 2007; Zhou et al., 2007). MATE1 and MATE2K mRNA was not detected in human intestine (Masuda et al., 2006), although mMate1 expression was detected in mouse intestine (Hiasa et al., 2006). Direct protein expression of hOCT1-3 in human intestine is lacking. Muller et al. (2005) used immunofluorescent staining with rOCT1, hOCT2, and hOCT3 antibodies to detect protein and subcellular localization in fixed human jejunum sections. No protein staining was observed for hOCT2, faint and diffuse cytosolic and lateral staining was observed with hOCT1, and hOCT3 was localized to the brush-border apical membrane of enterocytes (Muller et al., 2005). Transgenic mice deficient in Oct1 (Oct1(-/-)) had significantly lower intestinal accumulation of metformin following intravenous administration (Wang et al., 2002); suggesting that Oct1 is localized to the basolateral membrane in rodents. However, the rate of absorption in Oct1(-/-) was not different than wild-type mice following oral administration of metformin (Shu et al., 2008). Further studies are required to determine the localization and function of hOCT1-3 in human

intestine and the role they play in facilitating absorption of metformin and other hydrophilic cations.

hOCTN1 expression is approximately 7-fold lower than hOCTN2 (Kim et al., 2007). hOCTN1 may be localized to the mitochondria in intestine as it appears to be localized in liver (Lamhonwah and Tein, 2006) and in human derived intestinal cell model, Caco-2 (Lamhonwah et al., 2005). Rodent Octn2 was localized to the brush-border apical membrane in mouse intestine and is believed to function in mammals to facilitate sodium-dependent carnitine absorption (Kato et al., 2006). In summary, hOCTN2 appears to be the predominant novel cation and carnitine transporter in the intestine and likely is expressed on the apical membrane; however its role in facilitating absorption and intestinal accumulation of metformin remains unknown.

PMAT protein expression was detected in human intestine and localized to the brush-border apical membrane on enterocytes of the villus tips (Zhou et al., 2007). PMAT functions as a proton-symporter in which it translocates organic cations efficiently in the direction of an inward proton gradient (Xia et al., 2007). The apical localization of PMAT and its pH dependent uptake properties make it a more likely candidate than hOCT3 to facilitate uptake of metformin from the lumen into the enterocytes. This is due to lower lumen pH and hOCT3 proton-antiporter functionality (Kekuda et al., 1998). It is conceivable that PMAT facilitates metformin intestinal absorption; though no functional evidence *in vivo* or *in vitro* has implicated PMAT in intestinal absorption of metformin. Unlike in the liver and kidney, there is currently no definitive evidence implicating specific transport processes that mediate metformin dose-dependent absorption and intestinal accumulation. Based solely on intestinal localization and substrate specificity towards metformin, it is likely that PMAT

and hOCT3 function to take up metformin across the lumen membrane; however there is no evidence implicating basolateral transporters in intestinal absorption of metformin (Figure 1.4).

#### **1.F.5. Transporters Involved in Peripheral Tissues**

Metformin was shown to distribute throughout the body and accumulate in the liver, kidney, and intestine and to lesser extent in the heart, skeletal muscle, erythrocytes, and white adipose tissue (Wilcock et al., 1991; Wilcock and Bailey, 1994; Wang et al., 2002; Shu et al., 2008). hOCT1 mRNA has been detected in skeletal muscle, kidney, intestine, liver, placenta, granulocytes, lymphocytes, and spleen (Gorboulev et al., 1997; Koepsell et al., 2007). In contrast, hOCT2 mRNA expression was less broad was only detected in the kidney, placenta, and brain. hOCT3 strongest expression was found in skeletal muscle, kidney, placenta, brain, and heart (Grundemann et al., 1998; Wu et al., 2000a).

Unlike the kidney specific MATE2K, MATE1 has relatively broad tissue expression with the significant expression in the kidney, adrenal gland, testis, skeletal muscle, liver, uterus, and heart (Masuda et al., 2006). PMAT expression is highest in the brain, kidney, and intestine followed by skeletal muscle and heart (Engel et al., 2004; Barnes et al., 2006). Currently there are no data identifying and characterizing cation-selective transporters present in white adipocytes. In summary, metformin transporters hOCT1, hOCT3, MATE1, and PMAT have relatively broad tissue distribution and may facilitate uptake of metformin into peripheral tissues and organs. There still remains a significant body of work in the transporter field to elucidate the mechanisms by which metformin and similar hydrophilic drugs enter and exit the cellular compartments in the heart, skeletal muscle, and other peripheral tissues.

### **1.F.6. Pharmacogenomics of Metformin Transporters**

Genetic polymorphisms in cation-selective transporters have recently been identified and have implications in metformin pharmacokinetics and dynamics. For example, genetic factors have been attributed to over 90% of the variability observed in metformin renal clearance (Leabman and Giacomini, 2003; Yin et al., 2006). The most widely studied polymorphisms involve single-nucleotide polymorphisms (SNPs) for hOCT1 and hOCT2 that alter transport function of metformin and other cationic compounds (Shu et al., 2003; Shu et al., 2007; Shu et al., 2008; Wang et al., 2008; Chen et al., 2009a; Tzvetkov et al., 2009). Polymorphisms in MATE1 and MATE2K have also been studied in relation to alterations in metformin transport and disposition (Chen et al., 2009b; Kajiwara et al., 2009; Toyama et al., 2010). Currently there is no information regarding polymorphisms of PMAT.

#### **1.F.6.a. hOCT1 Polymorphisms**

Polymorphisms of hOCT1 have been widely studied due to the significant role this transporter plays in the liver disposition of metformin. From 247 genetically diverse samples, 14 SNPs and one 3-base pair polymorphisms, which resulted in a deletion of methionine residue at position 420 (420del), were identified for hOCT1 (Shu et al., 2003). Of the 15 polymorphisms, 6 SNPs resulted in altered hOCT1 expression. The frequency of these variant alleles in each ethnicity ranged from 0.1% upwards to 20%. hOCT1 activity was increased in one SNP at position 14 (serine to phenylalanine mutation) (hOCT1-S14F), where two other SNPs, hOCT1-R16C and hOCT1-P341L, caused a decrease in hOCT1 activity (Shu et al., 2003). hOCT1-R16C mutation was associated with decreased hOCT1 protein expression in individuals of European ancestry carrying this variant allele (Nies et al., 2009). Three SNPs were identified that completely abolished hOCT1 function. They were



hOCT1-G220V, -G401S, and -G465R, all of which were mutations of evolutionary conserved glycine residues that are likely integral for hOCT1 function (Shu et al., 2003).

Metformin pharmacokinetics and dynamics were examined for hOCT1 variant alleles that reduced or abolished hOCT1 function. Individuals containing variants hOCT1-R61C, -G401S, -G465R, or -420del had significantly higher AUC and  $C_{\max}$  values with decreases in their apparent volume of distribution ( $V_D$ ) and total oral clearance (Shu et al., 2008). However, the reduction in total oral clearance could not be attributed to renal clearance; therefore, supporting the potential involvement of biliary excretion in metformin elimination. Decreased hOCT1 function likely reduced liver exposure, fraction of drug excreted into the bile, and overall volume of distribution while increasing the fraction of drug excreted in the urine. The hOCT1-variant population had significantly higher glucose exposure and increased plasma insulin levels following an OGTT (Shu et al., 2007). In conclusion, hOCT1 polymorphisms affected the liver disposition of metformin, resulting in a decrease in efficacy.

A recent report examined metformin renal clearance in 103 healthy volunteers in the context of hOCT1-3 polymorphisms. Ten, fourteen, and six polymorphisms were identified in the 103 patients for hOCT1, hOCT2, and hOCT3, respectively (Tzvetkov et al., 2009). In addition one SNP for hOCTN1 and MATE1 were identified and examined in this study. Surprisingly, only the population containing hOCT1-variant alleles had significantly altered renal clearances, in which heterozygous and homozygous variant populations had increased metformin renal clearance (Tzvetkov et al., 2009). Similarly, Oct1(-/-) mice renal clearance of tetraethylammonium (TEA) was increased in relation to wild-type mice (Jonker et al., 2001). The increase in renal clearance was concluded to be due to the inability of the apical

hOCT1 to reabsorb metformin in the proximal tubules, although further studies are required to fully understand the effect of hOCT1 polymorphism on renal clearance of metformin and to understand the discrepancies between the two reports described here.

#### **1.F.6.b. hOCT2 Polymorphisms**

Over 20 polymorphisms of hOCT2 have been identified, of which four SNPs: hOCT2-M165I, -A270S, -R400C, and -K432Q had reduced transporter activity (Leabman et al., 2002). hOCT2-A270S was the most frequent variant allele (approximately 10-15% across different ethnicities) in which alanine at position 270 was replaced with serine. When expressed in HEK293 cells, hOCT2-A270S variant had similar affinity for metformin, but had an increase in transporter capacity and ultimately greater intrinsic transport clearance than hOCT2 reference control (Chen et al., 2009a). It was postulated that the mutation of alanine to serine provided an additional hydrogen binding site, which may increase the stability or post-translational processing of the transporter.

The effect of carrying hOCT2-A270S variant alleles is dependent on the haplotype associated with this SNP in each ethnicity. Heterozygous populations containing the hOCT2-A270S variant allele of European and African ancestries had significantly greater total renal clearance and active renal secretion of metformin than homozygous individuals with the reference allele (Chen et al., 2009a). Another report in 103 individuals of exclusively European ancestry found no effect of heterozygous hOCT2-A270S variant alleles on metformin renal clearance (Tzvetkov et al., 2009). Alternatively, heterozygous hOCT2-A270S populations of Han Chinese ancestry had significantly reduced total renal clearance and renal clearance by active secretion (Song et al., 2008; Wang et al., 2008). There were three haplotypes associated with the hOCT2-A270S found in Caucasians from Northern and

Western Europe, where only one haplotype was identified in Han Chinese populations which was not found in Caucasian or African populations (Chen et al., 2009a). The haplotype in the Han Chinese population contains four intronic SNPs specific to this population and likely accounts for the differences between the functional consequences of hOCT2-A270S variant allele. These studies have provided insight into sources of variability in metformin renal clearance and the role of hOCT2 *in vivo*; yet the limited numbers of studies are not conclusive enough to describe the liabilities associated with carrying hOCT2 variant alleles in relation to metformin elimination.

#### **1.F.6.c. MATE1 and MATE2K Polymorphisms**

MATE1 and MATE2K genetic polymorphisms have recently been identified (Chen et al., 2009b; Kajiwara et al., 2009). There are 15 identified SNPs for MATE1, of which there are 10 non-synonymous coding SNPs. The allele frequency in each ethnicity for these polymorphisms ranged between 0.5% and 9% (Chen et al., 2009b; Kajiwara et al., 2009). MATE1-G64D and MATE1-V480M have lost transport function completely, while MATE1-L125F, -A310V, -D328A, -V338I had significantly reduced transport function. MATE1-G64D loss of function was associated with decreased trafficking of the protein to the plasma membrane (Chen et al., 2009b; Kajiwara et al., 2009). Alternatively, a SNP to the MATE1 promoter region (position-66, T>C) significantly reduces association of two essential transcription factors, activating protein-1 and activating protein-2, reducing MATE1 transcription and protein expression (Ha Choi et al., 2009). MATE2K had 6 SNPs identified, with two non-synonymous SNPs of MATE2K-K64N and MATE2K-G211V that decreased MATE2K function. MATE2K-G211V, similar to MATE1-G64D, had a complete loss of metformin transport function due to the inability to be trafficked to the plasma membrane of

HEK293 cells (Kajiwara et al., 2009). The clinical significance of both MATE1 and MATE2K polymorphisms are currently being investigated. However, no difference in total oral clearance of metformin was observed between type II diabetic patients heterozygous for MATE1 and MATE2K variant alleles in relation to diabetics homozygous for the reference alleles (Toyama et al., 2010). In summary, MATE1 and MATE2K are polymorphic with relatively low population frequency. Variants of these transporters may account for some variability associated with metformin renal clearance, although larger and more detailed pharmacogenomic studies are needed.

## **1.G. THE CACO-2 CELL MODEL OF INTESTINAL EPITHELIUM**

### **1.G.1. Overview of Intestinal Absorption Processes**

Metformin can be absorbed across intestinal epithelium via two major routes: transcellular transport into and out of the enterocytes and paracellular transport in between adjacent enterocytes. Hydrophilic drugs like metformin require carrier-mediated pathways to undergo efficient transcellular transport due to its poor membrane permeability. This process requires vectorial transport in which apical and basolateral transporters work in conjunction to facilitate transcellular transport of the drug from the intestinal lumen into the blood. These processes are inherently saturable due to the nature of transporter-ligand interactions.

Alternatively, small hydrophilic drugs can be absorbed through the paracellular space between adjacent enterocytes. This pathway requires diffusing across the tight-junctions (TJs) into the lateral space and ultimately into the blood. TJs are intricate complexes formed in the apical portion of the lateral space and provide a barrier to water and small molecule paracellular transport (Kovbasnjuk et al., 1998; Van Itallie and Anderson, 2004). TJ are

made up of multiple transmembrane junctional proteins in detergent insoluble sphingolipid rich membrane rafts anchored in place by numerous cytosolic scaffolding proteins (Tsukamoto and Nigam, 1997). A major function of TJs are to maintain membrane polarity by restricting lipid movement between the apical and basolateral membranes (van Meer and Simons, 1986). In addition, TJ serve as a barrier or gate to prohibit solute flux. Hydrophilic solutes that have molecular radii less than 4 to 5 Å can diffuse through the pore of the TJ, where limited flux is observed with larger hydrophilic solutes (Knipp et al., 1997; Watson et al., 2001; Van Itallie et al., 2008). Paracellular transport of solutes traditionally has been considered a passive process governed by molecular diffusion properties. This perception has begun to shift as more evidence emerges revealing the dynamic and complex nature of TJs and understanding of their role in maintaining ion homeostasis (Van Itallie and Anderson, 2004). The size and hydrophilicity of metformin likely enable it to traverse through the paracellular space; thus, both transcellular and paracellular transport processes likely are involved in its intestinal absorption.

### **1.G.2. Overview of Caco-2 Cell Transwell™ Model**

*In vitro* intestinal cell models provide simplified systems to unravel the contributions of multiple processes involved in absorption. Caco-2 is an established cell-based model to study transport and absorption across human intestinal epithelium. This model originates from human colon adenocarcinoma cells and forms a monolayer of differentiated columnar “small-intestine like” epithelial cells (Hidalgo et al., 1989; Artursson, 1990). Similar to intestinal enterocytes, Caco-2 cells differentiate to form distinct apical and basolateral membranes separated by the presence of TJs. This model poses several key advantages over tissue models in that they form a structural monolayer free of mucus, submucosal connective

tissue, or muscle tissue. Additionally, Caco-2 cell monolayers are grown on porous membrane supports or Transwells™ that provide ready access to the basolateral (e.g. serosal) compartment as well as the apical (e.g. lumen) compartment (Figure 1.5A). This model allows for transport process across each membrane or across the monolayer to be monitored at varying times, concentrations, and in the presence of chemical modulators. Consequently, systematic experiments can be carried out to determine the relative contribution of transcellular and paracellular transport processes in overall absorption (Bourdet et al., 2006).

### **1.G.3. Cation-Selective Transporters Expressed in Caco-2 Cells**

Caco-2 cells originate from humans; therefore they express many relevant human intestinal transporters. Even though mRNA has been detected for many cation-selective intestinal transporters in Caco-2 cells (Englund et al., 2006; Seithel et al., 2006; Hilgendorf et al., 2007; Maubon et al., 2007; Hayeshi et al., 2008), protein expression, localization, and function have yet to be determined for the majority of the transporters capable of transporting metformin. hOCT1 mRNA is expressed in Caco-2 cells (Muller et al., 2005), although direct protein expression and localization is not clear. However, immunofluorescent staining with rat OCT1 antibody indicated apical localization in Caco-2 (Ng, 2002). AP uptake of ranitidine, an hOCT1 substrate, was efficient (apparent  $K_m$  0.45 mM), where its basolateral uptake was very inefficient (apparent  $K_m$  66.9 mM) (Lee et al., 2002; Bourdet and Thakker, 2006). This data supports that if hOCT1 is functionally active in Caco-2 cells it would be localized to the apical membrane.

hOCT2 mRNA was detected in Caco-2 cells and immunofluorescent staining with hOCT2 antibodies produced lateral and cytosolic staining (Muller et al., 2005). There is no evidence to support functionally active hOCT2 or other hOCTs on the basolateral membrane

in Caco-2 cells. TEA, an hOCT2 substrate, was inefficiently transported across the BL membrane of Caco-2 cells (Lee et al., 2002). hOCT3 mRNA and protein expression were detected in Caco-2 cells and hOCT3 was localized to the apical membrane (Muller et al., 2005). Uptake of 1-methyl-4-phenylpyrimidium ( $\text{MPP}^+$ ) across the AP membrane in Caco-2 cells was attributed to hOCT3 (Martel et al., 2001), although due to the polyspecificity of hOCTs to transport  $\text{MPP}^+$ , conclusive evidence for hOCT3 function in Caco-2 cells is lacking. hOCTN1 was detected in Caco-2 cells (Hayeshi et al., 2008), although it is localized to intracellular membranes of the mitochondria (Lamhonwah et al., 2005). Caco-2 cells express hOCTN2 on the apical membrane (Elimrani et al., 2003).

MATE1, MATE2K, and PMAT expression in Caco-2 cells are not known. PMAT is expressed on the apical membrane of intestinal enterocytes (Zhou et al., 2007); yet there is no evidence for its expression, function, and localization in Caco-2 cells. Future studies are warranted to determine the role of these transporters in facilitating cation absorption across Caco-2 cells and ultimately across the intestine. A schematic diagram of the known cation-selective transporters present in Caco-2 cells is depicted in Figure 1.5B.

#### **1.G.4. Transport of Metformin and Ranitidine across Caco-2 Cell Monolayers**

Metformin absorptive transport, e.g. transport from the apical to basolateral compartment, across Caco-2 cell monolayers has been examined in limited cases. The first report of metformin absorptive transport across Caco-2 cells was performed by Nicklin et al. in 1996. Metformin transport was linear up to 90 min, non-saturable, and not dependent upon transport direction (Nicklin et al., 1996). Apparent permeability ( $P_{\text{app}}$ ) of metformin was reported to be  $5.5 \times 10^{-6} \text{ cm s}^{-1}$ , which was 10-fold greater than the  $P_{\text{app}}$  for the paracellular probe compound mannitol (Nicklin et al., 1996). Interestingly,  $P_{\text{app}}$  of

metformin in the absorptive direction was significantly affected by decreasing extracellular pH, where  $P_{app}$  decreased by 50% when the pH was changed from 7.4 to 5.5, whereas mannitol transport was independent of pH (Nicklin et al., 1996). The significant difference between the  $P_{app}$  values of metformin and mannitol and the pH dependence of metformin  $P_{app}$  suggests that transcellular carrier-mediated processes facilitated metformin absorptive transport; yet overall transport was not saturable. The main deficiency in this report is that the concentrations examined were relatively high (e.g. 0.5 to 25 mM), where saturable transport processes would most likely be linear.

Additionally, metformin transport across Caco-2 cells and the parallel artificial membrane permeation assay (PAMPA) was determined to estimate the relative contributions of paracellular transport to its overall intestinal transport. Metformin  $P_{app}$  was  $1.09 \pm 0.62 \times 10^{-6} \text{ cm s}^{-1}$  and less than  $0.27 \times 10^{-6} \text{ cm s}^{-1}$  across Caco-2 monolayers and PAMPA, respectively (Saitoh et al., 2004). The contribution of paracellular transport was assumed be the difference between the Caco-2  $P_{app}$  and the PAMPA  $P_{app}$  value. In this approach, 88% of metformin absorptive transport was predicted to be via paracellular transport (Saitoh et al., 2004). This grossly simplified model failed to account for transcellular transport processes that potentially act on metformin in Caco-2 cells. In summary, there exists very little data on metformin transport across Caco-2 cells.

Detailed studies have been performed on other hydrophilic cationic drugs across Caco-2 cell monolayers. Ranitidine, an  $H_2$ -receptor antagonist, transport processes across Caco-2 cells have been studied extensively. Ranitidine absorptive transport was saturable across Caco-2 cell monolayers (Lee and Thakker, 1999). The drug was taken up efficiently across the apical membrane of Caco-2 cells by “OCT-like” transporters and effluxed across



the apical membrane by P-gp (Bourdet and Thakker, 2006). Ranitidine basolateral uptake and efflux was inefficient in relation to the apical uptake and efflux (Lee et al., 2002; Bourdet and Thakker, 2006); suggesting that the basolateral membrane was rate limiting to transcellular transport of ranitidine. A comprehensive kinetic modeling approach was implemented to estimate the relative contribution of transcellular and paracellular transport to overall absorptive transport of ranitidine. The results indicated that the absorptive transport was comprised of approximately 60% paracellular transport (Bourdet et al., 2006).

Surprisingly, the paracellular transport of ranitidine contained a saturable component. Ranitidine had been shown previously to increase the transepithelial electrical resistance (TEER) across Caco-2 monolayers in a concentration-dependent manner that was attributed to the cationic amine moiety (Gan et al., 1998). It was hypothesized that the saturable paracellular transport and subsequent increase in TEER was due to electrostatic interactions with the cationic drug and anionic residues of the tight-junction or lateral surface of the cell (Lee et al., 2002; Bourdet et al., 2006). It is conceivable that metformin would exhibit similar transcellular and paracellular transport processes in Caco-2 cells as ranitidine due to its relative size and net positive charge.

#### **1.G.5. Paracellular Transport and Claudins**

The molecular mechanisms for the saturable paracellular transport of ranitidine are not fully understood. However, recent evidence points to a family of TJ proteins, known as claudins. These proteins are believed to form pores in the TJ, where the relative pattern of claudin expression in the monolayer likely regulates the barrier properties of the monolayer to ions and solutes (Van Itallie and Anderson, 2006). Additionally, claudin isoforms have been identified that are known to increase barrier integrity (e.g. claudin-1 or -8) (Yu et al.,

2003; Banan et al., 2005) or to preferentially facilitate ion permeability across the TJ (e.g. claudin-2, -4, -7, -12, or -16) (Van Itallie et al., 2001; Colegio et al., 2003; Alexandre et al., 2005; Hou et al., 2005; Fujita et al., 2008). Claudins exert charge-selectivity by electrostatic interactions between the metal ions and specific charged amino acid residues in their first extracellular loop believed to form the pores (Colegio et al., 2002). In particular, claudin-2 preferentially facilitates metal cations such as  $\text{Na}^+$  and  $\text{Ca}^{+2}$  (Fujita et al., 2008; Yu et al., 2009) in addition to permitting flux of small neutral organic polyethylene glycol oligomers (Van Itallie et al., 2008). Therefore, it is possible that these proteins could facilitate paracellular transport of ranitidine, metformin, and other small organic cations. However, it remains unknown whether claudins can facilitate the paracellular transport of these compounds.

## **1.H. RATIONALE AND OVERVIEW OF PROPOSED RESEARCH**

Metformin exhibits higher than expected oral bioavailability considering its physiochemical properties; yet little work has been performed to understand this phenomenon. Metformin is well absorbed across the small intestine; however, the entire length of the small intestine is required for complete absorption (Vidon et al., 1988). The intestinal absorption of this drug in humans is dose-dependent (Tucker et al., 1981; Sambol et al., 1996b), indicating the presence of saturable transport processes. Furthermore, metformin accumulates in intestinal enterocytes (Bailey et al., 2008), which may result in a significant intestine related pharmacological response (Stepensky et al., 2002). Metformin has very limited passive membrane permeability (Kovo et al., 2008); therefore, carrier-mediated processes are most likely required for the efficient and dose-dependent absorption and

intestinal accumulation. There is substantial evidence to implicate cation-selective transporters in metformin disposition in the liver and its elimination in the kidney; however little to no evidence exists surrounding transporters involved in metformin absorption. Recent advances in genotyping has revealed that polymorphisms of hepatic and renal metformin transporters can account for significant portions of the clinical variability in both disposition and response (Shu et al., 2007; Shu et al., 2008; Chen et al., 2009a; Chen et al., 2009b; Kajiwara et al., 2009). Thus, elucidating the transport processes responsible for intestinal absorption and accumulation of metformin will provide insight into metformin pharmacology and overall disposition. In addition, identifying the transport processes involved in absorption will aid in understanding the mechanisms of metformin induced toxicity, patient variability, and overall clinical outcomes. The central hypotheses and specific aims of the dissertation project were designed to determine the mechanisms involved in carrier-mediated uptake and overall absorptive transport of metformin in the intestine that result in both the intestinal accumulation and the higher than expected oral bioavailability.

The following major hypotheses have been tested by the studies described in this dissertation:

1. The intestinal absorption of metformin is influenced by carrier-mediated transport processes as well as a novel paracellular facilitative diffusion mechanism.
2. Saturable paracellular transport of organic cations in intestinal epithelium is mediated by electrostatic interactions with charge-selective tight junction proteins (e.g. claudin-2 or claudin-12).

3. Intestinal accumulation of metformin is due to uptake across the apical membrane by specific cation-selective transporters and inefficient basolateral egress.

The **Specific Aims** designed to test these hypotheses are as follows:

**Specific Aim 1:** Determine the relative contribution of transcellular and paracellular transport to overall absorption transport of metformin across the intestinal epithelial Caco-2 cell model.

- a Determine metformin transport kinetics for overall absorptive transport and the transport kinetics associated with uptake and efflux processes at each membrane.
- b Estimate the rate of transcellular transport from overall paracellular transport by rate comparisons between basolateral efflux and the overall rate of absorptive transport.
- c Confirm transcellular transport estimates by fitting absorptive transport and cellular accumulation data to a kinetic model with fixed experimentally derived rate constants to estimate the relative contribution of transcellular and paracellular transport.

**Specific Aim 2:** Determine role of cation-selective tight junction proteins in the facilitative (paracellular) diffusion of metformin and similar hydrophilic cations across the TJ complex.

- a Evaluate organic cation paracellular transport across Caco-2 cell monolayers treated in the presence or absence of vitamin D<sub>3</sub>, which is known to induce expression of cation-selective claudin isoforms; also evaluate the transcellular transport processes potentially affected by vitamin D<sub>3</sub> treatment.

- b Determine the direct effects claudin-2 on organic cation paracellular transport by employing a claudin-2 expressing epithelial cell model under the control of an inducible promoter.

**Specific Aim 3:** Identify the predominant apical intestinal transporter(s) responsible for metformin apical uptake and accumulation in Caco-2 cells.

- a Confirm substrate specificity of organic cation transporters for metformin using cell models that are singly expressing candidate transporters.
- b Identify chemical inhibitors capable of selectively inhibiting individual or combinations of candidate cation-selective transporters identified in Aim (3a). Confirm potency and selectivity of metformin uptake inhibition in singly expressed transporter cell lines.
- c Employ a systematic chemical inhibition scheme to elucidate the relative contribution of each candidate transporter in facilitating metformin apical uptake in Caco-2 cells.

**TABLE 1.1. Pharmacokinetic Parameters for Orally Administered Metformin in Humans**

	Units	(Somogyi et al., 1987)	(Tucker et al., 1981)	(Pentikainen et al., 1979)	(Sambol et al., 1996b)	(Noel, 1979)	(Pentikainen, 1986)	(Shu et al., 2008)	(Tucker et al., 1981)
<b>Dose</b>	<b>g</b>	<b>0.25</b>	<b>0.5</b>	<b>0.5</b>	<b>0.85</b>	<b>1.0</b>	<b>1.0</b>	<b>1.0</b>	<b>1.5</b>
<b>T<sub>max</sub></b>	<b>h</b>	3.3 (0.8)	2.2 (0.3)	1.9 (0.43)	3.28 (0.38)	3.5 (0.3)	2.25 (0.44)	1.9 (0.52)	1.5 (0.4)
<b>C<sub>max</sub></b>	<b>µg ml<sup>-1</sup></b>	0.59 (0.24)	1.02 (0.34)	1.55 (0.24)	1.51 (0.15)	1.88 (0.11)	1.58 (0.07)	1.3 (0.1)	3.10 (0.93)
<b>AUC</b>	<b>µg h ml<sup>-1</sup></b>	4.26 (1.64)	6.71 (1.82)	9.08 (1.54)	11.65 (1.27)			7.7 (0.97)	18.40 (6.52)
<b>fe<sub>F</sub></b>	<b>%</b>		27 (11)						33 (14)
<b>fe<sub>U</sub></b>	<b>%</b>	50 (13)	63 (14)	51 (5)	43 (2)			19 (9)	48 (6)
<b>CL<sub>R</sub></b>	<b>ml min<sup>-1</sup></b>	527 (165)	525 (125)	444 (23)	481.7 (46.1)	596 (35)	542 (78)	666 (266)	519 (278)
<b>CL<sub>PO</sub></b>	<b>ml min<sup>-1</sup></b>		1319 (393)		1033.3 (100)				1552 (347)
<b>t<sub>1/2, P</sub></b>	<b>h</b>		5.43 (1.47)	2.63 (0.18)	7.2 (1.9)	2.14 (0.07)	2.21 (0.22)	7.3 (2.3)	5.98 (1.49)
<b>t<sub>1/2, U</sub></b>	<b>h</b>			8.93 (0.68)			11.3 (1.7)		
<b>V<sub>D</sub></b>	<b>L</b>		276 (68)	69 (4.5)		230 (29)			
<b>F</b>	<b>%</b>		55 (8)	60 (8)		52 (3)	33		50 (10)
<b>DF</b>		Tablet	Tablet	Tablet	Tablet	Solution	Tablet	Tablet	Tablet
<b>N</b>		7	4	3	9	6	6	8	4

Parameters presented in Table 1.1 represent mean values with the standard deviation in parenthesis. (T<sub>max</sub>) is the time associated with the maximal plasma drug concentration. (C<sub>max</sub>) represents the maximal plasma metformin concentration. (AUC) represents the area under curve of the metformin plasma concentration as a function of time. (fe<sub>F</sub>) represents the percent of metformin excreted in feces unchanged. (fe<sub>U</sub>) represents the percent of metformin excreted in the urine unchanged. (CL<sub>R</sub>) represents the renal clearance, while (CL<sub>PO</sub>) represents the total clearance. (t<sub>1/2,P</sub>) is the terminal plasma half-life of metformin following oral administration. (t<sub>1/2,U</sub>) is the terminal half-life approximated from urinary excretion rates. (V<sub>D</sub>) is the apparent volume of distribution of metformin calculated from compartmental analysis. (F) is the absolute oral bioavailability of metformin reported as a percent. (DF) represents the dosage form that was administered. (N) is the number of patients employed in each study.

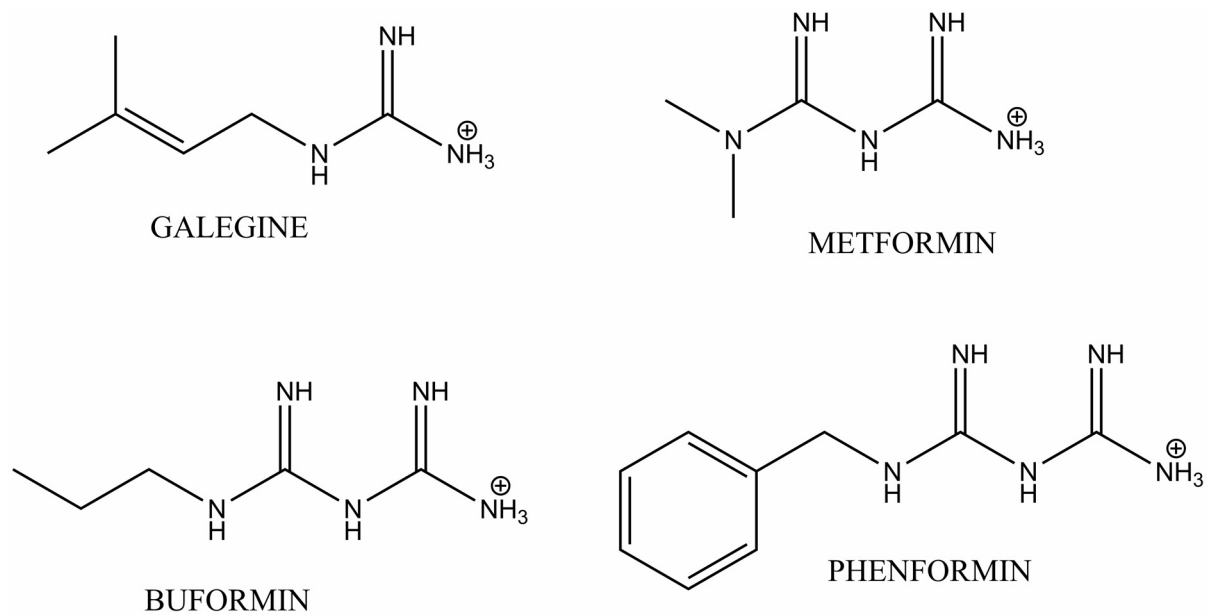


**Figure 1.1. Structures of Guanidine and Biguanide Compounds at Physiological pH**

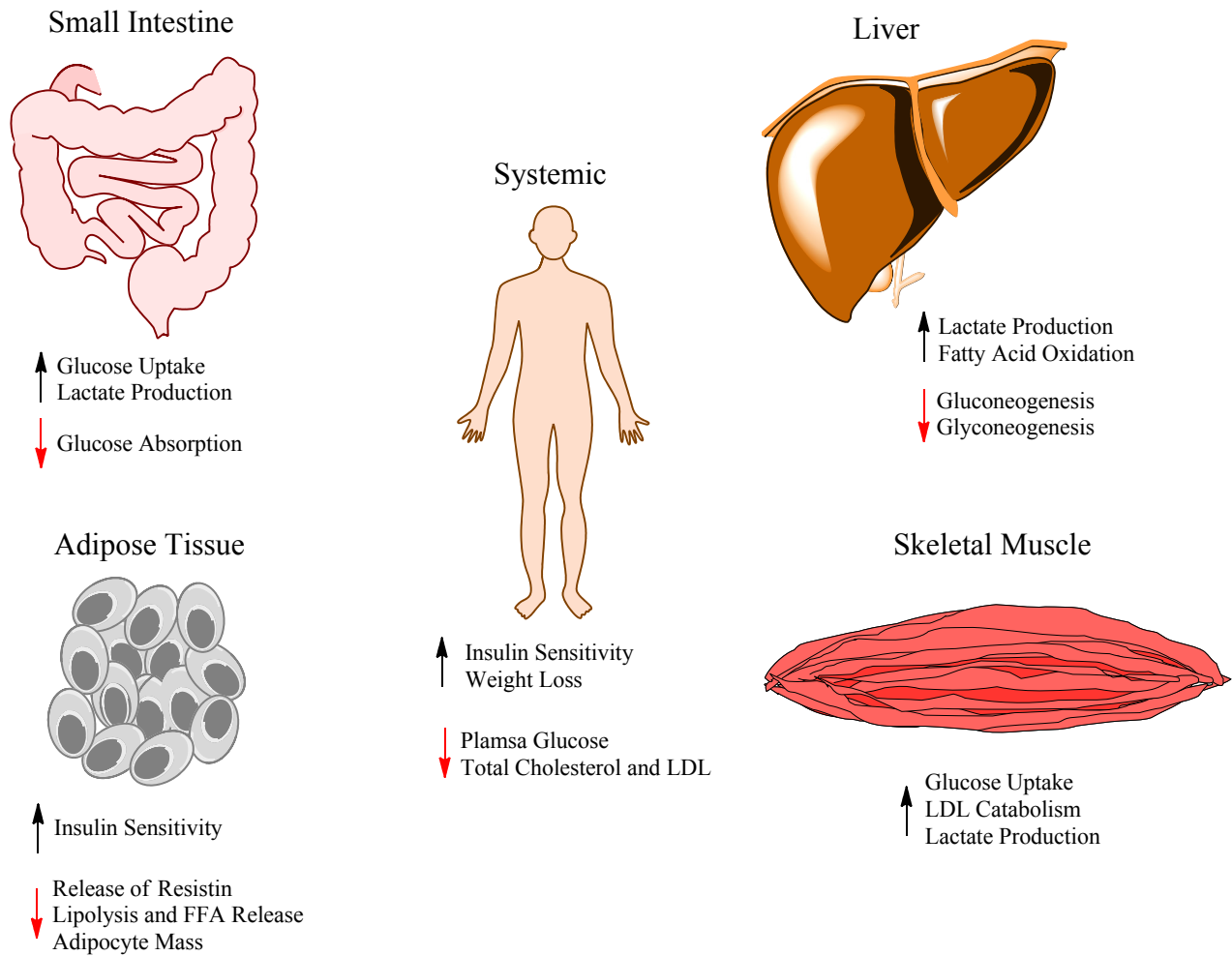


**Figure 1.2. Organ Specific and Systemic Pharmacologic Effects of Metformin.** Increases in the pharmacologic response are designated by black arrows, where decreases in the effects are designated by red arrows.



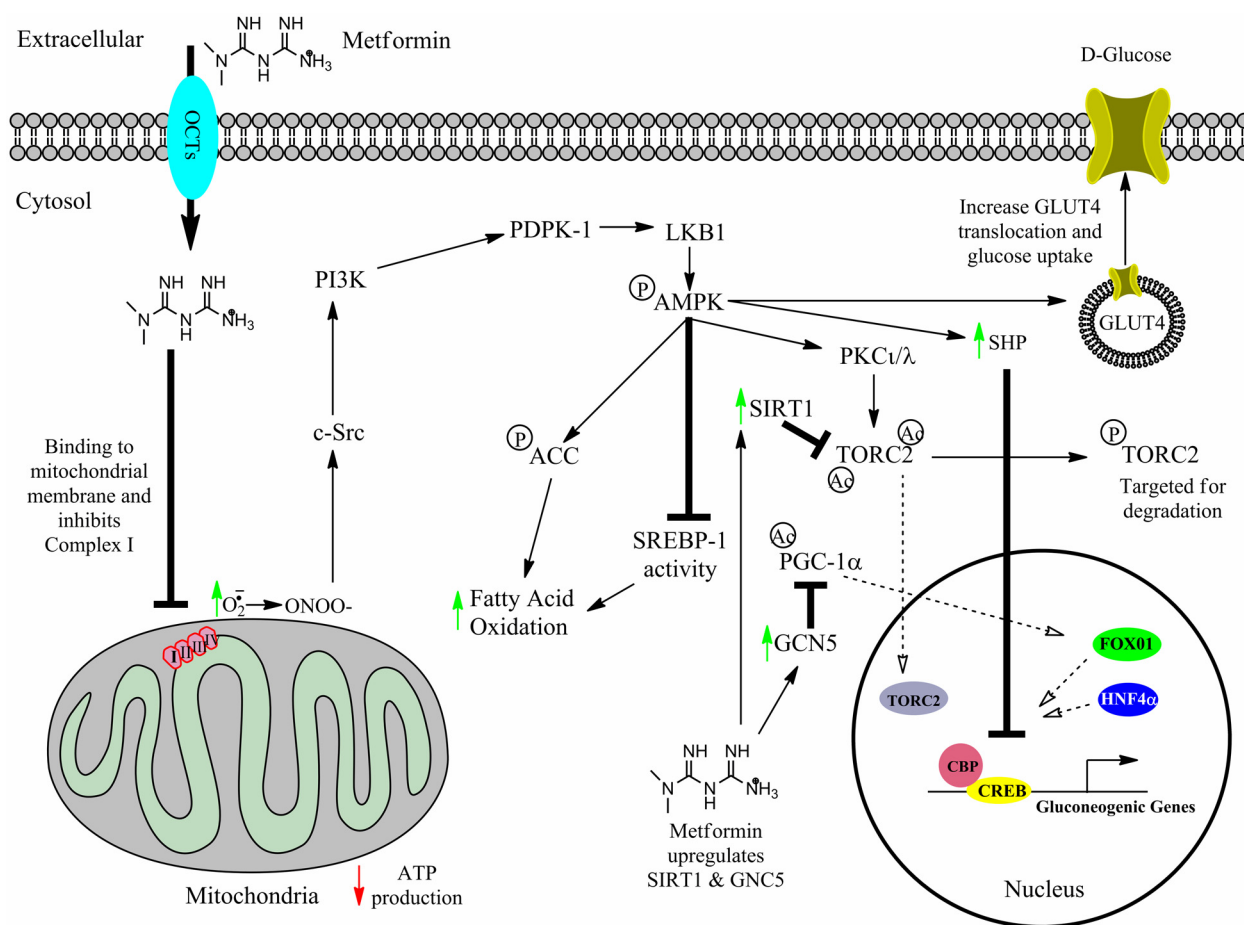


**Figure 1.3. Schematic Diagram of Metformin Cellular Pathways to Elicit Pharmacologic Responses.** Metformin enters the cell via organic cation transporters (OCTs), inhibits complex I of the mitochondrial respiratory chain, inducing superoxide formation, leading to peroxynitrite ( $ONOO^-$ ) formation, activating c-Src-PI3K-PDPK-1 pathway to activate LKB1-AMPK. AMPK activation decreases SREBP-1 translocation to the nucleus activity and phosphorylates ACC to increase fatty acid oxidation. AMPK activation increases GLUT4 translocation to the plasma membrane. AMPK activation decreases gluconeogenesis through PKC $\iota/\lambda$  phosphorylation of TORC2 targeting it for degradation. Additionally, metformin, through AMPK dependent and independent pathway, up regulates SIRT1 and GCN5 which inhibit TORC2 translocation to the nucleus by deacylation and PGC-1 $\alpha$  associated in the nucleus to FOXO1 by acetylation, respectively. Furthermore, metformin AMPK activation increases SHP expression which blocks CBP binding to FOXO1 and HNF4 $\alpha$ . Green arrows represent increased activity or expression, red arrows represent decreased activity, solid black arrows indicate agonist effects, bold bars indicate antagonist effects, and dashed arrows represent the mechanism perturbed by the preceding action.

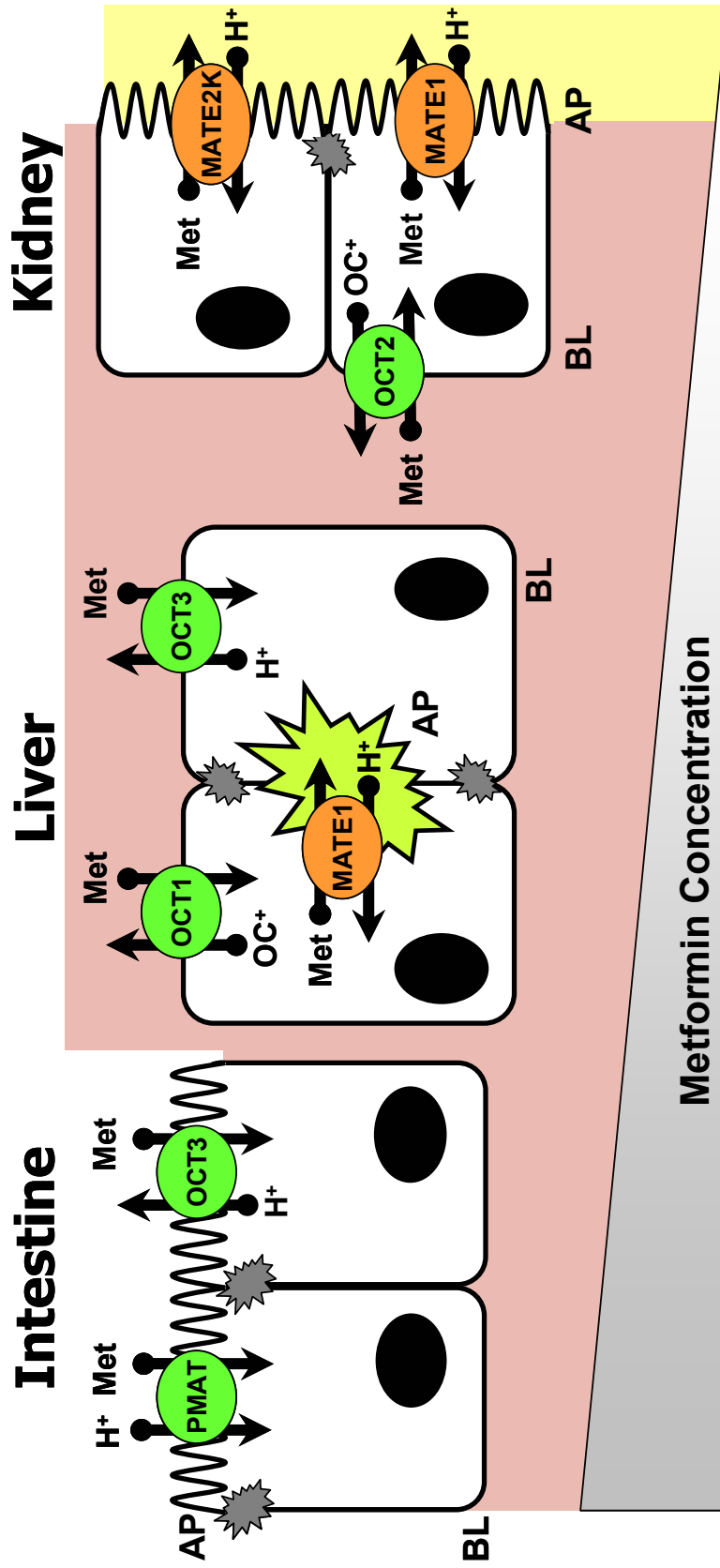


**Figure 1.4. Cation-Selective Transporters Implicated in Metformin Disposition in the Intestine, Liver, and Kidney.** The effective metformin concentration that each organ experiences decreases from the gut lumen to portal blood and ultimately systemic blood. In the intestine, PMAT and hOCT3 are present on the lumen apical membrane and potentially facilitate intestinal accumulation of metformin. In the liver hOCT1 and hOCT3 mediate uptake into hepatocytes, where MATE1 may facilitate biliary excretion of metformin. In the proximal tubule cells of the kidney, hOCT2 mediates uptake of metformin from the blood, while MATE1 and MATE2K efflux metformin into the urine.

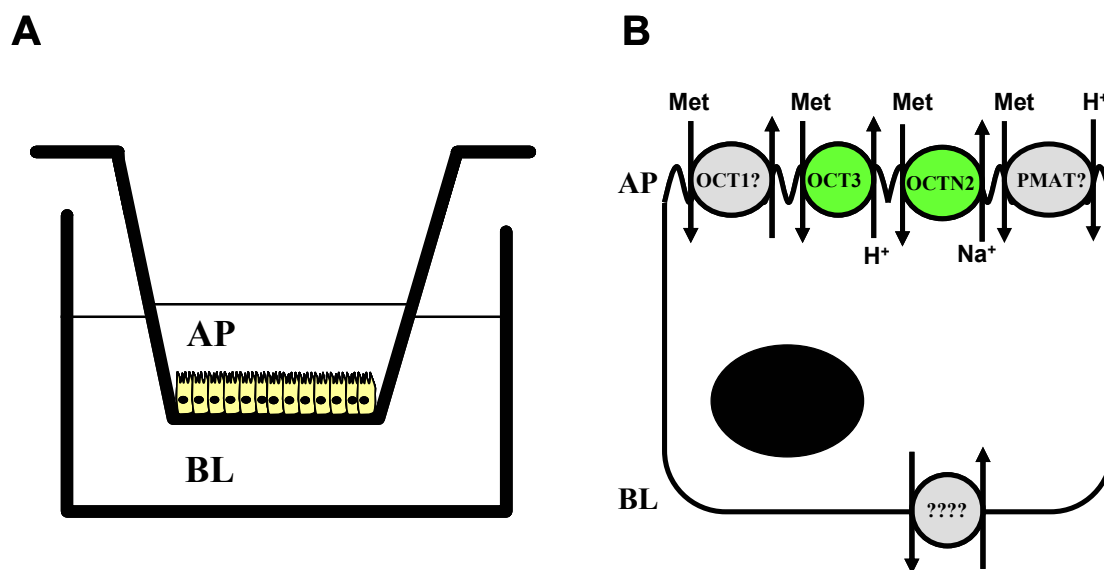


**Figure 1.5. Diagram of Caco-2 Transwell™ Model and Cation-Selective Transporter Expression and Localization in Caco-2 Cells.** A. Transwell™ experimental system with Caco-2 cells grown on porous membrane supports, providing access to both the apical (AP) and basolateral (BL) compartments for dosing and/or sampling. B. Proposed and known cation-selective transporters in Caco-2 cells. hOCT3 and hOCTN2 (green color) function, localization, and expression has been confirmed in Caco-2 cells. hOCT1 and PMAT (grey color) localization function, or expression has yet to be fully determined in Caco-2 cells. Currently there is no evidence for BL cation-selective transporters in Caco-2 cells.

## 1.1. REFERENCES

- Abdul-Ghani MA, Molina-Carrion M, Jani R, Jenkinson C and Defronzo RA (2008) Adipocytes in subjects with impaired fasting glucose and impaired glucose tolerance are resistant to the anti-lipolytic effect of insulin. *Acta Diabetol* **45**:147-150.
- ADA (2009) Standards of medical care in diabetes--2009. *Diabetes Care* **32 Suppl 1**:S13-61.
- Alexander GC, Sehgal NL, Moloney RM and Stafford RS (2008) National trends in treatment of type 2 diabetes mellitus, 1994-2007. *Arch Intern Med* **168**:2088-2094.
- Alexandre MD, Lu Q and Chen YH (2005) Overexpression of claudin-7 decreases the paracellular Cl<sup>-</sup> conductance and increases the paracellular Na<sup>+</sup> conductance in LLC-PK1 cells. *J Cell Sci* **118**:2683-2693.
- Anedda A, Rial E and Gonzalez-Barroso MM (2008) Metformin induces oxidative stress in white adipocytes and raises uncoupling protein 2 levels. *J Endocrinol* **199**:33-40.
- Aoki M, Terada T, Kajiwarra M, Ogasawara K, Ikai I, Ogawa O, Katsura T and Inui K (2008) Kidney-specific expression of human organic cation transporter 2 (OCT2/SLC22A2) is regulated by DNA methylation. *Am J Physiol Renal Physiol* **295**:F165-170.
- Artursson P (1990) Epithelial transport of drugs in cell culture. I: A model for studying the passive diffusion of drugs over intestinal absorptive (Caco-2) cells. *J Pharm Sci* **79**:476-482.
- Assan R, Heuclin C, Ganeval D, Bismuth C, George J and Girard JR (1977) Metformin-induced lactic acidosis in the presence of acute renal failure. *Diabetologia* **13**:211-217.
- Bailey CJ (1992) Biguanides and NIDDM. *Diabetes Care* **15**:755-772.
- Bailey CJ and Day C (1989) Traditional plant medicines as treatments for diabetes. *Diabetes Care* **12**:553-564.
- Bailey CJ and Day C (2004) Metformin: its botanical background. *Pract Diab Int* **21**:115-117.
- Bailey CJ, Flatt PR and Marks V (1989) Drugs inducing hypoglycemia. *Pharmacol Ther* **42**:361-384.
- Bailey CJ, Mynett KJ and Page T (1994) Importance of the intestine as a site of metformin-stimulated glucose utilization. *Br J Pharmacol* **112**:671-675.
- Bailey CJ and Nattrass M (1988) Treatment--metformin. *Baillieres Clin Endocrinol Metab* **2**:455-476.
- Bailey CJ and Turner RC (1996) Metformin. *N Engl J Med* **334**:574-579.

- Bailey CJ, Wilcock C and Day C (1992) Effect of metformin on glucose metabolism in the splanchnic bed. *Br J Pharmacol* **105**:1009-1013.
- Bailey CJ, Wilcock C and Scarpello JH (2008) Metformin and the intestine. *Diabetologia* **51**:1552-1553.
- Banan A, Zhang LJ, Shaikh M, Fields JZ, Choudhary S, Forsyth CB, Farhadi A and Keshavarzian A (2005) theta Isoform of protein kinase C alters barrier function in intestinal epithelium through modulation of distinct claudin isotypes: a novel mechanism for regulation of permeability. *J Pharmacol Exp Ther* **313**:962-982.
- Barnes K, Dobrzynski H, Foppolo S, Beal PR, Ismat F, Scullion ER, Sun L, Tellez J, Ritzel MW, Claycomb WC, Cass CE, Young JD, Billeter-Clark R, Boyett MR and Baldwin SA (2006) Distribution and functional characterization of equilibrative nucleoside transporter-4, a novel cardiac adenosine transporter activated at acidic pH. *Circ Res* **99**:510-519.
- Boden G and Shulman GI (2002) Free fatty acids in obesity and type 2 diabetes: defining their role in the development of insulin resistance and beta-cell dysfunction. *Eur J Clin Invest* **32 Suppl 3**:14-23.
- Boulias K, Katrakili N, Bamberg K, Underhill P, Greenfield A and Talianidis I (2005) Regulation of hepatic metabolic pathways by the orphan nuclear receptor SHP. *Embo J* **24**:2624-2633.
- Bourdet DL, Pollack GM and Thakker DR (2006) Intestinal absorptive transport of the hydrophilic cation ranitidine: a kinetic modeling approach to elucidate the role of uptake and efflux transporters and paracellular vs. transcellular transport in Caco-2 cells. *Pharm Res* **23**:1178-1187.
- Bourdet DL and Thakker DR (2006) Saturable absorptive transport of the hydrophilic organic cation ranitidine in Caco-2 cells: role of pH-dependent organic cation uptake system and P-glycoprotein. *Pharm Res* **23**:1165-1177.
- Bourron O, Daval M, Hainault I, Hajduch E, Servant JM, Gautier JF, Ferre P and Foufelle F (2010) Biguanides and thiazolidinediones inhibit stimulated lipolysis in human adipocytes through activation of AMP-activated protein kinase. *Diabetologia* **53**:768-778.
- Brown JB, Pedula K, Barzilay J, Herson MK and Latare P (1998) Lactic acidosis rates in type 2 diabetes. *Diabetes Care* **21**:1659-1663.
- Brunmair B, Staniek K, Gras F, Scharf N, Althaym A, Clara R, Roden M, Gnaiger E, Nohl H, Waldhausl W and Fornsinn C (2004) Thiazolidinediones, like metformin, inhibit respiratory complex I: a common mechanism contributing to their antidiabetic actions? *Diabetes* **53**:1052-1059.

- Carling D, Zammit VA and Hardie DG (1987) A common bicyclic protein kinase cascade inactivates the regulatory enzymes of fatty acid and cholesterol biosynthesis. *FEBS Lett* **223**:217-222.
- Caton PW, Nayuni N, Kieswich J, Khan N, Yaqoob M and Corder R (2010) Metformin suppresses hepatic gluconeogenesis through induction of SIRT1 and GCN5. *J Endocrinol* **In Press**.
- Chen Y, Li S, Brown C, Cheatham S, Castro RA, Leabman MK, Urban TJ, Chen L, Yee SW, Choi JH, Huang Y, Brett CM, Burchard EG and Giacomini KM (2009a) Effect of genetic variation in the organic cation transporter 2 on the renal elimination of metformin. *Pharmacogenet Genomics* **19**:497-504.
- Chen Y, Teranishi K, Li S, Yee SW, Hesselson S, Stryke D, Johns SJ, Ferrin TE, Kwok P and Giacomini KM (2009b) Genetic variants in multidrug and toxic compound extrusion-1, hMATE1, alter transport function. *Pharmacogenomics J* **9**:127-136.
- Cho YK, Choi YH, Kim SH and Lee MG (2009) Effects of Escherichia coli lipopolysaccharide on the metformin pharmacokinetics in rats. *Xenobiotica* **39**:946-954.
- Choi YH, Chung SJ and Lee MG (2008) Pharmacokinetic interaction between DA-8159, a new erectogenic, and metformin in rats: competitive inhibition of metabolism via hepatic CYP3A1/2. *Br J Pharmacol* **153**:1568-1578.
- Choi YH, Kim SG and Lee MG (2006) Dose-independent pharmacokinetics of metformin in rats: Hepatic and gastrointestinal first-pass effects. *J Pharm Sci* **95**:2543-2552.
- Choi YH, Lee I and Lee MG (2007) Effects of water deprivation on the pharmacokinetics of metformin in rats. *Biopharm Drug Dispos* **28**:373-383.
- Choi YH, Lee I and Lee MG (2010) Slower clearance of intravenous metformin in rats with acute renal failure induced by uranyl nitrate: contribution of slower renal and non-renal clearances. *Eur J Pharm Sci* **39**:1-7.
- Choi YH and Lee MG (2006) Effects of enzyme inducers and inhibitors on the pharmacokinetics of metformin in rats: involvement of CYP2C11, 2D1 and 3A1/2 for the metabolism of metformin. *Br J Pharmacol* **149**:424-430.
- Chou CH (2000) Uptake and dispersion of metformin in the isolated perfused rat liver. *J Pharm Pharmacol* **52**:1011-1016.
- Ciaraldi TP, Kong AP, Chu NV, Kim DD, Baxi S, Loviscach M, Plodkowski R, Reitz R, Caulfield M, Mudaliar S and Henry RR (2002) Regulation of glucose transport and insulin signaling by troglitazone or metformin in adipose tissue of type 2 diabetic subjects. *Diabetes* **51**:30-36.
- Clarke BF and Campbell IW (1977) Comparison of metformin and chlorpropamide in non-obese, maturity-onset diabetics uncontrolled by diet. *Br Med J* **2**:1576-1578.

- Cleasby ME, Dzamko N, Hegarty BD, Cooney GJ, Kraegen EW and Ye JM (2004) Metformin prevents the development of acute lipid-induced insulin resistance in the rat through altered hepatic signaling mechanisms. *Diabetes* **53**:3258-3266.
- Codario RA (2005) *Type 2 diabetes, pre-diabetes, and the metabolic syndrome : the primary care guide to diagnosis and management*. Humana Press, Totowa, N.J.
- Colegio OR, Van Itallie C, Rahner C and Anderson JM (2003) Claudin extracellular domains determine paracellular charge selectivity and resistance but not tight junction fibril architecture. *Am J Physiol Cell Physiol* **284**:C1346-1354.
- Colegio OR, Van Itallie CM, McCrea HJ, Rahner C and Anderson JM (2002) Claudins create charge-selective channels in the paracellular pathway between epithelial cells. *Am J Physiol Cell Physiol* **283**:C142-147.
- Corton JM, Gillespie JG, Hawley SA and Hardie DG (1995) 5-aminoimidazole-4-carboxamide ribonucleoside. A specific method for activating AMP-activated protein kinase in intact cells? *Eur J Biochem* **229**:558-565.
- Davies SP, Hawley SA, Woods A, Carling D, Haystead TA and Hardie DG (1994) Purification of the AMP-activated protein kinase on ATP-gamma-sepharose and analysis of its subunit structure. *Eur J Biochem* **223**:351-357.
- DeFronzo RA, Barzilai N and Simonson DC (1991) Mechanism of metformin action in obese and lean noninsulin-dependent diabetic subjects. *J Clin Endocrinol Metab* **73**:1294-1301.
- DeFronzo RA and Goodman AM (1995) Efficacy of metformin in patients with non-insulin-dependent diabetes mellitus. The Multicenter Metformin Study Group. *N Engl J Med* **333**:541-549.
- Despres JP and Lemieux I (2006) Abdominal obesity and metabolic syndrome. *Nature* **444**:881-887.
- Diamanti-Kandarakis E, Christakou CD, Kandaraki E and Economou FN Metformin: an old medication of new fashion: evolving new molecular mechanisms and clinical implications in polycystic ovary syndrome. *Eur J Endocrinol* **162**:193-212.
- Dresner A, Laurent D, Marcucci M, Griffin ME, Dufour S, Cline GW, Slezak LA, Andersen DK, Hundal RS, Rothman DL, Petersen KF and Shulman GI (1999) Effects of free fatty acids on glucose transport and IRS-1-associated phosphatidylinositol 3-kinase activity. *J Clin Invest* **103**:253-259.
- El-Mir MY, Nogueira V, Fontaine E, Averet N, Rigoulet M and Leverve X (2000) Dimethylbiguanide inhibits cell respiration via an indirect effect targeted on the respiratory chain complex I. *J Biol Chem* **275**:223-228.

- Elimrani I, Lahjouji K, Seidman E, Roy MJ, Mitchell GA and Qureshi I (2003) Expression and localization of organic cation/carnitine transporter OCTN2 in Caco-2 cells. *Am J Physiol Gastrointest Liver Physiol* **284**:G863-871.
- Engel K, Zhou M and Wang J (2004) Identification and characterization of a novel monoamine transporter in the human brain. *J Biol Chem* **279**:50042-50049.
- Englund G, Rorsman F, Ronnblom A, Karlbom U, Lazorova L, Grasjo J, Kindmark A and Artursson P (2006) Regional levels of drug transporters along the human intestinal tract: co-expression of ABC and SLC transporters and comparison with Caco-2 cells. *Eur J Pharm Sci* **29**:269-277.
- Fantus IG and Brosseau R (1986) Mechanism of action of metformin: insulin receptor and postreceptor effects in vitro and in vivo. *J Clin Endocrinol Metab* **63**:898-905.
- Fontbonne A, Charles MA, Juhan-Vague I, Bard JM, Andre P, Isnard F, Cohen JM, Grandmottet P, Vague P, Safar ME and Eschwege E (1996) The effect of metformin on the metabolic abnormalities associated with upper-body fat distribution. BIGPRO Study Group. *Diabetes Care* **19**:920-926.
- Fujita H, Sugimoto K, Inatomi S, Maeda T, Osanai M, Uchiyama Y, Yamamoto Y, Wada T, Kojima T, Yokozaki H, Yamashita T, Kato S, Sawada N and Chiba H (2008) Tight junction proteins claudin-2 and -12 are critical for vitamin D-dependent Ca<sup>2+</sup> absorption between enterocytes. *Mol Biol Cell* **19**:1912-1921.
- Fujita M, Nakanishi T, Shibue Y, Kobayashi D, Moseley RH, Shirasaka Y and Tamai I (2009) Hepatic Uptake of  $\gamma$ -Butyrobetaine, a Precursor of Carnitine Biosynthesis, in Rats. *Am J Physiol Gastrointest Liver Physiol*.
- Gan LS, Yanni S and Thakker DR (1998) Modulation of the tight junctions of the Caco-2 cell monolayers by H<sub>2</sub>-antagonists. *Pharm Res* **15**:53-57.
- Ganapathy ME, Huang W, Rajan DP, Carter AL, Sugawara M, Iseki K, Leibach FH and Ganapathy V (2000) beta-lactam antibiotics as substrates for OCTN2, an organic cation/carnitine transporter. *J Biol Chem* **275**:1699-1707.
- Garvey WT, Huecksteadt TP, Matthaei S and Olefsky JM (1988) Role of glucose transporters in the cellular insulin resistance of type II non-insulin-dependent diabetes mellitus. *J Clin Invest* **81**:1528-1536.
- Garvey WT, Maianu L, Zhu JH, Brechtel-Hook G, Wallace P and Baron AD (1998) Evidence for defects in the trafficking and translocation of GLUT4 glucose transporters in skeletal muscle as a cause of human insulin resistance. *J Clin Invest* **101**:2377-2386.
- Glube N, Closs E and Langguth P (2007) OCTN2-mediated carnitine uptake in a newly discovered human proximal tubule cell line (Caki-1). *Mol Pharm* **4**:160-168.



- Glube N and Langguth P (2008) Caki-1 cells as a model system for the interaction of renally secreted drugs with OCT3. *Nephron Physiol* **108**:p18-28.
- Gontier E, Fourme E, Wartski M, Blondet C, Bonardel G, Le Stanc E, Mantzarides M, Foehrenbach H, Pecking AP and Alberini JL (2008) High and typical 18F-FDG bowel uptake in patients treated with metformin. *Eur J Nucl Med Mol Imaging* **35**:95-99.
- Gorboulev V, Ulzheimer JC, Akhoundova A, Ulzheimer-Teuber I, Karbach U, Quester S, Baumann C, Lang F, Busch AE and Koepsell H (1997) Cloning and characterization of two human polyspecific organic cation transporters. *DNA Cell Biol* **16**:871-881.
- Grigat S, Fork C, Bach M, Golz S, Geerts A, Schomig E and Grundemann D (2009) The carnitine transporter SLC22A5 is not a general drug transporter, but it efficiently translocates mildronate. *Drug Metab Dispos* **37**:330-337.
- Grundemann D, Harlfinger S, Golz S, Geerts A, Lazar A, Berkels R, Jung N, Rubbert A and Schomig E (2005) Discovery of the ergothioneine transporter. *Proc Natl Acad Sci U S A* **102**:5256-5261.
- Grundemann D, Schechinger B, Rappold GA and Schomig E (1998) Molecular identification of the corticosterone-sensitive extraneuronal catecholamine transporter. *Nat Neurosci* **1**:349-351.
- Gugliucci A (2009) "Blinding" of AMP-dependent kinase by methylglyoxal: a mechanism that allows perpetuation of hepatic insulin resistance? *Med Hypotheses* **73**:921-924.
- Ha Choi J, Wah Yee S, Kim MJ, Nguyen L, Ho Lee J, Kang JO, Hesselson S, Castro RA, Stryke D, Johns SJ, Kwok PY, Ferrin TE, Goo Lee M, Black BL, Ahituv N and Giacomini KM (2009) Identification and characterization of novel polymorphisms in the basal promoter of the human transporter, MATE1. *Pharmacogenet Genomics* **19**:770-780.
- Hadden DR (2005) Goat's rue - French lilac - Italian fitch - Spanish sainfoin: gallega officinalis and metformin: the Edinburgh connection. *J R Coll Physicians Edinb* **35**:258-260.
- Hardie DG (2003) Minireview: the AMP-activated protein kinase cascade: the key sensor of cellular energy status. *Endocrinology* **144**:5179-5183.
- Hardie DG (2008) AMPK: a key regulator of energy balance in the single cell and the whole organism. *Int J Obes (Lond)* **32 Suppl 4**:S7-12.
- Hawley SA, Boudeau J, Reid JL, Mustard KJ, Udd L, Makela TP, Alessi DR and Hardie DG (2003) Complexes between the LKB1 tumor suppressor, STRAD alpha/beta and MO25 alpha/beta are upstream kinases in the AMP-activated protein kinase cascade. *J Biol* **2**:28.
- Hawley SA, Gadalla AE, Olsen GS and Hardie DG (2002) The antidiabetic drug metformin activates the AMP-activated protein kinase cascade via an adenine nucleotide-independent mechanism. *Diabetes* **51**:2420-2425.

- Hayeshi R, Hilgendorf C, Artursson P, Augustijns P, Brodin B, Dehertogh P, Fisher K, Fossati L, Hovenkamp E, Korjamo T, Masungi C, Maubon N, Mols R, Mullertz A, Monkkonen J, O'Driscoll C, Oppers-Tiemissen HM, Ragnarsson EG, Rooseboom M and Ungell AL (2008) Comparison of drug transporter gene expression and functionality in Caco-2 cells from 10 different laboratories. *Eur J Pharm Sci* **35**:383-396.
- He L, Sabet A, Djedjos S, Miller R, Sun X, Hussain MA, Radovick S and Wondisford FE (2009) Metformin and insulin suppress hepatic gluconeogenesis through phosphorylation of CREB binding protein. *Cell* **137**:635-646.
- Heishi M, Hayashi K, Ichihara J, Ishikawa H, Kawamura T, Kanaoka M, Taiji M and Kimura T (2008) Comparison of gene expression changes induced by biguanides in db/db mice liver. *J Toxicol Sci* **33**:339-347.
- Henry RR (1996) Glucose control and insulin resistance in non-insulin-dependent diabetes mellitus. *Ann Intern Med* **124**:97-103.
- Hermann L and Melander A (1992) Biguanides: basic aspects and clinical uses, in: *International Textbook of Diabetes Mellitus* (Alberti K, DeFronzo R, Keen H and Zimmet P eds), pp 773-795, John Wiley & Sons Inc., New York.
- Hermann LS, Schersten B, Bitzen PO, Kjellstrom T, Lindgarde F and Melander A (1994) Therapeutic comparison of metformin and sulfonylurea, alone and in various combinations. A double-blind controlled study. *Diabetes Care* **17**:1100-1109.
- Hiasa M, Matsumoto T, Komatsu T and Moriyama Y (2006) Wide variety of locations for rodent MATE1, a transporter protein that mediates the final excretion step for toxic organic cations. *Am J Physiol Cell Physiol* **291**:C678-686.
- Hidalgo IJ, Raub TJ and Borchardt RT (1989) Characterization of the human colon carcinoma cell line (Caco-2) as a model system for intestinal epithelial permeability. *Gastroenterology* **96**:736-749.
- Hilgendorf C, Ahlin G, Seithel A, Artursson P, Ungell AL and Karlsson J (2007) Expression of thirty-six drug transporter genes in human intestine, liver, kidney, and organotypic cell lines. *Drug Metab Dispos* **35**:1333-1340.
- Hirsch HA, Iliopoulos D, Tsiachlis PN and Struhl K (2009) Metformin selectively targets cancer stem cells, and acts together with chemotherapy to block tumor growth and prolong remission. *Cancer Res* **69**:7507-7511.
- Hou J, Paul DL and Goodenough DA (2005) Paracellin-1 and the modulation of ion selectivity of tight junctions. *J Cell Sci* **118**:5109-5118.
- Hundal RS, Krssak M, Dufour S, Laurent D, Lebon V, Chandramouli V, Inzucchi SE, Schumann WC, Petersen KF, Landau BR and Shulman GI (2000) Mechanism by which metformin reduces glucose production in type 2 diabetes. *Diabetes* **49**:2063-2069.

- Iannello S, Camuto M, Cavaleri A, Milazzo P, Pisano MG, Bellomia D and Belfiore F (2004) Effects of short-term metformin treatment on insulin sensitivity of blood glucose and free fatty acids. *Diabetes Obes Metab* **6**:8-15.
- Ito S, Kusuhara H, Kuroiwa Y, Wu C, Moriyama Y, Inoue K, Kondo T, Yuasa H, Nakayama H, Horita S and Sugiyama Y (2010) Potent and specific inhibition of mMate1-mediated efflux of type I organic cations in the liver and kidney by pyrimethamine. *J Pharmacol Exp Ther* **In Press**.
- Jackson RA, Hawa MI, Jaspan JB, Sim BM, Disilvio L, Featherbe D and Kurtz AB (1987) Mechanism of metformin action in non-insulin-dependent diabetes. *Diabetes* **36**:632-640.
- Jayasagar G, Krishna Kumar M, Chandrasekhar K, Madhusudan Rao C and Madhusudan Rao Y (2002) Effect of cephalixin on the pharmacokinetics of metformin in healthy human volunteers. *Drug Metabol Drug Interact* **19**:41-48.
- Jiralerspong S, Palla SL, Giordano SH, Meric-Bernstam F, Liedtke C, Barnett CM, Hsu L, Hung MC, Hortobagyi GN and Gonzalez-Angulo AM (2009) Metformin and pathologic complete responses to neoadjuvant chemotherapy in diabetic patients with breast cancer. *J Clin Oncol* **27**:3297-3302.
- Johnson AB, Webster JM, Sum CF, Heseltine L, Argyraki M, Cooper BG and Taylor R (1993) The impact of metformin therapy on hepatic glucose production and skeletal muscle glycogen synthase activity in overweight type II diabetic patients. *Metabolism* **42**:1217-1222.
- Jonker JW, Wagenaar E, Mol CA, Buitelaar M, Koepsell H, Smit JW and Schinkel AH (2001) Reduced hepatic uptake and intestinal excretion of organic cations in mice with a targeted disruption of the organic cation transporter 1 (Oct1 [Slc22a1]) gene. *Mol Cell Biol* **21**:5471-5477.
- Kajiwarra M, Terada T, Ogasawara K, Iwano J, Katsura T, Fukatsu A, Doi T and Inui K (2009) Identification of multidrug and toxin extrusion (MATE1 and MATE2-K) variants with complete loss of transport activity. *J Hum Genet* **54**:40-46.
- Karttunen P, Uusitupa M and Lamminsivu U (1983) The pharmacokinetics of metformin: a comparison of the properties of a rapid-release and a sustained-release preparation. *Int J Clin Pharmacol Ther Toxicol* **21**:31-36.
- Kato Y, Mikihiro S, Sugiura T, Wakayama T, Kubo Y, Kobayashi D, Sai Y, Tamai I, Iseki S and Tsuji A (2006) Organic cation/carnitine transporter OCTN2 (Slc22a5) is responsible for carnitine transport across the apical membranes of small intestinal epithelial cells in mouse. *Mol Pharmacol* **70**:829-837.
- Kekuda R, Prasad PD, Wu X, Wang H, Fei YJ, Leibach FH and Ganapathy V (1998) Cloning and functional characterization of a potential-sensitive, polyspecific organic cation transporter (OCT3) most abundantly expressed in placenta. *J Biol Chem* **273**:15971-15979.

- Kewalramani G, Puthanveetil P, Wang F, Kim MS, Deppe S, Abrahani A, Luciani DS, Johnson JD and Rodrigues B (2009) AMP-activated protein kinase confers protection against TNF- $\alpha$ -induced cardiac cell death. *Cardiovasc Res* **84**:42-53.
- Kim HR, Park SW, Cho HJ, Chae KA, Sung JM, Kim JS, Landowski CP, Sun D, Abd El-Aty AM, Amidon GL and Shin HC (2007) Comparative gene expression profiles of intestinal transporters in mice, rats and humans. *Pharmacol Res* **56**:224-236.
- Kim JY, Kim HJ, Kim KT, Park YY, Seong HA, Park KC, Lee IK, Ha H, Shong M, Park SC and Choi HS (2004) Orphan nuclear receptor small heterodimer partner represses hepatocyte nuclear factor 3/Foxa transactivation via inhibition of its DNA binding. *Mol Endocrinol* **18**:2880-2894.
- Kim YD, Park KG, Lee YS, Park YY, Kim DK, Nedumaran B, Jang WG, Cho WJ, Ha J, Lee IK, Lee CH and Choi HS (2008) Metformin inhibits hepatic gluconeogenesis through AMP-activated protein kinase-dependent regulation of the orphan nuclear receptor SHP. *Diabetes* **57**:306-314.
- Kimura N, Masuda S, Tanihara Y, Ueo H, Okuda M, Katsura T and Inui K (2005a) Metformin is a superior substrate for renal organic cation transporter OCT2 rather than hepatic OCT1. *Drug Metab Pharmacokinet* **20**:379-386.
- Kimura N, Okuda M and Inui K (2005b) Metformin Transport by Renal Basolateral Organic Cation Transporter hOCT2. *Pharm Res* **22**:255-259.
- Knipp GT, Ho NF, Barsuhn CL and Borchardt RT (1997) Paracellular diffusion in Caco-2 cell monolayers: effect of perturbation on the transport of hydrophilic compounds that vary in charge and size. *J Pharm Sci* **86**:1105-1110.
- Koepsell H, Lips K and Volk C (2007) Polyspecific organic cation transporters: structure, function, physiological roles, and biopharmaceutical implications. *Pharm Res* **24**:1227-1251.
- Koo SH, Flechner L, Qi L, Zhang X, Screatton RA, Jeffries S, Hedrick S, Xu W, Boussouar F, Brindle P, Takemori H and Montminy M (2005) The CREB coactivator TORC2 is a key regulator of fasting glucose metabolism. *Nature* **437**:1109-1111.
- Kovbasnjuk O, Leader JP, Weinstein AM and Spring KR (1998) Water does not flow across the tight junctions of MDCK cell epithelium. *Proc Natl Acad Sci U S A* **95**:6526-6530.
- Kovo M, Kogman N, Ovadia O, Nakash I, Golan A and Hoffman A (2008) Carrier-mediated transport of metformin across the human placenta determined by using the ex vivo perfusion of the placental cotyledon model. *Prenat Diagn* **28**:544-548.
- Kurth-Kraczek EJ, Hirshman MF, Goodyear LJ and Winder WW (1999) 5' AMP-activated protein kinase activation causes GLUT4 translocation in skeletal muscle. *Diabetes* **48**:1667-1671.

- Lamhonwah AM, Ackerley C, Onizuka R, Tilups A, Lamhonwah D, Chung C, Tao KS, Tellier R and Tein I (2005) Epitope shared by functional variant of organic cation/carnitine transporter, OCTN1, *Campylobacter jejuni* and *Mycobacterium paratuberculosis* may underlie susceptibility to Crohn's disease at 5q31. *Biochem Biophys Res Commun* **337**:1165-1175.
- Lamhonwah AM and Tein I (2006) Novel localization of OCTN1, an organic cation/carnitine transporter, to mammalian mitochondria. *Biochem Biophys Res Commun* **345**:1315-1325.
- Leabman MK and Giacomini KM (2003) Estimating the contribution of genes and environment to variation in renal drug clearance. *Pharmacogenetics* **13**:581-584.
- Leabman MK, Huang CC, Kawamoto M, Johns SJ, Stryke D, Ferrin TE, DeYoung J, Taylor T, Clark AG, Herskowitz I and Giacomini KM (2002) Polymorphisms in a human kidney xenobiotic transporter, OCT2, exhibit altered function. *Pharmacogenetics* **12**:395-405.
- Lee A and Morley JE (1998) Metformin decreases food consumption and induces weight loss in subjects with obesity with type II non-insulin-dependent diabetes. *Obes Res* **6**:47-53.
- Lee K, Ng C, Brouwer KL and Thakker DR (2002) Secretory transport of ranitidine and famotidine across Caco-2 cell monolayers. *J Pharmacol Exp Ther* **303**:574-580.
- Lee K and Thakker DR (1999) Saturable transport of H<sub>2</sub>-antagonists ranitidine and famotidine across Caco-2 cell monolayers. *J Pharm Sci* **88**:680-687.
- Lenhard JM, Kliever SA, Paulik MA, Plunket KD, Lehmann JM and Weiel JE (1997) Effects of troglitazone and metformin on glucose and lipid metabolism: alterations of two distinct molecular pathways. *Biochem Pharmacol* **54**:801-808.
- Lerin C, Rodgers JT, Kalume DE, Kim SH, Pandey A and Puigserver P (2006) GCN5 acetyltransferase complex controls glucose metabolism through transcriptional repression of PGC-1 $\alpha$ . *Cell Metab* **3**:429-438.
- Liu Z, Liu J, Jahn LA, Fowler DE and Barrett EJ (2009) Infusing lipid raises plasma free fatty acids and induces insulin resistance in muscle microvasculature. *J Clin Endocrinol Metab* **94**:3543-3549.
- Lochhead PA, Salt IP, Walker KS, Hardie DG and Sutherland C (2000) 5-aminoimidazole-4-carboxamide riboside mimics the effects of insulin on the expression of the 2 key gluconeogenic genes PEPCK and glucose-6-phosphatase. *Diabetes* **49**:896-903.
- Lord JM, Flight IH and Norman RJ (2003) Metformin in polycystic ovary syndrome: systematic review and meta-analysis. *Bmj* **327**:951-953.
- Lord JM, White SI, Bailey CJ, Atkins TW, Fletcher RF and Taylor KG (1983) Effect of metformin on insulin receptor binding and glycaemic control in type II diabetes. *Br Med J (Clin Res Ed)* **286**:830-831.

- Lucis OJ (1983) The status of metformin in Canada. *Can Med Assoc J* **128**:24-26.
- Lupi R, Del Guerra S, Tellini C, Giannarelli R, Coppelli A, Lorenzetti M, Carmellini M, Mosca F, Navalesi R and Marchetti P (1999) The biguanide compound metformin prevents desensitization of human pancreatic islets induced by high glucose. *Eur J Pharmacol* **364**:205-209.
- Martel F, Grundemann D, Calhau C and Schomig E (2001) Apical uptake of organic cations by human intestinal Caco-2 cells: putative involvement of ASF transporters. *Naunyn Schmiedebergs Arch Pharmacol* **363**:40-49.
- Masuda S, Terada T, Yonezawa A, Tanihara Y, Kishimoto K, Katsura T, Ogawa O and Inui K (2006) Identification and functional characterization of a new human kidney-specific H<sup>+</sup>/organic cation antiporter, kidney-specific multidrug and toxin extrusion 2. *J Am Soc Nephrol* **17**:2127-2135.
- Maubon N, Le Vee M, Fossati L, Audry M, Le Ferrec E, Bolze S and Fardel O (2007) Analysis of drug transporter expression in human intestinal Caco-2 cells by real-time PCR. *Fundam Clin Pharmacol* **21**:659-663.
- McBride A and Hardie DG (2009) AMP-activated protein kinase--a sensor of glycogen as well as AMP and ATP? *Acta Physiol (Oxf)* **196**:99-113.
- McLelland J (1985) Recovery from metformin overdose. *Diabet Med* **2**:410-411.
- Meier Y, Eloranta JJ, Darimont J, Ismail MG, Hiller C, Fried M, Kullak-Ublick GA and Vavricka SR (2007) Regional distribution of solute carrier (SLC) mRNA expression along the human intestinal tract. *Drug Metab Dispos.*
- Misbin RI, Green L, Stadel BV, Gueriguian JL, Gubbi A and Fleming GA (1998) Lactic acidosis in patients with diabetes treated with metformin. *N Engl J Med* **338**:265-266.
- MMWR (2004) Prevalence of overweight and obesity among adults with diagnosed diabetes--United States, 1988-1994 and 1999-2002. *MMWR Morb Mortal Wkly Rep* **53**:1066-1068.
- Motohashi H, Sakurai Y, Saito H, Masuda S, Urakami Y, Goto M, Fukatsu A, Ogawa O and Inui K (2002) Gene expression levels and immunolocalization of organic ion transporters in the human kidney. *J Am Soc Nephrol* **13**:866-874.
- Muller J, Lips KS, Metzner L, Neubert RH, Koepsell H and Brandsch M (2005) Drug specificity and intestinal membrane localization of human organic cation transporters (OCT). *Biochem Pharmacol* **70**:1851-1860.
- Musi N, Hirshman MF, Nygren J, Svanfeldt M, Bavenholm P, Rooyackers O, Zhou G, Williamson JM, Ljunqvist O, Efendic S, Moller DE, Thorell A and Goodyear LJ (2002) Metformin increases AMP-activated protein kinase activity in skeletal muscle of subjects with type 2 diabetes. *Diabetes* **51**:2074-2081.

- Nattrass M and Alberti KG (1978) Biguanides. *Diabetologia* **14**:71-74.
- Ng C (2002) Novel Cation-Sensitive Mechanisms for Intestinal Absorption and Secretion of Famotidine and Ranitidine: Potential Clinical Implications, in: *Pharmacy*, pp 186, University of North Carolina at Chapel Hill, Chapel Hill.
- Nicklin P, Keates AC, Page T and Bailey CJ (1996) Transfer of metformin across monolayers of human intestinal Caco-2 cells and across rat intestine. *International Journal of Pharmaceutics* **128**:155-162.
- Nies AT, Herrmann E, Brom M and Keppler D (2008) Vectorial transport of the plant alkaloid berberine by double-transfected cells expressing the human organic cation transporter 1 (OCT1, SLC22A1) and the efflux pump MDR1 P-glycoprotein (ABCB1). *Naunyn Schmiedebergs Arch Pharmacol* **376**:449-461.
- Nies AT, Koepsell H, Winter S, Burk O, Klein K, Kerb R, Zanger UM, Keppler D, Schwab M and Schaeffeler E (2009) Expression of organic cation transporters OCT1 (SLC22A1) and OCT3 (SLC22A3) is affected by genetic factors and cholestasis in human liver. *Hepatology* **50**:1227-1240.
- Nishikawa T, Edelstein D, Du XL, Yamagishi S, Matsumura T, Kaneda Y, Yorek MA, Beebe D, Oates PJ, Hammes HP, Giardino I and Brownlee M (2000) Normalizing mitochondrial superoxide production blocks three pathways of hyperglycaemic damage. *Nature* **404**:787-790.
- Noel M (1979) Kinetic study of normal and sustained release dosage forms of metformin in normal subjects. *Res Clin Pharmacol* **1**:33-44.
- Ohira M, Miyashita Y, Murano T, Watanabe F and Shirai K (2009) Metformin promotes induction of lipoprotein lipase in skeletal muscle through activation of adenosine monophosphate-activated protein kinase. *Metabolism* **58**:1408-1414.
- Ohnhaus EE, Berger W, Duckert F and Oesch F (1983) The influence of dimethylbiguanide on phenprocoumon elimination and its mode of action. A drug interaction study. *Klin Wochenschr* **61**:851-858.
- Ohnhaus EE, Berger W and Nars PW (1978) The effect of different doses of dimethylbiguanide (DMB) on liver blood flow, blood glucose and plasma immunoreactive insulin in anaesthetized rats. *Biochem Pharmacol* **27**:789-793.
- Ota S, Horigome K, Ishii T, Nakai M, Hayashi K, Kawamura T, Kishino A, Taiji M and Kimura T (2009) Metformin suppresses glucose-6-phosphatase expression by a complex I inhibition and AMPK activation-independent mechanism. *Biochem Biophys Res Commun* **388**:311-316.
- Otsuka M, Matsumoto T, Morimoto R, Arioka S, Omote H and Moriyama Y (2005) A human transporter protein that mediates the final excretion step for toxic organic cations. *Proc Natl Acad Sci U S A* **102**:17923-17928.

- Owen MR, Doran E and Halestrap AP (2000) Evidence that metformin exerts its anti-diabetic effects through inhibition of complex 1 of the mitochondrial respiratory chain. *Biochem J* **348 Pt 3**:607-614.
- Palanivel R and Sweeney G (2005) Regulation of fatty acid uptake and metabolism in L6 skeletal muscle cells by resistin. *FEBS Lett* **579**:5049-5054.
- Pedersen O, Nielsen O, Bak J, Richelsen B, Beck-Nielsen H and Sorensen N (1989) The effects of metformin on adipocyte insulin action and metabolic control in obese subjects with type 2 diabetes. *Diabet Med* **6**:249-256.
- Pentikainen PJ (1986) Bioavailability of metformin. Comparison of solution, rapidly dissolving tablet, and three sustained release products. *Int J Clin Pharmacol Ther Toxicol* **24**:213-220.
- Pentikainen PJ, Neuvonen PJ and Penttila A (1979) Pharmacokinetics of metformin after intravenous and oral administration to man. *Eur J Clin Pharmacol* **16**:195-202.
- Rattan R, Giri S, Hartmann L and Shridhar V (2009) Metformin attenuates ovarian cancer cell growth in an AMP- kinase dispensable manner. *J Cell Mol Med*.
- Rea R and Donnelly R (2006) Effects of metformin and oleic acid on adipocyte expression of resistin. *Diabetes Obes Metab* **8**:105-109.
- Ren T, He J, Jiang H, Zu L, Pu S, Guo X and Xu G (2006) Metformin reduces lipolysis in primary rat adipocytes stimulated by tumor necrosis factor- $\alpha$  or isoproterenol. *J Mol Endocrinol* **37**:175-183.
- Robert F, Fendri S, Hary L, Lacroix C, Andrejak M and Lalau JD (2003) Kinetics of plasma and erythrocyte metformin after acute administration in healthy subjects. *Diabetes Metab* **29**:279-283.
- Roden M, Stingl H, Chandramouli V, Schumann WC, Hofer A, Landau BR, Nowotny P, Waldhausl W and Shulman GI (2000) Effects of free fatty acid elevation on postabsorptive endogenous glucose production and gluconeogenesis in humans. *Diabetes* **49**:701-707.
- Rodgers JT, Lerin C, Haas W, Gygi SP, Spiegelman BM and Puigserver P (2005) Nutrient control of glucose homeostasis through a complex of PGC-1 $\alpha$  and SIRT1. *Nature* **434**:113-118.
- Runge S, Mayerle J, Warnke C, Robinson D, Roser M, Felix SB and Friesecke S (2008) Metformin-associated lactic acidosis in patients with renal impairment solely due to drug accumulation? *Diabetes Obes Metab* **10**:91-93.
- Saitoh R, Sugano K, Takata N, Tachibana T, Higashida A, Nabuchi Y and Aso Y (2004) Correction of permeability with pore radius of tight junctions in Caco-2 monolayers



- improves the prediction of the dose fraction of hydrophilic drugs absorbed by humans. *Pharm Res* **21**:749-755.
- Sambol NC, Brookes LG, Chiang J, Goodman AM, Lin ET, Liu CY and Benet LZ (1996a) Food intake and dosage level, but not tablet vs solution dosage form, affect the absorption of metformin HCl in man. *Br J Clin Pharmacol* **42**:510-512.
- Sambol NC, Chiang J, O'Conner M, Liu CY, Lin ET, Goodman AM, Benet LZ and Haram JH (1996b) Pharmacokinetics and pharmacodynamics of metformin in healthy subjects and patients with noninsulin-dependent diabetes mellitus. *J Clin Pharmacol* **36**:1012-1021.
- Sasaki H, Asanuma H, Fujita M, Takahama H, Wakeno M, Ito S, Ogai A, Asakura M, Kim J, Minamino T, Takashima S, Sanada S, Sugimachi M, Komamura K, Mochizuki N and Kitakaze M (2009) Metformin prevents progression of heart failure in dogs: role of AMP-activated protein kinase. *Circulation* **119**:2568-2577.
- Schatz H, Katsilambros N, Nierle C and Pfeiffer EE (1972) The effect of biguanides on secretion and biosynthesis of insulin in isolated pancreatic islets of rats. *Diabetologia* **8**:402-407.
- Scheen AJ (1996) Clinical Pharmacokinetics of Metformin. *Clin. Pharmacokinet.* **30**:359-371.
- Scheen AJ (2005) Drug interactions of clinical importance with antihyperglycaemic agents: an update. *Drug Saf* **28**:601-631.
- Scheen AJ, de Magalhaes AC, Salvatore T and Lefebvre PJ (1994) Reduction of the acute bioavailability of metformin by the alpha-glucosidase inhibitor acarbose in normal man. *Eur J Clin Invest* **24 Suppl 3**:50-54.
- Seidowsky A, Nseir S, Houdret N and Fourrier F (2009) Metformin-associated lactic acidosis: a prognostic and therapeutic study. *Crit Care Med* **37**:2191-2196.
- Seithel A, Karlsson J, Hilgendorf C, Bjorquist A and Ungell A (2006) Variability in mRNA expression of ABC- and SLC-transporters in human intestinal cells: comparison between human segments and Caco-2 cells. *Eur J Pharm Sci* **28**:291-299.
- Shu Y, Brown C, Castro RA, Shi RJ, Lin ET, Owen RP, Sheardown SA, Yue L, Burchard EG, Brett CM and Giacomini KM (2008) Effect of genetic variation in the organic cation transporter 1, OCT1, on metformin pharmacokinetics. *Clin Pharmacol Ther* **83**:273-280.
- Shu Y, Leabman MK, Feng B, Mangravite LM, Huang CC, Stryke D, Kawamoto M, Johns SJ, DeYoung J, Carlson E, Ferrin TE, Herskowitz I and Giacomini KM (2003) Evolutionary conservation predicts function of variants of the human organic cation transporter, OCT1. *Proc Natl Acad Sci U S A* **100**:5902-5907.
- Shu Y, Sheardown SA, Brown C, Owen RP, Zhang S, Castro RA, Ianculescu AG, Yue L, Lo JC, Burchard EG, Brett CM and Giacomini KM (2007) Effect of genetic variation in the organic cation transporter 1 (OCT1) on metformin action. *J Clin Invest* **117**:1422-1431.

- Sogame Y, Kitamura A, Yabuki M and Komuro S (2009) A comparison of uptake of metformin and phenformin mediated by hOCT1 in human hepatocytes. *Biopharm Drug Dispos* **30**:476-484.
- Somogyi A, Stockley C, Keal J, Rolan P and Bochner F (1987) Reduction of metformin renal tubular secretion by cimetidine in man. *Br J Clin Pharmacol* **23**:545-551.
- Song IS, Shin HJ and Shin JG (2008) Genetic variants of organic cation transporter 2 (OCT2) significantly reduce metformin uptake in oocytes. *Xenobiotica* **38**:1252-1262.
- Song NN, Li QS and Liu CX (2006) Intestinal permeability of metformin using single-pass intestinal perfusion in rats. *World J Gastroenterol* **12**:4064-4070.
- Song S, Andrikopoulos S, Filippis C, Thorburn AW, Khan D and Proietto J (2001) Mechanism of fat-induced hepatic gluconeogenesis: effect of metformin. *Am J Physiol Endocrinol Metab* **281**:E275-282.
- Stepensky D, Friedman M, Raz I and Hoffman A (2002) Pharmacokinetic-pharmacodynamic analysis of the glucose-lowering effect of metformin in diabetic rats reveals first-pass pharmacodynamic effect. *Drug Metab Dispos* **30**:861-868.
- Steppan CM, Bailey ST, Bhat S, Brown EJ, Banerjee RR, Wright CM, Patel HR, Ahima RS and Lazar MA (2001) The hormone resistin links obesity to diabetes. *Nature* **409**:307-312.
- Stumvoll M, Nurjhan N, Perriello G, Dailey G and Gerich JE (1995) Metabolic effects of metformin in non-insulin-dependent diabetes mellitus. *N Engl J Med* **333**:550-554.
- Suter M, Riek U, Tuerk R, Schlattner U, Wallimann T and Neumann D (2006) Dissecting the role of 5'-AMP for allosteric stimulation, activation, and deactivation of AMP-activated protein kinase. *J Biol Chem* **281**:32207-32216.
- Tamai I, Nakanishi T, Kobayashi D, China K, Kosugi Y, Nezu J, Sai Y and Tsuji A (2004) Involvement of OCTN1 (SLC22A4) in pH-dependent transport of organic cations. *Mol Pharm* **1**:57-66.
- Tamai I, Ohashi R, Nezu J, Yabuuchi H, Oku A, Shimane M, Sai Y and Tsuji A (1998) Molecular and functional identification of sodium ion-dependent, high affinity human carnitine transporter OCTN2. *J Biol Chem* **273**:20378-20382.
- Tamai I, Yabuuchi H, Nezu J, Sai Y, Oku A, Shimane M and Tsuji A (1997) Cloning and characterization of a novel human pH-dependent organic cation transporter, OCTN1. *FEBS Lett* **419**:107-111.
- Tanihara Y, Masuda S, Sato T, Katsura T, Ogawa O and Inui K (2007) Substrate specificity of MATE1 and MATE2-K, human multidrug and toxin extrusions/H(+)-organic cation antiporters. *Biochem Pharmacol* **74**:359-371.

- Towler MC and Hardie DG (2007) AMP-activated protein kinase in metabolic control and insulin signaling. *Circ Res* **100**:328-341.
- Toyama K, Yonezawa A, Tsuda M, Masuda S, Yano I, Terada T, Osawa R, Katsura T, Hosokawa M, Fujimoto S, Inagaki N and Inui K (2010) Heterozygous variants of multidrug and toxin extrusions (MATE1 and MATE2-K) have little influence on the disposition of metformin in diabetic patients. *Pharmacogenet Genomics* **20**:135-138.
- Tsuda M, Terada T, Mizuno T, Katsura T, Shimakura J and Inui K (2009a) Targeted disruption of the multidrug and toxin extrusion 1 (mate1) gene in mice reduces renal secretion of metformin. *Mol Pharmacol* **75**:1280-1286.
- Tsuda M, Terada T, Ueba M, Sato T, Masuda S, Katsura T and Inui K (2009b) Involvement of human multidrug and toxin extrusion 1 in the drug interaction between cimetidine and metformin in renal epithelial cells. *J Pharmacol Exp Ther* **329**:185-191.
- Tsukamoto T and Nigam SK (1997) Tight junction proteins form large complexes and associate with the cytoskeleton in an ATP depletion model for reversible junction assembly. *J Biol Chem* **272**:16133-16139.
- Tucker GT, Casay C, Phillips PJ, Connor H, Ward JD and Woods HF (1981) Metformin kinetics in healthy subjects and in patients with diabetes mellitus. *J Clin. Pharmac.* **12**:235-246.
- Tuthill A, McKenna MJ, O'Shea D and McKenna TJ (2008) Weight changes in type 2 diabetes and the impact of gender. *Diabetes Obes Metab* **10**:726-732.
- Tzvetkov MV, Vormfelde SV, Balen D, Meineke I, Schmidt T, Sehr D, Sabolic I, Koepsell H and Brockmoller J (2009) The effects of genetic polymorphisms in the organic cation transporters OCT1, OCT2, and OCT3 on the renal clearance of metformin. *Clin Pharmacol Ther* **86**:299-306.
- UKPDS (1998) Effect of intensive blood-glucose control with metformin on complications in overweight patients with type 2 diabetes (UKPDS 34). UK Prospective Diabetes Study (UKPDS) Group. *Lancet* **352**:854-865.
- Van Itallie C, Rahner C and Anderson JM (2001) Regulated expression of claudin-4 decreases paracellular conductance through a selective decrease in sodium permeability. *J Clin Invest* **107**:1319-1327.
- Van Itallie CM and Anderson JM (2004) The molecular physiology of tight junction pores. *Physiology (Bethesda)* **19**:331-338.
- Van Itallie CM and Anderson JM (2006) Claudins and epithelial paracellular transport. *Annu Rev Physiol* **68**:403-429.
- Van Itallie CM, Holmes J, Bridges A, Gookin JL, Coccaro MR, Proctor W, Colegio OR and Anderson JM (2008) The density of small tight junction pores varies among cell types and is increased by expression of claudin-2. *J Cell Sci* **121**:298-305.

- van Meer G and Simons K (1986) The function of tight junctions in maintaining differences in lipid composition between the apical and the basolateral cell surface domains of MDCK cells. *Embo J* **5**:1455-1464.
- Verhaagh S, Schweifer N, Barlow DP and Zwart R (1999) Cloning of the mouse and human solute carrier 22a3 (Slc22a3/SLC22A3) identifies a conserved cluster of three organic cation transporters on mouse chromosome 17 and human 6q26-q27. *Genomics* **55**:209-218.
- Vidon N, Chaussade S, Noel M, Franchisseur C, Huchet B and Bernier JJ (1988) Metformin in the digestive tract. *Diabetes Res Clin Pract* **4**:223-229.
- Walker J, Jijon HB, Diaz H, Salehi P, Churchill T and Madsen KL (2005) 5-aminoimidazole-4-carboxamide riboside (AICAR) enhances GLUT2-dependent jejunal glucose transport: a possible role for AMPK. *Biochem J* **385**:485-491.
- Wang DS, Jonker JW, Kato Y, Kusuhara H, Schinkel AH and Sugiyama Y (2002) Involvement of organic cation transporter 1 in hepatic and intestinal distribution of metformin. *J Pharmacol Exp Ther* **302**:510-515.
- Wang DS, Kusuhara H, Kato Y, Jonker JW, Schinkel AH and Sugiyama Y (2003) Involvement of organic cation transporter 1 in the lactic acidosis caused by metformin. *Mol Pharmacol* **63**:844-848.
- Wang ZJ, Yin OQ, Tomlinson B and Chow MS (2008) OCT2 polymorphisms and in-vivo renal functional consequence: studies with metformin and cimetidine. *Pharmacogenet Genomics* **18**:637-645.
- Warram JH, Martin BC, Krolewski AS, Soeldner JS and Kahn CR (1990) Slow glucose removal rate and hyperinsulinemia precede the development of type II diabetes in the offspring of diabetic parents. *Ann Intern Med* **113**:909-915.
- Watanabe K, Sawano T, Terada K, Endo T, Sakata M and Sato J (2002) Studies on intestinal absorption of sulpiride (1): carrier-mediated uptake of sulpiride in the human intestinal cell line Caco-2. *Biol Pharm Bull* **25**:885-890.
- Watson CJ, Rowland M and Warhurst G (2001) Functional modeling of tight junctions in intestinal cell monolayers using polyethylene glycol oligomers. *Am J Physiol Cell Physiol* **281**:C388-397.
- Werner EA and Bell J (1921) The preparation of methylguanidine, and of  $\beta\beta$ -dimethylguanidine by the interaction of dicyanodiamide, and methylammonium and dimethylammonium chlorides respectively. *J Chem Soc, Transactions* **121**:1790-1795.
- Wilcock C and Bailey CJ (1990) Sites of metformin-stimulated glucose metabolism. *Biochem Pharmacol* **39**:1831-1834.

- Wilcock C and Bailey CJ (1991) Reconsideration of inhibitory effect of metformin on intestinal glucose absorption. *J Pharm Pharmacol* **43**:120-121.
- Wilcock C and Bailey CJ (1994) Accumulation of metformin by tissues of the normal and diabetic mouse. *Xenobiotica* **24**:49-57.
- Wilcock C, Wyre ND and Bailey CJ (1991) Subcellular distribution of metformin in rat liver. *J Pharm Pharmacol* **43**:442-444.
- Woods A, Johnstone SR, Dickerson K, Leiper FC, Fryer LG, Neumann D, Schlattner U, Wallimann T, Carlson M and Carling D (2003) LKB1 is the upstream kinase in the AMP-activated protein kinase cascade. *Curr Biol* **13**:2004-2008.
- Wu X, George RL, Huang W, Wang H, Conway SJ, Leibach FH and Ganapathy V (2000a) Structural and functional characteristics and tissue distribution pattern of rat OCTN1, an organic cation transporter, cloned from placenta. *Biochim Biophys Acta* **1466**:315-327.
- Wu X, Huang W, Ganapathy ME, Wang H, Kekuda R, Conway SJ, Leibach FH and Ganapathy V (2000b) Structure, function, and regional distribution of the organic cation transporter OCT3 in the kidney. *Am J Physiol Renal Physiol* **279**:F449-458.
- Wu X, Huang W, Prasad PD, Seth P, Rajan DP, Leibach FH, Chen J, Conway SJ and Ganapathy V (1999) Functional characteristics and tissue distribution pattern of organic cation transporter 2 (OCTN2), an organic cation/carnitine transporter. *J Pharmacol Exp Ther* **290**:1482-1492.
- Wulffele MG, Kooy A, de Zeeuw D, Stehouwer CD and Gansevoort RT (2004) The effect of metformin on blood pressure, plasma cholesterol and triglycerides in type 2 diabetes mellitus: a systematic review. *J Intern Med* **256**:1-14.
- Xia L, Engel K, Zhou M and Wang J (2007) Membrane localization and pH-dependent transport of a newly cloned organic cation transporter (PMAT) in kidney cells. *Am J Physiol Renal Physiol* **292**:F682-690.
- Xia L, Zhou M, Kalhorn TF, Ho HT and Wang J (2009) Podocyte-specific expression of organic cation transporter PMAT: implication in puromycin aminonucleoside nephrotoxicity. *Am J Physiol Renal Physiol* **296**:F1307-1313.
- Yabuuchi H, Tamai I, Nezu J, Sakamoto K, Oku A, Shimane M, Sai Y and Tsuji A (1999) Novel membrane transporter OCTN1 mediates multispecific, bidirectional, and pH-dependent transport of organic cations. *J Pharmacol Exp Ther* **289**:768-773.
- Yamagata K, Daitoku H, Shimamoto Y, Matsuzaki H, Hirota K, Ishida J and Fukamizu A (2004) Bile acids regulate gluconeogenic gene expression via small heterodimer partner-mediated repression of hepatocyte nuclear factor 4 and Foxo1. *J Biol Chem* **279**:23158-23165.

- Yin OQ, Tomlinson B and Chow MS (2006) Variability in renal clearance of substrates for renal transporters in chinese subjects. *J Clin Pharmacol* **46**:157-163.
- Yu AS, Cheng MH, Angelow S, Gunzel D, Kanzawa SA, Schneeberger EE, Fromm M and Coalson RD (2009) Molecular basis for cation selectivity in claudin-2-based paracellular pores: identification of an electrostatic interaction site. *J Gen Physiol* **133**:111-127.
- Yu AS, Enck AH, Lencer WI and Schneeberger EE (2003) Claudin-8 expression in Madin-Darby canine kidney cells augments the paracellular barrier to cation permeation. *J Biol Chem* **278**:17350-17359.
- Zhang L, Dresser MJ, Gray AT, Yost SC, Terashita S and Giacomini KM (1997) Cloning and functional expression of a human liver organic cation transporter. *Mol Pharmacol* **51**:913-921.
- Zheng D, MacLean PS, Pohnert SC, Knight JB, Olson AL, Winder WW and Dohm GL (2001) Regulation of muscle GLUT-4 transcription by AMP-activated protein kinase. *J Appl Physiol* **91**:1073-1083.
- Zhou G, Myers R, Li Y, Chen Y, Shen X, Fenyk-Melody J, Wu M, Ventre J, Doebber T, Fujii N, Musi N, Hirshman MF, Goodyear LJ and Moller DE (2001) Role of AMP-activated protein kinase in mechanism of metformin action. *J Clin Invest* **108**:1167-1174.
- Zhou M, Xia L and Wang J (2007) Metformin transport by a newly cloned proton-stimulated organic cation transporter (plasma membrane monoamine transporter) expressed in human intestine. *Drug Metab Dispos* **35**:1956-1962.
- Zou MH, Hou XY, Shi CM, Kirkpatrick S, Liu F, Goldman MH and Cohen RA (2003) Activation of 5'-AMP-activated kinase is mediated through c-Src and phosphoinositide 3-kinase activity during hypoxia-reoxygenation of bovine aortic endothelial cells. Role of peroxynitrite. *J Biol Chem* **278**:34003-34010.
- Zou MH, Kirkpatrick SS, Davis BJ, Nelson JS, Wiles WG, Schlattner U, Neumann D, Brownlee M, Freeman MB and Goldman MH (2004) Activation of the AMP-activated protein kinase by the anti-diabetic drug metformin in vivo. Role of mitochondrial reactive nitrogen species. *J Biol Chem* **279**:43940-43951.

## **CHAPTER 2**

### **MECHANISMS UNDERLYING SATURABLE INTESTINAL ABSORPTION OF METFORMIN**

This chapter was published in *Drug Metabolism and Disposition* **36**(8):1650–1658, 2008.

Reprinted with permission of the American Society for Pharmacology and Experimental Therapeutics. All rights reserved.

Copyright © 2008 by The American Society for Pharmacology and Experimental Therapeutics

## 2.A. ABSTRACT

The purpose of the study was to elucidate mechanisms of metformin absorptive transport to explain the dose-dependent absorption observed in humans. Apical (AP) and basolateral (BL) uptake and efflux as well as AP to BL (absorptive) transport across Caco-2 cell monolayers were evaluated over a range of concentrations. Transport was concentration-dependent and consisted of saturable and nonsaturable components ( $K_m \sim 0.05$  mM,  $J_{\max} \sim 1.0$  pmol min<sup>-1</sup> cm<sup>-2</sup>, and  $K_{d, \text{transport}} \sim 10$  nL min<sup>-1</sup> cm<sup>-2</sup>). AP uptake data also supported the presence of saturable and nonsaturable components ( $K_m \sim 0.9$  mM,  $V_{\max} \sim 330$  pmol min<sup>-1</sup> mg protein<sup>-1</sup>, and  $K_{d, \text{uptake}} \sim 0.04$  μL min<sup>-1</sup> mg protein<sup>-1</sup>). BL efflux was rate-limiting to transcellular transport of metformin; AP efflux was 7-fold greater than BL efflux and was not inhibited by [N-(4-[2-(1,2,3,4-tetrahydro-6,7-dimethoxy-2-isoquinolinyl)ethyl]-phenyl)-9,10-dihydro-5-methoxy-9-oxo-4-acridine carboxamide], a P-glycoprotein inhibitor. AP efflux was *trans*-stimulated by metformin and prototypical substrates of organic cation transporters, suggesting that a cation-specific bidirectional transport mechanism mediated the AP efflux of metformin. BL efflux of intracellular metformin was much less efficient in comparison with the overall transport, with BL efflux clearance accounting for ~7% and ~13% of the overall transport clearance at 0.05 mM and 10 mM metformin concentrations, respectively. Kinetic modeling of cellular accumulation and transport processes fits the data and supports the finding that transport occurs almost exclusively via the paracellular route (~90%) and that the paracellular transport is saturable. This report provides strong evidence of a saturable mechanism in the paracellular space and provides insight into possible mechanisms for the dose-dependence of metformin absorption *in vivo*.



## 2.B. INTRODUCTION

Metformin is an oral antihyperglycemic agent that has been widely used in the management of non-insulin-dependent diabetes mellitus. The oral bioavailability of metformin ranges between 40% and 60%; it is primarily excreted unchanged in the urine, with negligible metabolism (Tucker et al., 1981; Scheen, 1996); approximately 20-30% of the dose is recovered in the feces unchanged (Tucker et al., 1981; Vidon et al., 1988). The oral absorption of metformin is high considering its hydrophilic nature (e.g. calculated log D -6.13 at pH 7) (Saitoh et al., 2004) and net positive charge at intestinal pH values (pKa 12.4) (Figure 2.1). It is believed to be predominantly absorbed in the upper part of the intestine, and estimated time for its complete absorption is approximately 6 h (Tucker et al., 1981; Scheen, 1996). The elimination half-life after oral administration of metformin is more likely a reflection of the rate of absorption than true elimination of the drug (Tucker et al., 1981). In other words, metformin exhibits flip-flop kinetics where the slow absorption of metformin is the rate-limiting factor in its disposition.

Clinical trials with metformin have demonstrated decreased bioavailability at higher doses, suggesting saturable intestinal absorption (Noel, 1979; Tucker et al., 1981; Sambol et al., 1996; Scheen, 1996). When metformin was co-administered orally with the histamine H<sub>2</sub>-receptor antagonist cimetidine, metformin plasma concentrations were increased and renal tubular secretion was decreased, implying a role of the organic cation transporters in metformin elimination (Somogyi et al., 1987). However, in the same study, a significant change in metformin absorption due to cimetidine co-administration was not observed, as determined by total urinary recovery of metformin, suggesting no

interactions associated with their intestinal absorption. Recent work with single-pass intestinal perfusion in rats with metformin showed that permeability in the duodenum was concentration-dependent, suggesting the involvement of a carrier-mediated saturable mechanism (Song et al., 2006). Conversely, another study concluded that there was a dose-independent linear absorption of metformin in rats (Choi et al., 2006), although the doses used in this study were high (50-200 mg/kg), thus potentially saturating any carrier-mediated absorption over the dose range examined. It is clear that the mechanisms responsible for the dose-dependent absorption of metformin in humans need to be better understood.

Metformin is a substrate for organic cation transporters (OCTs) in both the kidney (OCT2) (Kimura et al., 2005a; Kimura et al., 2005b; Terada et al., 2006) and the liver (OCT1) (Wang et al., 2002; Kimura et al., 2005a). Oct1 also was implicated in the intestinal secretion of metformin following IV administration in mice (Wang et al., 2002). Detectable message levels for hOCT1, hOCT2, hOCT3, hOCTN1, and hOCTN2 have been found in human intestinal tissue (Ming et al., 2005; Muller et al., 2005; Englund et al., 2006; Seithel et al., 2006). In addition, metformin has been identified as a substrate for the multidrug and toxin extrusion (MATE) antiporters, MATE1 and MATE2-K (Masuda et al., 2006; Terada et al., 2006; Tsuda et al., 2007). Although MATE2-K, a kidney specific isoform, is believed to be involved in metformin elimination (Masuda et al., 2006), the role of MATE antiporters on metformin absorption is unknown. Metformin is also a substrate for the newly identified proton-coupled transporter, the plasma-membrane monoamine transporter (PMAT), that has been

localized on the apical membrane of human epithelial cells and may facilitate metformin absorption (Zhou et al., 2007).

The present study was undertaken to elucidate the transport mechanisms involved in the intestinal absorption of metformin. The approach used was similar to the one used to recently elucidate the absorptive mechanism of another hydrophilic cation, ranitidine (Bourdet et al., 2006). The current studies reveal a complex transport mechanism that involves the interaction of metformin with AP uptake and efflux transporters and also a paracellular transport mechanism. The postulated mechanism(s) of metformin transport helps to explain the saturable, dose-dependent absorption of metformin observed in humans.

## 2.C. METHODS

### Materials

The Caco-2 cell line was obtained from ATCC (Manassas, VA, USA). Eagle's minimum essential medium (EMEM) with Earle's salts and L-glutamate, nonessential amino acids (NEAA, 100x), and penicillin-streptomycin-amphotericin B solution (100x), fetal bovine serum (FBS), and HEPES (1M) were obtained from Invitrogen Corporation (Carlsbad, CA, USA). Hank's balanced salt solution (HBSS) with calcium and magnesium was purchased from Mediatech Inc. (Hendon, VA, USA). Metformin, quinidine, 1-methyl-4-phenyl pyridinium (MPP), tetraethylammonium bromide (TEA), Triton-X100, and D-(+) glucose were purchased from Sigma Chemical Co. (St. Louis, MO, USA). [N-(4-[2-(1,2,3,4-tetrahydro-6,7-dimethoxy-2-isoquinoliny)ethyl]-phenyl)-9,10-dihydro-5-methoxy-9-oxo-4-acridine carboxamide] (GW918) was a gift from GlaxoSmithKline (Research Triangle Park, NC, USA). [ $^{14}\text{C}$ ]Metformin (54  $\mu\text{Ci}/\mu\text{mol}$ ) and [ $^{14}\text{C}$ ]Mannitol (53  $\mu\text{Ci}/\mu\text{mol}$ ) were purchased from Moravek Biochemicals and Radiochemicals (Brea, CA, USA) and were determined to be  $\geq 96\%$  pure by the manufacturer.

### Cell Culture

Caco-2 cells were cultured at 37°C in EMEM with 10% FBS, 1% NEAA, and 100 U/ml penicillin, 100  $\mu\text{g}/\text{mL}$  streptomycin, and 0.25  $\mu\text{g}/\text{mL}$  amphotericin B in an atmosphere of 5%  $\text{CO}_2$  and 90% relative humidity. The cells were passaged following 90% confluency using trypsin-EDTA, and plated at a 1:5 ratio in 75- $\text{cm}^2$  T flasks. The cells (passage numbers 25 to 40) were seeded at a density of 60,000 cells/ $\text{cm}^2$  on polycarbonate membranes of Transwells™ (12 mm i.d., 0.4  $\mu\text{m}$  pore size, 1  $\text{cm}^2$ , Costar,

Cambridge, MA, USA). Medium was changed the day following seeding and every other day thereafter (AP volume 0.4 mL, BL volume 1.5 mL). The Caco-2 cell monolayers were used 21-28 days post seeding. Transepithelial electrical resistance (TEER) was measured to ensure monolayer integrity. Measurements were obtained using an EVOM Epithelial Tissue Voltohmmeter and an Endohm-12 electrode (World Precision Instruments, Sarasota, FL, USA). Cell monolayers with TEER values greater than 300  $\Omega \cdot \text{cm}^2$  were used in transport experiments.

### **Transport Studies**

Transport studies involved only AP to BL (absorptive) direction, and were conducted as described previously with minor deviations (Bourdet and Thakker, 2006). Cell monolayers were preincubated with transport buffer solution (HBSS with 25 mM D-glucose and 10 mM HEPES), pH 7.2) for 30 min at 37°C. The buffer in the donor (AP) compartment was replaced with 0.4 mL of transport buffer containing various concentrations of [ $^{14}\text{C}$ ]metformin with or without 0.2 mM quinidine for absorptive transport. The pH in both AP and BL compartments was maintained at 7.2 for all transport studies. Appearance of metformin in the receiver (BL) compartment was monitored as a function of time in the linear region of transport and under sink conditions. For experiments examining the role of cation selective transport, cell monolayers were preincubated in the absence or presence of quinidine (0.2 mM) in the AP compartment for 30 min prior to initiating the transport study. For experiments examining the role of cation selective uptake, cell monolayers were preincubated in the absence or presence of quinidine (0.2 mM) in the AP compartment for 30 min. At the conclusion of the experiment, cellular accumulation was determined following washing

with 4°C transport buffer three times in each compartment. After this, the cell monolayers were allowed to dry, excised from the insert, and placed in 300 µL of 1% Triton-X100 for 3 hours, while shaking. The solution was then centrifuged at 10,000 rpm for 10 min and the supernatant was analyzed. [<sup>14</sup>C]Metformin in the receiver compartment and in the cellular compartment was measured using liquid scintillation counting (1600 TR Liquid Scintillation Analyzer, Packard Instrument Company, Downers Grove, IL, USA). Protein content was determined by the BCA protein assay (Pierce, Rockford, IL, USA) with bovine serum albumin as a standard. TEER was measured prior to and following transport experiments to ensure monolayer integrity throughout the experiment and to monitor the effects of metformin and other compounds on the monolayer integrity. Cell monolayers with TEER  $\leq 300 \Omega \cdot \text{cm}^2$  were discarded. Effect of metformin on the cell monolayers was also assessed by measuring [<sup>14</sup>C]mannitol transport in the presence and absence of varying concentrations of unlabeled metformin in the AP donor compartment.

### **Uptake Kinetics**

All uptake studies were conducted using methods previously reported with minor deviations (Bourdet and Thakker, 2006). Caco-2 cell monolayers were preincubated for 30 min in transport buffer. Experiments were initiated by replacing the donor compartment buffer (0.4 ml for AP and 1.5 ml for BL) with transport buffer containing various concentrations of [<sup>14</sup>C]metformin. AP and BL uptake was determined over 5 and 30 min (the linear uptake region), respectively. The pH in both AP and BL compartments was 7.2 for all uptake experiments. Cell monolayers were washed three

times with 4°C transport buffer and metformin cellular accumulation and protein content was measured as described under “Transport Studies”.

### **Efflux Studies:**

Cell monolayers were preincubated in transport buffer at 37°C for 30 min, after which they were preloaded from the AP side for 60 min with 0.5 mM [<sup>14</sup>C]metformin. The cells were then washed three times with 4°C transport buffer, placed in contact with the 37°C transport buffer in the AP and BL compartments, and the amount of metformin appearing in each compartment was determined at the indicated time points. To assess the effects of P-gp, transport buffer with GW918 (1 µM), a potent P-gp and BCRP inhibitor, was added to each compartment during the preloading and efflux experiments. To evaluate *trans*-stimulation/inhibition by other cationic compounds, transport buffer containing metformin (5 mM), MPP (0.05 mM), TEA (10 mM), or quinidine (0.2 mM) was added to the AP or BL compartment prior to the measurement of efflux. All efflux experiments were conducted in buffer at pH 7.2. The appearance of [<sup>14</sup>C]metformin in the AP and BL compartments was monitored as a function of time, and efflux clearance was determined in the linear range of efflux. For all efflux studies, cellular accumulation following pre-loading for 60 min was determined at the commencement of each experiment to serve as the starting intracellular concentrations (C<sub>o</sub>) of metformin for efflux rate constant and clearance calculations.

### **Data Analysis**

Transport of metformin is expressed in terms of apparent permeability (P<sub>app</sub>) and is described by the following equation:

$$P_{app} = \frac{dX/dt}{(A * C_o)} \quad (1)$$

where  $dX/dt$  is the mass of metformin ( $X$ ) transported over time ( $t$ ),  $A$  is the surface area of the Transwell™ porous membrane insert, and  $C_o$  is the initial concentration in the donor compartment. Similarly, transport can be expressed as flux and is described by the following equation:

$$J = \frac{dX/dt}{A} \quad (2)$$

Kinetic constants ( $J_{\max}$ ,  $K_m$ ,  $K_{d, \text{transport}}$ ) were obtained for transport data by fitting a model incorporating one saturable and one nonsaturable component to metformin transport using the following equation (Eq. (3A)):

$$J = \frac{(J_{\max} * C)}{(K_m + C)} + K_{d, \text{transport}} * C \quad (3A)$$

where  $C$  is the metformin concentration,  $J_{\max}$  is the maximal flux,  $K_m$  is the Michaelis-Menten constant, and  $K_{d, \text{transport}}$  is the nonsaturable component of transport.

Uptake data were fit to a model describing one saturable and one nonsaturable component (Eq. (3B))

$$\text{Uptake Rate} = \frac{(V_{\max} * C)}{(K_m + C)} + K_{d, \text{uptake}} * C \quad (3B)$$

where  $C$  is the metformin concentration,  $V_{\max}$  is the maximal velocity,  $K_m$  is the Michaelis-Menten constant, and  $K_{d, \text{uptake}}$  is the nonsaturable component of uptake.

Clearance (CL) values for efflux across both membrane barriers (e.g. AP and BL) and transport of metformin from the AP to BL compartment were calculated using Eq. (4):

$$CL = \frac{dX/dt}{C_o} \quad (4)$$



where  $dX/dt$  represents the mass of metformin ( $X$ ) effluxed or transported over time ( $t$ ) in the linear region of efflux and transport and  $C_o$  is the estimated initial intracellular concentration or donor concentration of metformin during efflux and transport experiments, respectively. In all instances, clearance values were calculated from experiments with 1 cm<sup>2</sup> Transwell™ surface area. Initial intracellular concentrations were calculated using the amount loaded following initial preloading into the Caco-2 cells and cellular volume of 3.66 µL mg protein<sup>-1</sup> (Blais et al., 1987; Dantzig and Bergin, 1990) or 0.732 µL for 1 cm<sup>2</sup> Transwell™ insert with average protein content 0.2 mg. *Trans*-stimulation/inhibition values were reported as % control values of their efflux clearance in the linear range of efflux at 15 min.

### Mathematical Model

A compartmental modeling approach was implemented to examine the accumulation and transport of metformin in Caco-2 cells as described previously (Bourdet et al., 2006). The three-compartment model structure can be seen in Figure 2.2. Differential equations describing the transfer of mass between compartments of the model in Figure 2.2 are:

$$\frac{dX_1}{dt} = -(k_{12} + k_{13}) * X_1 + k_{21} * X_2 \quad (5)$$

$$\frac{dX_2}{dt} = k_{12} * X_1 - (k_{21} + k_{23}) * X_2 + k_{32} * X_3 \quad (6)$$

$$\frac{dX_3}{dt} = k_{23} * X_2 + k_{13} * X_1 - k_{32} * X_3 \quad (7)$$

where  $X_1$ ,  $X_2$ , and  $X_3$  represent the mass of drug in the AP, cellular, and BL compartments, respectively. First-order rate constants (min<sup>-1</sup>) signify parameters associated with AP uptake ( $k_{12}$ ), AP efflux ( $k_{21}$ ), BL uptake ( $k_{32}$ ), BL efflux ( $k_{23}$ ), and

paracellular transport ( $k_{13}$ ). Reverse paracellular flux ( $k_{31}$ ) was omitted from the model due to the large AP to BL concentration gradient and the assumptions of sink conditions. Parameter estimates were obtained by simultaneously modeling cellular accumulation and transport of metformin using nonlinear least-squares regression (WinNonlin, Pharsight, Mountain View, CA, USA). A weighting scheme of  $1/Y$  and the Gauss-Newton minimization method were used for each modeling exercise. Parameter estimates for BL efflux ( $k_{23}$ ) and BL uptake ( $k_{32}$ ) were fixed during modeling using experimentally derived values to allow for more accurate estimation of the remaining parameters. BL efflux ( $k_{23}$ ) was calculated from the following equation:

$$k_{23} = \frac{dX/dt}{X_0} \quad (8)$$

where  $X$  is the mass of metformin effluxed into the BL compartment as a function of time ( $t$ ) and  $X_0$  is the initial mass following preloading of the cells. AP and BL uptake rate constants were calculated using the equation for uptake rate in terms of the experimentally derived kinetic parameters reported previously (Bourdet et al., 2006). The rate constants ( $k_{12}$  and  $k_{32}$ ) were calculated by using the kinetic parameters ( $V_{\max}$ ,  $K_m$ , and  $K_d$ , uptake) associated with AP and BL uptake. The initial rate of uptake into the cellular compartment (e.g.  $X_2$ ) is described by the following equation:

$$\frac{dX_2}{dt_{\text{initial}}} = k_{12(\text{or } 32)} * X_{1(\text{or } 3)} \quad (9)$$

where  $dX_2/dt_{\text{initial}}$  is the initial rate of uptake of metformin mass ( $X$ ) into the cell. The initial rate of metformin uptake rate also can be described by a model containing one saturable and one nonsaturable component, Eq. (3B). By expressing metformin

concentration in terms of mass ( $X$ ) divided by the donor compartment volume ( $V_{AP}$  (or BL)), the initial uptake rate is represented in the following equation as:

$$\frac{dX_2}{dt_{initial}} = \frac{V_{max} * X_{1(or 3)}}{K_m * V_{AP(or BL)} + X_{1(or 3)}} + \frac{K_{d,uptake} * X_{1(or 3)}}{V_{AP(or BL)}} \quad (10)$$

where  $V_{max}$  is the maximal velocity,  $K_m$  is the Michaelis-Menten constant,  $K_{d, uptake}$  is the nonsaturable component of uptake, and  $V_{AP}$  (or BL) is the volume of the donor compartment. Substitution of Eq. (10) into Eq. (9) enables calculation of the rate constant from the experimentally determined kinetic parameters as follows:

$$k_{12 (or 32)} = \frac{V_{max}}{(K_m * V_{AP(or BL)} + X_{1(or 3)})} + \frac{K_{d,uptake}}{V_{AP(or BL)}} \quad (11)$$

where  $V_{max}$  values and  $K_d$  values were multiplied by the average protein content of the monolayers (0.20 mg protein on a 1 cm<sup>2</sup> Transwell™ insert) to remove the dependency of protein content from the uptake rate constants. All data are expressed as mean  $\pm$  SD from three measurements. Statistical significance was evaluated using unpaired  $t$  tests. Validation of the model and goodness of fit were assessed by the %CV values for each parameter estimate, parameter sensitivity, and correlation matrices.

### **Simulation of Transcellular and Paracellular Transport**

The transcellular and paracellular contributions to transport of metformin were determined by implementing parameter estimates from the modeling exercises and simulating the appearance of metformin in the receiver (BL) compartment using subsets of the differential equations, Eq. (5-7), containing rate constants that describe solely transcellular and paracellular transport. The equations for the simulations were:

Paracellular:

$$dX_1/dt = -k_{13} * X_1 \quad (12)$$

$$dX_3/dt = k_{13} * X_1 \quad (13)$$

Transcellular:

$$dX_1/dt = -k_{12} * X_1 + k_{21} * X_2 \quad (14)$$

$$dX_2/dt = k_{12} * X_1 - (k_{21} + k_{23}) * X_2 + k_{32} * X_3 \quad (15)$$

$$dX_3/dt = k_{23} * X_2 - k_{32} * X_3 \quad (16)$$

## 2.D. RESULTS

### Absorptive Transport and Apical Cellular Uptake of Metformin as a Function of Concentration in Caco-2 Cell Monolayers

The absorptive transport across Caco-2 monolayers of metformin and its AP uptake as a function of concentration are shown in Figure 2.3. For clarity, absorptive transport (subsequently referred to as “transport”) refers to movement of drug from the AP compartment across the cell monolayer and into the BL compartment. Uptake and efflux will refer to movement of drug across only one membrane barrier (AP or BL). Metformin transport was linear up to 90 min with less than 1% of metformin transported at all concentrations. The apparent permeability ( $P_{app}$ ) decreased from  $4.7 \pm 0.2 \text{ nm sec}^{-1}$  at  $10 \mu\text{M}$  to  $2.1 \pm 0.3 \text{ nm sec}^{-1}$  at  $5 \text{ mM}$ , providing evidence for saturable transport of metformin across Caco-2 monolayers (Figure 2.3A, left axis). The transport, in terms of flux ( $J$ ), was modeled as a function of metformin donor concentration (Figure 2.3A, right axis). The transport vs. concentration data were best fit to a model containing one saturable and one nonsaturable component (refer to Eq. (3A) in Methods). This model was previously fit to describe the transport of hydrophilic cations, ranitidine and famotidine (Lee and Thakker, 1999). The  $J_{max}$  and apparent  $K_m$  estimated for the transport were  $1.02 \pm 0.46 \text{ pmol min}^{-1} \text{ cm}^{-2}$  and  $0.06 \pm 0.03 \text{ mM}$ , respectively. The nonsaturable transport coefficient,  $K_{d, \text{ transport}}$ , was  $13.4 \pm 0.77 \text{ nL min}^{-1} \text{ cm}^{-2}$ . Comparison of the  $K_{d, \text{ transport}}$  value to the saturable component of transport ( $J_{max} / K_m$ :  $18.5 \text{ nL min}^{-1} \text{ cm}^{-2}$ ) suggests that ~60% of the overall metformin absorptive transport at low concentrations ( $\ll K_m$ ) occurs via a saturable process.

Metformin (0.5 mM) AP uptake was rapid, but failed to reach steady state by 45 minutes (inset of Figure 2.3B). The initial AP uptake rate (determined over 5 min, the linear region of AP uptake) of metformin as a function of concentration was described by a model with one saturable and one nonsaturable component (Figure 2.3B). The  $V_{\max}$  and apparent  $K_m$  estimated for AP metformin uptake were  $331 \pm 68 \text{ pmol min}^{-1} \text{ mg protein}^{-1}$  and  $0.9 \pm 0.2 \text{ mM}$ , respectively (Table 2.1). The nonsaturable component of AP uptake,  $K_{d, \text{uptake}}$ , was estimated to be  $0.036 \pm 0.011 \text{ }\mu\text{L min}^{-1} \text{ mg protein}^{-1}$ . Comparison of the  $K_{d, \text{uptake}}$  value to the saturable component of uptake ( $V_{\max} / K_m$ :  $0.40 \text{ }\mu\text{L min}^{-1} \text{ mg protein}^{-1}$ ) suggests that ~90% of the overall metformin uptake at low concentrations ( $\ll K_m$ ) is via a saturable process (Table 2.1). The data are consistent with a saturable, carrier-mediated AP uptake process for metformin in Caco-2 cells.

Metformin BL uptake into Caco-2 cells was significantly lower than AP uptake, and was linear up to 30 min (data not shown). BL uptake kinetic parameters ( $V_{\max}$  and  $K_m$ ) were obtained from concentration dependence of BL uptake in the linear range of BL uptake (30 min) from 0.01 to 5 mM dosing concentrations (Table 2.1). BL uptake data did not support the incorporation of a term for nonsaturable uptake ( $K_{d, \text{uptake}}$ ), as was observed previously for ranitidine BL uptake (Bourdet and Thakker, 2006). It should be noted however, that the BL uptake studies never fully reach  $V_{\max}$ , therefore model predictions of  $K_m$  may underestimate the true apparent  $K_m$  for BL uptake. We acknowledge this potential deficiency, but due to the significantly high  $K_m$  estimate (~12 mM) this parameter will play little role in the disposition of metformin at concentrations achieved in the BL compartment in the Caco-2 cell system or at physiological

concentrations achieved in the blood. Therefore the kinetic estimates were adequate for calculation of BL uptake rate constant ( $k_{32}$ ) (refer to Eq. (11) in Methods section).

### **AP and BL Efflux of Metformin from Preloaded Cell Monolayers**

A comparison of the AP uptake to transport suggests that the saturable AP uptake clearance is far more efficient than the saturable transport clearance of metformin (Table 2.1), suggesting that BL efflux out of the cell may limit transcellular transport. To investigate the rate of efflux from the cell, appearance of metformin in the AP and BL compartments from cells preloaded with 0.5 mM [ $^{14}\text{C}$ ]metformin was monitored as a function of time over the linear region (up to 90 min) of efflux (Figure 2.4A). Metformin exhibited 7-fold higher AP efflux clearance than the BL efflux clearance, suggesting that the efflux across the AP membrane is assisted by an efflux transporter and that BL efflux is inefficient. The polarity between AP and BL efflux clearance values indicates that the BL membrane is rate limiting to transcellular transport. The AP efflux was not inhibited by 1  $\mu\text{M}$  GW918, a P-glycoprotein (P-gp) inhibitor (Hyafil et al., 1993) (Figure 2.4B), thus ruling out the role of P-gp in the AP efflux of metformin; however, AP efflux was significantly inhibited by quinidine ( $p < 0.001$ ). This result supports previous reports that metformin is not a substrate for P-gp (Song et al., 2006).

*Trans*-stimulation experiments have been conducted previously to determine whether there is a bidirectional carrier-mediated efflux mechanism for other small molecules (Villalobos and Braun, 1998; Mizuuchi et al., 1999; Zhang et al., 1999; Bourdet and Thakker, 2006). Therefore, *trans*-stimulation of metformin efflux by unlabelled metformin and prototypical OCT substrates/inhibitors was examined by measuring the efflux following preloading (0.5 mM [ $^{14}\text{C}$ ]metformin) the Caco-2 cell

monolayers (Figure 2.4B). AP efflux was *trans*-stimulated by unlabeled metformin (5 mM), MPP (0.05 mM), and TEA (10 mM). The presence of quinidine in the AP compartment significantly reduced the AP efflux clearance of [<sup>14</sup>C]metformin from  $10.2 \pm 0.4 \text{ nL min}^{-1}$  (control) to  $1.7 \pm 0.3 \text{ nL min}^{-1}$  (+ 0.2 mM quinidine), abolishing the polarity between AP and BL efflux of metformin (data not shown). In addition, the presence of quinidine trapped  $72.3 \pm 0.8\%$  of the initial intracellular metformin in the cell following the 90 min efflux experiment, in comparison to control (no quinidine) where  $19.9 \pm 2.1\%$  remained (data not shown). The stimulation of [<sup>14</sup>C]metformin AP efflux by unlabeled metformin and prototypical OCT substrates, TEA and MPP, supports the presence of a cation-selective bidirectional transporter in the AP membrane that facilitates metformin uptake and secretion from the cell. BL efflux was not capable of *trans*-stimulation/inhibition by unlabeled metformin, MPP, TEA, or quinidine (Figure 2.4C).

#### **Inefficient Basolateral Efflux Limits Transcellular Transport of Metformin across Caco-2 Cell Monolayers.**

Transcellular transport of hydrophilic cations like metformin requires vectoral transport, comprised of both AP uptake and BL efflux from the cell. In Caco-2 cells, AP uptake of metformin is highly efficient (Table 2.1), while BL efflux appears to be rate limiting to transcellular transport. Therefore, the rate of BL efflux can serve as a surrogate rate of transcellular transport and as an estimate of the relative contribution of this pathway to the overall transport of metformin. Transport (flux) increased from  $1.2 \pm 0.03$  to  $126 \pm 19 \text{ pmol min}^{-1} \text{ cm}^{-2}$  (~100 fold) as donor concentration increased from 0.05 mM to 10 mM (200 fold) (Figure 2.5A). The BL efflux rate increased from  $0.3 \pm 0.03$  to



$7.85 \pm 0.2 \text{ pmol min}^{-1} \text{ cm}^{-2}$  (~26 fold) as the donor concentration increased from 0.05 mM to 10 mM (Figure 2.5A). The ~26 fold increase in BL efflux rate correlated with the increase in estimated intracellular metformin concentration ( $C_o$ ), which increased from  $0.19 \pm 0.02 \text{ mM}$  to  $4.93 \pm 0.19 \text{ mM}$  (~26 fold increase) as the loading concentration increased from 0.05 to 10 mM (inset of Figure 2.5B). The BL efflux rates for 0.05 and 10 mM loading concentrations could only account for ~25% and ~6% of the overall transport, respectively (Figure 2.5A). This result leads to the conclusion that metformin transport must occur predominantly via the paracellular route.

Transport (flux) and BL efflux rates are dependent upon the donor concentration or the initial intracellular concentrations, respectively. Clearance values correct for the driving force concentrations and represent the efficiency of metformin transported from AP to BL compartment during transport or across the BL membrane during BL efflux. Transport and BL efflux clearance values ( $1 \text{ cm}^2$  Transwell™ insert) were determined following 0.05 or 10 mM AP dose or loading dose, respectively (Figure 2.5B). Transport clearance significantly decreased from  $24 \pm 1 \text{ nL min}^{-1}$  to  $13 \pm 2 \text{ nL min}^{-1}$  from 0.05 mM to 10 mM donor concentrations, respectively. This ~50% reduction in transport clearance from low to high concentration was indicative of saturable transport processes. The BL efflux clearance values for 0.05 and 10 mM were not significantly different (Figure 2.5B), although the initial loading concentration ( $C_o$ ) increased ~26 fold (inset of Figure 2.5B). The BL efflux clearance could only account for ~7% and ~13% of the overall transport clearance at 0.05 mM and 10 mM metformin concentrations, respectively. These data suggest that transcellular transport can account for ~10% of the overall transport of metformin across Caco-2 cell monolayers.

## **The Relationship between Absorptive Transport and Cellular Accumulation of Metformin**

The transport and cellular accumulation of metformin from the AP compartment (0.05 mM) as a function of time were evaluated simultaneously in Caco-2 cells in the absence or presence of the cation-selective inhibitor, quinidine (0.2 mM) (Figure 2.6A, D respectively). Cellular accumulation describes the mass of drug accumulated in the cell at a fixed period of time. This value takes into account multiple processes, e.g. uptake and efflux, at both the AP and BL membranes. The cellular accumulation of metformin exceeded the transport throughout the experiment (Figure 2.6A), confirming that the uptake into the cell was not the rate limiting step to transport of metformin. In the presence of quinidine, the cellular accumulation and transport decreased significantly compared to control, and the cellular accumulation failed to exceed the amount of metformin transported (Figure 2.6D).

Kinetic modeling of the transport and cellular accumulation data was performed using the model outlined in Figure 2 with fixed experimentally derived parameters ( $k_{23}$ ) and ( $k_{32}$ ), representing BL efflux rate constant and BL uptake rate constant, respectively. BL efflux rate constant ( $k_{23}$ ) was fixed because BL efflux was linear over the 90 min (Figure 2.4A) and the clearance remained unchanged irrespective of cellular concentrations (Figure 2.5B). BL uptake rate constant ( $k_{32}$ ) was calculated from  $V_{\max}$  and  $K_m$  parameters experimentally derived (Table 2.1), although this rate constant should play a negligible role in metformin disposition due to low concentrations of metformin in the BL compartment, e.g. <1% dose transported after 90 min. When assessing model goodness of fit, the estimate for AP uptake rate constant ( $k_{12}$ ) was highly correlated with

the AP efflux rate constant ( $k_{21}$ ). The correlation of these parameter estimates was not unexpected, for these processes work in opposite directions on the same membrane and affect the disposition of the same adjacent compartments. In addition, the estimated AP uptake rate constant ( $k_{12} = 0.000156 \text{ min}^{-1}$ ) was in good agreement with the experimentally derived and calculated rate constant ( $k_{12} = 0.000199 \text{ min}^{-1}$ ) obtained from  $V_{\text{max}}$ ,  $K_m$ , and  $K_{d, \text{ uptake}}$  values for AP uptake in Eq. (11) (Methods section). The model was highly sensitive to the three iterated parameters: ( $k_{12}$ ), ( $k_{21}$ ), and ( $k_{13}$ ). The paracellular rate constant ( $k_{13}$ ) did not have any correlation with the other two iterated parameters, ( $k_{12}$ ) or ( $k_{21}$ ).

Parameter estimates were generated from simultaneously modeling the cellular accumulation and transport of metformin (0.05 mM) in the presence or absence of the cation transporter inhibitor, quinidine (0.2 mM) (Table 2.2). In the presence of quinidine, the rate constant associated with AP uptake ( $k_{12}$ ) decreased by approximately 90%, which was consistent with the inhibition of carrier-mediated uptake process and subsequent decrease in cellular accumulation of metformin (Table 2.2, Figure 2.6D). Inhibition by quinidine caused a 3 fold decrease in apparent permeability ( $P_{\text{app, total}}$ ) and a 7 fold decrease in cellular accumulation of metformin (Figure 2.6D). The paracellular rate constant ( $k_{13}$ ) decreased by approximately 50% in the presence of quinidine (Table 2.2). The ability of quinidine to decrease both transcellular and paracellular transport of a hydrophilic cation, ranitidine, has been observed previously (Bourdet et al., 2006).

## **Relative Contribution of Transcellular and Paracellular Transport Pathways to Absorptive Transport of Metformin**

The relative contribution of paracellular and transcellular transport to the overall transport of metformin (0.05 mM) were estimated to be 9% and 91%, respectively (Table 2.3); these values were derived based on the parameter estimates obtained from modeling with subsets of the differential equations expressing solely paracellular or transcellular rate constants (Eq. (12-16)) and were consistent with the estimates based on experimental values for transport and BL efflux. Quinidine (0.2 mM) caused a substantial decrease in the permeability ( $P_{app, total}$ ), and there was a good correspondence between the experimental and predicted  $P_{app, total}$  values (Table 2.3). Model predictions showed that the decrease in the permeability was likely due to a decrease in both transcellular permeability ( $P_{app, trans}$ ) and paracellular permeability ( $P_{app, para}$ ). In the presence of quinidine, the predicted relative contributions of transcellular and paracellular transport were estimated to be 3% and 97%, respectively (Table 2.3).

The relative contribution of transcellular and paracellular transport was estimated at three widely separated metformin concentrations: 0.05 mM (near the apparent  $K_m$  for absorptive transport and below apparent  $K_m$  for AP uptake), 0.5 mM (above apparent  $K_m$  for absorptive transport and near the apparent  $K_m$  for AP uptake), and 10 mM (above apparent  $K_m$  for both transport and AP uptake). The  $P_{app, total}$  values for metformin at 0.05, 0.5, and 10 mM were  $5.0 \pm 0.57$ ,  $3.9 \pm 0.56$ , and  $1.4 \pm 0.24$  nm sec<sup>-1</sup>, respectively (Table 2.3), showing a decrease with concentration. Cellular accumulation of metformin did not reach steady state by 90 min at both the 0.05 and 0.5 mM concentrations, while at

the 10 mM metformin concentration steady state concentration in the cell appeared to be achieved at ~90 min (Figure 2.6C).

Kinetic modeling yielded parameter estimates that described the transport and accumulation data (Table 2.2). The model fit to the experimental data is presented in Figure 2.6A-C. The experimental  $P_{app, total}$  was in good agreement with the model predicted  $P_{app, total}$  (Table 2.3). The estimated AP uptake rate constant ( $k_{12}$ ) significantly decreased with increase in metformin donor concentration, which is consistent with a saturable AP uptake mechanism (Table 2.2). The rate constant estimates for paracellular transport ( $k_{13}$ ) decreased with increasing metformin donor concentrations (Table 2.2). For all three concentrations, the majority (~90-95%) of the metformin transport was estimated to be via the paracellular route, with only ~5-10% of the transport through the transcellular mechanism (Table 2.3). Both the predicted  $P_{app, trans}$  and predicted  $P_{app, para}$  decreased significantly with increasing metformin concentration (Table 2.3). The predicted  $P_{app, para}$  decreased from 4.5 to 1.3 nm sec<sup>-1</sup> as concentration increased from 0.05 and 10 mM, an approximately 70% decrease. The permeability of the paracellular marker [<sup>14</sup>C]mannitol did not change significantly from control ( $P_{app}$  5.8 ± 0.7 nm sec<sup>-1</sup>) in the presence of 0.05, 0.5, and 10 mM metformin or in the presence of quinidine (Table 2.3).

## 2.E. DISCUSSION

The transport and AP uptake of metformin in Caco-2 cell monolayers contain saturable components (Figure 2.3A,B). To our knowledge, this is the first report of dose-dependent transport of metformin in a cell-based *in vitro* system. The saturable component did not appear to play a dominant role in the transport of metformin, particularly at high concentrations (Figure 2.3A, right axis), yet there is clear evidence for saturable transport of metformin in the plot of apparent permeability ( $P_{app}$ ) as a function of concentration (Figure 2.3A, left axis). When compared with the low affinity/high capacity AP uptake (apparent  $K_m \sim 0.8$  mM,  $V_{max} \sim 330$  pmol min<sup>-1</sup> mg protein<sup>-1</sup>), the saturable component of transport exhibited distinctly different kinetic behavior (apparent  $K_m \sim 0.05$  mM, derived  $V_{max} \sim 5$  pmol min<sup>-1</sup>mg protein<sup>-1</sup>, see footnote to Table 2.1), and was only 25% as efficient as the apical uptake ( $(V_{max} / K_m)_{AP \text{ to BL Transport}} \sim 0.1$   $\mu\text{L min}^{-1}$  mg protein<sup>-1</sup> vs.  $(V_{max} / K_m)_{AP} \sim 0.4$   $\mu\text{L min}^{-1}$  mg protein<sup>-1</sup>, Table 2.1). This discrepancy between the kinetic parameters for the transport and AP uptake suggests that the dose-dependent transport of metformin was not mediated solely by the AP uptake mechanism and associated transcellular processes.

The AP uptake and cellular accumulation of metformin appeared to reach steady state at 90 min for 10mM donor concentration (Figure 2.6C), but not for 0.05 and 0.5mM donor concentrations (Figure 2.6A,B). The inability to achieve steady-state over 90 min at 0.05 and 0.5 mM was surprising considering that the hydrophilic cation ranitidine (0.5 mM) achieved steady-state cellular concentrations at  $\sim 15$  min (Bourdet and Thakker, 2006). This was likely due to both restricted BL efflux and the presence of an efficient and high capacity bidirectional transport mechanism on the AP membrane.

Both AP uptake and cellular accumulation of metformin were strongly inhibited by quinidine (Figure 2.6D), a potent inhibitor of OCTs (Bourdet et al., 2005; Kimura et al., 2005b), MATE1 (Ohta et al., 2006), and P-gp (Adachi et al., 2001). Further, *trans*-inhibition by quinidine caused over a 5 fold reduction in AP efflux, suggesting that the AP uptake and efflux may be OCT mediated. The AP efflux was subject to *trans*-stimulation by metformin and prototypical cation transporter substrates, TEA and MPP (Figure 2.4B), further supporting the involvement of one or more OCT transporters in AP uptake and efflux. Organic cation transporters on the AP membrane of intestinal epithelium, in particular OCT3, are facilitative transporters that have been shown to transport cations bidirectionally in conjunction with electrochemical gradient or membrane potential (Schneider et al., 2005). Although the exact transporter(s) implicated are not known, these studies provide strong evidence supporting an “OCT-like” bidirectional uptake/efflux transport mechanism on the AP membrane in Caco-2 cells for metformin. To our knowledge, this the first report of metformin AP efflux from an intestinal cell model system.

In comparison to the AP efflux, the BL efflux of metformin was quite inefficient (Figure 2.4A), and appeared to occur via passive diffusion as evidenced by little change in the BL efflux clearance over a wide concentration range (Figure 2.5B). The inefficient BL efflux appeared to be the rate-limiting step for the transcellular transport of metformin, resulting in its accumulation in the cells over the 90 min transport experiments (Fig 6A-C). These results provided an explanation for why transport would be predominantly paracellular although metformin was efficiently taken up into Caco-2 cells.

The results for the transport, uptake, and efflux kinetic experiments revealed that metformin traverses Caco-2 cell monolayers predominantly via a saturable paracellular mechanism. A kinetic modeling approach was employed to estimate the relative contributions of trans- and paracellular transport. The modeling provides a more complete evaluation of the processes associated with transport and is able to estimate the relative contributions of paracellular and transcellular transport for drugs under a variety of experimental conditions (e.g. different concentrations, presence of inhibitors). At 0.05 mM donor concentration, approximately 90% of the metformin transport is estimated to occur via the paracellular route, whereas only approximately 10% would occur via the transcellular pathway (Table 2.3). This was in excellent agreement with experimental transport and efflux data, where ~7% of the transport could be accounted for by BL efflux for 0.05 mM metformin donor concentration (Figure 2.5B).

The kinetic modeling supports the results that suggest that metformin is transported predominantly via the paracellular route. However, it is difficult to reconcile this with the experimental observation that the permeability is concentration-dependent (i.e. transport is saturable) in Caco-2 cells (Figure 2.3A). The apparent permeability values ( $P_{app, total}$ ) of metformin decreased from  $5.0 \pm 0.57 \text{ nm sec}^{-1}$  to  $1.4 \pm 0.24 \text{ nm sec}^{-1}$  from a dose of 0.05 mM to 10 mM, most of which is attributed to a decrease in the paracellular permeability,  $P_{app, para}$  (Table 2.3). The permeability of mannitol, a prototypical paracellular transport marker, remained unchanged in the presence of varying metformin concentrations (Table 2.3). Therefore, the decrease in paracellular permeability is likely due to saturable interactions between metformin and a macromolecule, presumably a protein, in the paracellular space of Caco-2 cell



monolayers, and not due to gross changes in the paracellular space or in the tight junctions. It has been postulated that a saturable paracellular mechanism may be due to a cation-selective saturable mechanism in the paracellular space involving charge-charge interactions (Lee and Thakker, 1999; Bourdet et al., 2006). Further studies are required to elucidate the mechanisms of this saturable paracellular transport mechanism. Anionic amino acid residues of tight junction protein family, claudins, have been shown to confer cationic charge selectivity, i.e.  $\text{Na}^+$  permeability, to the paracellular pathway (Colegio et al., 2002; Van Itallie et al., 2003). It can be postulated that metformin may saturate these anionic sites in the tight junction, restricting its own transport at high concentrations.

The data presented in this study on metformin provide the most convincing evidence for a saturable process in the paracellular space acting on a small molecule. The results further show that metformin is taken up into the cells across the AP membrane via a cation-selective transporter. Once inside the cell, it is effluxed poorly across the BL membrane but much more efficiently across the AP membrane, perhaps via an AP transporter that serves as a cation-exchanger. It has been shown that metformin bioavailability in humans was dose-dependent (Noel, 1979; Tucker et al., 1981; Sambol et al., 1996; Scheen, 1996). In order for transcellular processes to account for the dose-dependent absorption, vectoral transport of metformin must exist, in which both AP and BL transporters are needed to transport the drug from the lumen into the blood. Provided Caco-2 cell monolayers are an appropriate cellular model for intestinal absorption of hydrophilic cationic compounds such as metformin, saturable absorption could not occur via transcellular transport because of inefficient efflux across the BL membrane. Rather, the saturable absorption *in vivo* could occur via the paracellular route which accounted

for ~90% of the transport of metformin across the Caco-2 cell monolayers. Based on these results, a hypothesis is formulated that attempts to relate the transport behavior of metformin in the Caco-2 cell culture model of intestinal epithelium to its likely behavior in human subjects (depicted as the “sponge effect” in Figure 2.7) upon oral administration. It can be speculated that a portion of the metformin dose is sequestered in the enterocytes due to the lack of an efficient BL efflux transporter mechanism. In addition, metformin is prevented from AP efflux due to a higher luminal concentration of the drug that maintains the net flow of drug in the inward direction. Some of the metformin dose is absorbed across the intestinal epithelium via the cation-selective facilitative diffusion in the paracellular space (Figure 2.7A). As the dose passes through the intestine, the luminal concentration decreases below the achievable intracellular concentrations of metformin, and AP efflux occurs via the bidirectional “OCT-like” transport mechanism. The effluxed dose of metformin can be absorbed across the paracellular space via the cation-selective saturable mechanism or taken up back into the enterocytes (Figure 2.7B). At high doses, ( $\geq 850$  mg or  $\geq 20$  mM luminal concentration) the transport mechanisms are saturated and thus a smaller fraction of administered doses would be absorbed via the saturable mechanism. The data presented in this report provide an explanation for why the fraction absorbed for metformin, one of the most widely prescribed drugs on the market, could fall from ~0.9 to ~0.4 as the dose is raised to 2.0 g in humans (Tucker et al., 1981). Further studies to identify the exact mechanism(s) of the saturable paracellular process will lead to better understanding of how metformin and other small hydrophilic cations traverse and navigate through tight junctions and the effects this process has on their disposition. Conceivably, a saturable paracellular

transport mechanism could be contributing to the elimination of metformin and other hydrophilic cations in the kidney and other tight junction containing organs/tissues.

## **LEGENDS FOR FIGURES**

**Figure 2.1. Structure of metformin.**

**Figure 2.2. Schematic representation of the three-compartment model describing the transport of metformin across Caco-2 cell monolayers.** Compartments represent the AP ( $X_1$ ), cellular ( $X_2$ ), and BL ( $X_3$ ) chambers. Rate constants associated with transmembrane movement of drug are denoted as follows: AP uptake ( $k_{12}$ ), AP efflux ( $k_{21}$ ), BL uptake ( $k_{32}$ ), and BL efflux ( $k_{23}$ ). The rate constant ( $k_{13}$ ) is associated with metformin transport in the paracellular space. Reverse paracellular flux ( $k_{31}$ ) was omitted from the model and assumed to be negligible under sink conditions.

**Figure 2.3. Concentration-dependent transport, apparent permeability, and AP uptake of metformin in Caco-2 cells.** The apparent permeability ( $P_{app}$ ) of metformin (●) as a function of donor concentration is shown in Panel A (left axis). The concentration dependence of the transport (AP to BL) (Panel A) and the AP uptake (Panel B) of metformin in Caco-2 cells are shown with the fitted lines for the transport/uptake data (solid), the saturable (dashed), and nonsaturable (dotted) components, respectively. Appearance of metformin (▲) in the BL compartment (A) and uptake into the cell (B) were monitored in the linear time range for transport and AP uptake at 60 min and 5 min, respectively. The time course for AP uptake (0.5 mM donor concentration) can be seen in Figure 2.3B (inset). Data represent mean  $\pm$  SD; n=3.

**Figure 2.4. Efflux of preloaded metformin across the AP and BL membranes of Caco-2 cells.** (A) Time course of metformin efflux into AP (●) and BL (○) compartments. *Trans*-stimulation/inhibition by organic cations of metformin AP efflux (Panel B) and BL efflux (Panel C). The *trans*-stimulation/inhibition experiment was performed after preloading 0.5 mM [ $^{14}$ C]metformin (refer to Methods) by replacing the transport buffer in the AP or BL compartment with a buffer containing GW918 (1  $\mu$ M) (918), metformin (5 mM) (MET), MPP (0.05 mM), TEA (10 mM), or quinidine (0.2 mM) (QND) and monitoring [ $^{14}$ C]metformin appearance in the AP or BL compartments for 15 min. *Trans*-stimulation/inhibition experiments are reported as relative % of the control (CON) value. Data represent mean  $\pm$  SD; n=3. \*p<0.05 compared to control; \*\*p<0.01 compared to control; \*\*\*p<0.001 compared to control.

**Figure 2.5. Relative rates and clearance values of transport (AP-BL) and BL efflux of metformin across Caco-2 cell monolayers.** A. Transport (AP-BL) and BL efflux (BL) rates over 90 min for initial AP donor concentration ( $C_o$ ) of 0.05 mM (black bars, left y-axis) and 10 mM (open bars, right y-axis) metformin. B. Transport clearance and BL efflux clearance values (1 cm<sup>2</sup> Transwell™ inserts) for initial AP donor concentration ( $C_o$ ) of 0.05 mM (black bars) and 10 mM (open bars). Inset depicts the estimated initial cellular concentrations ( $C_o$ ), following 60 min incubation of cells with 0.05 (black bars) and 10 mM (open bars) [ $^{14}$ C]metformin in the AP compartment (refer to Methods section). Data represent mean  $\pm$  SD; n=3. \*\*\*p<0.001 for 0.05 mM compared to 10 mM, “ns” not significantly different between 0.05 mM and 10 mM values.

**Figure 2.6. Concentration dependence of metformin transport and cellular accumulation in Caco-2 cells.** Metformin appearance in the BL compartment (○) and cellular accumulation (●) were monitored as a function of time at dosing concentrations of 0.05 mM (A), 0.5 mM (B), 10 mM (C), and 0.05 mM in the presence of quinidine (0.2 mM) (D). Lines indicate the best fit of the kinetic model (Fig. 2.2) to the metformin BL appearance (dotted) and cellular accumulation (solid) data. Data represent mean  $\pm$  SD; n=3.

**Figure 2.7. Schematic of the proposed “sponge” hypothesis for dose-dependent absorption of metformin.** (A) Metformin dose travels from the proximal to distal regions of the intestine and undergoes predominantly saturable paracellular transport and also saturable AP uptake into the cells. The BL membrane barrier restricts transcellular transport of metformin, sequestering the drug in the cell. (B) As luminal concentration decreases and becomes less than the intracellular concentrations of metformin, AP “OCT” like bidirectional transporter(s) effluxes metformin into the lumen and allows for transport through the paracellular space or re-uptake into the cells.

## TABLES

**Table 2.1. Estimated kinetic parameter for AP uptake, BL uptake, and absorptive (AP to BL) transport of metformin in Caco-2 cells.**

Transport Site/Direction	$V_{\max}$ [pmol min <sup>-1</sup> (mg protein <sup>-1</sup> )]	$K_m$ [mM]	$K_d$ [μL min <sup>-1</sup> (mg protein <sup>-1</sup> )]	$V_{\max} / K_m$ [μL min <sup>-1</sup> (mg protein <sup>-1</sup> )]
AP <sup>a</sup>	331 ± 68	0.9 ± 0.2	0.036 ± 0.011	0.37
BL <sup>b</sup>	619 ± 15	12.3 ± 0.4	n/a <sup>c</sup>	0.05
AP to BL Transport <sup>d</sup>	5.1 ± 0.2	0.06 ± 0.03	0.067 ± 0.004	0.09

<sup>a</sup> Initial AP uptake data (5 min) are presented in Figure 2.2B with model fits used to generate kinetic parameter estimates using nonlinear-least squares regression analysis.

<sup>b</sup> BL uptake kinetic parameters were obtained from concentration dependence of BL uptake in the linear uptake range (30 min) from 0.01 to 5 mM dosing concentrations.

<sup>c</sup> BL uptake data did not support the incorporation of a term for nonsaturable uptake. n/a: not applicable.

<sup>d</sup> AP to BL transport kinetic parameters,  $J_{\max}$  and  $K_{d, \text{transport}}$ , were divided by the average protein content in a Caco-2 monolayer (0.2 mg for 1 cm<sup>2</sup> Transwell™ insert) and  $J_{\max}$  was expressed as the maximal velocity,  $V_{\max}$ , for comparison.

**Table 2.2. Effects of donor concentration and inhibition by quinidine on kinetic parameters for metformin transport and cellular accumulation in Caco-2 cells.**

Parameter	Metformin Donor Concentrations[mM]									
	0.05		0.50		10		0.05 + Quinidine <sup>a</sup>			
	Estimate (min <sup>-1</sup> )	CV%	Estimate (min <sup>-1</sup> )	CV%	Estimate (min <sup>-1</sup> )	CV%	Estimate (min <sup>-1</sup> )	CV%	Estimate (min <sup>-1</sup> )	CV%
$k_{12}$	0.000156	8	0.000114	11	0.000029	13	0.000017	33		
$k_{21}$	0.0119	26	0.0135	31	0.0205	29	0.00919	134		
$k_{23}$	0.00107	N.A <sup>b</sup>	0.00107	N.A <sup>b</sup>	0.00107	N.A <sup>b</sup>	0.00107	N.A <sup>b</sup>		
$k_{32}$	0.00001	N.A <sup>c</sup>	0.00001	N.A <sup>c</sup>	0.00001	N.A <sup>c</sup>	0.00001	N.A <sup>c</sup>		
$k_{13}$	0.000054	4	0.000048	5	0.000015	4	0.000022	6		

Transport and cellular accumulation data were fit simultaneously using the model equations detailed under *Materials and Methods*.

N.A. not applicable

<sup>a</sup> Quinidine [0.2 mM] was added to the AP donor compartment containing metformin [0.05 mM]

<sup>b</sup>  $k_{23}$  was experimentally derived using eq. 8 and fixed.

<sup>c</sup>  $k_{32}$  was experimentally derived using eq. 11 and fixed.



**Table 2.3. Relative contribution of paracellular and transcellular transport to overall transport of metformin as a function of donor concentration in Caco-2 cells.**

Metformin Concentration (mM)	Experimental		Metformin Model Prediction				
	Mannitol $P_{app, total}^a \times 10^{-7}$ (cm s <sup>-1</sup> )	Metformin $P_{app, total}$ (cm s <sup>-1</sup> ) $\times 10^{-7}$	$P_{app, total}^b \times 10^{-7}$ (cm s <sup>-1</sup> )	$P_{app, trans}^c \times 10^{-7}$ (cm s <sup>-1</sup> )	$P_{app, para}^c \times 10^{-7}$ (cm s <sup>-1</sup> )	% Trans <sup>d</sup>	% Para <sup>d</sup>
0.05	5.4 ± 1.7	5.0 ± 0.57	4.9	0.4	4.5	9	91
0.5	5.1 ± 0.9	3.9 ± 0.56	4.3	0.3	4.0	7	93
10	5.4 ± 0.9	1.4 ± 0.24	1.3	0.1	1.3	5	95
0.05 + QND <sup>e</sup>	5.9 ± 1.3	1.7 ± 0.15	1.9	0.1	1.8	3	97
Control	5.8 ± 0.7						

<sup>a</sup> Determined from AP to BL transport of [<sup>14</sup>C]mannitol in the presence of varying concentrations of unlabeled metformin over 90 min transport experiment. Control value equals mannitol flux in the absence of metformin or quinidine. Data represent mean ± SD; n=3.

<sup>b</sup> Determined from the model prediction of total metformin transported as a function of time.

<sup>c</sup> Determined from simulation of amount of metformin transported as a function of time using a subset of the overall kinetic model incorporating solely paracellular or transcellular transport.

<sup>d</sup> Determined from the predicted paracellular or transcellular permeability as a percentage of the total predicted permeability

<sup>e</sup> Metformin (0.05mM) transport and model predictions in the presence of quinidine (QND) (0.2 mM) in the AP donor compartment.

**FIGURES:**

**Figure 2.1.**

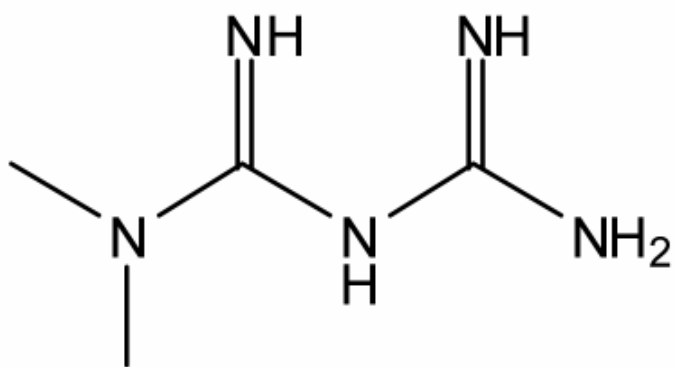


Figure 2.2.

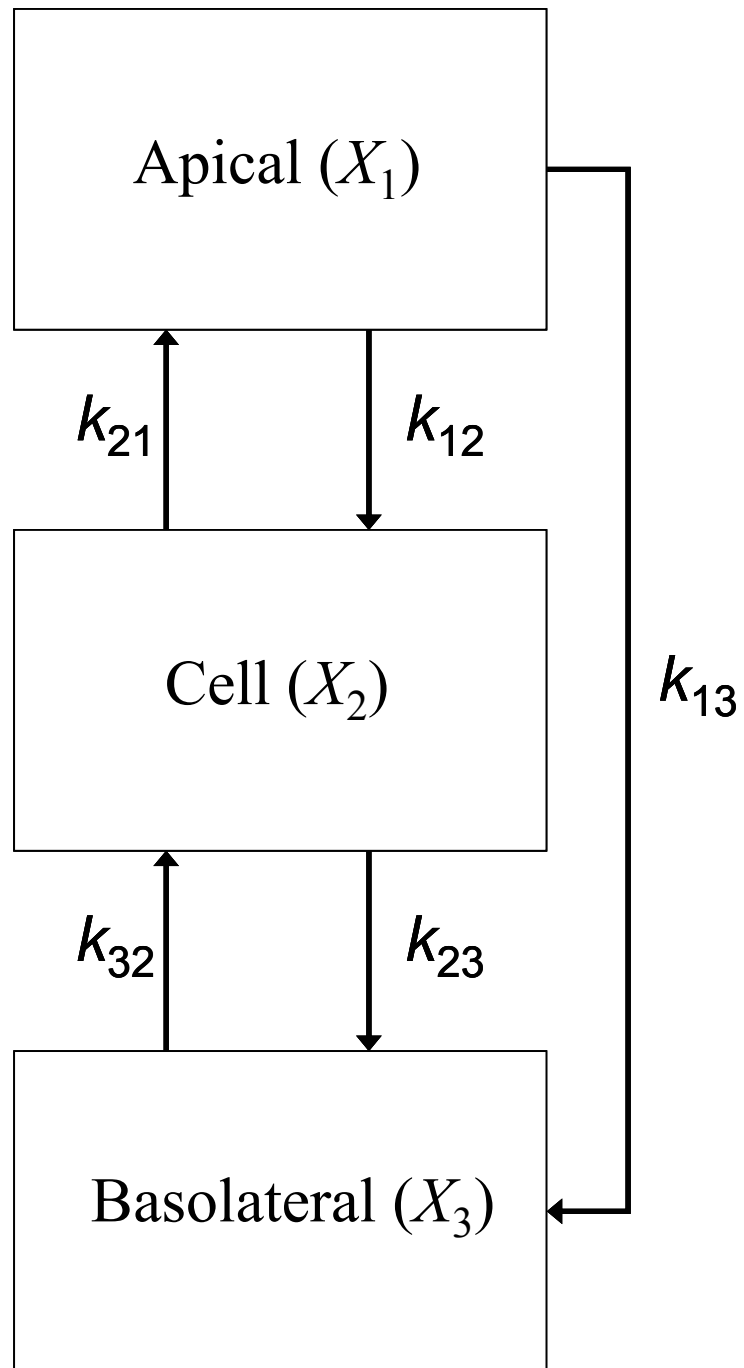
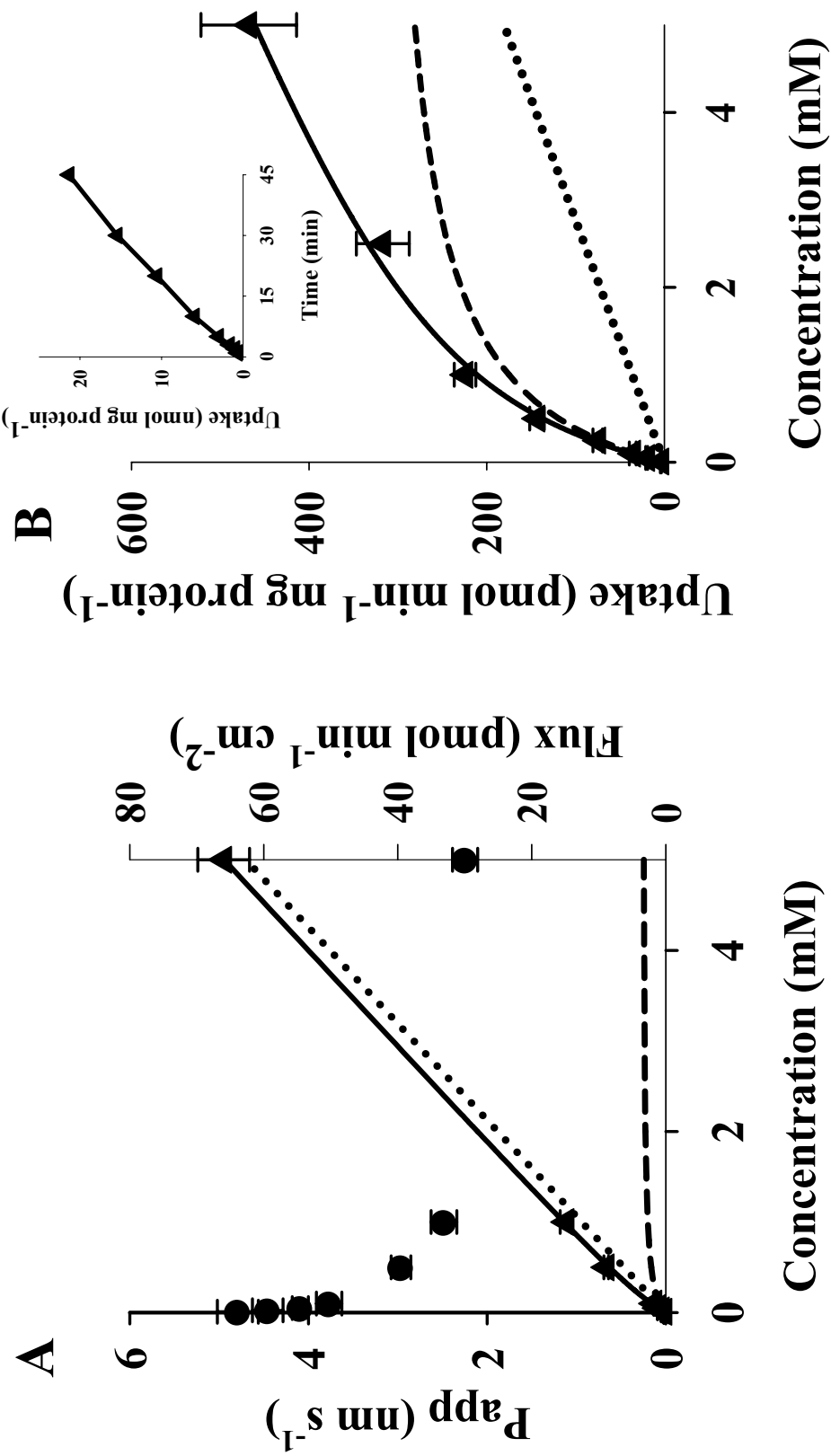


Figure 2.3.



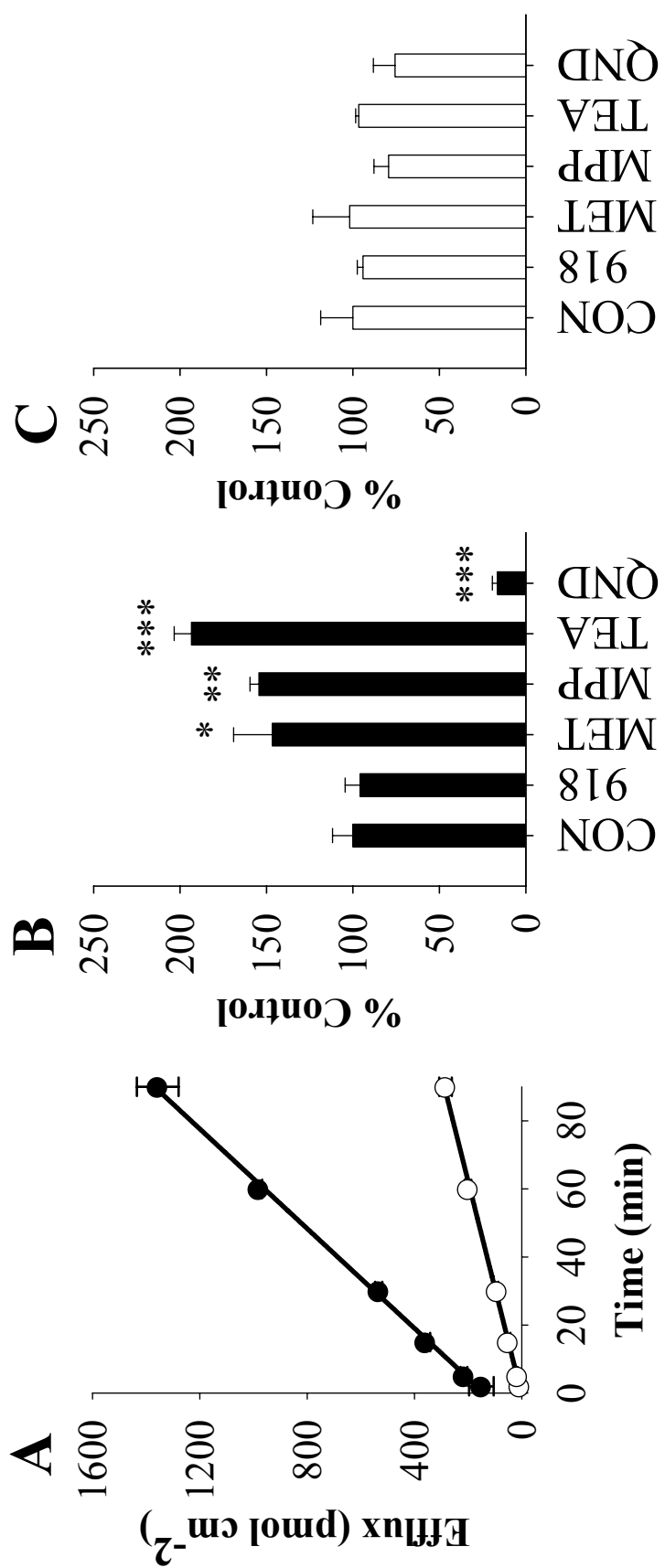


Figure 2.4.

Figure 2.5.

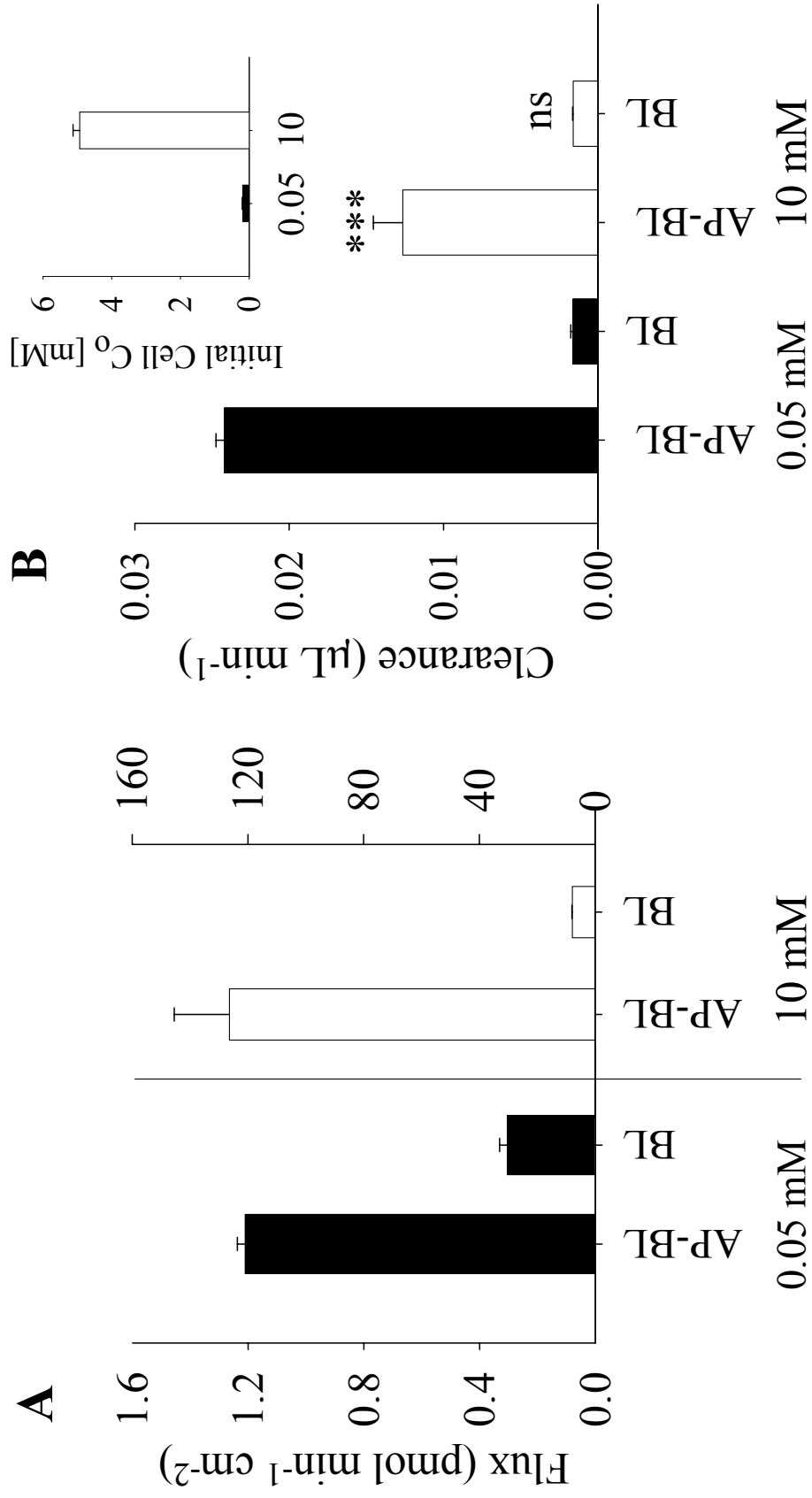


Figure 2.6.

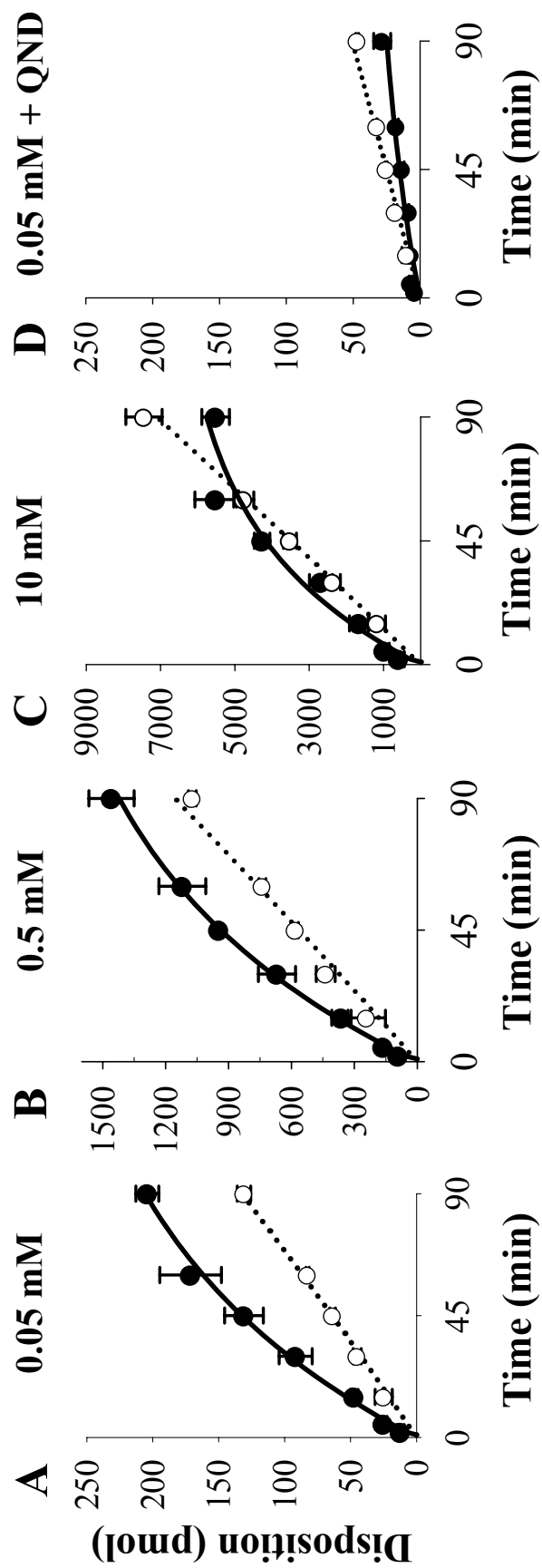
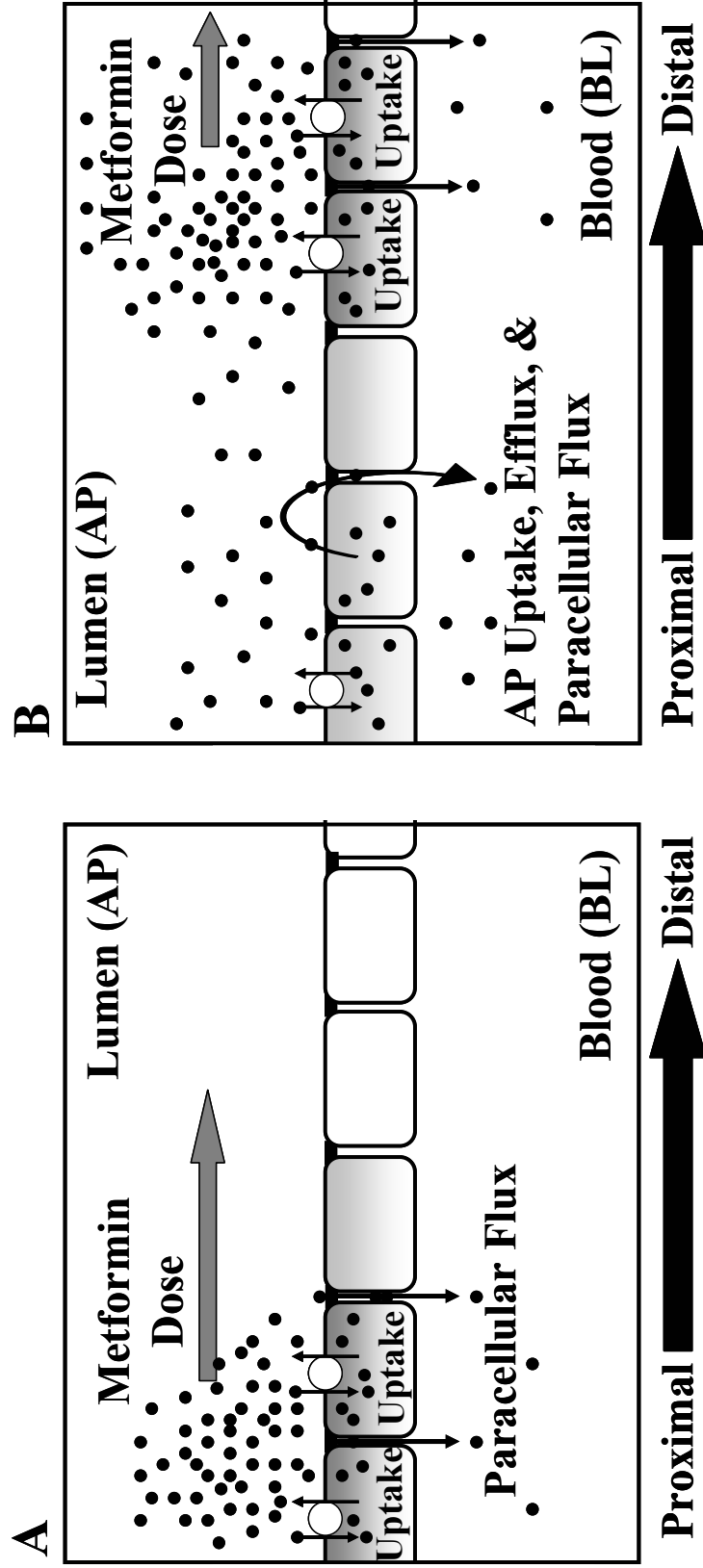


Figure 2.7.





## 2.F. REFERENCES

- Adachi Y, Suzuki H and Sugiyama Y (2001) Comparative studies on in vitro methods for evaluating in vivo function of MDR1 P-glycoprotein. *Pharm Res* **18**:1660-1668.
- Blais A, Bissonnette P and Berteloot A (1987) Common characteristics for Na<sup>+</sup>-dependent sugar transport in Caco-2 cells and human fetal colon. *J. Membr. Biol.* **99**:113-125.
- Bourdet DL, Pollack GM and Thakker D (2006) Intestinal absorptive transport of the hydrophilic cation ranitidine: A kinetic modeling approach to elucidate the role of uptake and efflux transporters and paracellular vs. transcellular transport in Caco-2 cells. *Pharm Res* **23**:1178-1187.
- Bourdet DL, Pritchard JB and Thakker DR (2005) Differential substrate and inhibitory activities of ranitidine and famotidine toward human organic cation transporter 1 (hOCT1; SLC22A1), hOCT2 (SLC22A2), and hOCT3 (SLC22A3). *J Pharmacol Exp Ther* **315**:1288-1297.
- Bourdet DL and Thakker DR (2006) Saturable absorptive transport of the hydrophilic organic cation ranitidine in Caco-2 cells: role of pH-dependent organic cation uptake system and P-glycoprotein. *Pharm Res* **23**:1165-1177.
- Choi YH, Kim SG and Lee MG (2006) Dose-independent pharmacokinetics of metformin in rats: Hepatic and gastrointestinal first-pass effects. *J Pharm Sci* **95**:2543-2552.
- Colegio OR, Van Itallie CM, McCrea HJ, Rahner C and Anderson JM (2002) Claudins create charge-selective channels in the paracellular pathway between epithelial cells. *Am J Physiol Cell Physiol* **283**:C142-147.
- Dantzig AH and Bergin L (1990) Uptake of cephalosporin, cephalixin by a dipeptide transport carrier in the human intestinal cell line, Caco-2. *Biochim Biophys Acta* **1027**:211-217.
- Englund G, Rorsman F, Ronnblom A, Karlbom U, Lazorova L, Grasjo J, Kindmark A and Artursson P (2006) Regional levels of drug transporters along the human intestinal tract: co-expression of ABC and SLC transporters and comparison with Caco-2 cells. *Eur J Pharm Sci* **29**:269-277.
- Hyafil F, Vergely C, Du Vignaud P and Grand-Perret T (1993) In vitro and in vivo reversal of multidrug resistance by GF120918, an acridonecarboxamide derivative. *Cancer Res* **53**:4595-4602.
- Kimura N, Masuda S, Tanihara Y, Ueo H, Okuda M, Katsura T and Inui K (2005a) Metformin is a superior substrate for renal organic cation transporter OCT2 rather than hepatic OCT1. *Drug Metab Pharmacokinet* **20**:379-386.

- Kimura N, Okuda M and Inui K (2005b) Metformin Transport by Renal Basolateral Organic Cation Transporter hOCT2. *Pharm Res* **22**:255-259.
- Lee K and Thakker D (1999) Saturable transport of H<sub>2</sub>-antagonists ranitidine and famotidine across Caco-2 cell monolayers. *J Pharm Sci* **88**:680-687.
- Masuda S, Terada T, Yonezawa A, Tanihara Y, Kishimoto K, Katsura T, Ogawa O and Inui K (2006) Identification and functional characterization of a new human kidney-specific H<sup>+</sup>/organic cation antiporter, kidney-specific multidrug and toxin extrusion 2. *J Am Soc Nephrol* **17**:2127-2135.
- Ming X, Bourdet DL and Thakker DR (2005) Gene expression profile of human organic cation transporters along the gastrointestinal tract and in Caco-2 cells. *AAPS Annual Meeting Nashville, TN, USA*.
- Mizuuchi H, Katsura T, Saito H, Hashimoto Y and Inui KI (1999) Transport characteristics of diphenhydramine in human intestinal epithelial Caco-2 cells: contribution of pH-dependent transport system. *J Pharmacol Exp Ther* **290**:388-392.
- Muller J, Lips KS, Metzner L, Neubert RH, Koepsell H and Brandsch M (2005) Drug specificity and intestinal membrane localization of human organic cation transporters (OCT). *Biochem Pharmacol* **70**:1851-1860.
- Noel M (1979) Kinetic study of normal and sustained release dosage forms of metformin in normal subjects. *Res Clin Florums* **1**:33-44.
- Ohta KY, Inoue K, Hayashi Y and Yuasa H (2006) Molecular identification and functional characterization of rat multidrug and toxin extrusion type transporter 1 as an organic cation/H<sup>+</sup> antiporter in the kidney. *Drug Metab Dispos* **34**:1868-1874.
- Saitoh R, Sugano K, Takata N, Tachibana T, Higashida A, Nabuchi Y and Aso Y (2004) Correction of permeability with pore radius of tight junctions in Caco-2 monolayers improves the prediction of the dose fraction of hydrophilic drugs absorbed by humans. *Pharm Res* **21**:749-755.
- Sambol NC, Chiang J, O'Conner M, Liu CY, Lin ET, Goodman AM, Benet LZ and Haram JH (1996) Pharmacokinetics and pharmacodynamics of metformin in healthy subjects and patients with noninsulin-dependent diabetes mellitus. *J Clin Pharmacol* **36**:1012-1021.
- Scheen AJ (1996) Clinical Pharmacokinetics of Metformin. *Clin. Pharmacokinet.* **30**:359-371.
- Schneider E, Machavoine F, Pleau JM, Bertron AF, Thurmond RL, Ohtsu H, Watanabe T, Schinkel AH and Dy M (2005) Organic cation transporter 3 modulates murine

- basophil functions by controlling intracellular histamine levels. *J Exp Med* **202**:387-393.
- Seithel A, Karlsson J, Hilgendorf C, Bjorquist A and Ungell A (2006) Variability in mRNA expression of ABC- and SLC-transporters in human intestinal cells: comparison between human segments and Caco-2 cells. *Eur J Pharm Sci* **28**:291-299.
- Somogyi A, Stockley C, Keal J, Rolan P and Bochner F (1987) Reduction of metformin renal tubular secretion by cimetidine in man. *Br J Clin Pharmacol* **23**:545-551.
- Song N, Li Q and Liu C (2006) Intestinal Permeability of Metformin using Single-Pass Intestinal Perfusion in Rats. *World J Gastroenterol* **12**:4064-4070.
- Terada T, Masuda S, Asaka J, Masahiro T, Katsura T and Inui K (2006) Molecular Cloning, Functional Characterization and Tissue Distribution of Rat H<sup>+</sup>/Organic Cation Antiporter MATE1. *Pharm Res* **23**:1696-1701.
- Tsuda M, Terada T, Asaka J, Ueba M, Katsura T and Inui K (2007) Oppositely directed H<sup>+</sup> gradient functions as a driving force of rat H<sup>+</sup>/organic cation antiporter MATE1. *Am J Physiol Renal Physiol* **292**:F593-598.
- Tucker GT, Casay C, Phillips PJ, Connor H, Ward JD and Woods HF (1981) Metformin kinetics in healthy subjects and in patients with diabetes mellitus. *J Clin. Pharmac.* **12**:235-246.
- Van Itallie CM, Fanning AS and Anderson JM (2003) Reversal of charge selectivity in cation or anion-selective epithelial lines by expression of different claudins. *Am J Physiol Renal Physiol* **285**:F1078-1084.
- Vidon N, Chaussade S, Noel M, Franchisseur C, Huchet B and Bernier JJ (1988) Metformin in the digestive tract. *Diabetes Res Clin Pract* **4**:223-229.
- Villalobos AR and Braun EJ (1998) Substrate specificity of organic cation/H<sup>+</sup> exchange in avian renal brush-border membranes. *J Pharmacol Exp Ther* **287**:944-951.
- Wang D, Jonker JW, Kato Y, Kusuhara H, Schinkel A and Sugiyama Y (2002) Involvement of Organic Cation Transporter 1 in Hepatic and Intestinal Distribution of Metformin. *J Pharmacol Exp Ther* **302**:510-515.
- Zhang L, Gorset W, Dresser MJ and Giacomini KM (1999) The interaction of n-tetraalkylammonium compounds with a human organic cation transporter, hOCT1. *J Pharmacol Exp Ther* **288**:1192-1198.
- Zhou M, Xia L and Wang J (2007) Metformin transport by a newly cloned proton-stimulated organic cation transporter (plasma membrane monoamine transporter) expressed in human intestine. *Drug Metab Dispos* **35**:1956-1962.

## **CHAPTER 3**

### **VITAMIN D<sub>3</sub> ENHANCES PARACELLULAR TRANSPORT OF METFORMIN ACROSS CACO-2 CELL MONOLAYERS VIA INDUCTION OF CLAUDIN-2**

This chapter will be submitted to the journal of the *Proceedings of the National Academy of Sciences* and is formatted in the style of this journal.

### 3.A. ABSTRACT

Metformin undergoes predominantly paracellular transport across the intestinal cell model, Caco-2; yet this process had a significant saturable component (Proctor, et al. *Drug Metab Dispos.* 2008; **35**(8),1650-58). It was hypothesized that saturable paracellular transport was mediated by pores formed by members of tight-junction (TJ) protein family, claudins. These proteins, in particular claudin-2, confer paracellular ion selectivity by electrostatic interactions between charged amino acid residues in their first extracellular loops believed to form the pores in the TJs. The active form of vitamin D<sub>3</sub>, 1 $\alpha$ ,25-dihydroxyvitamin D<sub>3</sub> (1,25-(OH)<sub>2</sub>D<sub>3</sub>), is known to induce claudin-2 and -12 expression in Caco-2 cells (Fujita et. al. *Mol Biol Cell* 2008; 19(5), 1912-21). The goal of this study was to evaluate how 1,25-(OH)<sub>2</sub>D<sub>3</sub>-treatment affects the paracellular transport of organic cations, such as metformin, across Caco-2 cell monolayers (clone P27.7). 1,25(OH)<sub>2</sub>D<sub>3</sub>-treatment caused an increase in the paracellular transport of organic cations, guanidine and metformin, in a size-dependent manner. Surprisingly, the transport of non-charged paracellular probes decreased significantly across 1,25(OH)<sub>2</sub>D<sub>3</sub> treated Caco-2 cell monolayers. Of over 30 genes associated with TJ formation or regulation, only claudin-2 was selectively induced (3-4 fold) by 1,25(OH)<sub>2</sub>D<sub>3</sub>-treatment. The results presented provide novel insight into the role of claudin-2 in facilitating organic cation transport and the nature of claudin-2 pores in TJs. Additionally, the present study characterizes the modulation of the pore populations in the TJs of intestinal epithelium by vitamin D<sub>3</sub>, providing molecular mechanisms to explain its dual physiological role to enhance cation-selectivity and increase intestinal barrier-integrity in the intestine.

### 3.B. INTRODUCTION

Metformin is the most widely prescribed oral anti-hyperglycemic agent for the treatment of non-insulin dependent diabetes mellitus. Despite its widespread use, the disposition and pharmacodynamic properties of metformin remain under active investigation (1-3). Metformin is generally well tolerated, though gastrointestinal side effects of diarrhea, nausea, abdominal discomfort, and anorexia are common (4). These symptoms are typically transient and subside over time. However, approximately 3% of patients become refractory to metformin therapy due to intolerance surrounding these side effects (5). The mechanism(s) responsible for the gastrointestinal effects are not known. The intestine is a major site for metformin overall glucose-lowering effect (6). This has been attributed to its ability to increase peripheral glucose uptake and stimulate anaerobic glucose metabolism in the intestine (7, 8), resulting in increased lactate production and secretion. In instances of acute systemic accumulation of the drug, this process can potentially lead to elevated lactate plasma concentrations and ultimately to lactic acidosis, a rare but potential fatal adverse event. Metformin is very hydrophilic with a net positive charge at physiological pH ( $pK_a$  12.4), and thus should have poor membrane permeability and overall absorption (refer to Figure 3.2A). Instead, the drug accumulates significantly in intestinal enterocytes (8) and is well absorbed with an oral bioavailability (500 mg dose) of 50-60%, although it is dose-dependent and highly variable (9-11), suggesting the involvement of intestinal transporters in its oral absorption.

Recent work in a well established intestinal epithelial model, Caco-2 cell monolayers, has shown that metformin undergoes saturable absorptive transport (Chapter

2, (12)). When dosed on the apical side, metformin was efficiently taken up across the AP membrane of Caco-2 cells by one or more organic cation transporter(s); however, egress across the BL membrane was so inefficient that very little metformin was transported across the cell monolayers via the transcellular route. Cellular kinetic studies showed that the overall metformin transport in the absorptive direction was predominately (>90%) paracellular. Surprisingly, the absorptive transport of metformin had a distinct saturable component to its paracellular transport (12). This phenomenon of saturable paracellular transport, although most clearly demonstrated with metformin, has been observed with other hydrophilic cationic drugs, ranitidine and famotidine (13, 14).

Small hydrophilic compounds, particularly those that have net charge at physiological pH, cross the intestinal epithelium via the paracellular route. Transport across this route is generally quite inefficient because the paracellular space represents approximately 1/10000 of the overall surface area on the apical cell membrane that is available to compounds for absorptive transcellular transport due to the presence of microvilli on the apical membrane (15). The narrow and tortuous paracellular space further contributes to the inefficient transport of compounds via this route. The third and perhaps the most important reason for inefficient paracellular transport is the presence of tight junctions, which severely restrict the passage of compounds through the paracellular space. The passage of compounds through the paracellular space is believed to occur via convective diffusion, a passive transport process. Therefore it was surprising that metformin exhibited saturable transport behavior even when over 90% of the compound traversed the cell monolayers via the paracellular route. We hypothesize that the saturable paracellular transport of metformin is due to electrostatic interactions within the

tight junctions (TJ) that facilitates paracellular transport of cationic metformin, analogous to the known electrostatic interactions that facilitate paracellular transport of the inorganic metal ions, calcium and sodium (16, 17).

The TJ form pores in the paracellular space by specific interactions between the extracellular domains of a family of proteins called claudins that are projected into the intercellular space from two adjoining cells (18). Claudins have been implicated in increasing barrier integrity (e.g. claudin-1 or -8) (19, 20) or preferentially facilitating ion permeability across the TJ by forming charge-selective pores (e.g. claudin-2, -4, -7, -12, or -16) (17, 21-24). The latter group of claudins confers charge-selectivity by electrostatic interactions between metal ions and specific charged amino acid residues in first extracellular loop believed to form the pores in the TJ (16). Claudin-2, in particular, exhibits its charge-selectivity through electrostatic interactions in the side chain carboxyl group of aspartate-65 of the first extracellular loop; altering this key residue reduced cation permeability (25). Claudin-2 pores are not only charge-selective but also size restricted to permeation of both charged and non-charged species, alike. Transport studies with noncharged polyethylene glycol oligomers (PEGs) revealed that over expressing claudin-2 in Madin-Darby Canine Kidney (MDCK) cell monolayers significantly increased the pore density of the monolayer; however, the radius of the pores remained relatively constant at approximately 4 Å (26).

Provided metformin molecular radius is smaller than 4 Å, it is conceivable that the saturable paracellular transport of the cationic metformin observed across Caco-2 cell monolayers can be facilitated by claudin-2 or other cation-selective claudins. We have employed a Caco-2 cell model, in which claudins-2 and -12 can be induced by treatment



of the cells with  $1\alpha,25$ -dihydroxyvitamin  $D_3$  ( $1,25$ -(OH) $_2D_3$ ) (17), to examine the potential role claudin-2 and/or claudin-12 have on metformin absorptive transport. The results in this study provide the first evidence that claudin-2 facilitates paracellular transport of metformin and other small hydrophilic cations through electrostatic interactions. Interestingly, treatment of Caco-2 cells with  $1,25$ -(OH) $_2D_3$  stimulated the transport of hydrophilic cations like metformin on one hand, but also attenuated paracellular transport of neutral molecules, such as mannitol, presumably via modulation of pores that regulate the paracellular transport of neutral molecules. This is the first report of an agent that selectively stimulates the paracellular transport of organic cations, and at the same time attenuates the transport of hydrophilic neutral molecules.

### 3.C. RESULTS

#### Vitamin D<sub>3</sub>-treatment Causes an Increase in Cation Permeability across Caco-2 Cell Monolayers

The magnitude of the effect of 1,25-(OH)<sub>2</sub>D<sub>3</sub>-treatment on calcium transport across Caco-2 cell monolayers has been shown to be dependent upon the specific clone utilized (27). Therefore, the Caco-2 P27.7 clone was used in this report to maximize the 1,25-(OH)<sub>2</sub>D<sub>3</sub> effect on metformin absorptive transport. This clone was first isolated by limited dilution from Caco-2 parental cells (HTB-37) passage 27 by Schmiedlin-Ren et al. in 1997 and has been used extensively for vitamin D<sub>3</sub> induction of cytochrome P450 isoform 3A4 (CYP3A4) intestinal metabolism (28, 29). The P27.7 Caco-2 cells forms high resistance monolayers (TEER ~1000 Ω\*cm<sup>2</sup>) in relation to the parental Caco-2 cell monolayers (TEER ~500 Ω\*cm<sup>2</sup>); therefore small perturbations to metformin paracellular transport can be detected in P27.7 Caco-2 cells. As reported previously (16, 34), treatment of Caco-2 cells with 1,25-(OH)<sub>2</sub>D<sub>3</sub> [100 nM] for 3 days caused a 50% drop in TEER (Figure 3.1A). Concurrently, the rate of absorptive (AP to BL) and secretory (BL to AP) transport of [<sup>45</sup>Ca<sup>+2</sup>] [1 mM], expressed as apparent permeability (P<sub>app</sub>), increased by 3.63 ± 0.14 and 2.87 ± 0.10 fold, respectively (Figure 3.1D) under linear transport conditions (Figure 3.1B). Interestingly, the control P<sub>app</sub> for [<sup>45</sup>Ca<sup>+2</sup>] [1 mM] did not change between the absorptive and secretory transport directions. Transcellular calcium transport functions in the absorptive direction in an energy dependent process (30, 31); therefore the increased secretory transport of [<sup>45</sup>Ca<sup>+2</sup>] (1 mM) observed across 1,25-(OH)<sub>2</sub>D<sub>3</sub>-treated Caco-2 cell monolayers represents only paracellular transport. The secretory P<sub>app</sub> was reduced by approximately 25% (p<0.01) in relation to the absorptive

$P_{app}$  for  $[^{45}\text{Ca}^{+2}]$  [1 mM], with values of  $12.1 \pm 0.4$  and  $16.7 \pm 0.7$  nm/s, respectively (Figure 3.1C). These data support the hypothesis that 1,25-(OH)<sub>2</sub>D<sub>3</sub>-treatment increased transcellular  $[^{45}\text{Ca}^{+2}]$  transport by approximately 25%, and increased paracellular  $[^{45}\text{Ca}^{+2}]$  transport by approximately 75%. The absorptive  $P_{app}$  values for  $[^{45}\text{Ca}^{+2}]$  decreased by ~50% ( $p < 0.05$ ) at a higher concentration [5 mM] for both the control group and 1,25-(OH)<sub>2</sub>D<sub>3</sub>-treated group (Figure 3.1C), suggesting that  $[\text{Ca}^{+2}]$  across the monolayer was saturable. Vitamin D<sub>3</sub> caused a 75% increase in the paracellular transport of  $[^{45}\text{Ca}^{+2}]$  [1mM] in the absorptive direction; therefore, the 50% reduction in the absorptive  $P_{app}$  of  $[^{45}\text{Ca}^{+2}]$  [5mM] in the 1,25-(OH)<sub>2</sub>D<sub>3</sub>-treated group clearly demonstrated saturable paracellular transport of  $[\text{Ca}^{+2}]$  in the absorptive direction. Although the raw  $P_{app}$  values decreased approximately 50%, the fold increase in  $P_{app}$  for the absorptive  $P_{app}$  of  $[^{45}\text{Ca}^{+2}]$  did not change between the [1mM] and [5mM] donor concentrations (Figure 3.1D).

Interestingly, 1,25-(OH)<sub>2</sub>D<sub>3</sub>-treatment [100nM] caused a modest but significant increase in the absorptive  $P_{app}$  of the hydrophilic organic cation, metformin, where the  $P_{app}$  values increased from  $2.3 \pm 0.3$  to  $2.9 \pm 0.2$  nm s<sup>-1</sup> ( $p < 0.05$ ) (Figure 3.2B). Since metformin was shown to be transported across Caco-2 cell monolayers predominantly via the paracellular route (12), it is reasonable to postulated that 1,25-(OH)<sub>2</sub>D<sub>3</sub> caused the increase in metformin permeability by up-regulating claudin-2 and claudin-12 in the TJ of these cells (17). A much smaller increase in metformin permeability compared to that of  $[\text{Ca}^{+2}]$  ions caused by 1,25-(OH)<sub>2</sub>D<sub>3</sub> may reflect a much larger volume (radius) of the organic cation compared to  $[\text{Ca}^{+2}]$ . To determine if the effect of 1,25-(OH)<sub>2</sub>D<sub>3</sub> on the  $P_{app}$  of metformin across Caco-2 cell monolayers could apply to other small hydrophilic organic cations and to evaluate if it also was dependent on the size of the cation, transport

of a small panel of hydrophilic organic cations across Caco-2 cell monolayers was examined using cells treated with 1,25-(OH)<sub>2</sub>D<sub>3</sub> [100nM] or vehicle control. Figure 3.2A depicts space-filling chemical structures of the organic cations guanidine, metformin, and TEA, in addition to the uncharged mannitol, which provide an estimate of the relative size of these molecules. Molecular radius estimates were determined for these compounds and other reported hydrophilic cations using molecular modeling approaches (Table 3.1). The radius estimates for the organic cations guanidine, metformin, and TEA were estimated to be 2.56, 3.28, and 3.74 Å, respectively. Mannitol was estimated to have a slightly larger molecular radius of 3.92 Å (Table 3.1). Cation-selective claudins, in particular claudin-2, are known to facilitate ion and small solute flux in a size-dependent manner (25, 26); therefore, if these pores were involved, the effects on absorptive transport would affect the smaller guanidine to a larger extent than metformin or TEA. Indeed,  $P_{app}$  values of guanidine increased by almost 2-fold from  $13.5 \pm 0.8$  to  $23.9 \pm 1.7$  nm s<sup>-1</sup> ( $p < 0.001$ ) (Figure 3.2B-C). The  $P_{app}$  values for a larger cation than metformin, TEA, did not change significantly by 1,25-(OH)<sub>2</sub>D<sub>3</sub>-treatment, although the mean  $P_{app}$  value for 1,25-(OH)<sub>2</sub>D<sub>3</sub> treatment group for TEA appeared to decrease somewhat.

### **Effect of 1,25-(OH)<sub>2</sub>D<sub>3</sub>-treatment on the Absorptive Transport of Neutral Hydrophilic Compounds Across Caco-2 Cell Monolayers**

Surprisingly, the absorptive  $P_{app}$  across monolayers treated with 1,25-(OH)<sub>2</sub>D<sub>3</sub> decreased by ~25% from  $0.92 \pm 0.08$  to  $0.69 \pm 0.09$  nm s<sup>-1</sup> ( $p < 0.01$ ) for the neutral paracellular probe, mannitol (Figure 3.2B-C). To further examine the effect of 1,25-(OH)<sub>2</sub>D<sub>3</sub>-treatment on neutral hydrophilic paracellular molecules, the permeability of a

series of PEG oligomers with varying molecular weight and size was examined across control and 1,25-(OH)<sub>2</sub>D<sub>3</sub>-treated Caco-2 cell monolayers. The  $P_{app}$  values of the PEG oligomers across 1,25-(OH)<sub>2</sub>D<sub>3</sub>-treated and vehicle-treated Caco-2 cell monolayers, plotted as a function of the hydrodynamic radii ( $r$ ), are depicted in Figure 3.2D. The relationship between  $P_{app}$  values and hydrodynamic radii in the control cell monolayers was similar to the previously reported relationship (26, 32, 33), suggesting two populations of TJ pores, those that allow transport of compounds smaller than 4 Å in a size-dependent manner, and those that allow transport of larger molecules in a size-independent manner. Interestingly, 1,25-(OH)<sub>2</sub>D<sub>3</sub>-treatment caused a significant decrease in the mean  $P_{app}$  ( $p < 0.001$ ) for PEG<sub>3.2Å</sub>; while not significant, the mean  $P_{app}$  value for PEG<sub>3.5Å</sub> also decreased in relation to control values. Thus, the reduction in mannitol  $P_{app}$  upon 1,25-(OH)<sub>2</sub>D<sub>3</sub>-treatment of Caco-2 cell monolayers was observed for other hydrophilic neutral molecules of similar size. The size-restricted pore radius calculated by the ratio of PEG<sub>3.2Å</sub> and PEG<sub>3.5Å</sub> permeability values using Eq. 3.6 for control and 1,25-(OH)<sub>2</sub>D<sub>3</sub>-treated Caco-2 (P27.7) cell monolayers was 3.9 and 4.0 Å, respectively. This size-restricted pore radius of ~4 Å was identical to the value obtained in the Caco-2 BBe clone (26). These data suggest that 1,25-(OH)<sub>2</sub>D<sub>3</sub> treatment caused a reduction in the size-restricted pore number, without affecting the pore size.

### **Vitamin D<sub>3</sub>-treatment Does Not Affect Transcellular Transport Processes of Metformin in Caco-2 Cell Monolayers**

The transcellular transport processes of metformin were examined in both treatment groups to determine if the ~25% increase in absorptive transport of metformin could be attributed to 1,25-(OH)<sub>2</sub>D<sub>3</sub> related increase in AP uptake, cellular accumulation,

and/or BL efflux. Initial AP uptake (5 min) of metformin remained unchanged in the Caco-2 cell monolayers treated in the presence or absence of 1,25-(OH)<sub>2</sub>D<sub>3</sub>, with uptake values of  $1.39 \pm 0.10$  and  $1.30 \pm 0.11$  (pmol\*min<sup>-1</sup>\*mg protein<sup>-1</sup>) for control and 1,25-(OH)<sub>2</sub>D<sub>3</sub>-treated Caco-2 cells, respectively (Figure 3.3A). AP and BL efflux clearance, as determined in the linear range of efflux and corrected for initial cellular concentration following 60min loading of metformin [10μM], did not change significantly by 1,25-(OH)<sub>2</sub>D<sub>3</sub>-treatment (Figure 3.3B). In both treatment groups, BL efflux was ~5 fold lower than AP efflux, as was observed previously for metformin transport across Caco-2 cell monolayers (12). Cellular accumulation (C<sub>o</sub>) following a 60min absorptive transport experiment at 0.01 and 10 mM AP metformin donor concentrations was not affected by treatment with 1,25-(OH)<sub>2</sub>D<sub>3</sub> (Figure 3.3C). Thus, the transcellular transport processes of metformin remain unchanged in Caco-2 cell monolayers treated with 1,25-(OH)<sub>2</sub>D<sub>3</sub>, and can not account for the increase in the absorptive permeability across Caco-2 cell monolayers caused by 1,25-(OH)<sub>2</sub>D<sub>3</sub>-treatment.

#### **Expression of Claudin-2 among Claudins is Selectively Induced by Vitamin D<sub>3</sub> in Caco-2 (P27.7) Cells.**

Metformin and guanidine absorptive transport increased when Caco-2 cells were treated with 1,25-(OH)<sub>2</sub>D<sub>3</sub> (Figure 3.2C), while the transcellular transport processes remained unchanged (Figure 3.3). These results suggested that 1,25-(OH)<sub>2</sub>D<sub>3</sub> increased absorptive transport of metformin and guanidine via the paracellular route, while decreasing the absorptive transport of neutral paracellular probes. It is known that 1,25-(OH)<sub>2</sub>D<sub>3</sub>-treatment induces mRNA and protein expression of claudin-2 and claudin-12 in Caco-2 BBe cells (17), and E-cadherin protein expression in parental Caco-2 cells (34).

In both studies, the effect of 1,25-(OH)<sub>2</sub>D<sub>3</sub>-treatment on the expression of only a subset of tight-junction proteins was evaluated. Furthermore, it is not known whether the effects 1,25-(OH)<sub>2</sub>D<sub>3</sub>-treatment on TJ protein expression that were previously observed would be observed in Caco-2 P27.7 cells. Hence, the effect of 1,25-(OH)<sub>2</sub>D<sub>3</sub>-treatment on mRNA expression was determined corresponding to 30 genes that encode proteins responsible for TJ structure and for regulation of TJ function using RT-PCR analysis (refer to Table 3.S1 in Supplemental Material). Of the 30 genes examined, 21 targets passed the specified criteria to be detected in the assay and produced single products at the predicted size (Figure 3.S1 in Supplemental Material). Expression of each gene was reported relative to the housekeeping gene product, GAPDH, and comparison was performed using the  $\Delta\Delta C_t$  method (35). The relative expression of each gene in Caco-2 cells treated with 1,25-(OH)<sub>2</sub>D<sub>3</sub> and vehicle control are depicted in Figure 3.4A. The relative expression of Claudin-2 mRNA was 4-fold higher in 1,25-(OH)<sub>2</sub>D<sub>3</sub>-treated Caco-2 cells in comparison to control (Figure 3.4A (Inset)). Claudin-12 mRNA remained unchanged with 1,25-(OH)<sub>2</sub>D<sub>3</sub> treatment, which was inconsistent with previous reports that 1,25-(OH)<sub>2</sub>D<sub>3</sub> increased claudin-12 expression 3 to 4-fold in Caco-2 cells, albeit in a different clone, Caco-2 BBe (17). The relative expression of mRNA for adipocyte-specific adhesion molecule (ASAM) and claudin-16 decreased by approximately 65% in the 1,25-(OH)<sub>2</sub>D<sub>3</sub>-treated Caco-2 cells in comparison to control cells, while expression of mRNA for claudin-1, -3, and -4, and -15 decreased by approximately 40% (Figure 3.4B). Relative expression of mRNA for occludin, epithelial membrane protein 2 (EMP2), and the junction adhesion molecule A (F11R) increased by approximately 40% in the 1,25-(OH)<sub>2</sub>D<sub>3</sub>-treated Caco-2 cells in comparison to control cells. Claudin-7 mRNA

expression in control Caco-2 cells was detected with  $C_t$  values at approximately 34 cycles, although the mRNA levels in the 1,25-(OH) $_2$ D $_3$ -treated Caco-2 cells fell below the detection limit (e.g. >35 cycles) and was deemed undetected (data not shown).

The effect of 1,25-(OH) $_2$ D $_3$ -treatment on claudin-2 protein expression in Caco-2 P27.7 cells was evaluated in addition to the expression of claudin-4, -7, and occludin proteins (Figure 3.4C). Claudin-4 mRNA decreased approximately 40% in the 1,25-(OH) $_2$ D $_3$ -treated cells and is known to significantly increase monolayer resistance and reduce metal cation paracellular transport (22, 23); therefore claudin-4 protein was examined to determine if 1,25-(OH) $_2$ D $_3$  acted to increase cation-selectivity of the monolayer by simultaneously up-regulating claudin-2 and down-regulating claudin-4. As stated above, claudin-7 mRNA was detected in the control Caco-2 cells, but fell out of range in the 1,25-(OH) $_2$ D $_3$  treated Caco-2 cells. In addition claudin-7 has been implicated in increasing metal cation paracellular transport and decreasing anion transport (21, 36); thus, the protein of this claudin isoform was evaluated. Occludin mRNA increased significantly following 1,25-(OH) $_2$ D $_3$ -treatment; therefore, the effects of 1,25-(OH) $_2$ D $_3$ -treatment on occludin protein expression were examined.

Similar to the mRNA data, only claudin-2 protein significantly increased (~300% N=4,  $p<0.05$ ) with 1,25-(OH) $_2$ D $_3$ -treatment in relation to control Caco-2 cell protein expression (Figure 3.4C). Claudin-4, claudin-7, and occludin remained unchanged between treatment groups. The protein expression data did not support the mRNA expression increase of occludin or the decrease in relative expression decrease of claudin-4. In summary, 1,25-(OH) $_2$ D $_3$  selectively induced claudin-2 expression in Caco-2 P27.7



cells, while the expression of other TJ proteins or the corresponding mRNA was altered to a lesser extent.

The relative expression of organic cation transporters was examined in Caco-2 cells treated with 1,25-(OH)<sub>2</sub>D<sub>3</sub> or vehicle control to further confirm the transport data, which suggested that metformin transcellular transport processes remained unchanged by 1,25-(OH)<sub>2</sub>D<sub>3</sub>-treatment. Caco-2 cells express many organic cation transporters (OCTs), such as OCT1 (SLC22A1), OCT3 (SLC22A3), and OCTN2 (SLC22A5) (37, 38). Metformin is known to be a substrate for human OCT1 (39) and OCT3 (40), and OCTN2 is the most abundant cation transporter in Caco-2 cells (38), although metformin substrate specificity towards this transporter has yet to be determined. Metformin recently has been identified as a substrate for a newly cloned transporter, the plasma membrane monoamine transporter (PMAT, SLC29A4), which has been shown to be expressed on the AP membrane of human intestine enterocytes (3). The expression of this transporter in Caco-2 cells is unknown. The relative expression of OCT1,-3, -N2, and PMAT was measured using quantitative PCR. The relative expression of OCT1,-3, and -N2 remained unchanged in Caco-2 cells treated with 1,25-(OH)<sub>2</sub>D<sub>3</sub> (Figure 3.4A-B). PMAT mRNA was detected in both control and 1,25-(OH)<sub>2</sub>D<sub>3</sub>-treated Caco-2 cells. This is the first report of PMAT expression in Caco-2 cells. The relative expression of this cation transporter was at the same level as OCTN2, and significantly greater than OCT1 and OCT3 expression (Figure 3.4A). The relative expression of PMAT decreased ~30% ( $p<0.05$ ) in the 1,25-(OH)<sub>2</sub>D<sub>3</sub>-treated Caco-2 cells. In summary, known cation transporter expression in Caco-2 cells did not increase following treatment with 1,25-

(OH)<sub>2</sub>D<sub>3</sub>, supporting metformin functional data that transcellular transport processes were not affected.

### 3.D. DISCUSSION

We have shown previously in parental Caco-2 HTB-37 cells (12) and again in this study using Caco-2 P7.7 cells that metformin was transported efficiently across the AP membrane by a bidirectional organic cation transporter(s); yet the drug cannot escape the cellular compartment due to inefficient BL efflux resulting in accumulation. Consequently, metformin absorptive transport was predominantly (>90%) paracellular with a clearly saturable component (Chapter 2) (12). The aim of this work was to elucidate the mechanism of this novel saturable paracellular transport observed with metformin and potentially other small hydrophilic organic cations. It was hypothesized that saturable paracellular transport of metformin was due to a facilitative diffusion process driven by electrostatic interactions within the TJ, analogous to similar interactions known to mediate paracellular transport of metal ions.

To test this hypothesis we studied the effect of vitamin D<sub>3</sub>, in particular the active vitamin D<sub>3</sub> metabolite, 1,25-dihydroxyvitamin D<sub>3</sub> (1,25-(OH)<sub>2</sub>D<sub>3</sub>), on metformin paracellular transport across Caco-2 cell monolayers. The results presented here confirm previous reports (17, 41) that 1,25-(OH)<sub>2</sub>D<sub>3</sub>-treatment reduced overall monolayer resistance and increased the calcium paracellular transport in Caco-2 cell monolayers. In the Caco-2 BBe cells, this effect was shown to be due to 1,25-(OH)<sub>2</sub>D<sub>3</sub> specifically up-regulating both claudin-2 and -12 protein expression (17). However, our results in the Caco-2 P27.7 cells revealed that only claudin-2 mRNA and protein expression were significantly increased (~3-4 fold) with 1,25-(OH)<sub>2</sub>D<sub>3</sub>-treatment. Expression of claudin-12, -15, and -16 in monolayers have been shown to increase cation paracellular transport (17, 24, 42), yet the relative mRNA expression for each of these proteins was either

unchanged (claudin-12) or decreased (claudin-15, and -16) as a result of 1,25-(OH)<sub>2</sub>D<sub>3</sub>-treatment (Figure 3.4A-B). The difference between the Caco-2 P27.7 and Caco-2 BBe clone in relation to claudin-12 vitamin D<sub>3</sub> regulation deserves future study.

Nevertheless, 1,25-(OH)<sub>2</sub>D<sub>3</sub> increased the overall cation-selectivity of the Caco-2 P27.7 monolayer through select induction of claudin-2. Claudin-2 has been studied extensively in relation to facilitating paracellular transport of metal cations, such as sodium and calcium (17, 23, 25, 42-44). It is believed that claudin-2 forms pores in the TJ and facilitates transport of cations by electrostatic interactions between key anionic amino-acid residues in the first extracellular loop, in particular the carboxyl group of aspartate-65 (25). The role this protein on transport of small organic cations is less understood. Recently, Yu et al. (2009) evaluated methylamine, ethylamine, trimethylamine (TMA), and TEA permeability across MDCK cells expressing claudin-2 under an inducible promoter. Although the results revealed a size-dependent increase in the permeability of organic cations with claudin-2 expression, the permeability of the organic cations was measured indirectly by electrophysiological measurements (e.g. dilution potentials) and at concentrations that are supra-physiological (75mM donor solutions). The study also employed inducible promoters to account for the endogenous claudins that may alter paracellular transport of the ions studied, but they failed to account for the effect of additional claudin-2 expression on the monolayer integrity by monitoring the flux of neutral paracellular probes (e.g. mannitol or PEG). Over expression of claudin protein in MDCK cells are known to increase overall permeability across the monolayer presumably by overloading the TJs with protein, while still producing a desired effect on monolayer resistance and dilution potential (data not

shown). Therefore, alterations to the monolayer may have confounded the data and produced effects not directly attributed to claudin-2 electrostatics.

In this report, physiologic levels of the active metabolite of vitamin D<sub>3</sub> selectively increased claudin-2 protein expression resulting in a size-dependent increase in guanidine and metformin absorptive transport (Figure 3.2C). However, 1,25-(OH)<sub>2</sub>D<sub>3</sub> had no effect on the transcellular transport processes of metformin. Therefore, the increase observed in metformin absorptive transport across Caco-2 cells treated with 1,25-(OH)<sub>2</sub>D<sub>3</sub> can only be attributed to an increase in paracellular transport. 1,25-(OH)<sub>2</sub>D<sub>3</sub>-treatment did not increase the transport of neutral hydrophilic solutes, indicating that the enhanced paracellular transport caused by 1,25-(OH)<sub>2</sub>D<sub>3</sub>-treatment was dependent on both size and charge. These observations taken together provide overwhelming evidence implicating claudin-2 in facilitating paracellular transport of metformin and similar organic cations.

1,25-(OH)<sub>2</sub>D<sub>3</sub>-treatment caused a significant reduction in the absorptive permeability of the neutral paracellular probe mannitol (Figure 3.2C). Mannitol molecular radius was estimated using molecular modeling approaches to be 3.92 Å (Table 3.1), which was approximately equal to the calculated values of the size-restricted pore radius for control and 1,25-(OH)<sub>2</sub>D<sub>3</sub>-treated Caco-2 cell monolayers of 3.9 and 4.0 Å, respectively. In addition, this molecular radius estimate may underestimate the true hydrodynamic radius of mannitol, which has been shown experimentally to be approximately 4.2 Å (45). Moreover, mannitol paracellular transport was not affected by claudin-2 expression in MDCK C7 cell monolayers (26, 43) indicating that it was unable to permeate the claudin-2 associated size- and charge-restricted pore system. In other words, mannitol absorptive transport represents permeation through pores in the TJ that

are relatively size-independent. Therefore, 1,25-(OH)<sub>2</sub>D<sub>3</sub>-treatment appeared to increase the monolayer barrier-integrity by reducing the number of size-independent pores or restricted these pores to reduce the flux of mannitol.

Under basic molecular sieving assumptions, attenuation of transport through the size-independent pathway likely contributed to an equal or greater reduction of transport through these pores for the smaller solutes such as metformin and guanidine in relation to the effect on mannitol transport. Thus, 1,25-(OH)<sub>2</sub>D<sub>3</sub>-treatment presumably reduced metformin and guanidine passive transport through one pathway; yet their overall transport was significantly increased (Figure 3.3C). This observation supports the hypothesis that the true effect of 1,25-(OH)<sub>2</sub>D<sub>3</sub> on increasing the cation-selective pores may be underestimated by only measuring transport of the organic cations. However, the structure and proteins involved in forming the size-independent pores remains unknown. Furthermore, it is not known whether charged solutes (e.g. metformin) exhibit similar diffusion properties as neutral molecules of similar size. In summary, this is the first report of simultaneous modulation of the two paracellular pore systems with opposing effects and supports previous reports for two distinctly different pore systems that affect hydrophilic solutes: a charge- and size-dependent pathway and a size-independent pathway. Further studies are warranted to examine the molecular mechanism responsible for the effects of 1,25-(OH)<sub>2</sub>D<sub>3</sub> on both the size-independent and size- and charge-dependent paracellular routes.

Claudin-2 protein expression was increased approximately 3 to 4 fold following 1,25-(OH)<sub>2</sub>D<sub>3</sub>-treatment, most likely resulting in the size-dependent increase in calcium, guanidine, and metformin transport (Figures 3.1B and 3.2B-C). Expression of claudin-2

protein in MDCK cell monolayers resulted in both an increase in the cation paracellular transport (25) as well as a size-dependent increase in small non-charged PEG oligomers with hydrodynamic radii less than 4 Å (e.g. PEG<sub>3,2</sub>) (26, 33). The observed increase in small non-charged PEG flux was not attributed to an increase in the radius of the size-restricted pore (26), supporting that claudin-2 enhanced the number of size-restricted pores in the monolayer. Based on the previous reports outlined above, the increase in claudin-2 protein should have resulted in an increase in the pore number as measured by an increase in the flux of PEG<sub>3,2</sub> molecules. In contrast, the transport of the small non-charged PEG<sub>3,2</sub> was decreased significantly following 1,25-(OH)<sub>2</sub>D<sub>3</sub>-treatment (Figure 3.2D). Because the size-restricted pore radius for the cell monolayers treated with 1,25-(OH)<sub>2</sub>D<sub>3</sub> or vehicle control appeared to be nearly identical, the decrease in the permeability of PEG<sub>3,2</sub> molecule must be due to a decrease in the number of the size-restricted pores in the monolayer.

If small PEG oligomers and small cations are both capable of permeating claudin-2 pores, then the respective decrease and increase in each pathway suggests that 1,25-(OH)<sub>2</sub>D<sub>3</sub> enhanced the number of claudin-2 pores, while significantly reducing other size-restricted pores resulting in a net decrease in monolayer porosity. It would seem reasonable to assume that other pore-forming proteins would need to be displaced in order to decrease the effective porosity of the monolayer while simultaneously increasing the cation-selective size-restricted pores. It is conceivable that the significant decrease in claudin-1, -3, -15, -16, and/or ASAM mRNA expression as a result of 1,25-(OH)<sub>2</sub>D<sub>3</sub>-treatment was a potential compensatory mechanism to allow for increased claudin-2 cation-selective pores, while reducing the overall porosity of the monolayer. For

example, the junction adhesion molecule A (JAM-A or F11R) was increased by approximately 40% in vitamin D<sub>3</sub>-treated cells (Figure 3.4B). F11R gene silencing in mice was shown to significantly increase intestinal expression of claudin-10 and -15 (46); therefore, the 1,25-(OH)<sub>2</sub>D<sub>3</sub>-associated increase in JAM-A expression may have led to a reduction in claudin-15 pores in the monolayer.

There have been several reports linking vitamin D<sub>3</sub> deficiency to the risk of inflammatory bowel disease (IBD) and Crohn's disease (47). Furthermore, vitamin D<sub>3</sub>-treatment decreased disease progression and mortality rates in transgenic mice deficient in interleukin-10, the prevalent preclinical model to study IBD and Crohn's disease (48). A recent report also has shown that 1,25-(OH)<sub>2</sub>D<sub>3</sub> can increase barrier integrity and wound healing in the Caco-2 cell model (34). In the latter study, Caco-2 HTB-37 cells were less susceptible to dextran sulfate sodium disruption of monolayer integrity following pretreatment for 24 h with 10nM of 1,25-(OH)<sub>2</sub>D<sub>3</sub>. They attributed the increase in barrier integrity to vitamin D<sub>3</sub> induced expression of E-cadherin and ZO-1 and maintenance of TEER following injury (34). Interestingly, we did not observe a statistically different increase in E-cadherin or ZO-1 mRNA expression following 1,25-(OH)<sub>2</sub>D<sub>3</sub>-treatment in our Caco-2 P27.7 cell model. Potential differences between Caco-2 culture conditions, clone variations, and duration of 1,25-(OH)<sub>2</sub>D<sub>3</sub>-treatment (24 vs. 72 h) may account for this discrepancy. The results presented here demonstrate for the first time the effect of 1,25-(OH)<sub>2</sub>D<sub>3</sub> *in vitro* on simultaneously increasing barrier integrity and cation-selectivity of intestinal epithelium as determined through direct measurement of both cation and small noncharged solute flux and provide expression changes to several TJ associated proteins that may be responsible for this effect.



In conclusion, the work presented in this report provides a molecular mechanism to explain the saturable paracellular transport observed with metformin across intestinal epithelium. We have shown selective induction of claudin-2 protein by 1,25-(OH)<sub>2</sub>D<sub>3</sub> in Caco-2 P27.7 cells that result in increased cation-selective pores capable of facilitating diffusion of these small charged solutes. This process is distinctly different from the paracellular transport of neutral paracellular probes, revealing a complex and dynamic system that involves electrostatic interactions, diffusion, and charge accessibility. This novel finding is the first direct evidence that physiologically relevant TJ modulation can enhance transport of charged organic solutes, while still maintaining overall barrier integrity. Moreover, 1,25-(OH)<sub>2</sub>D<sub>3</sub>-treatment in Caco-2 P27.7 cells simultaneously increased both paracellular cation flux and the barrier integrity of the monolayer. This was achieved by 1,25-(OH)<sub>2</sub>D<sub>3</sub>-treatment, which altered both the size-restricted and size-independent pore systems of the monolayer. A schematic representation of the proposed effect 1,25-(OH)<sub>2</sub>D<sub>3</sub>-treatment on paracellular transport of metformin and other hydrophilic solutes is depicted in Figure 3.5. This work provides novel mechanistic information on how metformin and other similar compounds are absorbed across intestinal epithelium. Additionally, these findings have potential implications in our understanding of the distribution and elimination of metformin and other small charged solutes in other barrier tissues with well formed tight-junctions.

### 3.E. MATERIALS AND METHODS

#### Materials

Eagle's minimum essential medium (EMEM) with Earle's salts and L-glutamate, nonessential amino acids (NEAA, 100x), penicillin-streptomycin-amphotericin B solution (100x), fetal bovine serum (FBS), and HEPES (1M) were obtained from Invitrogen Corporation (Carlsbad, CA, USA). PEG200, PEG40, and PEG900 were obtained from Fluka Chemical (Sigma-Aldrich, St. Louis, MO, USA). Purified PEG28 was obtained from Polypure AS (Oslo, Norway). 1-Naphthylisocyanate (1-NIC) was obtained from Acros Organics (ThermoFisher Scientific, Pittsburgh PA, USA). Hank's balanced salt solution (HBSS) with calcium and magnesium was purchased from Mediatech, Inc. (Mannassas, VA, USA). Metformin, guanidine, 1-methyl-4-phenylpyridinium (MPP<sup>+</sup>), tetraethylammonium bromide (TEA), sodium-dodecyl sulfate (SDS), D-(+) glucose, and SYBR Green JumpStartTaq ReadyMix™ were purchased from Sigma Chemical Co. (St. Louis, MO, USA). 1,25-(OH)<sub>2</sub>D<sub>3</sub> was obtained from BIOMOL (Enzo Life Sciences, Plymouth Meeting, PA, USA). [<sup>14</sup>C]Metformin (54 μCi/μmol), [<sup>14</sup>C]guanidine (53 μCi/μmol), and [<sup>14</sup>C]mannitol (55 μCi/μmol) was purchased from Moravek Biochemicals and Radiochemicals (Brea, CA, USA). [<sup>14</sup>C]TEA (51 μCi/μmol) and <sup>45</sup>CaCl<sub>2</sub> (451 μCi/μmol) were purchased from New England Nuclear (PerkinElmer, Waltham, MA, USA). RT-PCR primer pairs for TJ gene products were purchased from Qiagen, Inc. (Valencia, CA, USA) as QuantiTech Primer Assays™ (the names of the genes, accession, and assay numbers are reported in Supplemental Material, Table 3.S1). All other RT-PCR primers were custom designed and synthesized by Invitrogen (Carlsbad, CA, USA). The Caco-2 cell line (P27.7) was obtained

generously from Dr. Mary F. Paine (Eshelman School of Pharmacy, UNC-Chapel Hill, Chapel Hill, NC).

### **Caco-2 Cell Culture**

Caco-2 cells were cultured at 37°C in EMEM with 10% FBS, 1% NEAA, and 100 U/ml penicillin, 100 µg/mL streptomycin, and 0.25 µg/mL amphotericin B in an atmosphere of 5% CO<sub>2</sub> and 90% relative humidity. The cells were passaged following 90% confluency using trypsin-EDTA, and plated at a 1:10 ratio in 75-cm<sup>2</sup> T flasks. The cells (passage numbers 31 to 36) were seeded at a density of 60,000 cells/cm<sup>2</sup> on polycarbonate membranes of Transwells™ (12 mm, 0.4 µm pore size, Corning Life Science, Lowell, MA, USA). Medium was changed the day following seeding and every other day thereafter (apical (AP) volume 0.5 mL, basolateral (BL) volume 1.5 mL). The Caco-2 cell monolayers were used 21-28 days post seeding. Cells were treated in both the AP and BL compartments with 1,25-(OH)<sub>2</sub>D<sub>3</sub> [100nM] or vehicle (0.01% ethanol) in cell culture medium for three days prior to transport experiment. Transepithelial electrical resistance (TEER) was measured to ensure monolayer integrity and the extent of claudin induction by 1,25-(OH)<sub>2</sub>D<sub>3</sub>. Measurements were done using an EVOM Epithelial Tissue Voltohmmeter and an Endohm-12 electrode (World Precision Instruments, Sarasota, FL, USA). Cell monolayers with TEER values greater than 400 Ω·cm<sup>2</sup> were used in transport experiments.

### **Absorptive (AP-BL) Transport Studies:**

Transport studies were conducted as described previously with minor deviations (12, 49). Cell monolayers treated for 3 days with 1,25-(OH)<sub>2</sub>D<sub>3</sub> [100nM] or vehicle control were preincubated with transport buffer solution (HBSS with 25 mM D-glucose

and 10 mM HEPES, pH 7.4) for 30 min at 37°C. The buffer in the donor compartment was replaced with 0.4 ml (AP) or 1.5 ml (BL) of transport buffer containing [ $^{45}\text{Ca}^{+2}$ ] (0.2  $\mu\text{Ci/ml}$ ), [ $^{14}\text{C}$ ]-guanidine (0.1  $\mu\text{Ci/ml}$ ), [ $^{14}\text{C}$ ]-metformin (0.15  $\mu\text{Ci/ml}$ ), [ $^{14}\text{C}$ ]-TEA (0.1  $\mu\text{Ci/ml}$ ), or [ $^{14}\text{C}$ ]-mannitol (0.1  $\mu\text{Ci/ml}$ ). For measurement of calcium transport, [ $^{45}\text{Ca}^{+2}$ ] in transport buffer was spiked into the donor compartment without additional calcium [1mM] or at 5mM CaCl [5mM]. All other compounds assessed were dosed at 10 $\mu\text{M}$  unless otherwise noted. The pH in both AP and BL compartments was maintained at 7.4 for all transport studies. Appearance of compounds into the receiver compartment (BL for absorptive transport or AP for secretory transport) was monitored as a function of time in the linear region of transport and under sink conditions. The radioisotope-labeled compounds were quantified using liquid scintillation spectrometry (1600 TR Liquid Scintillation Analyzer, Packard Instrument Company, Downers Grove, IL, USA).

### **Uptake, Efflux, and Cellular Accumulation Studies**

Transcellular transport processes (e.g. uptake, efflux, and cellular accumulation) of metformin were evaluated across Caco-2 cell monolayers that were treated for 3 days with 1,25-(OH) $_2\text{D}_3$  [100nM] or vehicle control using methods established previously (12) with minor deviations. During uptake experiments, cell monolayers were preincubated for 30 min in transport buffer. Uptake experiments were initiated by replacing the buffer in the donor compartment with transport buffer containing [ $^{14}\text{C}$ ]metformin (0.15 $\mu\text{Ci/mL}$ ) at a final concentration of 10 $\mu\text{M}$ . The AP uptake into the Caco-2 cell monolayers was determined during the initial linear uptake range at 5 min. Uptake was stopped by washing the cell monolayers with 4°C transport buffer three times in each compartment at the indicated time point. The cell monolayers were allowed to dry, excised from the

insert, and placed in 500  $\mu$ L of 0.1% SDS in 0.1N NaOH for 3 hours, while shaking. Protein content of the cell lysate was determined by the bicinchoninic acid (BCA) protein assay (Pierce, Rockford, IL, USA) with bovine serum albumin as a standard. Metformin in the cell lysate was analyzed by liquid scintillation spectrometry, and the rate of initial uptake of metformin was determined.

Metformin efflux across the AP and BL membranes of Caco-2 cell monolayers was determined using cells that were treated for 3 days with 1,25-(OH)<sub>2</sub>D<sub>3</sub> [100nM] or vehicle control. Cell monolayers were preincubated in transport buffer at 37°C for 30 min, after which they were preloaded from the AP side by incubating for 60 min with 10 $\mu$ M [<sup>14</sup>C]metformin. The cells were then washed three times with 4°C transport buffer, placed in contact with the 37°C transport buffer in the AP and BL compartments, and the amount of metformin appearing in each compartment was determined at 15, 30, and 60 min. All efflux experiments were conducted in pH 7.4 buffer. The appearance of [<sup>14</sup>C]metformin in the AP and BL compartments was monitored as a function of time. Efflux clearance was determined in the linear range of efflux. Cellular accumulation was determined in separate wells following preloading of metformin ([10 $\mu$ M] and [10mM]) from the AP compartment for 60 min. The cellular accumulation studies provided the starting intracellular concentrations (C<sub>0</sub>) of metformin for efflux clearance calculations.

#### **Polyethylene Glycol (PEG) Permeability Assay**

To evaluate the effect of 1,25-(OH)<sub>2</sub>D<sub>3</sub> on paracellular pores, independent of charge-selectivity, the apparent permeability (P<sub>app</sub>) was determined for a series of noncharged polyethylene glycols (PEGs) across Caco-2 cell monolayers in the presence or absence of 1,25-(OH)<sub>2</sub>D<sub>3</sub> [100nM]. This was achieved by measuring absorptive

transport of PEG oligomers across cell monolayers using a method originally proposed by Watson and colleagues (32) that involves pre-column fluorescent derivatization with 1-NIC and HPLC separation with fluorescent detection (26, 50). Briefly, cell monolayers were preincubated with transport buffer for 30 minutes. The experiment was initiated by replacing the buffer in the donor compartment with transport buffer containing a 5mg/ml mixture of PEG200, PEG400, and PEG900 at a ratio of 2:0.5:1 by weight. Receiver compartments were sampled 0, 60, 120, and 180 minutes. Samples were spiked with an internal standard (20µg purified PEG28) prior to further handling. Samples were dried down in a water bath at 55°C under a stream of nitrogen gas. The samples were derivatized by addition of 20µL of 1-NIC in 100µL of acetone, followed by vortexing for 4 hours at 25°C, and finally adding 50µL of methanol and 500µl of H<sub>2</sub>O to quench excess reagent. The contents of the reaction mixture were extracted twice with diethyl ether. The aqueous phase was transferred to an HPLC vial for analysis. The derivatized PEGs in aqueous sample (100µL) were separated on a bare-silica column (Waters Spherisorb 5.0-µm Silica column, 4.6x150mm, Waters Corporation, Milford, MA, USA). The PEG oligomers were quantified by integration of the HPLC peaks (fluorescence emission detection, excitation at 232 nm, emission at 358nm). Each PEG was quantified using a standard curve obtained with analyte/internal standard (PEG28) peak area ratios.

#### **Quantitative Polymerase Chain Reaction (PCR) to Determine the Expression of Tight Junction and Cation-selective Transporter Genes in Caco-2 Cells Treated with 1,25-Dihydroxyvitamine D<sub>3</sub>**

The expression of genes coding for TJ proteins in Caco-2 cells was determined by quantitative PCR using established methods (51) with minor deviations. Total RNA was

isolated from Caco-2 cell monolayers that were treated with 1,25-(OH)<sub>2</sub>D<sub>3</sub> [100nM] or vehicle control for three days using RNeasy Mini Prep columns (Qiagen, Valencia CA). RNA samples underwent DNA digestion by TURBO DNase (Ambion/Applied Biosystems, Austin, TX, USA) to remove potential genomic DNA contamination. cDNA was synthesized from total Caco-2 RNA (5µg) using Superscript III reverse transcriptase (Invitrogen Corporation, Carlsbad, CA). An equal amount of RNA was included in a No-RT control for each separate RNA sample. Real-time PCR was preformed with 1:50 dilutions (or with 1:10 dilutions for determination of claudin-2 and claudin-16 expression) of the cDNA (in triplicate). For each primer set studied, No-RT and No-Template reaction negative controls were analyzed. Quantitative PCR reactions (25µL total volume) were performed using SYBR Green JumpStartTaq ReadyMix™ (Sigma–Aldrich Co., St. Louis, MO) containing primer pairs at 0.9 or 0.3 µM final reaction concentration and 5 µL of cDNA or negative controls. RT-PCR amplification was performed in a Rotor-Gene 3000 (Corbett Research, Mortlake, Australia) thermal cycler at 95°C for 3 min followed by 40 cycles at 94°C for 15 s, 54°C for 20 s, and 72°C for 25 s. Melting curve analysis was performed following amplification by heating the reactions from 50 to 99°C in 0.2°C intervals while monitoring fluorescence. All primer pairs, except glyceraldehyde 3-phosphate dehydrogenase (GAPDH), organic cation transporter 1 (OCT1), OCT3, novel cation and carnitine transporter 2 (OCTN2), and the plasma membrane monoamine transporter (PMAT), were obtained as QuantiTect™ Primer Assays (Qiagen, Valencia, CA, USA). The gene name, accession number, and assay number are listed in Table 3.S1 in Supplemental Data. QuantiTect™ Primer Assays are bioinformatically validated primer sets that are optimized for use in SYBR Green-based

detection and are designed to have ~100% PCR efficiency for quantitative comparisons. Primer pairs produced single melt temperatures; the amplified products were analyzed using gel electrophoresis (2% agarose gel with 0.5 µg/mL ethidium bromide) to ensure singular products at the appropriate size (Figure 3.S1 in Supplemental Data). The lowest signal threshold at which all amplified samples were above the background was set (approximately 0.2 fluorescence units) and the cycle at which each sample crossed the threshold, or cycle threshold ( $C_t$ ), was determined. Gene products which failed to amplify above the threshold by cycle 35 were assigned as not detected (ND) and were not included in further comparisons. Amplification efficiency for each individual reaction was monitored, as given by the Rotor-Gene software (v.5) comparative quantification function. Amplification efficiencies for all reactions were approximately 100%; therefore no adjustment to the  $C_t$  values was needed.

Human GAPDH expression was determined in each RT-PCR run and served as the normalization control. cDNA preparation, fluorescence threshold, and PCR conditions were identical to those used for target genes in order to calculate the expression of TJ and cation transporter genes in relation to GAPDH. The relative expression for each target gene was calculated by  $2^{\Delta C_t}$ , where  $\Delta C_t = (C_{t, \text{GAPDH}} - C_{t, \text{gene}})$ ; therefore setting the expression value of GAPDH to 1.0. Experimental error was estimated for each gene in each treatment group by comparing the CV (%) of the average  $C_t$  value of that gene,  $\text{error} = [(2^{\%CV})/100] \cdot [\text{relative expression value}]$ . Statistical differences between the relative expression of gene products of control and 1,25-(OH)<sub>2</sub>D<sub>3</sub>-treated Caco-2 cells was determined using the  $\Delta\Delta C_t$  method (35) with unpaired t-test statistical analysis.



### **Gel Electrophoresis and Immunoblotting:**

Immunoblots were performed using methods described previously (42, 52) with minor deviations. Anti-human claudin-2 mouse monoclonal antibody (mAb) (1:4000), anti-human claudin-4 mouse mAb (1:4000), anti-human claudin-7 mouse mAb (1:1500), and anti-human occludin mouse mAb (1:1500 dilution) were obtained from Zymed (Invitrogen, Carlsbad CA, USA). Claudin-12 antibody was purchased from Invitrogen (Carlsbad, CA, USA), but failed to produce distinct bands at the appropriate molecular weight and was not pursued further (data not shown). Caco-2 cells were grown on 1-cm<sup>2</sup> Transwell™ supports for 21 day culture with or without 3-day treatment with 100nM of 1,25-(OH)<sub>2</sub>D<sub>3</sub>. SDS-sample buffer (40% glycerol, 0.25 M Tris (pH 6.8), 8% SDS, 0.4% 2-mercaptoethanol, and ~0.004% bromophenol blue, 100μl) was added to the insert, incubated at room temperature for 10min to lyse the cells, and then frozen at -80°C for future immunoblot analysis. Equal volumes of lysates were subjected to sodium dodecyl sulfate polyacrylamide gel electrophoresis (SDS-PAGE) (13% polyacrylamide gels for claudins, 8% gels for occludin) and transferred to nitrocellulose membranes (0.45μm, Bio-Rad Laboratories, Hercules, CA, USA). Antigen-antibody complexes were detected using horseradish peroxidase conjugated secondary antibodies by enhanced chemiluminescence (ECL) (Amersham Biosciences, GE Healthcare, Piscataway, NJ, USA). Immunoblot protein concentrations were determined by optical densitometry at the identical scan and intensity settings (Odyssey™ Infrared Imaging System, LI-COR Biosciences, Lincoln, NE, USA). TJ protein expression in 1,25-(OH)<sub>2</sub>D<sub>3</sub>-treated Caco-2 cells was reported relative to the expression of these proteins in untreated Caco-2 cells.

## Conformational Search and Molecular Volume Calculation for Organic Solutes

The conformational search and molecular volume calculations were performed on the protonated (e.g. cationic) structure of each organic cation. Each compound was first subjected to a conformational search using stochastic search algorithm (53). The conformational space was searched exhaustively by perturbing both dihedral angle of all rotation bonds and Cartesian coordinates of each atom in the molecule by some small amounts, i.e. 30 degrees and  $[-1\text{\AA}, 1\text{\AA}]$  (the sign was determined randomly), respectively. The current chirality of all constrained chiral centers (that are not easily invertible) in the molecule had been retained during the search. The potential energy setup for conformational evaluation as well as the partial charge calculation employed MMFF94x force field (54, 55) with all explicit hydrogens, and the calculations were conducted in the MOE 2007.09 package (Chemical Computing Group, Montreal, Quebec, Canada). The conformers of the lowest potential energy were rendered to energy minimization prior to be submitted to Gaussian 03 (Gaussian, Inc., Wallingford, CT, USA) for the quantum mechanic calculations. The molecular volume of each molecule was defined as the volume inside a contour of 0.001 electrons/Bohr<sup>3</sup> density and computed by the Hartree-Fock method with 6-311+G basis set (56-59). This value was the volume enclosed by the van der Waals surface (60, 61), which was composed of the union of the spherical atomic surfaces defined by the van der Waals radius of each component atom in the molecule. The geometry had been further optimized within Gaussian 03 at the same level by the Berny algorithm.

## Data Analysis

Transport of the compounds examined this report was expressed as the apparent permeability ( $P_{app}$ ) and is described by the following equation:

$$P_{app} = \frac{dX/dt}{(A * C_o)} \quad (1)$$

where  $dX/dt$  is the mass of compound (X) transported over time (t), A is the surface area of the Transwell™ porous membrane, and  $C_o$  is the initial concentration in the donor compartment. All data are expressed as mean  $\pm$  SD from 4 measurements. Statistical significance was evaluated using unpaired *t* tests or 2-way analysis of variance analysis (ANOVA) with Bonferroni's post-test correction as noted.

Metformin uptake data, reported as amount taken up per minute, were corrected for total protein content of the monolayer, and expressed as  $\text{pmol} \cdot \text{min}^{-1} \cdot \text{mg protein}^{-1}$ . Efflux clearance ( $CL_{eff}$ ) values at both membrane barriers (e.g. AP and BL) were calculated using Eq. (3.2):

$$CL_{eff} = \frac{dX/dt}{C_o} \quad (3.2)$$

where  $dX/dt$  represents the mass of metformin effluxed (X) into the AP or BL compartment over time (t), determined in the linear region of efflux, and  $C_o$  is the estimated initial intracellular concentration of metformin. Initial intracellular concentrations, which is another term for cellular accumulation, were calculated from the amount loaded into the Caco-2 cells, using the cellular volume of  $3.66 \mu\text{L}/\text{mg protein}$  (62, 63) or  $0.732 \mu\text{L}/\text{cells}$  on  $1 \text{ cm}^2$  Transwell™ insert with average protein content  $0.2 \text{ mg}$ .

The hydrodynamic radius for each PEG molecule was calculated by Eq. 3.3 reported previously (64):

$$r = 0.29(M)^{0.454} \quad (3.3)$$

where  $r$  is the hydrodynamic radius in Å and  $M$  is the molecular mass of each PEG oligomer. Statistical significance was determined using two-way ANOVA with Bonferroni post-test analysis. PEG permeability studies were done with  $n=4$  for each treatment group. Experiments were repeated in triplicate.

The size-restricted pore radius, or paracellular aqueous pore radius, of the Caco-2 cell monolayers was calculated from the ratio of the corrected paracellular  $P_{app}$  of pairs of two small PEG species with radii 3.2 and 3.5 Å using a Renkin molecular sieving function as described previously (25, 65). Briefly, the pore size in terms of radius ( $R$ ) of the Caco-2 cell monolayer was determined the ratio of apparent permeability values of each solute to the following equation:

$$\frac{P_{app,x}}{P_{app,y}} = \frac{r_y F(r_x / R)}{r_x F(r_y / R)} \quad (3.4)$$

where  $x$  and  $y$  are a solute pair,  $r$  is the radius of each respective solute,  $R$  is the radius of the pore system, and  $F(r/R)$  is the Renkin function that is described by the following equation:

$$F\left(\frac{r}{R}\right) = \left(1 - \left(\frac{r}{R}\right)\right)^2 \left[1 - 2.104\left(\frac{r}{R}\right) + 2.09\left(\frac{r}{R}\right)^3 - 0.95\left(\frac{r}{R}\right)^5\right] \quad (3.5)$$

By substituting Eq. 3.5 into Eq. 3.4, the final equation used to calculate the radius of the pore in Caco-2 system was derived and seen below in Eq. 3.6:

$$\frac{P_{app,x}}{P_{app,y}} = \frac{r_y}{r_x} \left[ \frac{\left(1 - \left(\frac{r_x}{R}\right)\right)^2 \left[1 - 2.104\left(\frac{r_x}{R}\right) + 2.09\left(\frac{r_x}{R}\right)^3 - 0.95\left(\frac{r_x}{R}\right)^5\right]}{\left(1 - \left(\frac{r_y}{R}\right)\right)^2 \left[1 - 2.104\left(\frac{r_y}{R}\right) + 2.09\left(\frac{r_y}{R}\right)^3 - 0.95\left(\frac{r_y}{R}\right)^5\right]} \right] \quad (3.6)$$

The calculated pore radius (R) was determined using the mean  $P_{app}$  values obtained for each solute. Radius values were determined for both control and vitamin D<sub>3</sub> treated Caco-2 cell monolayers for each solute pair.

### **3.F. ACKNOWLEDGEMENTS:**

We would like to acknowledge Dr. Simon Wang (UNC-Eshelman School of Pharmacy, UNC-Chapel Hill, Chapel Hill, NC) for his contribution to this work regarding molecular modeling and helpful insight regarding radius estimates. We would also like to acknowledge Dr. Christina Van Itallie and Jennifer Holmes (UNC-School of Medicine, UNC-Chapel Hill) for their contributions to this work and invaluable technical assistance, resources, and intellectual discussions. We acknowledge Dr. Mary F. Paine (UNC-Eshelman School of Pharmacy, UNC-Chapel Hill, Chapel Hill, NC) for generously providing the Caco-2 P27.7 cells and for her help and resources during these studies. Funding for this work was provided by Amgen, Inc. and the PhRMA Foundation in the form of pre-doctoral fellowships awarded to William Proctor.

## TABLES AND FIGURES

**Table 3.1. Calculated molecular radius for hydrophilic organic solutes in relation to reported values.**

Compound	Molar Volume <sup>a</sup>	Calculated Radius <sup>b</sup>	Range of Reported Radius	References
	cm <sup>3</sup> /mol	Å	Å	
Methylamine	33.04	2.36	1.9 - 2.7	(25, 65, 66)
Guanidine	42.35	2.56	NA	
1-Methylguanidine	63.79	2.94	NA	
Metformin	89.15	3.28	NA	
TEA	131.52	3.74	3.3 - 4.0	(25, 67)
Mannitol	152.43	3.92	3.6 - 4.3	(45, 65, 66, 68)
Atenolol	221.51	4.45	4.2 - 4.8	(65, 66)

<sup>a</sup> Molar volume was determined by Gaussian 3.0 software for each compound using the most thermodynamically favored confirmation (refer to methods section).

<sup>b</sup> Calculated radius values were determined from molar volume values assuming volume of a sphere. NA: not available

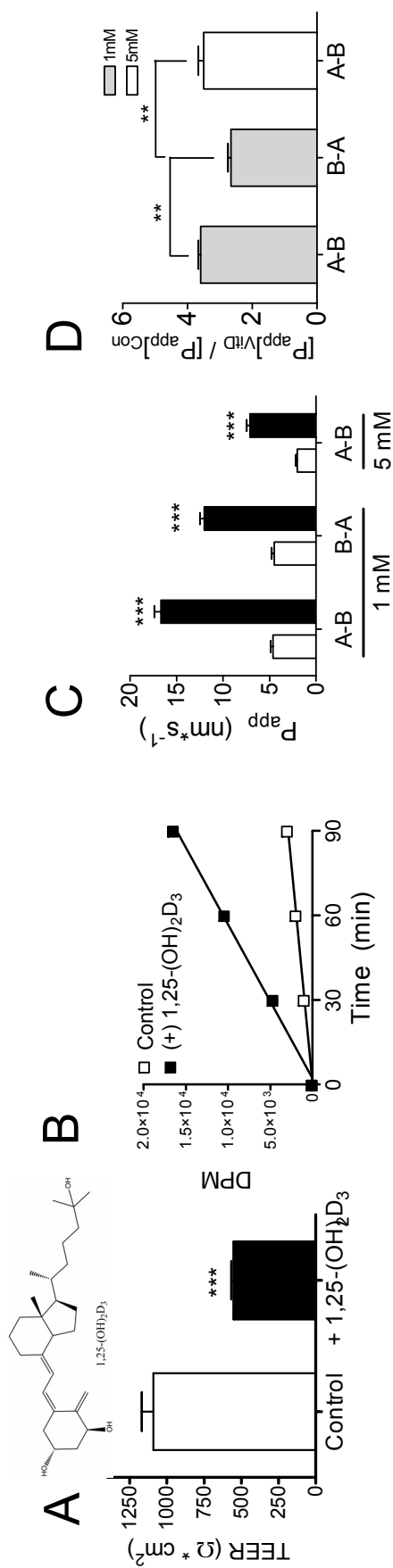


**Figure 3.1. Vitamin D<sub>3</sub>-mediated induction of calcium transport across Caco-2 cell monolayers.** (A) The effect of 3-day treatment 1,25-(OH)<sub>2</sub>D<sub>3</sub> (structure of 1,25-(OH)<sub>2</sub>D<sub>3</sub> is depicted above graph) on TEER. (B) Appearance of [<sup>45</sup>Ca<sup>+2</sup>] in the receiver compartment was measured as a function of time across Caco-2 cell monolayers, treated 3 days prior to transport experiment (■) with 1,25-(OH)<sub>2</sub>D<sub>3</sub> [100nM] or (□) with vehicle control. Apparent permeability (P<sub>app</sub>) of [<sup>45</sup>Ca<sup>+2</sup>] in both the absorptive (A-B) and secretory (B-A) directions for [1mM] donor concentration and A-B transport for [5mM] donor concentrations are reported as raw values (C) or as the ratio of the 1,25-(OH)<sub>2</sub>D<sub>3</sub>-treated P<sub>app</sub> (P<sub>app</sub>[VITD]), and the control cell P<sub>app</sub> (P<sub>app</sub>[Con]), for [1mM] (grey bars) and [5mM] (open bars) (D). Statistical differences between control and vitamin D<sub>3</sub>-treated (+1,25-(OH)<sub>2</sub>D<sub>3</sub>) monolayers were performed using 2-way ANOVA with Bonferroni post-test analysis. Data represents mean ± S.D; n=4 \*\*p<0.01, \*\*\*p<0.001.



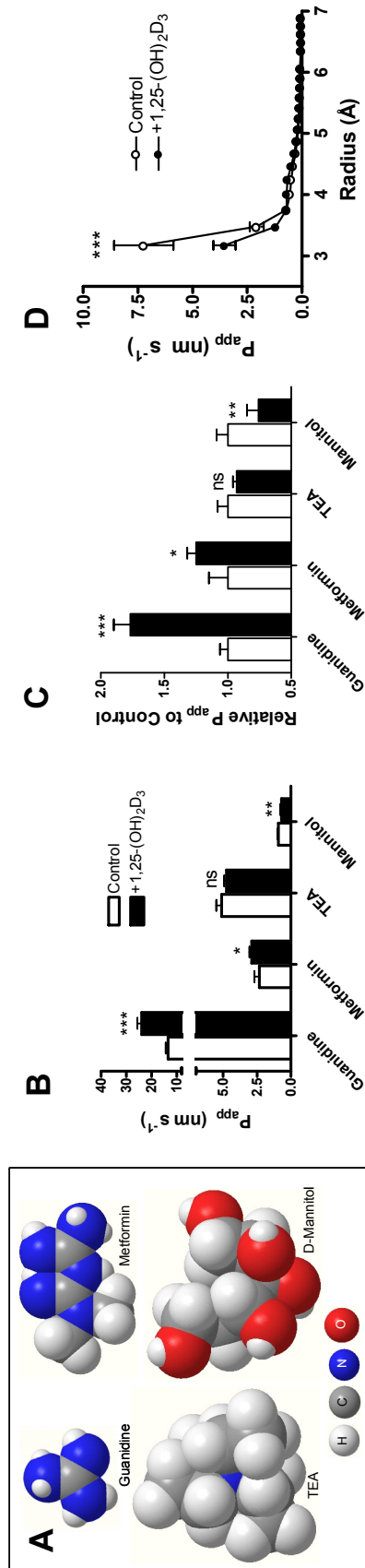


**Figure 3.2: Effect of vitamin D<sub>3</sub>-treatment on absorptive transport of hydrophilic compounds across Caco-2 cell monolayers.** The structures of the hydrophilic compounds are depicted with space-filling models (A). Apparent permeability ( $P_{app}$ ) for guanidine, metformin, TEA, and mannitol in the absorptive (AP-BL) direction at 10  $\mu$ M donor concentrations across Caco-2 cells treated for 3 days prior to the transport experiment with 1,25-(OH)<sub>2</sub>D<sub>3</sub> [100nM] (closed bars) or vehicle control (open bars); permeability values are reported as raw values (B) or relative to control values (C). The absorptive transport for guanidine was linear and obeyed sink conditions (e.g. < 10% of compound transported) up to 60 min, while transport of metformin, TEA, and mannitol was linear to hydrodynamic radius across Caco-2 cells treated for 3 days with 1,25-(OH)<sub>2</sub>D<sub>3</sub> [100nM] (●) or vehicle control (○) (D). Statistical difference was determined by 2-way ANOVA with Bonferroni post-test analysis. Data represent mean  $\pm$  SD, n=4. \*p<0.05, \*\*p<0.01, \*\*\*p<0.001, ns (not significant).

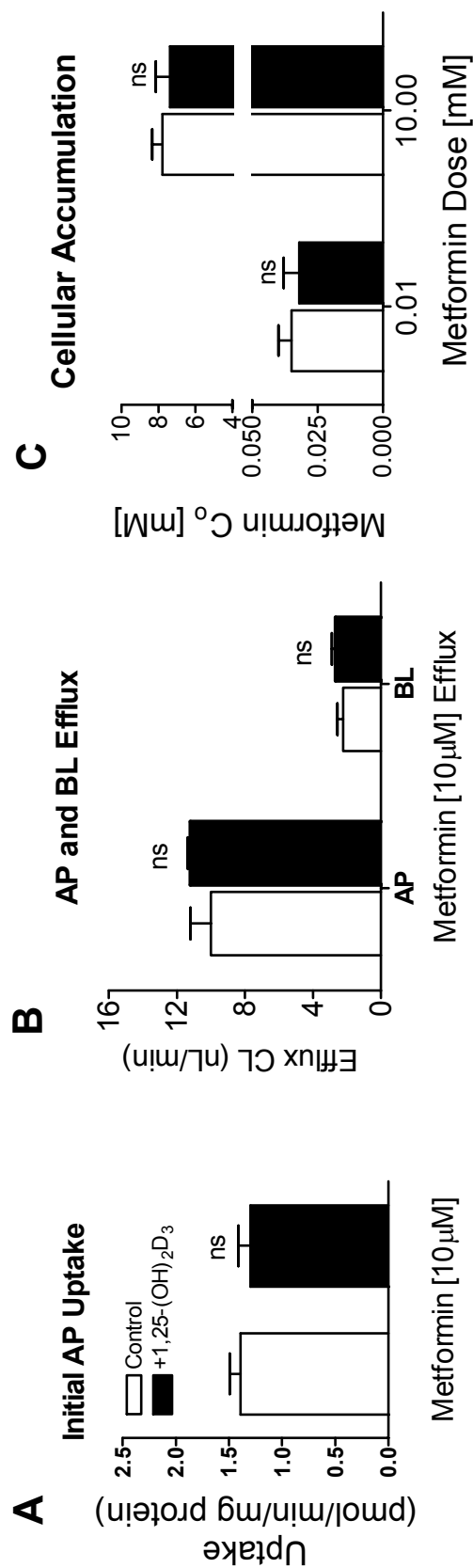


**Figure 3.3: Transcellular transport of metformin is not affected by vitamin D<sub>3</sub>-treatment.** (A) Initial AP uptake of metformin [10µM] in the 1,25(OH)<sub>2</sub>D<sub>3</sub>-treated [100 nM] (closed bars) or vehicle control (open bars) cells; (B) AP and BL efflux clearance following AP metformin [10µM] loading for 60 min in 1,25(OH)<sub>2</sub>D<sub>3</sub>-treated [100 nM] (closed bars) or vehicle control (open bars) cells. (C) Cellular accumulation of metformin reported as cellular concentration (C<sub>0</sub>) following AP dosing of metformin for 60 min at 0.01 and 10.0 mM donor concentrations in the 1,25(OH)<sub>2</sub>D<sub>3</sub>-treated [100 nM] (closed bars) or vehicle control (open bars) cells. Cellular concentration was determined based on the volume of Caco-2 cells of 3.66 µL mg protein<sup>-1</sup> [(62, 63) (refer to Methods section)]. Data represents mean ± S.D; n=4, ns (not significant)

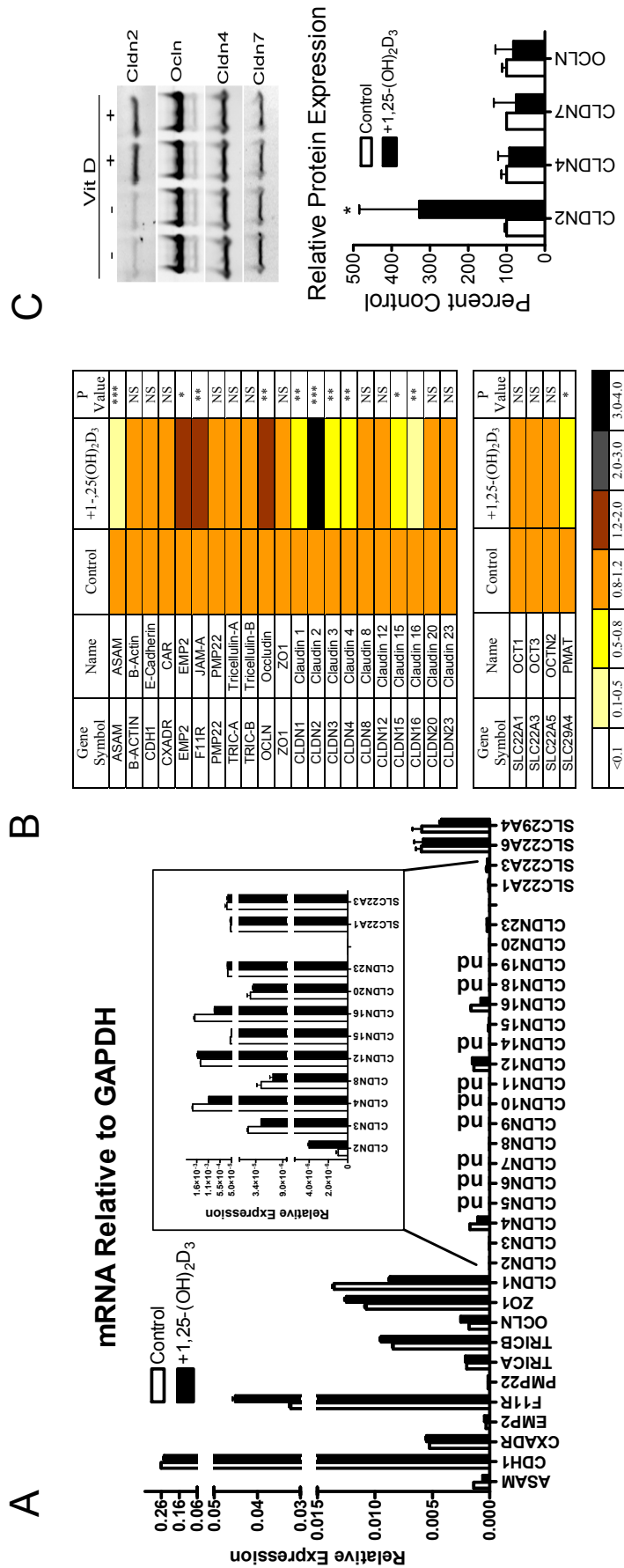


**Figure 3.4. Effect of vitamin D<sub>3</sub>-treatment on tight-junction gene products and protein expression.** (A) mRNA expression of TJ proteins and organic cation transporters relative to GAPDH expression in Caco-2 cell monolayers treated for 3 days with 1,25-(OH)<sub>2</sub>D<sub>3</sub> [100nM] (closed bars) or vehicle control (open bars). Data represents mean  $\pm$  S.D., n=3. The relative expression data is depicted in relation to control mRNA expression values in panel B (the font in the table is too small). (C, top panel) Protein expression measured by a representative Western blot of claudin-2 (CLDN2), occludin (Ocln), claudin-4 (CLDN4), and claudin-7 (CLDN7) in cells that were treated for 3 days with 1,25-(OH)<sub>2</sub>D<sub>3</sub> [100nM] (+Vit D) and control (- Vit D). The change in each TJ protein levels were calculated relative to control values by densitometry analysis (C, bottom panel). Data represent mean  $\pm$  S.D., n=4. \*p<0.05, \*\*p<0.01, \*\*\*p<0.001, nd (not detected).

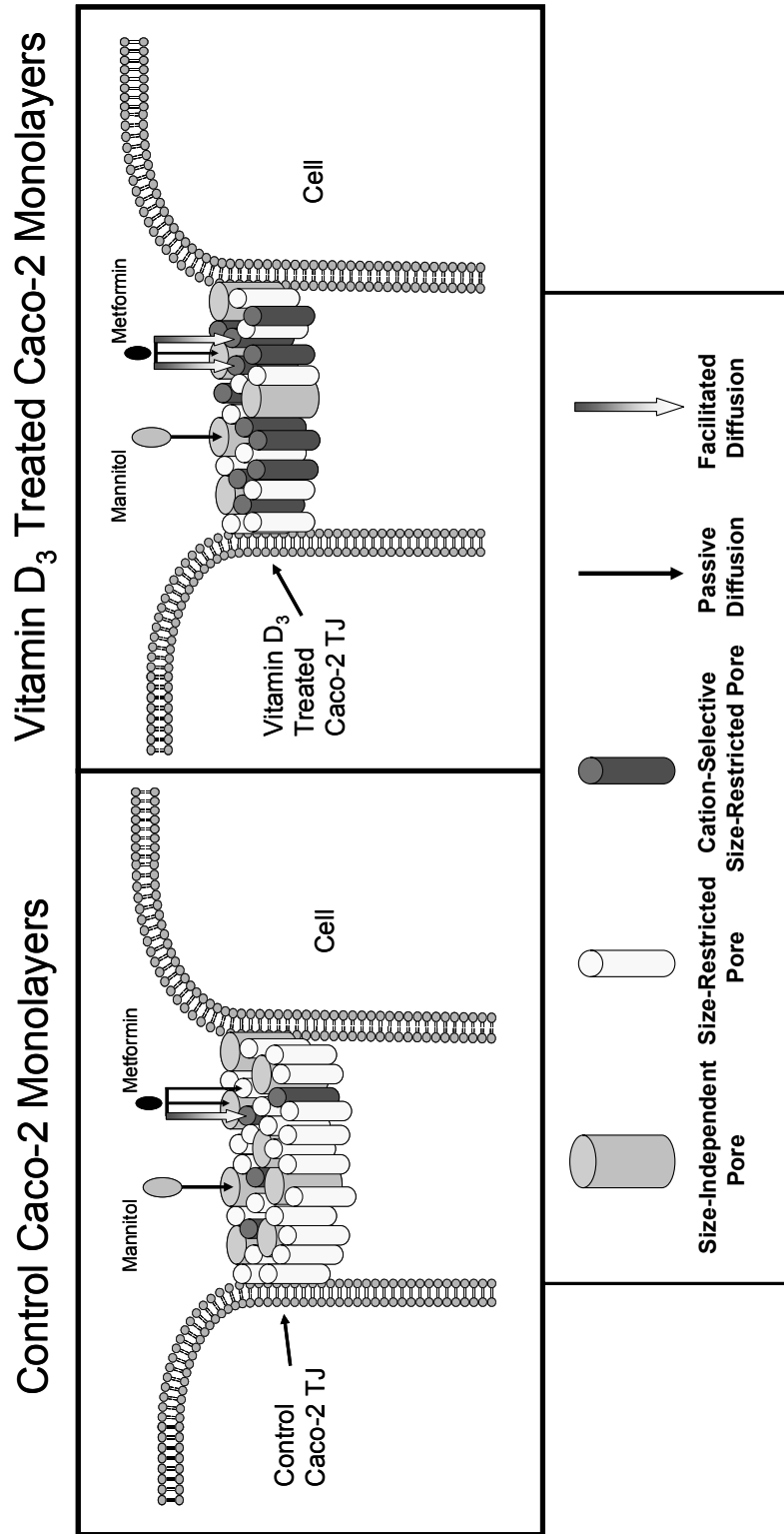


**Figure 3.5: Schematic diagram of the effects of vitamin D<sub>3</sub> on the tight junctions in Caco-2 P27.7 cell monolayers.** Mannitol and metformin paracellular permeation is postulated to be affected by vitamin D<sub>3</sub> induced changes to the TJ pore populations. Mannitol can only permeate through the size-independent pore, while metformin can diffuse through both the size-independent and size-restricted pores. In addition, the cation-selective pores formed by claudin-2 can also facilitate metformin paracellular transport. Vitamin D<sub>3</sub>-treatment causes a reduction in the size-independent pore, causing a decrease in mannitol and metformin passive diffusion through this pore. Additionally, vitamin D<sub>3</sub>-treatment increases the number of claudin-2 cation-selective size-restricted pores at the TJ facilitating metformin diffusion through the TJ, while simultaneously reducing the overall porosity of size-restricted pore of the monolayer.

### 3.G. SUPPLEMENTAL MATERIAL

**Table 3.S1:** List of primer sequences and amplified product size for TJ and cation-selective transporters gene products

Gene	Name	Accession	5' Primer	3' Primer	Product Size (bp)
GAPDH	GAPDH	NM_002046	GACCCCTTCATTGACCTCAACTAC	TTGACGGTGCATGGAATTT	80
ACTB	B-Actin	NM_001101	GCGGGAAATCGTGGTGACATT	GATGGAGTTGAAGTAGTTTCGTG	232
ASAM	ASAM	NM_024769	NA (QT00079751)	NA (QT00079751)	71
CDH1	E-Cadherin	NM_004360	NA (QT00080143)	NA (QT00080143)	84
CLDN1	Claudin-1	NM_021101	NA (QT00225764)	NA (QT00225764)	122
CLDN2	Claudin-2	NM_020384	NA (QT00089481)	NA (QT00089481)	128
CLDN3	Claudin-3	NM_001306	NA (QT00201376)	NA (QT00201376)	109
CLDN4	Claudin-4	NM_001305	NA (QT00241073)	NA (QT00241073)	103
CLDN5	Claudin-5	NM_003277	NA (QT00232197)	NA (QT00232197)	110
CLDN6	Claudin-6	NM_021195	NA (QT00235193)	NA (QT00235193)	96
CLDN7	Claudin-7	NM_001307	NA (QT00236061)	NA (QT00236061)	94
CLDN8	Claudin 8	NM_199328	NA (QT00212268)	NA (QT00212268)	110
CLDN9	Claudin 9	NM_020982	NA (QT00209482)	NA (QT00209482)	98
CLDN10	Claudin 10	NM_182848	NA (QT01012200)	NA (QT01012200)	103
CLDN11	Claudin 11	NM_005602	NA (QT00008085)	NA (QT00008085)	110
CLDN12	Claudin 12	NM_012129	NA (QT01012186)	NA (QT01012186)	145
CLDN14	Claudin 14	NM_012130	NA (QT00234731)	NA (QT00234731)	67
CLDN15	Claudin 15	NM_014343	NA (QT00202048)	NA (QT00202048)	66
CLDN16	Claudin 16	NM_006580	NA (QT00029655)	NA (QT00029655)	78
CLDN18	Claudin 18	NM_0010020206	NA (QT00039550)	NA (QT00039550)	138
CLDN19	Claudin 19	NM_148960	NA (QT00083475)	NA (QT00083475)	105
CLDN20	Claudin 20	NM_001001346	NA (QT00218057)	NA (QT00218057)	75
CLDN23	Claudin 23	NM_194284	NA (QT00213402)	NA (QT00213402)	60
CXADR	CAR	NM_001338	NA (QT00075460)	NA (QT00075460)	80
EMP2	EMP2	NM_001424	NA (QT00100695)	NA (QT00100695)	77
F11R	JAM-A	NM_016946	NA (QT00083972)	NA (QT00083972)	65
JAM3	JAM-3	NM_032801	NA (QT00024997)	NA (QT00024997)	81
OCN	Occludin	NM_002538	NA (QT00081844)	NA (QT00081844)	69
PMP22	PMP22	NM_000304	NA (QT00050064)	NA (QT00050064)	101
MARVELD2	TRIC-A	NM_144724	NA (QT01154986)	NA (QT01154986)	136
MARVELD2	TRIC-B	NM_001038603	NA (QT01154993)	NA (QT01154993)	80
TJPI	ZO1	NM_003257	NA (QT00077308)	NA (QT00077308)	75
SLC22A1	OCT1	NM_003057	GACGCCGAGAACCTGGG	GGTAGGCAAGTATGAGG	198
SLC22A3	OCT3	NM_021977	GGAGTTCTGCTCTGTCAGG	GGAATGTGGACTGCCAAGTT	216
SLC22A5	OCTN2	NM_003060	AGTGGGCTATTTGGGCTTT	GGTCGTAGGCACCAAGGTAA	398
SLC29A4	PMAT	NM_001040661	TTCATCACGGACGTGGACTA	CGTCGCAGATGCTGATAAAA	202

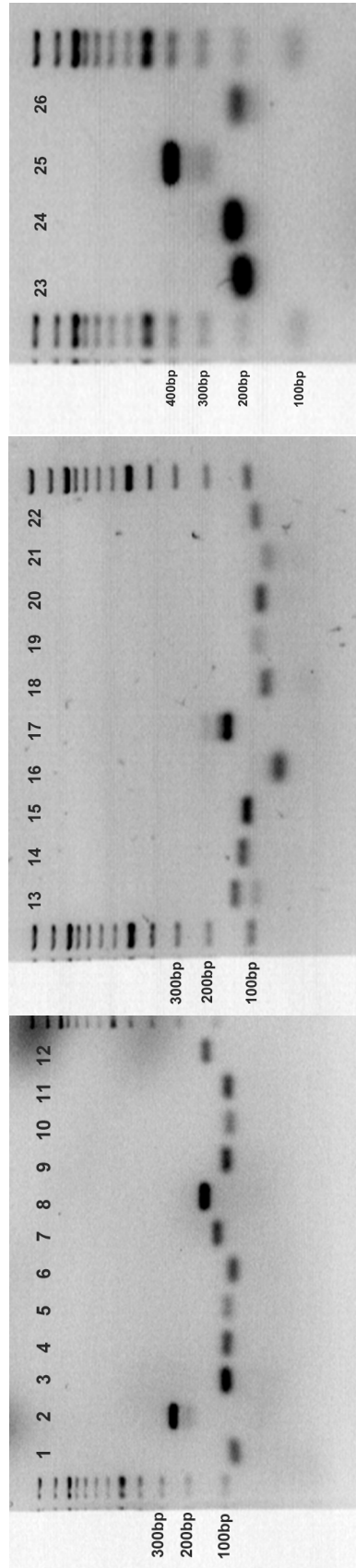


**Figure 3.S1. Gel electrophoresis of the reverse transcription-polymerase chain reaction (RT-PCR) primer products.** RT-PCR amplified products were separated on 2% agarose with 0.5µg/ml ethidium bromide. PCR primer amplified products designated in each lane as follows: (1) ASAM (2) B-ACTIN (3) CDH1 (4) CXADR (5) EMP2 (6) F11R (7)PMP22 (8)TRICA (9) TRICB (10) OCLN (11) ZO1 (12) CLDN1 (13) CLDN2 (14)CLDN3 (15) CLDN4 (16) CLDN8 (17) CLDN12 (18) CLDN15 (19) CLDN16 (20) CLDN20 (21) CLDN23 (22) GAPDH (23) SLC22A1 (24) SLC22A3 (25) SLC22A5 (26) SLC29A4. Amplified products and accession numbers for each primer pair can be seen in Table 3.S1 in Supplemental Material.

### 3.H. REFERENCES

1. Shu, Y., Sheardown, S. A., Brown, C., Owen, R. P., Zhang, S., Castro, R. A., Ianculescu, A. G., Yue, L., Lo, J. C., Burchard, E. G., Brett, C. M. & Giacomini, K. M. (2007) *J Clin Invest* **117**, 1422-31.
2. Shu, Y., Brown, C., Castro, R. A., Shi, R. J., Lin, E. T., Owen, R. P., Sheardown, S. A., Yue, L., Burchard, E. G., Brett, C. M. & Giacomini, K. M. (2008) *Clin Pharmacol Ther* **83**, 273-80.
3. Zhou, M., Xia, L. & Wang, J. (2007) *Drug Metab Dispos* **35**, 1956-62.
4. Bailey, C. J. & Nattrass, M. (1988) *Baillieres Clin Endocrinol Metab* **2**, 455-76.
5. Hermann, L. & Melander, A. (1992) in *International Textbook of Diabetes Mellitus*, eds. Alberti, K., DeFronzo, R., Keen, H. & Zimmet, P. (John Wiley & Sons Inc., New York), pp. 773-95.
6. Stepensky, D., Friedman, M., Raz, I. & Hoffman, A. (2002) *Drug Metab Dispos* **30**, 861-8.
7. Bailey, C. J., Mynett, K. J. & Page, T. (1994) *Br J Pharmacol* **112**, 671-5.
8. Bailey, C. J., Wilcock, C. & Scarpello, J. H. (2008) *Diabetologia* **51**, 1552-3.
9. Tucker, G. T., Casay, C., Phillips, P. J., Connor, H., Ward, J. D. & Woods, H. F. (1981) *J Clin. Pharmac.* **12**, 235-246.
10. Scheen, A. J. (1996) *Clin. Pharmacokinet.* **30**, 359-371.
11. Sambol, N. C., Chiang, J., O'Conner, M., Liu, C. Y., Lin, E. T., Goodman, A. M., Benet, L. Z. & Haram, J. H. (1996) *J Clin Pharmacol* **36**, 1012-1021.
12. Proctor, W. R., Bourdet, D. L. & Thakker, D. R. (2008) *Drug Metab Dispos* **36**, 1650-8.

13. Bourdet, D. L., Lee, K. & Thakker, D. R. (2004) *J Med Chem* **47**, 2935-8.
14. Bourdet, D. L., Pollack, G. M. & Thakker, D. R. (2006) *Pharm Res* **23**, 1178-87.
15. Soergel, K. H. (1993) *Gastroenterology* **105**, 1247-50.
16. Colegio, O. R., Van Itallie, C. M., McCrea, H. J., Rahner, C. & Anderson, J. M. (2002) *Am J Physiol Cell Physiol* **283**, C142-7.
17. Fujita, H., Sugimoto, K., Inatomi, S., Maeda, T., Osanai, M., Uchiyama, Y., Yamamoto, Y., Wada, T., Kojima, T., Yokozaki, H., Yamashita, T., Kato, S., Sawada, N. & Chiba, H. (2008) *Mol Biol Cell* **19**, 1912-21.
18. Van Itallie, C. M. & Anderson, J. M. (2006) *Annu Rev Physiol* **68**, 403-29.
19. Banan, A., Zhang, L. J., Shaikh, M., Fields, J. Z., Choudhary, S., Forsyth, C. B., Farhadi, A. & Keshavarzian, A. (2005) *J Pharmacol Exp Ther* **313**, 962-82.
20. Yu, A. S., Enck, A. H., Lencer, W. I. & Schneeberger, E. E. (2003) *J Biol Chem* **278**, 17350-9.
21. Alexandre, M. D., Lu, Q. & Chen, Y. H. (2005) *J Cell Sci* **118**, 2683-93.
22. Van Itallie, C., Rahner, C. & Anderson, J. M. (2001) *J Clin Invest* **107**, 1319-27.
23. Colegio, O. R., Van Itallie, C., Rahner, C. & Anderson, J. M. (2003) *Am J Physiol Cell Physiol* **284**, C1346-54.
24. Hou, J., Paul, D. L. & Goodenough, D. A. (2005) *J Cell Sci* **118**, 5109-18.
25. Yu, A. S., Cheng, M. H., Angelow, S., Gunzel, D., Kanzawa, S. A., Schneeberger, E. E., Fromm, M. & Coalson, R. D. (2009) *J Gen Physiol* **133**, 111-27.



26. Van Itallie, C. M., Holmes, J., Bridges, A., Gookin, J. L., Coccaro, M. R., Proctor, W., Colegio, O. R. & Anderson, J. M. (2008) *J Cell Sci* **121**, 298-305.
27. Fleet, J. C., Eksir, F., Hance, K. W. & Wood, R. J. (2002) *Am J Physiol Gastrointest Liver Physiol* **283**, G618-25.
28. Schmiedlin-Ren, P., Thummel, K. E., Fisher, J. M., Paine, M. F., Lown, K. S. & Watkins, P. B. (1997) *Mol Pharmacol* **51**, 741-54.
29. Paine, M. F., Leung, L. Y., Lim, H. K., Liao, K., Oganessian, A., Zhang, M. Y., Thummel, K. E. & Watkins, P. B. (2002) *J Pharmacol Exp Ther* **301**, 174-86.
30. Fleet, J. C. & Wood, R. J. (1999) *Am J Physiol* **276**, G958-64.
31. Kumar, R. (1995) *J Cell Biochem* **57**, 392-8.
32. Watson, C. J., Rowland, M. & Warhurst, G. (2001) *Am J Physiol Cell Physiol* **281**, C388-97.
33. Van Itallie, C. M., Holmes, J., Bridges, A. & Anderson, J. M. (2009) *Ann N Y Acad Sci* **1165**, 82-7.
34. Kong, J., Zhang, Z., Musch, M. W., Ning, G., Sun, J., Hart, J., Bissonnette, M. & Li, Y. C. (2008) *Am J Physiol Gastrointest Liver Physiol* **294**, G208-16.
35. Livak, K. J. & Schmittgen, T. D. (2001) *Methods* **25**, 402-8.
36. Alexandre, M. D., Jeansonne, B. G., Renegar, R. H., Tatum, R. & Chen, Y. H. (2007) *Biochem Biophys Res Commun* **357**, 87-91.
37. Hayer-Zillgen, M., Bruss, M. & Bonisch, H. (2002) *Br J Pharmacol* **136**, 829-36.

38. Englund, G., Rorsman, F., Ronnblom, A., Karlbom, U., Lazorova, L., Grasjo, J., Kindmark, A. & Artursson, P. (2006) *Eur J Pharm Sci* **29**, 269-77.
39. Kimura, N., Masuda, S., Tanihara, Y., Ueo, H., Okuda, M., Katsura, T. & Inui, K. (2005) *Drug Metab Pharmacokinet* **20**, 379-86.
40. Nies, A. T., Koepsell, H., Winter, S., Burk, O., Klein, K., Kerb, R., Zanger, U. M., Keppler, D., Schwab, M. & Schaeffeler, E. (2009) *Hepatology* **50**, 1227-40.
41. Chirayath, M. V., Gajdzik, L., Hulla, W., Graf, J., Cross, H. S. & Peterlik, M. (1998) *Am J Physiol* **274**, G389-96.
42. Van Itallie, C. M., Fanning, A. S. & Anderson, J. M. (2003) *Am J Physiol Renal Physiol* **285**, F1078-84.
43. Amasheh, S., Meiri, N., Gitter, A. H., Schoneberg, T., Mankertz, J., Schulzke, J. D. & Fromm, M. (2002) *J Cell Sci* **115**, 4969-76.
44. Hou, J., Gomes, A. S., Paul, D. L. & Goodenough, D. A. (2006) *J Biol Chem* **281**, 36117-23.
45. Schultz, S. G. & Solomon, A. K. (1961) *J Gen Physiol* **44**, 1189-99.
46. Laukoetter, M. G., Nava, P., Lee, W. Y., Severson, E. A., Capaldo, C. T., Babbitt, B. A., Williams, I. R., Koval, M., Peatman, E., Campbell, J. A., Dermody, T. S., Nusrat, A. & Parkos, C. A. (2007) *J Exp Med* **204**, 3067-76.
47. Lim, W. C., Hanauer, S. B. & Li, Y. C. (2005) *Nat Clin Pract Gastroenterol Hepatol* **2**, 308-15.
48. Cantorna, M. T., Munsick, C., Bemiss, C. & Mahon, B. D. (2000) *J Nutr* **130**, 2648-52.
49. Bourdet, D. L. & Thakker, D. R. (2006) *Pharm Res* **23**, 1165-77.

50. Rissler, K., Wytenbach, N. & Bornsen, K. (1998) *J. Chromatogr. A* **822**, 189-206.
51. Holmes, J. L., Van Itallie, C. M., Rasmussen, J. E. & Anderson, J. M. (2006) *Gene Expr Patterns* **6**, 581-8.
52. Van Itallie, C. M., Fanning, A. S., Bridges, A. & Anderson, J. M. (2009) *Mol Biol Cell* **20**, 3930-40.
53. Ferguson, D. M. & Raber, D. J. (1989) *Journal of the American Chemical Society* **111**, 4371-4378.
54. Halgren, T. A. (1999) *Journal of Computational Chemistry* **20**, 730-748.
55. Halgren, T. A. (1999) *Journal of Computational Chemistry* **20**, 720-729.
56. Blaudeau, J. P., McGrath, M. P., Curtiss, L. A. & Radom, L. (1997) *Journal of Chemical Physics* **107**, 5016-5021.
57. Raghavachari, K., Binkley, J. S., Seeger, R. & Pople, J. A. (1980) *The Journal of Chemical Physics* **72**, 650-654.
58. McLean, A. D. & Chandler, G. S. (1980) *The Journal of Chemical Physics* **72**, 5639-5648.
59. Curtiss, L. A., McGrath, M. P., Blaudeau, J.-P., Davis, N. E., Binning, R. C. & Radom, L. (1995) *Journal of Chemical Physics* **103**, 6104.
60. Whitley, D. (1998) *Journal of Mathematical Chemistry* **23**, 377-397.
61. Petitjean, M. (1994) *Journal of Computational Chemistry* **15**, 507-523.
62. Blais, A., Bissonnette, P. & Berteloot, A. (1987) *J. Membr. Biol.* **99**, 113-125.

63. Dantzig, A. H. & Bergin, L. (1990) *Biochim Biophys Acta* **1027**, 211-217.
64. Ruddy, S. B. & Hadzija, B. W. (1992) *Drug Des Discov* **8**, 207-24.
65. Knipp, G. T., Ho, N. F., Barsuhn, C. L. & Borchardt, R. T. (1997) *J Pharm Sci* **86**, 1105-10.
66. Avdeef, A. (2010) *Pharm Res* **In Press**.
67. Wang, H. Z. & Veenstra, R. D. (1997) *J Gen Physiol* **109**, 491-507.
68. Steward, M. C. (1982) *J Physiol* **322**, 419-39.

## **CHAPTER 4**

### **CLAUDIN-2 FACILITATES PARACELLULAR TRANSPORT OF SMALL ORGANIC CATIONS ACROSS EPITHELIAL MONOLAYERS: A MOLECULAR MECHANISM FOR SATURABLE PARACELLULAR TRANSPORT OF METFORMIN AND OTHER ORGANIC CATIONS**

#### 4.A. ABSTRACT

Metformin paracellular transport was increased following treatment with the active metabolite of vitamin D<sub>3</sub>. It was shown that a tight-junction (TJ) protein, claudin-2, was selectively induced by this treatment. Claudin-2 is a transmembrane protein that is believed to form pores in the TJ that preferentially transports cations through electrostatic interactions with anionic residues in its extracellular loops (Yu et al., 2009). The goal of this report was to determine whether claudin-2 protein directly interacts with metformin and similar organic cations. To achieve this, the absorptive transport of a small panel of organic cations, including metformin, was examined across a LLC-PK<sub>1</sub> epithelial cell model that exogenously expressed claudin-2 under the control of an inducible promoter (Van Itallie et al., 2003). Monolayer integrity was monitored by mannitol transport, which increased upwards of 40% at high levels of claudin-2 induction. Increasing claudin-2 protein expression to a maximum at which mannitol transport was not significantly increased resulted in a 12-, 4-, and 2-fold increase in [Ca<sup>+2</sup>], guanidine, and 1-methylguanidine absorptive transport. This was the first direct evidence that claudin-2 facilitated diffusion of organic cations at levels that did not affect overall monolayer integrity. Surprisingly, metformin and tetraethylammonium (TEA) transport were not affected by claudin-2 expression. Using molecular radius estimates for guanidine and 1-methylguanidine and their respective changes to absorptive transport, the claudin-2 pore radius was estimated to be approximately 4 Å. This estimate was not different from the basal uninduced size-restricted LLC-PK<sub>1</sub> pore radius, supporting a previous report that claudin-2 expression did not alter pore size but increases porosity in MDCK C7 cells (Van Itallie et al., 2008).

#### **4.B. INTRODUCTION**

Metformin has been shown to be primarily absorbed across Caco-2 cell monolayers, the established intestinal cell model, via the paracellular route (Proctor et al., 2008). Although metformin was taken up efficiently across the apical (AP) membrane of Caco-2 cells, the transcellular route contributed very little to the absorptive transport of metformin because metformin could not egress efficiently from the cells across the basolateral (BL) membrane, presumably due to the absence of a cation-selective efflux transporter at the BL membrane. Cellular kinetic studies clearly demonstrated that the overall absorptive transport of metformin was partially saturable (Proctor et al., 2008) despite the preponderance of paracellular transport. This observation provided the most striking evidence for saturable paracellular transport acting on an organic cation, which has been proposed previously (Gan et al., 1998; Lee and Thakker, 1999; Bourdet et al., 2006).

The molecular mechanism responsible for the saturable paracellular transport acting on metformin and other hydrophilic cations across Caco-2 cell monolayers is unknown; however it was postulated to involve interactions between the drugs and the family of tight-junction (TJ) proteins known as claudins. Claudins are transmembrane proteins believed to form pores in the TJ that affect both barrier integrity and charge-selectivity of the monolayers (Van Itallie and Anderson, 2004). Specific claudin isoforms have been shown to confer charge-selectivity through charged amino acid residues of the first extracellular loop that facilitate paracellular ion permeability by electrostatic interactions (Colegio et al., 2002; Colegio et al., 2003). For example, cation-selective claudins preferentially facilitate paracellular transport of  $\text{Na}^+$  and  $\text{Ca}^{+2}$  ions

mediated by electrostatic interactions with negatively charged residues that line the pores (Colegio et al., 2003; Yu et al., 2009). There are five known cation-selective claudin isoforms: claudin-2, -10b, -12, -15, and -16 (Amasheh et al., 2002; Van Itallie et al., 2003; Hou et al., 2005; Van Itallie et al., 2006; Fujita et al., 2008). These claudins are regionally expressed throughout the body (Rahner et al., 2001; Fujita et al., 2006) and have distinct functions in regulating ion homeostasis and maintaining barrier integrity for both ion and solute flux (Van Itallie and Anderson, 2006; Amasheh et al., 2009b).

Claudin-2 is the most widely studied cation-selective claudin. Claudin-2 expressed in the Madin-Darby Canine Kidney (MDCK) C7 epithelial cells resulted in a 6-fold increase in  $\text{Na}^+$  and  $\text{K}^+$  ion permeability, while not affecting neutral paracellular probe compound mannitol (Amasheh et al., 2002). It has been shown to facilitate metal cation flux through electrostatic interactions with an aspartic acid residue at position 65 of its first extracellular loop (Colegio et al., 2003; Yu et al., 2009). Over-expression of claudin-2 in Caco-2 cells reduced the monolayer resistance and increased both  $\text{Na}^+$  and  $\text{Ca}^{+2}$  paracellular transport (Fujita et al., 2008). Additionally, claudin-2 pores have been shown to be capable of passively diffusing small noncharged hydrophilic solutes, provided their hydrodynamic radii were below 4 Å (Van Itallie et al., 2008). The ability to diffuse small hydrophilic solutes appears to be unique to claudin-2, where expression of the anionic-selective claudin-4 increased monolayer resistance but did not affect transport of noncharged solutes (Van Itallie et al., 2008; Van Itallie et al., 2009b). The ability of claudin-2 to modulate cation-selectivity across the monolayer in addition to permitting flux of small hydrophilic neutral solutes made this claudin isoform an ideal



candidate to explore potential molecular mechanisms responsible for saturable paracellular transport of metformin.

As stated above, the effect of claudin-2 expression on the transport of metal cations is well established; however the role that this protein plays in paracellular transport of organic cations remains largely unknown. Yu et al. (2009) reported that the transport of small organic cations such as methylamine (MA), ethylamine (EA), and tetramethylammonium (TMA) was affected by electrostatic interactions with claudin-2 expressed in MDCK monolayers. This phenomenon was size-dependent and was partially ablated when aspartic acid-65 was replaced with asparagine (Yu et al., 2009). Although a thorough and comprehensive study, the experimental conditions and the compounds selected did not allow for direct determination of claudin-2 mediated transport of organic cations. Further study is necessary to explicitly demonstrate claudin-2 mediated paracellular transport of organic cations.

The goal of this work was to test the hypothesis that claudin-2 facilitates paracellular transport of small hydrophilic organic cations (e.g. metformin) across epithelial monolayers. A previously developed and characterized cell line that stably expresses claudin-2 with the ability to control its expression (Van Itallie et al., 2003) was employed to test this hypothesis. The results presented here demonstrate, for the first time, direct evidence for facilitated paracellular transport of small organic cations mediated by claudin-2. Furthermore, the magnitude of the effect of claudin-2 was proportional to the relative size of the cation; thus providing a new tool to probe the claudin-2 associated pore properties.

#### 4.C. MATERIALS AND METHODS

##### Materials

Dulbecco's minimum essential medium (DMEM) with D-glucose (4.5g/L) L-glutamate, penicillin-streptomycin-amphotericin B solution (100x), and HEPES (1M) were obtained from Invitrogen Corporation (Carlsbad, CA, USA). Tetracycline screened fetal bovine serum (TS-FBS) was obtained from Hyclone, Inc (ThermoFisher Scientific, Pittsburgh PA, USA). PEG200, PEG40, and PEG900 were obtained from Fluka Chemical (Sigma-Aldrich, St. Louis, MO, USA). Purified PEG28 was obtained from Polypure AS (Oslo, Norway). 1-Naphthylisocyanate (1-NIC) was obtained from Acros Organics (ThermoFisher Scientific, Pittsburgh PA, USA). Hank's balanced salt solution (HBSS) with calcium and magnesium was purchased from Mediatech, Inc. (Mannassas, VA, USA). Metformin, guanidine, 1-methylguanidine, 1-ethylguanidine, tetraethylammonium bromide (TEA), sodium-dodecyl sulfate (SDS), D-(+) glucose, benzoin, tris(hydroxymethyl)aminomethane (TRIS) base, sodium sulfite,  $\beta$ -mercaptoethanol ( $\beta$ -ME), and doxycycline hyclate were purchased from Sigma-Aldrich (St. Louis, MO, USA). [ $^{14}\text{C}$ ]Metformin (54 mCi/mmol), [ $^{14}\text{C}$ ]guanidine (53 mCi/mmol), and [ $^{14}\text{C}$ ]mannitol (55 mCi/mmol) was purchased from Moravek Biochemicals and Radiochemicals (Brea, CA, USA). [ $^{14}\text{C}$ ]TEA (3.5 mCi/mmol) and [ $^{45}\text{Ca}^{+2}$ ] (451 mCi/mmol) was purchased from New England Nuclear (PerkinElmer, Waltham, MA, USA). The LLC-PK<sub>1</sub> Tet-Off parental and LLC-PK<sub>1</sub> PT2:13 (clone 13 of claudin-2 expressing LLC-PK<sub>1</sub> cells) cell lines were obtained generously from Drs. Christina Van Itallie and James M. Anderson (UNC School of Medicine, UNC-Chapel Hill, Chapel Hill, NC, USA).

### **LLC-PK<sub>1</sub> Cell Culture**

LLC-PK<sub>1</sub> cells were cultured and handled using established procedures (Van Itallie et al., 2003) with minor deviations. LLC-PK<sub>1</sub> cells were cultured at 37°C in DMEM with 10% TS-FBS, and 100 U/ml penicillin, 100 µg/mL streptomycin, 0.25 µg/mL amphotericin B, and 50 ng/mL of doxycycline in an atmosphere of 5% CO<sub>2</sub> and 90% relative humidity. The cells were passaged following 90% confluency using trypsin-EDTA, and plated at a 1:10 ratio in 75-cm<sup>2</sup> T flasks. The cells within 5 passages of each other were seeded at a density of 250,000 cells/cm<sup>2</sup> on polycarbonate membranes of Transwells™ (12 mm i.d., 0.4 µm pore size, Corning Life Science, Lowell, MA, USA). Doxycycline concentrations in the culture medium were varied between 0 and 50 ng/ml to modulate claudin-2 expression in PT2:13 LLC-PK<sub>1</sub> cells, with a decrease in doxycycline concentration resulting in an increase in claudin-2 expression. LLC-PK<sub>1</sub> parental cells were cultured consistently with 50 ng/ml of doxycycline. Medium was changed the day following seeding and every other day thereafter (AP volume 0.5 mL, BL volume 1.5 mL). LLC-PK<sub>1</sub> cell monolayers were used 4-5 days post seeding. Transepithelial electrical resistance (TEER) was measured to ensure monolayer integrity and the extent of claudin-2 expression. Measurements were obtained using an EVOM Epithelial Tissue Voltohmmeter and an Endohm-12 electrode (World Precision Instruments, Sarasota, FL, USA). Cell monolayers with TEER values greater than 100 Ω·cm<sup>2</sup> were used in transport experiments.

### **Absorptive (Apical to Basolateral) Transport Studies:**

Transport studies were conducted as described previously (Van Itallie et al., 2003) with minor deviations. The LLC-PK<sub>1</sub> cells were derived from porcine kidney, endogenously express porcine organic cation transporters (OCTs), and preferentially transport TEA and metformin in the secretory (BL to AP) direction in relation to the absorptive direction (Hull et al., 1976; Saito et al., 1992; Song et al., 2008). To minimize transcellular transport of organic cations across LLC-PK<sub>1</sub> cell monolayers, all transport experiments were performed in the AP to BL direction. Cell monolayers were preincubated with transport buffer solution (HBSS with 25 mM D-glucose and 10 mM HEPES, pH 7.4) for 30 min at 37°C. The buffer in the donor compartment was replaced with 0.4 ml (AP) of transport buffer containing [<sup>45</sup>Ca<sup>+2</sup>] (0.2 µCi/ml), [<sup>14</sup>C]-guanidine (0.1 µCi/ml), [<sup>14</sup>C]-metformin (0.15 µCi/ml), [<sup>14</sup>C]-TEA (0.1 µCi/ml), [<sup>14</sup>C]-mannitol (0.1 µCi/ml), or 1-methylguanidine. For measurement of calcium transport, [<sup>45</sup>Ca<sup>+2</sup>] was spiked into the buffer of the AP donor compartment in transport buffer without additional calcium. All compounds assessed were dosed at 10µM unless otherwise noted. The pH in both AP and BL compartments was maintained at 7.4 for all transport studies. Appearance of compound into the receiver compartment (BL) was monitored as a function of time in the linear region of transport and under sink conditions. The mass of the radiolabeled compound in each sample was measured using liquid scintillation spectrometry (1600 TR Liquid Scintillation Analyzer, Packard Instrument Company, Downers Grove, IL, USA) for [<sup>45</sup>Ca<sup>+2</sup>], guanidine, metformin, TEA, and mannitol transport. 1-Methylguanidine was analyzed by liquid chromatography coupled to tandem

mass-spectrometry following derivatization with benzoin with 1-ethylguanidine as an internal standard control (refer to derivatization protocol outlined below).

### **Guanidine Derivatization with Benzoin**

The amount of 1-methylguanidine transported across LLC-PK<sub>1</sub> cells with varying levels of claudin-2 expression was performed by pre-column derivatization with benzoin to form a stable product using methods outlined previously (Hung et al., 1984; Kai et al., 1984; Sparidans et al., 1999) with minor deviations. Briefly, 200µl of sample (either standard or unknown sample in transport buffer) was added at 4°C to 100µL of 4 mM benzoin in 2-methoxyethanol contained in a 1.5 mL polypropylene centrifuge tube. Then a 100µL of a chilled mixture containing 0.1 M β-ME, 0.2 M sodium sulfite, and 0.5µM 1-ethylguanidine (all final concentration) was added to the tube. Finally, 200µL of 3N sodium hydroxide was added. The solution was vortexed to ensure homogenous mixture and then placed in a boiling water bath (98°C) for 2 min. The faint yellow solution was cooled in an ice bath and the solution was neutralized with 200µL of a 1:1 mixture of 4N hydrochloric acid and 1 M TRIS buffer (pH 9.2). The solution was mixed by vortexing and the samples were then transferred to 96 well plates for LC-MS/MS analysis.

### **Liquid Chromatography Coupled to Tandem Mass-Spectrometry (LC-MS/MS)**

#### **Analysis of Derivatized Guanidine Products**

The derivatized samples were analyzed using an LC-MS/MS system fitted with a HTC PAL autosampler injector (LEAP Technologies, Carrboro, NC, USA) in line with two Shimadzu 10ADvp HPLC pumps (Shimadzu Scientific Instruments, Columbia, MD, USA) coupled to ABI Sciex 4000 Triple Quadrupole LC/MS/MS Mass Spectrometer (Applied Biosystems, Toronto, Canada). HPLC mobile phases consisted of water with

0.1% formic acid (mobile phase A) and acetonitrile with 0.1% formic acid (mobile phase B). Standards or unknown derivatized samples of 1-methylguanidine and 1-ethylguanidine products were injected (15  $\mu$ l) and retained on Aquasil™ C18 columns (50x2.1 mm diameter, 3 $\mu$ m particle size) (ThermoFisher Scientific, Pittsburgh PA, USA) and eluted using a linear gradient from 5% to 95% mobile phase B from 0.5 to 3.5 min at a flow rate of 0.4 mL/min. The column was re-equilibrated at 5% mobile phase B from 3.5 to 4.5 min. Flow was diverted from the mass-spectrometer source for the first minute. Ions were formed using positive electrospray ionization (ESI+) with ionization source potential at 3500 V and a source temperature of 500°C. The 1-methylguanidine and 1-ethylguanidine products were detected using Multiple-Reaction Monitoring™ (MRM) with parent ion  $\rightarrow$  daughter ion transitions of 250.2 $\rightarrow$ 194.2 m/z and 264  $\rightarrow$ 235.1 m/z, respectively. A sample chromatogram for both products at their respective MS/MS transitions with predicted fragmentations can be seen in Figure 4.2A. Peaks for 1-methylguanidine and 1-ethylguanidine eluted off the column at 2.6 and 2.7 min, respectively. Unknown samples were quantified using analyte peak area / internal standard peak area ratios fit to a standard curve. Standard curves were linear between 0.001 and 10 $\mu$ M standard concentration (Figure 4.2B), with the first detectable peak at 1nM. The lower-limit of quantitation (LLOQ) was determined as 3 times the standard deviation of blank samples divided by the slope of the calibration curve. The 1-methylguanidine product had a LLOQ of approximately 5nM. All unknown samples were bracketed by standards and above the LLOQ.

### **Polyethylene Glycol (PEG) Permeability Assay**

The pore characteristics of LLC-PK<sub>1</sub> PT2:13 cells in the absence of claudin-2 expression (e.g. +50ng/mL doxycycline) were examined using the PEG oligomer permeability assays outlined in Chapter 3 and using previously reported methods (Van Itallie et al., 2008). This work was performed by Dr. Christina Van Itallie (UNC School of Medicine, UNC-Chapel Hill, Chapel Hill, NC). Briefly, the apparent permeability ( $P_{app}$ ) of a series of noncharged polyethylene glycols (PEGs) across LLC-PK<sub>1</sub> PT2:13 cells cultured in the presence of 50ng/mL doxycycline were determined. Following pre-incubation with transport buffer for 30 min, the experiment was initiated by replacing the buffer in the donor compartment with transport buffer containing a 5mg/ml mixture of PEG200, PEG400, and PEG900 at a ratio of 2:0.5:1 by weight. Receiver compartments were sampled at 0, 60, 120, and 180 minutes. The samples were spiked with an internal standard (20µg purified PEG28) prior to further handling, dried down under a stream of nitrogen gas at 55°C, and derivatized by addition of 20µL of 1-NIC in 100µL of acetone and vortexing for 4 hours at 25°C; 50µL of methanol, and 500µl of H<sub>2</sub>O were added to quench excess reagent. The excess reagents were extracted twice by diethyl ether. The remaining aqueous phase was transferred to an HPLC vial for analysis. The aqueous samples (100µL) were separated on a bare-silica column (Waters Spherisorb 5.0-µm Silica column, 4.6x150mm, Waters Corporation, Milford, MA). PEG oligomers peaks were quantified from integrated HPLC peaks using fluorescent emission detection (excitation wavelength=232 nm, emission energy=358nm). Each PEG was quantified by correcting for internal standard (PEG28) peak area and the concentration associated with the analyte/area ratio was determined from a standard curve.

## **Gel Electrophoresis and Immunoblotting of Claudin-2 Protein Expression**

Immunoblotting were performed using methods described previously (Van Itallie et al., 2003; Van Itallie et al., 2009a) with minor deviations. Western blot analysis for semi-quantitation of claudin-2 protein expression were performed by Jennifer Holmes (UNC School of Medicine, UNC-Chapel Hill, Chapel Hill, NC) on cell lysates isolated following transport experiments at varying levels of doxycycline. Anti-human claudin-2 mouse monoclonal antibody (mAb) (1:1500) and rat anti-ZO-1 mAb (R40.76) (1:100 dilution) were obtained from Zymed (Invitrogen, Carlsbad CA, USA). LLC-PK<sub>1</sub> wells were lysed following transport experiment with 100µl of SDS-sample buffer (40% glycerol, 0.25 M Tris (pH 6.8), 8% SDS, 0.4% 2-mercaptoethanol, and ~0.004% bromophenol blue) that was added to the insert, incubated at room temperature for 10min, and then frozen at -80°C for future immunoblot analysis. Equal volumes (10µL) of lysate were subjected to sodium dodecyl sulfate polyacrylamide gel electrophoresis (SDS-PAGE) and transferred to nitrocellulose membranes (0.45µm, Bio-Rad Laboratories, Hercules, CA, USA). Antigen-antibody complexes were detected using horseradish peroxidase conjugated secondary antibodies by enhanced chemiluminescence (ECL) (Amersham Biosciences, GE Healthcare, Piscataway, NJ, USA). Immunoblot protein concentrations for the target protein and loading control were determined by optical densitometry at the identical scan and intensity settings (Odyssey™ Infrared Imaging System, LI-COR Biosciences, Lincoln, NE, USA). Claudin-2 protein expression was determined relative to the loading control of ZO-1. Four LLC-PK<sub>1</sub> wells were analyzed for each doxycycline concentration examined.



## Conformational Search and Molecular Volume Calculation for Organic Solutes

The conformational search and molecular volume calculations were performed on the protonated (e.g. cationic) structure of each organic cation (Figure 4.1). The conformational search and molecular modeling data presented here was performed by Dr. Simon Wang (UNC-Eshelman School of Pharmacy, UNC-Chapel Hill, Chapel Hill, NC). Each compound was first subjected to a conformational search using stochastic search algorithm (Ferguson and Raber, 1989). The conformational space was searched exhaustively by perturbing both dihedral angle of all rotation bonds and Cartesian coordinates of each atom in the molecule by some small amounts, i.e. 30 degrees and  $[-1\text{\AA}, 1\text{\AA}]$  (the sign was determined randomly), respectively. The current chirality of all constrained chiral centers (that are not easily invertible) in the molecule had been retained during the search. The potential energy setup for conformational evaluation as well as the partial charge calculation employed MMFF94x force field (Halgren, 1999b; Halgren, 1999a) with all explicit hydrogens, and the calculations were conducted in the MOE 2007.09 package (Chemical Computing Group, Montreal, Quebec, Canada). The conformers of the lowest potential energy were rendered to energy minimization prior to be submitted to Gaussian 03 (Gaussian, Inc., Wallingford, CT, USA) for the quantum mechanic calculations. The molecular volume of each molecule was defined as the volume inside a contour of 0.001 electrons/Bohr<sup>3</sup> density and computed by the Hartree-Fock method with 6-311+G basis set (McLean and Chandler, 1980; Raghavachari et al., 1980; Curtiss et al., 1995; Blauddau et al., 1997). This value was the volume enclosed by the van der Waals surface (Petitjean, 1994; Whitley, 1998), which was composed of the union of the spherical atomic surfaces defined by the van der Waals radius of each

component atom in the molecule. The geometry had been further optimized within Gaussian 03 at the same level by the Berny algorithm.

### Data Analysis

Transport of the compounds is expressed in terms of apparent permeability ( $P_{app}$ ) and is described by the following equation:

$$P_{app} = \frac{dX/dt}{(A * C_o)} \quad (4.1)$$

where  $dX/dt$  is the mass of compound (X) transported over time (t), A is the surface area of the Transwell™ porous membrane, and  $C_o$  is the initial concentration in the donor compartment.  $P_{app}$  data also are reported relative to their  $P_{app}$  values obtained across parental LLC-PK<sub>1</sub> cells (e.g. without claudin-2). All data are expressed as mean  $\pm$  SD from 3 measurements unless otherwise noted. Statistical significance was evaluated using unpaired *t* tests or one-way analysis of variance (ANOVA) with Bonferroni's post-test correction.

The hydrodynamic radius for each PEG was calculated by the following equation reported previously (Ruddy and Hadzija, 1992):

$$r = 0.29(M)^{0.454} \quad (4.2)$$

where *r* is the hydrodynamic radius in Å and *M* is the molecular mass of each PEG oligomer.

The size-restricted pore radius, or paracellular aqueous pore radius, of the LLC-PK<sub>1</sub> cell monolayers, was calculated from the ratio of the corrected paracellular permeability of pairs of two small solutes. Briefly, the pore radius (*R*) was calculated using a modified Renkin molecular sieving equation as described previously (Knipp et

al., 1997; Van Itallie et al., 2008; Yu et al., 2009) and outlined in detail in Chapter 3. The final equation implemented can be seen below:

$$\frac{P_{app,x}}{P_{app,y}} = \frac{r_y}{r_x} \left[ \frac{\left(1 - \left(\frac{r_x}{R}\right)\right)^2 \left[1 - 2.104\left(\frac{r_x}{R}\right) + 2.09\left(\frac{r_x}{R}\right)^3 - 0.95\left(\frac{r_x}{R}\right)^5\right]}{\left(1 - \left(\frac{r_y}{R}\right)\right)^2 \left[1 - 2.104\left(\frac{r_y}{R}\right) + 2.09\left(\frac{r_y}{R}\right)^3 - 0.95\left(\frac{r_y}{R}\right)^5\right]} \right] \quad (4.3)$$

where  $r$  is the radius of solute (x or y) with corresponding  $P_{app}$  values. The claudin-2 pore radius was determined using the ratio of permeability values for pairs of organic cations that significantly increased in the presence of claudin-2 expression. The ratio of these corrected permeability values from two organic cations was fit to Eq. (4.3) to estimate the claudin-2 associated pore radius ( $R$ ).

#### **4.D. RESULTS**

##### **Claudin-2 Expression in LLC-PK<sub>1</sub> PT2:13 Monolayers Increased Cation-selectivity and Calcium Transport**

Modulation of claudin-2 protein expression by varying doxycycline concentrations and measurements of the associated effects on monolayer resistance were performed to establish that the reported results (Van Itallie et al., 2003) could be reproduced in our laboratory and do not represent new findings. Claudin-2 protein expression was examined in LLC-PK<sub>1</sub> parental (P) and LLC-PK<sub>1</sub> PT2:13 monolayers cultured with 0, 0.01, 0.10, 1.0, and 10 ng/ml of doxycycline in relation to the loading control, ZO-1 (Figure 4.3A). As expected, the expression of claudin-2 protein was tightly regulated by the presence or absence of doxycycline in the culture media in LLC-PK<sub>1</sub> PT2:13 cell monolayers, with decreasing doxycycline concentrations resulting in increased claudin-2 expression. Claudin-2 protein expression relative to ZO-1 increased from  $0.07 \pm 0.01$  to  $0.52 \pm 0.12$  as doxycycline concentrations decreased from 10 ng/ml to 0 (Figure 4.3B-C). Overall claudin-2 expression in PT2:13 LLC-PK<sub>1</sub> monolayers cultured in the absence of doxycycline increased approximately 700-fold relative to the claudin-2 protein levels in parental LLC-PK<sub>1</sub> monolayers, or approximately 90-fold relative to the cells cultured with 10 ng/ml doxycycline (Figure 4.4C). Furthermore, over-expression of claudin-2 was controlled by titrating doxycycline concentrations that resulted in 14-fold changes in protein expression (Figure 4.4B-C).

The monolayer resistance, as measured by TEER, was reduced markedly as claudin-2 expression increased (Figure 4.4A). Parental LLC-PK<sub>1</sub> cell monolayers had TEER values of  $379 \pm 7 \Omega \text{ cm}^2$  (n=12), indicating low sodium conductance. The increase

of claudin-2 expression caused a decrease in TEER that was related to the expression level of claudin-2 until a minimum resistance of approximately  $160 \Omega \text{ cm}^2$  was reached in cells with maximal claudin-2 expression. The 60% reduction in TEER due to claudin-2 expression in LLC-PK<sub>1</sub> was similar to previous reports with this cell line (Van Itallie et al., 2003).

Claudin-2 expression in LLC-PK<sub>1</sub> monolayers has been shown to reverse the charge-selectivity of the monolayer from anionic to cationic by creating pores that are capable of facilitating diffusion of metal ions such as sodium (Van Itallie et al., 2003). To accurately assess the flux of small metal cations, we examined the effect of claudin-2 expression on  $[^{45}\text{Ca}^{+2}]$  permeability.  $[^{45}\text{Ca}^{+2}]$  absorptive transport was evaluated across parental and LLC-PK<sub>1</sub> PT2:13 monolayers cultured in the presence of varying doxycycline concentrations (Figure 4.4B).  $[^{45}\text{Ca}^{+2}] P_{\text{app}}$  increased with increasing claudin-2 expression, with approximately a 12-fold increase at maximal claudin-2 expression. There was a small but significant ( $p < 0.05$ ) increase in  $[^{45}\text{Ca}^{+2}] P_{\text{app}}$  (from  $10 \pm 0.2$  to  $13.0 \pm 1.0 \text{ nm s}^{-1}$ ) in PT2:13 monolayers with maximal suppression of claudin-2 expression over that of the parental cells.

The calcium  $P_{\text{app}}$  and TEER data clearly support the role of claudin-2 in forming cation-selective pores that facilitate the paracellular diffusion of calcium and sodium. The effect of claudin-2 expression on the permeability of neutral small molecular probe for paracellular transport, mannitol, was examined to determine how claudin-2 affected overall monolayer integrity. Mannitol  $P_{\text{app}}$  did not increase significantly across LLC-PK<sub>1</sub> PT2:13 cell monolayers that were cultured with  $\geq 0.10 \text{ ng/ml}$  doxycycline in relation to parental LLC-PK<sub>1</sub> mannitol  $P_{\text{app}}$  (Figure 4.4C). Small but significant increases in

mannitol  $P_{app}$  were observed in LLC-PK<sub>1</sub> PT2:13 cell monolayers treated with 0.01 ng/ml doxycycline (~20%,  $p < 0.05$ ) and untreated cells (~40%,  $p < 0.01$ ) in relation to parental LLC-PK<sub>1</sub> cell monolayers.

### **Claudin-2 Facilitates Paracellular Permeability of Organic Cations in a Size-Dependent Manner without Affecting the Size-Restricted Pore Radius**

The absorptive transport of guanidine, 1-methylguanidine, metformin, and TEA were measured across parental and PT2:13 LLC-PK<sub>1</sub> monolayers treated with varying concentrations of doxycycline. The  $P_{app}$  for the four organic cations and mannitol, reported relative to their permeability in the parental LLC-PK<sub>1</sub> cell monolayers are depicted in Figure 4.5A. Guanidine and 1-methylguanidine  $P_{app}$  increased significantly with increasing claudin-2 expression (e.g. decreasing doxycycline concentrations), while metformin and TEA  $P_{app}$  did not increase significantly (Figure 4.5). The increase in  $P_{app}$  for guanidine and 1-methylguanidine appeared to plateau across PT2:13 LLC-PK<sub>1</sub> monolayers cultured with  $\leq 0.01$  ng/ml doxycycline, as was the case for claudin-2 protein expression, TEER, and [<sup>45</sup>Ca<sup>+2</sup>] transport.  $P_{app}$  for guanidine increased approximately 4-fold from  $32.2 \pm 1.1$  to  $121.4 \pm 2.6$  nm s<sup>-1</sup> in claudin-2 over-expressing cells over parental cells (Figure 4.5). The  $P_{app}$  value for 1-methylguanidine increased by approximately 2-fold ( $32 \pm 2.0$  to  $66.8 \pm 11.1$  nm s<sup>-1</sup> ( $p < 0.01$ )) in claudin-2 over-expressing cells compared to control cells. Metformin and TEA  $P_{app}$  remained unchanged in the absence (Control) or presence (+Cldn2) of claudin-2 expression in LLC-PK<sub>1</sub> cell monolayers (Figure 4.5).

Epithelial cell monolayers have been shown to contain two or more pore systems that allow solutes to pass through the paracellular space (Knipp et al., 1997; Watson et

al., 2001; Seki et al., 2008; Van Itallie et al., 2008). Claudin-2 is believed to create pores that are size- and charge-dependent, with literature reported pore radius values ranging between 3.25 and 4.0 Å (Van Itallie et al., 2008; Yu et al., 2009). Therefore, the size-restricted claudin-2 pore radius was determined in PT2:13 LLC-PK<sub>1</sub> monolayers expressing claudin-2.

In order to estimate this value, the molecular radius for each organic solute had to be consistently and thoroughly estimated. Molecular radius values were calculated from the molar volumes assuming spherical volumes. Values of molecular radius for each cation paneled in addition to other hydrophilic cations for which there were literature values are outlined in Table 4.1. The empirical calculations were rigorous estimates of molar volume using similar assumptions and parameters which allowed for each value to be compared directly. As shown in Table 4.1, the molecular volume calculations potentially underestimate the true hydrodynamic radii of the organic solutes; therefore, calculations of the predicted pore radius using these values should be considered to be an estimate.

The claudin-2 pore radius was estimated by fitting the ratios of guanidine and 1-methylguanidine claudin-2 associated  $P_{app}$  values and fitting these values to the Renkin molecular sieving equation (Eq. (4.3)) with their respective molecular radius (Table 4.1). Claudin-2 associated  $P_{app}$  values for each organic cation were determined by subtracting the mean  $P_{app}$  values across the parental cell line (e.g. without claudin-2) from the mean  $P_{app}$  values obtained in the claudin-2 induced LLC-PK<sub>1</sub> cells at the maximal doxycycline concentration that did not significantly increase mannitol  $P_{app}$  values relative to parental mannitol  $P_{app}$  values (e.g. 0.1 ng/ml doxycycline). This correction removed any

difference in transcellular transport processes between the compounds and accounted for only the transport associated with claudin-2 pores. The claudin-2 pore radius (R) was calculated to be 4.2 Å, which was consistent with 4.0 Å radius previously reported using noncharged PEG oligomers (Van Itallie et al., 2008).

To determine whether the size-restricted claudin-2 pore radius was significantly different from the un-induced cell line, the pore radius of the PT2:13 cell line in the presence of 50ng/ml doxycycline was determined using the ratios of PEG<sub>3.2Å</sub>, PEG<sub>3.5Å</sub>, and PEG<sub>3.8Å</sub> permeability values as described previously (Van Itallie et al., 2008; Van Itallie et al., 2009a). The paracellular transport of these three small PEG oligomers are known to represent the flux through the size-restricted permeability pore system and can be used to determine this pore radius in PT2:13 LLC-PK<sub>1</sub> cell monolayers in the absence of claudin-2 expression. The permeability of the size dependent first phase was corrected by subtracting the second linear phase by linear regression. The pore radius was then calculated from the ratio of the corrected paracellular permeabilities of pairs of two small PEG oligomers. Each PEG pair  $P_{app}$  ratio fit to Eq. (4.3) provided an estimate for R and all three values were averaged to give an average size-restricted pore radius for the uninduced monolayer. The PEG oligomer permeability profile across un-induced LLC-PK<sub>1</sub> PT2:13 cell monolayers as a function of hydrodynamic radius is depicted in Figure 4.6. This profile clearly demonstrates a two or more pore system, where the first high capacity phase permits diffusion of PEG oligomers  $\leq 4\text{Å}$  and a second linear phase where PEG oligomers with  $>4\text{Å}$  radius are not as efficiently transported (Figure 4.6). The calculated pore radius (R) for this monolayer using (PEG<sub>3.2Å</sub> / PEG<sub>3.5Å</sub>), (PEG<sub>3.2Å</sub> / PEG<sub>3.8Å</sub>), and (PEG<sub>3.5Å</sub> / PEG<sub>3.8Å</sub>) permeability ratios were 3.99, 4.05, and 4.07 Å. The



average pore radius of the size-restricted pore in LLC-PK<sub>1</sub> cells in the absence of claudin-2 was 4.0 Å, which was not significantly different from the calculated claudin-2 associated pore radius using 1-methylguanidine and guanidine P<sub>app</sub> ratio outlined above.

#### **4.E. DISCUSSION**

Claudin-2 has been shown to confer cation-selectivity across the monolayer, where expression was linked to an increase in metal cation flux and a decrease in monolayer resistance (Amasheh et al., 2002; Colegio et al., 2003; Van Itallie et al., 2003; Fujita et al., 2008; Yu et al., 2009). It was shown that claudin-2 mediated cation flux through electrostatics between an anionic residue (aspartic acid at position 65) in its first extracellular loop and the metal ions (Yu et al., 2009); suggesting that claudin-2 forms pores in the TJ that preferentially transport cations. The majority of the aforementioned studies employed indirect electrophysiological measurements to determine the effects of claudin-2 expression on ion flux. Direct measurement of cation flux modulated by claudin-2 expression is generally lacking in the literature.

The results presented in Chapter 3 of this dissertation demonstrated that vitamin D<sub>3</sub>-treatment in Caco-2 cells (clone P27.7) caused a significant increase in metformin paracellular transport as well as another hydrophilic cation, guanidine. In this cell model, only claudin-2 mRNA and protein expression were significantly increased (e.g. 3-4-fold) by vitamin D<sub>3</sub>-treatment. Although the data clearly supported involvement of claudin-2 in the facilitating paracellular transport of metformin, direct evidence implicating claudin-2 was missing due to the numerous genes vitamin D<sub>3</sub>-treatment could affect (Fleet et al., 2002; Kong et al., 2008; Fan et al., 2009). In this study, the effects of claudin-2 protein expression on paracellular transport of a small panel of organic cations was evaluated to assess if claudin-2 indeed increased paracellular permeability of small organic cations by forming cation-selective pores.

To this end, transport of small organic cations, including metformin, was evaluated across LLC-PK<sub>1</sub> monolayers that overexpress claudin-2 protein under the control of an inducible promoter. LLC-PK<sub>1</sub> parental cells confer anionic-selectivity that can be switched to a cation-selectivity when claudin-2 protein is introduced (Van Itallie et al., 2003). This model was selected because the parental LLC-PK<sub>1</sub> cells have very low levels of endogenously expressed claudin-2 protein, and hence if claudin-2 caused an increase in the permeability of small organic cations; large signal to noise could be achieved using this model. The ability to control claudin-2 expression in LLC-PK<sub>1</sub> cell monolayers was a particularly useful feature of this model because of two inherent advantages: 1) the ability to directly measure the effect of claudin-2 expression in the same cells with consistent endogenous transcellular and paracellular transport processes and 2) the ability to systematically increase claudin-2 protein expression without affecting the overall monolayer integrity.

LLC-PK<sub>1</sub> cell monolayers at the very least endogenously express claudin-1 and claudin-4, with low levels of endogenous claudin-2 expression (Van Itallie et al., 2003); therefore, background claudin related paracellular transport needed to be accounted for. In addition, LLC-PK<sub>1</sub> cells endogenously express porcine organic cation transporters (OCTs) (Saito et al., 1992; Li et al., 2004) that potentially can affect  $P_{app}$  of organic cations. Metformin and TEA transport in the BL to AP direction was greater than AP to BL direction across LLC-PK<sub>1</sub> cell monolayers (Saito et al., 1992; Song et al., 2008), indicative of active cation-selective transcellular transport processes. Guanidine, guanidine analogues (e.g. 1-methylguanidine and metformin), and quaternary ammonium analogues (e.g. TMA, TEA) have been shown to interact with OCTs (Gorboulev et al.,

1997; Kimura et al., 2005; Kimura et al., 2009). Consequently,  $P_{app}$  for organic cations selected in Figure 4.1 across LLC-PK<sub>1</sub> cell monolayers likely represented both paracellular and transcellular processes. By subtracting the  $P_{app}$  across the parental cells from the  $P_{app}$  across the PT2:13 cells, the contribution of transcellular and paracellular transport processes were eliminated, leaving only the claudin-2-associated permeability. The role of claudin-2 in facilitating paracellular transport of metformin and other hydrophilic cations with similar charge environments was examined by employing this approach.

Introduction of claudin-2 protein in the monolayer has the potential to not only increase the cation-selective pores in the monolayer, but also affect the monolayer integrity. However, few reports have accurately assessed the effects on monolayer integrity in their claudin-2 over-expressed system. In this report, high levels of claudin-2 expression in the monolayer caused increases upwards of 40% in the transport of mannitol (Figure 4.4C). This finding contradicts previous reports in MDCK C7 cell monolayers in which induced claudin-2 expression did not alter mannitol transport (Amasheh et al., 2002; Van Itallie et al., 2008). Mannitol paracellular transport is believed to occur via the size- and charge-independent pore system not related to claudin-2 expression (Van Itallie et al., 2008). A possible explanation for the increase in mannitol permeability was that claudin-2 expression exceeded the capacity of the monolayer to insert claudin-2 properly into the TJ; therefore remaining claudin-2 either residing in vesicles or anchored to the TJ disrupted the overall integrity of the monolayer. This observation further justifies the need to adequately assess effects to the monolayer integrity when employing over-expressed models with claudin-2 or other TJ proteins.

The data presented in this report provide for the first time direct evidence that claudin-2 increased the permeability of organic cations at expression levels which did not affect the permeability of the neutral paracellular probe, mannitol. Guanidine and 1-methylguanide transport significantly increased with increasing claudin-2 expression (Figures 4.6). The magnitude of effect was proportional to molecular radius (Table 4.1), supporting that claudin-2-facilitated transport of organic cations was size-dependent. Interestingly, metformin transport remained unchanged across LLC-PK<sub>1</sub> cells expressing claudin-2. This was in contrast to the observation that induction of claudin-2 in Caco-2 cells caused an increase in metformin permeability (Chapter 3). Claudin-2 did not seem to affect the permeability of TEA in both the systems.

The guanidine and 1-methylguanidine transport data presented here support the hypothesis that small hydrophilic cation paracellular transport was affected by claudin-2 expression, most likely through electrostatic interactions. Contrary to what was expected, metformin transport was not affected by claudin-2 protein expression. The estimated molecular radius of TEA was close to the claudin-2 size-restricted pore radius; therefore, it was not surprising that claudin-2 overexpression had no effect on TEA permeability. In addition, the charge on TEA may not be accessible to electrostatic interactions due to shielding by the four ethyl groups (refer to Figure 4.1 space-filling model). In contrast metformin has resonance that distributes the positive charge across the biguanide moiety providing ample surface area for electrostatic interactions between the extracellular loops of claudin-2. Therefore, it was surprising that the permeability of metformin, with its estimated radius of 3.25 Å, was not affected by overexpression of claudin-2. It is conceivable that metformin molecular radius calculated here was significantly

underestimated, and that its true hydrodynamic radius was closer to the size limit of claudin-2 pores. For example, mannitol radius was underestimated by 0.3 Å in the molecular modeling approach relative to its experimentally derived hydrated radius of 4.2 Å (Table 4.1 and (Schultz and Solomon, 1961)). Refining estimates for metformin hydrated radius is warranted to better understand how this ion in solution fits into the size-restricted claudin-2 pores.

Additionally, the apparent inability of metformin to transport through claudin-2 pores raised the question whether the claudin-2 pore radius was smaller in the LLC-PK<sub>1</sub> cells in relation to the vitamin D<sub>3</sub>-induced Caco-2 cell model (Chapter 3). The claudin-2 pore radius was estimated by fitting the ratio of the claudin-2-associated  $P_{app}$  values of guanidine and 1-methylguanidine and their respective hydrodynamic radii to a molecular sieving equation as described previously (Knipp et al., 1997; Watson et al., 2001; Van Itallie et al., 2008). To our surprise, the claudin-2 pore radius was estimated to be 4.2 Å, which was not significantly different from the size-restricted pores in the uninduced LLC-PK<sub>1</sub> monolayers or from the ~4 Å claudin-2-associated pore radius reported in the literature (Van Itallie et al., 2008; Van Itallie et al., 2009b). The estimate was also consistent with the calculated radius of the size-restricted pore for Caco-2 cells in the presence or absence of induced claudin-2 expression (Chapter 3).

Provided the estimates for the claudin-2 pore radius were accurate, the increase in Ca<sup>2+</sup>, guanidine, and 1-methylguanidine transport supports the work by Van Itallie and colleagues (2008) that over-expressing claudin-2 protein increases porosity and not the pore radius of the size-restricted pathway. However, prior to this report it was unclear whether pore estimates using non-charged solutes accurately represent the claudin-2

associated pore capable of transporting cations. The novel finding in this report was that claudin-2 associated pore radius was shown to be approximately 4 Å, regardless of whether the estimates were determined from organic cation permeabilities or by noncharged solutes permeability. Nevertheless, claudin-2 expression confers cation-selectivity to the monolayer by increasing the flux of cations to a greater extent than the neutral molecules. In this study,  $\text{Ca}^{2+}$ , guanidine, and 1-methylguanidine  $P_{\text{app}}$  increased 12-, 4-, and 2-fold, respectively (Figure 4.4B and Figure 4.5). Over-expressing claudin-2 in MDCK C7 cells, which have low endogenous claudin-2 (Amasheh et al., 2002), only resulted in a maximal increase in PEG<sub>3.2</sub> and PEG<sub>3.5</sub>  $P_{\text{app}}$  of 1.5-fold (Van Itallie et al., 2008; Van Itallie et al., 2009b). In other words, claudin-2 appears to create a pore complex that has an approximate radius 4 Å that significantly enhances the cation-selectivity of the monolayer, while to a lesser extent increases the “leaky” nature of the monolayer to allow flux of small non-charged solutes.

The observation that the size-restricted pore radius of LLC-PK<sub>1</sub> remains constant while paracellular transport of guanidine and 1-methylguanidine increased supports that claudin-2 increases the overall porosity of the monolayer. There are conflicting reports as to whether claudin-2 expression increased the number of parallel strands or fibrils in the TJs, which may represent the pore forming structures. Exogenous expression of claudin-2 in MDCKII, which already express significant levels of endogenous claudin-2, resulted in the number of TJ fibrils or strands to increase (Colegio et al., 2003). These data support that claudin-2 expression increases TJ fibrils and consequently the porosity of the monolayer. In another report, exogenously expressed claudin in MDCK cells did not increase the number of fibrils or strands in relation to the control cells (Yu et al.,

2009). Claudin-8 that was exogenously expressed in MDCKII cells caused a decrease in endogenous canine claudin-2 expression, while not affecting the fibril or strand number in the TJs (Angelow et al., 2007). It was concluded that claudin-8 was able to replace endogenous claudin-2 strands in the TJ, altering the cation-selectivity of the monolayer. It is possible that the opposite could occur in which claudin-2 replaces other claudin strands that are not responsible for forming pores (e.g. claudin-4); thereby increasing the porosity while not altering the number of TJ strands. How claudin-2 expression regulates porosity of the monolayer and the structure of these pores remains unknown; however functional data in this report and other literature reports support that claudin-2 expression significantly alters the number of pores capable of facilitating transport of cations and to a lesser extent noncharged species.

The effect of claudin-2 expression on paracellular transport of organic cations was evaluated at the maximal expression at which mannitol transport was not significantly increased (e.g. cells cultured with doxycycline  $\geq 0.1$  ng/ml). This allowed for meaningful conclusions to be obtained regarding the effect of only the claudin-2 associated transport without general disruption of the monolayer. Yu et al. (2009) recently reported the effect of claudin-2 expression on paracellular permeability of organic cations using indirect measurement (e.g. dilution potential). The contribution of endogenous claudin-2 to the transport of each solute was subtracted to obtain only claudin-2 associated permeability (Yu et al., 2009). However, potential alterations to overall monolayer integrity due to claudin-2 expression were not determined; therefore, the increase in organic cation transport observed may not truly estimate the claudin-2 pore electrostatics. In addition, the cations paneled in the aforementioned study had significantly different charge



environments (e.g. primary amines vs. quaternary amines). Differences in organic cation  $P_{app}$  observed may not be due solely to changes in molecular radius, but to differences in charge accessibility. Lastly, the previous report indirectly measured the solute flux using electrophysiological measurements at concentrations that were supra-physiologic (e.g. 75 mM) (Yu et al., 2009). These factors taken together raise concern over the conclusions drawn regarding organic cation transport and the true radius of the claudin-2 associated pore.

In conclusion, the work presented here provides the first direct evidence for claudin-2 mediated paracellular transport of small organic cations. It remains unknown why metformin transport was unaffected by claudin-2 expression in this system, while it appeared to be facilitated by claudin-2 in Caco-2 cells treated with the active metabolite of vitamin D<sub>3</sub>. Further studies are warranted with larger guanidine analogues, such as biguanide or 1-ethylguanidine, which are closer to the size of metformin. This approach will allow for more accurate assessment of the true claudin-2 pore radius. Furthermore, potential differences between the claudin-2 environments in Caco-2 cells in relation to LLC-PK<sub>1</sub> cells may account for functional differences observed here; thus, the studies outlined in this report should be performed in other claudin-2 expressed cell systems, such as MDCK C7. Although unlikely, one cannot rule out that there were other proteins than claudin-2 involved in the vitamin D<sub>3</sub>-associated increase in the paracellular permeability across Caco-2 cell monolayers. Employing siRNA knock-down approaches in the vitamin D<sub>3</sub>-treated Caco-2 cell model may provide more conclusive evidence for the role of claudin-2 in facilitating paracellular transport of metformin.

Claudin-2 is ubiquitously expressed throughout the small intestine, although protein localization was shown to be restricted primarily to the undifferentiated crypts and crypt-villus axis (Rahner et al., 2001; Escaffit et al., 2005). For that reason, the effect claudin-2 has on the absorption of small organic cations is not apparent. Claudin-2 pores may facilitate the absorption of small organic cations along the crypt-villus axis, where transcellular transport processes are not functional. The size cutoff associated with claudin-2 pores likely does not make this a viable pathway to enhance absorption for the majority of hydrophilic drugs on the market or in development; yet this work provides important insight into the role this protein may play in gastrointestinal disorders. For example, claudin-2 expression in fully differentiated enterocytes has been shown to be increased in disease states such as inflammatory bowel disease (IBD) (Amasheh et al., 2009a), Crohn's disease (Zeissig et al., 2007), and gastrointestinal carcinomas (Aung et al., 2006). The elevated claudin-2 levels may be responsible for these gastrointestinal maladies, where increased absorption or excretion of small cationic and non-charged solutes result in an osmotic imbalance. Further studies in the appropriate preclinical models are necessary to assess the implications of enhanced intestinal expression of claudin-2 on intestinal excretion or absorption of hydrophilic solutes.

#### **4.F. ACKNOWLEDGEMENTS**

We would like to acknowledge Dr. Simon Wang (UNC-Eshelman School of Pharmacy, UNC-Chapel Hill, Chapel Hill, NC) for his contribution to this work regarding molecular modeling and helpful insight regarding radius estimates. We would also like to acknowledge Dr. Christina Van Itallie and Jennifer Holmes (UNC-School of Medicine, UNC-Chapel Hill) for their contributions to this work and invaluable technical assistance, resources, and intellectual discussions. Funding for this work was provided by the PhRMA Foundation in the form of a Pre-Doctoral Fellowship in Pharmaceutics awarded to William Proctor.

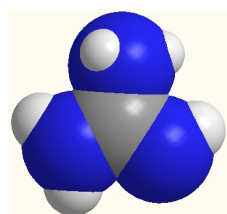
## TABLES AND FIGURES

**Table 4.1. Calculated Molecular Radius for Hydrophilic Organic Solutes in Relation to Reported Values**

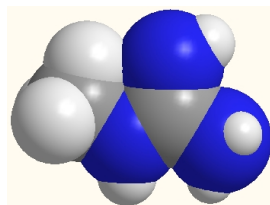
Compound	Molar Volume <sup>A</sup>	Calculated Radius <sup>B</sup>	Range of Reported Radius	References
	cm <sup>3</sup> /mol	Å	Å	
Methylamine	33.04	2.36	1.9 - 2.7	[1,2,3]
Guanidine	42.35	2.56	NA	
1-Methylguanidine	63.79	2.94	NA	
Metformin	89.15	3.28	NA	
TEA	131.52	3.74	3.3 - 4.0	[3,4]
Mannitol	152.43	3.92	3.6 - 4.3	[1,2,5,6]
Atenolol	221.51	4.45	4.2 - 4.8	[1,2]

<sup>A</sup> Molar volume was determined by Gaussian 3.0 software for each compound using the most thermodynamically favored confirmation (refer to methods section). <sup>B</sup> Calculated radius was determined from molar volume values assuming volume of a sphere. NA: not available

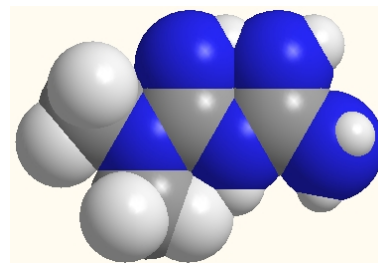
References: [1] (Knipp et al., 1997) [2] (Avdeef, 2010) [3] (Yu et al., 2009) [4] (Wang and Veenstra, 1997) [5] (Steward, 1982) [6] (Schultz and Solomon, 1961).



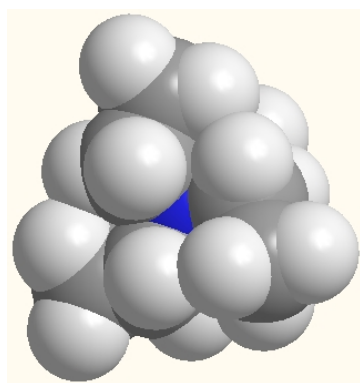
**Guanidine**



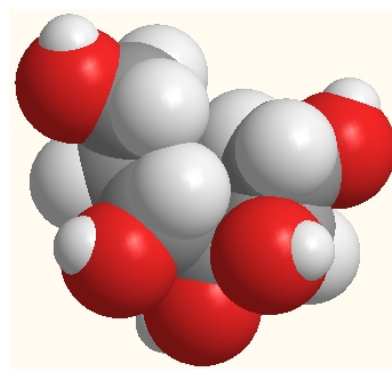
**1-Methylguanidine**



**Metformin**



**TEA**



**D-Mannitol**



**Carbon**



**Hydrogen**



**Nitrogen**



**Oxygen**

**Figure 4.1. Space-filling Structures for Hydrophilic Organic Solutes Guanidine, 1-Methylguanidine, Metformin, TEA, and D-Mannitol.**

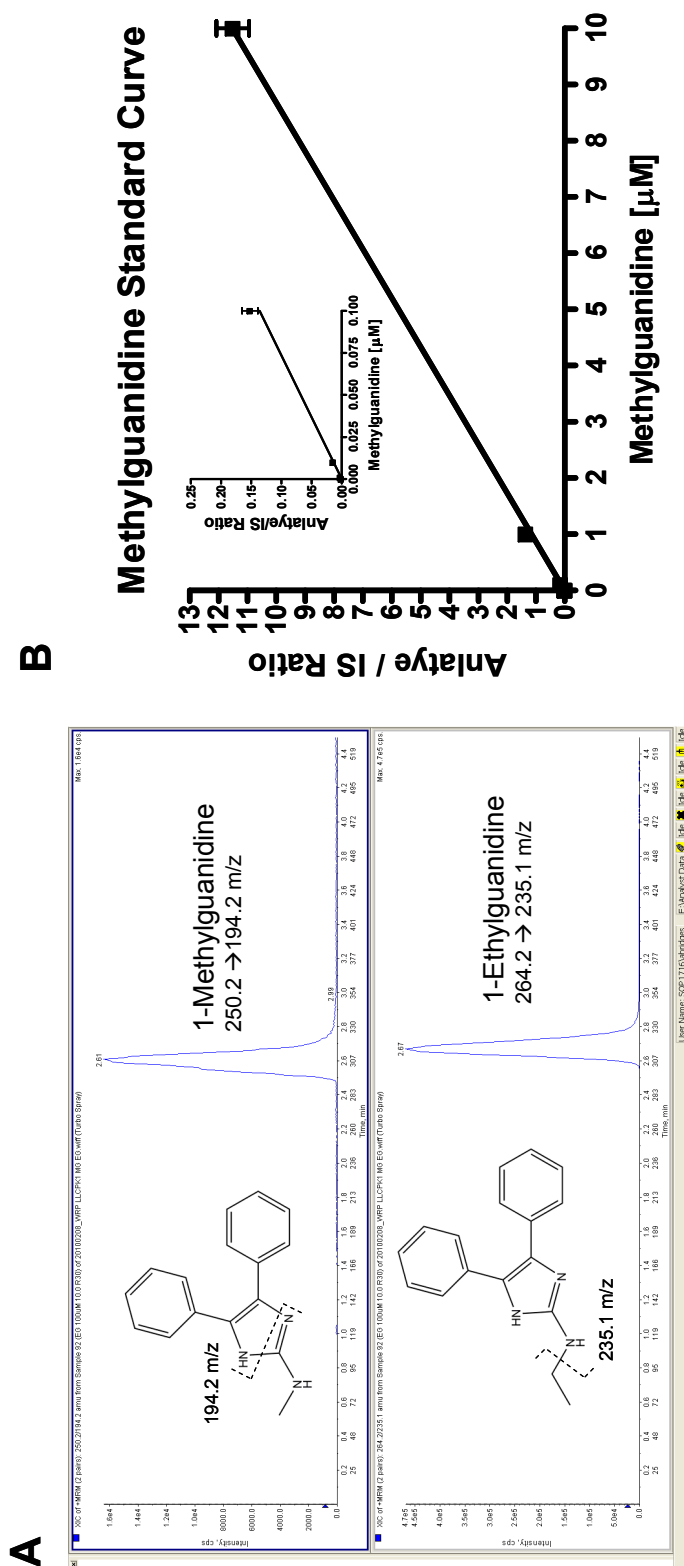


**Figure 4.2. LC-MS/MS Chromatograms and Standard Curve for 1-Methylguanidine Quantitative Analysis.** A. Sample chromatograms for the 1-methylguanidine and 1-ethylguanidine derivatized products with MS/MS transitions of 250.2  $\rightarrow$  194.2 m/z and 264.2  $\rightarrow$  235.1 m/z, respectively. The structure for each product and predicted fragmentation pattern is depicted in the inset of each chromatogram. B. The standard curve for the 1-Methylguanidine derivatized product from 1nM to 10 $\mu\text{M}$  initial concentrations is reported in terms of the 1-methylguanidine product peak area / 1-ethylguanidine product peak area ratio. Inset of panel B depicts the standard curve from 1nM to 100nM. Points represent mean  $\pm$  S.D. for 3 separate injections. Solid lines represent linear regression fit to the standard curve data.

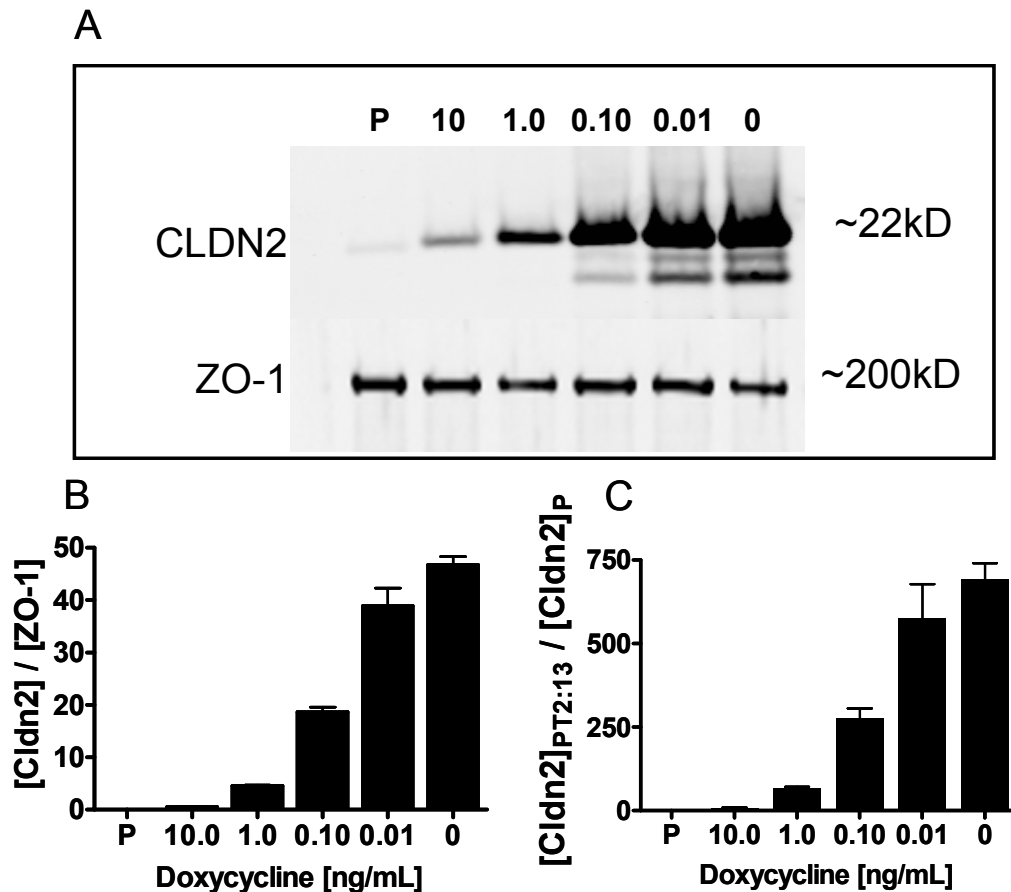


**Figure 4.3. Western Blot Analysis of Claudin-2 Expression in LLC-PK<sub>1</sub> Parental and PT2:13 LLC-PK<sub>1</sub> Cells with Decreasing Doxycycline Concentration.** A. Claudin-2 [CLDN2] protein expression was determined by Western Blot analysis of cell lysate from parental LLC-PK<sub>1</sub> cells (P) and PT2:13 LLC-PK<sub>1</sub> cells cultured with varying concentrations of doxycycline: 10 ng/ml (10.0), 1 ng/ml (1.0), 0.1 ng/ml (0.10), 0.01 ng/ml (0.01), and 0 ng/ml (0) with zonal occludin-1 [ZO-1] expression employed as a loading control. B. Claudin-2 relative to ZO-1 protein expression in parental LLC-PK<sub>1</sub> cells and PT2:13 cells cultured with varying doxycycline concentrations. C. The ratio of claudin-2 protein in the PT2:13 LLC-PK<sub>1</sub> cells ([CLDN2]<sub>PT2:13</sub>) and parental LLC-PK<sub>1</sub> cells ([Cldn2]<sub>P</sub>) at various doxycycline concentrations. Data represent mean  $\pm$  S.D with 4 measurements.

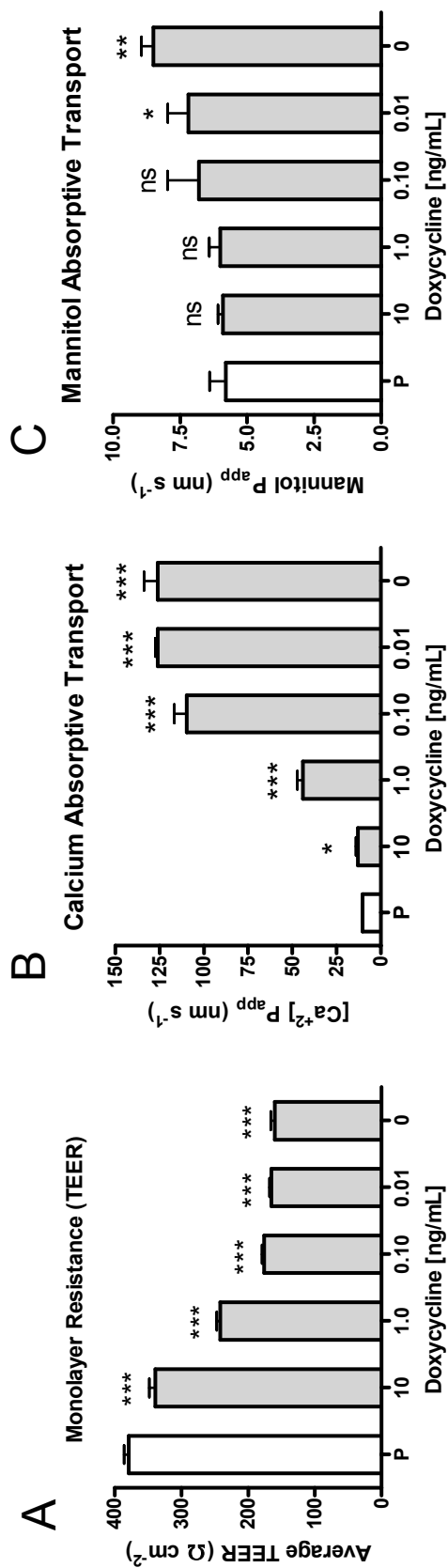


**Figure 4.4. The Effect of Claudin-2 Expression on Monolayer Resistance (TEER) and Paracellular Transport of Calcium and Mannitol.** A. TEER was measured across parental (P) (open bars) and PT2:13 LLC-PK<sub>1</sub> monolayers cultured with varying concentrations of doxycycline: 10 ng/ml (10), 1 ng/ml (1), 0.1 ng/ml (0.1), 0.01 ng/ml (0.01), and 0 ng/ml (0) (grey bars) as previously reported (Van Itallie et al., 2003). TEER data represent means  $\pm$  S.D. of 12 measurements. Permeability values of tracer levels of [ $^{45}\text{Ca}^{+2}$ ] (B) and [ $^{14}\text{C}$ ]mannitol (C) were determined in the absorptive (AP to BL) direction across LLC-PK<sub>1</sub> PT2:13 monolayers with varying doxycycline concentrations in relation to permeability values across parental LLC-PK<sub>1</sub> monolayers. Data represent mean  $\pm$  S.D. with 3 measurements. \* $p < 0.05$ , \*\* $p < 0.01$ , \*\*\* $p < 0.001$  in relation to values for parental LLC-PK<sub>1</sub> monolayers.



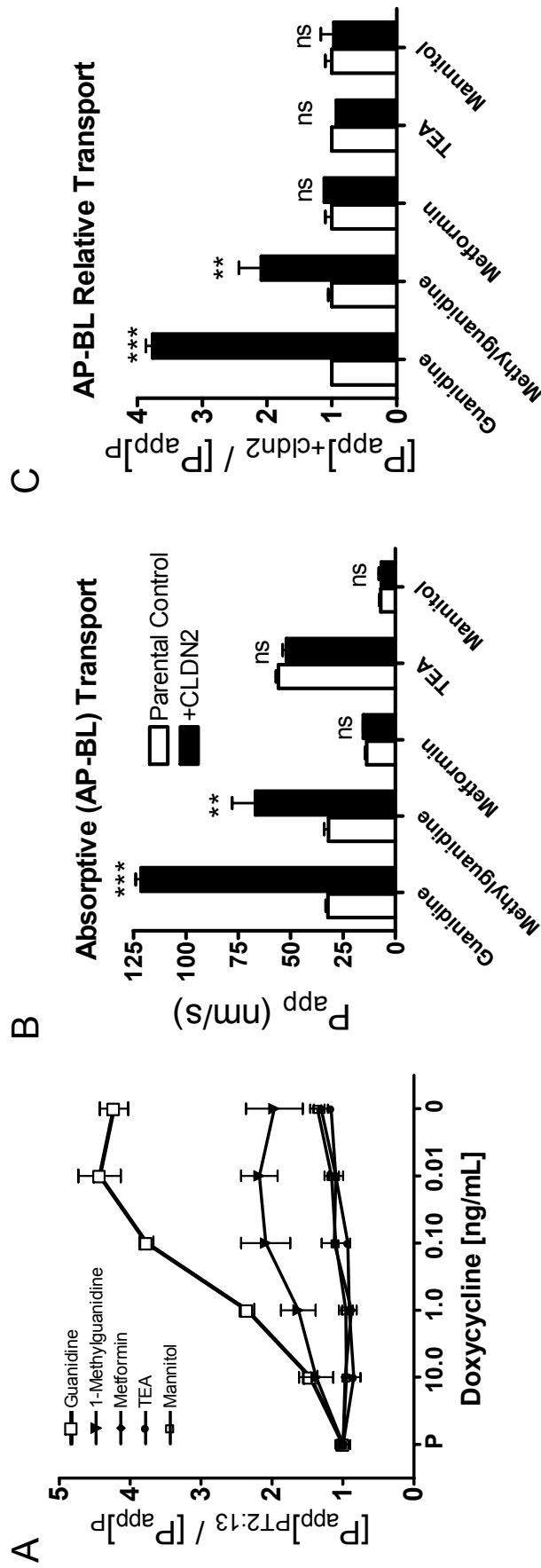


**Figure 4.5. Claudin-2 Dependent Increase in Paracellular Transport of Organic Cations Across LLC-PK<sub>1</sub> Cell Monolayers.** (A). The ratio of apparent permeability ( $P_{app}$ ) values for cationic guanidine (□), 1-methylguanidine (▼), metformin (◆), TEA (●) and the neutral paracellular probe mannitol (■) at [10μM] across PT2:13 and parental LLC-PK<sub>1</sub> monolayers cultured with varying concentrations of doxycycline in the absorptive (AP-BL) direction. The  $P_{app}$  values for each compound across the parental LLC-PK<sub>1</sub> cell monolayers (open bars) and PT2:13 LLC-PK<sub>1</sub> cell monolayers cultured with 0.1 ng/mL doxycycline (+CLDN2) (closed bars), which was the lowest doxycycline concentration that did not significantly increase mannitol transport are represented in (B) or relative  $P_{app}$  to parental control (C). Data represent mean  $\pm$  S.D. with 3 measurements. \*\* $p < 0.01$ , \*\*\* $p < 0.001$  relative to parental (P) LLC-PK<sub>1</sub>  $P_{app}$  values. ns: not significant

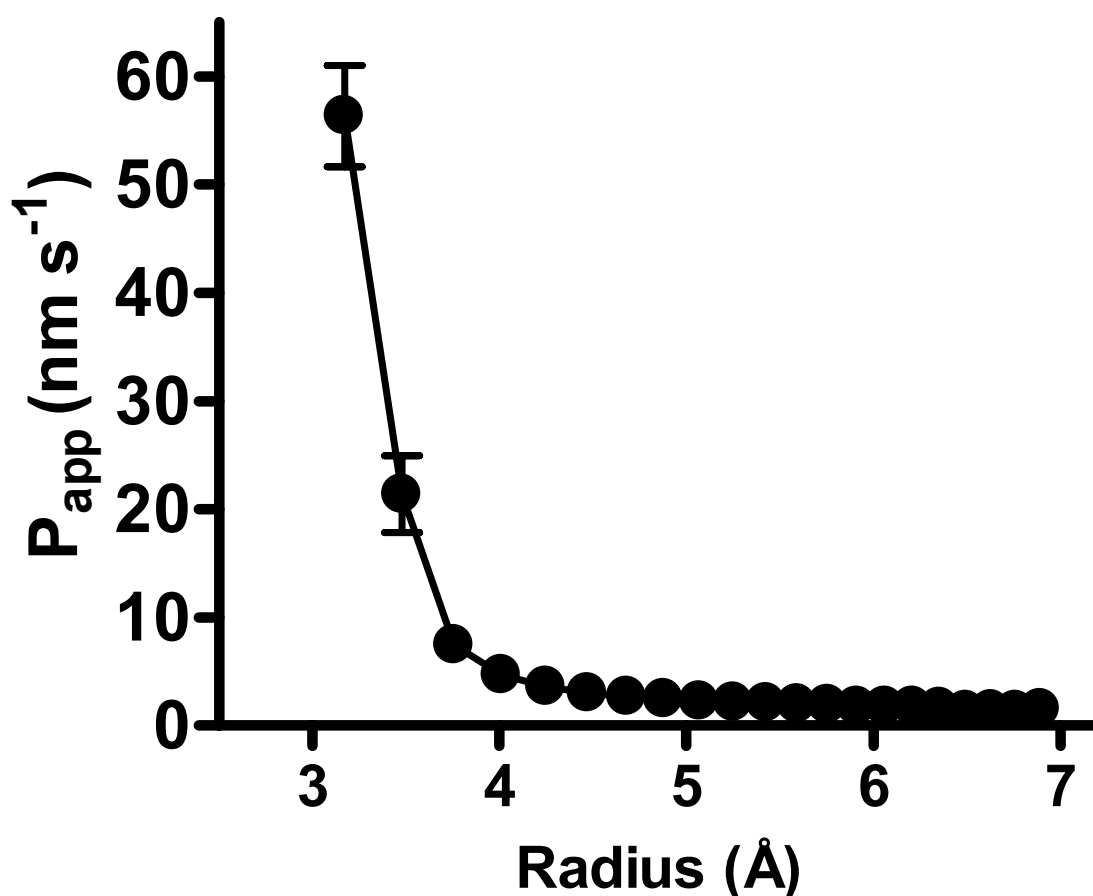


**Figure 4.6. Polyethylene Glycol (PEG) Oligomer Permeability as a Function of Hydrodynamic Radius in Un-Induced PT2:13 LLC-PK<sub>1</sub> Monolayers.** Polyethylene glycol (PEG) oligomer permeability was evaluated across PT2:13 LLC-PK<sub>1</sub> monolayers that were cultured in the presence of 50 ng/ml doxycycline and plotted as a function of their calculated hydrodynamic radius. Similar data have been reported previously for PEG permeability across MDCKII, MDCK C7, and Caco-2 cell monolayers (Van Itallie et al., 2008). Data represent mean  $\pm$  S.D. with 4 measurements.

#### 4.G. REFERENCES

- Amasheh S, Dullat S, Fromm M, Schulzke JD, Buhr HJ and Kroesen AJ (2009a) Inflamed pouch mucosa possesses altered tight junctions indicating recurrence of inflammatory bowel disease. *Int J Colorectal Dis* **24**:1149-1156.
- Amasheh S, Meiri N, Gitter AH, Schoneberg T, Mankertz J, Schulzke JD and Fromm M (2002) Claudin-2 expression induces cation-selective channels in tight junctions of epithelial cells. *J Cell Sci* **115**:4969-4976.
- Amasheh S, Milatz S, Krug SM, Markov AG, Gunzel D, Amasheh M and Fromm M (2009b) Tight junction proteins as channel formers and barrier builders. *Ann N Y Acad Sci* **1165**:211-219.
- Angelow S, Schneeberger EE and Yu AS (2007) Claudin-8 expression in renal epithelial cells augments the paracellular barrier by replacing endogenous claudin-2. *J Membr Biol* **215**:147-159.
- Aung PP, Mitani Y, Sanada Y, Nakayama H, Matsusaki K and Yasui W (2006) Differential expression of claudin-2 in normal human tissues and gastrointestinal carcinomas. *Virchows Arch* **448**:428-434.
- Avdeef A (2010) Leakiness and Size Exclusion of Paracellular Channels in Cultured Epithelial Cell Monolayers-Interlaboratory Comparison. *Pharm Res* **In Press**.
- Blaudeau JP, McGrath MP, Curtiss LA and Radom L (1997) Extension of Gaussian-2 (G2) theory to molecules containing third-row atoms K and Ca. *Journal of Chemical Physics* **107**:5016-5021.
- Bourdet DL, Pollack GM and Thakker DR (2006) Intestinal absorptive transport of the hydrophilic cation ranitidine: a kinetic modeling approach to elucidate the role of uptake and efflux transporters and paracellular vs. transcellular transport in Caco-2 cells. *Pharm Res* **23**:1178-1187.
- Colegio OR, Van Itallie C, Rahner C and Anderson JM (2003) Claudin extracellular domains determine paracellular charge selectivity and resistance but not tight junction fibril architecture. *Am J Physiol Cell Physiol* **284**:C1346-1354.
- Colegio OR, Van Itallie CM, McCrea HJ, Rahner C and Anderson JM (2002) Claudins create charge-selective channels in the paracellular pathway between epithelial cells. *Am J Physiol Cell Physiol* **283**:C142-147.
- Curtiss LA, McGrath MP, Blaudeau J-P, Davis NE, Binning RC and Radom L (1995) Extension of Gaussian-2 theory to molecules containing third-row atoms Ga-Kr. *Journal of Chemical Physics* **103**:6104.

- Escaffit F, Boudreau F and Beaulieu JF (2005) Differential expression of claudin-2 along the human intestine: Implication of GATA-4 in the maintenance of claudin-2 in differentiating cells. *J Cell Physiol* **203**:15-26.
- Fan J, Liu S, Du Y, Morrison J, Shipman R and Pang KS (2009) Up-regulation of transporters and enzymes by the vitamin D receptor ligands, 1 $\alpha$ ,25-dihydroxyvitamin D<sub>3</sub> and vitamin D analogs, in the Caco-2 cell monolayer. *J Pharmacol Exp Ther* **330**:389-402.
- Ferguson DM and Raber DJ (1989) A new approach to probing conformational space with molecular mechanics: random incremental pulse search. *Journal of the American Chemical Society* **111**:4371-4378.
- Fleet JC, Eksir F, Hance KW and Wood RJ (2002) Vitamin D-inducible calcium transport and gene expression in three Caco-2 cell lines. *Am J Physiol Gastrointest Liver Physiol* **283**:G618-625.
- Fujita H, Chiba H, Yokozaki H, Sakai N, Sugimoto K, Wada T, Kojima T, Yamashita T and Sawada N (2006) Differential expression and subcellular localization of claudin-7, -8, -12, -13, and -15 along the mouse intestine. *J Histochem Cytochem* **54**:933-944.
- Fujita H, Sugimoto K, Inatomi S, Maeda T, Osanai M, Uchiyama Y, Yamamoto Y, Wada T, Kojima T, Yokozaki H, Yamashita T, Kato S, Sawada N and Chiba H (2008) Tight junction proteins claudin-2 and -12 are critical for vitamin D-dependent Ca<sup>2+</sup> absorption between enterocytes. *Mol Biol Cell* **19**:1912-1921.
- Gan LS, Yanni S and Thakker DR (1998) Modulation of the tight junctions of the Caco-2 cell monolayers by H<sub>2</sub>-antagonists. *Pharm Res* **15**:53-57.
- Gorboulev V, Ulzheimer JC, Akhoundova A, Ulzheimer-Teuber I, Karbach U, Quester S, Baumann C, Lang F, Busch AE and Koepsell H (1997) Cloning and characterization of two human polyspecific organic cation transporters. *DNA Cell Biol* **16**:871-881.
- Halgren TA (1999a) MMFF VI. MMFF94s option for energy minimization studies. *Journal of Computational Chemistry* **20**:720-729.
- Halgren TA (1999b) MMFF VII. Characterization of MMFF94, MMFF94s, and other widely available force fields for conformational energies and for intermolecular-interaction energies and geometries. *Journal of Computational Chemistry* **20**:730-748.
- Hou J, Paul DL and Goodenough DA (2005) Paracellin-1 and the modulation of ion selectivity of tight junctions. *J Cell Sci* **118**:5109-5118.
- Hull RN, Cherry WR and Weaver GW (1976) The origin and characteristics of a pig kidney cell strain, LLC-PK. *In Vitro* **12**:670-677.

- Hung YL, Kai M, Nohta H and Ohkura Y (1984) High-performance liquid chromatographic analyser for guanidino compounds using benzoin as a fluorogenic reagent. *J Chromatogr* **305**:281-294.
- Kai M, Miyazaki T and Ohkura Y (1984) High-performance liquid chromatographic measurement of guanidino compounds of clinical importance in human urine and serum by pre-column fluorescence derivatization using benzoin. *J Chromatogr* **311**:257-266.
- Kimura N, Masuda S, Katsura T and Inui K (2009) Transport of guanidine compounds by human organic cation transporters, hOCT1 and hOCT2. *Biochem Pharmacol* **77**:1429-1436.
- Kimura N, Masuda S, Tanihara Y, Ueo H, Okuda M, Katsura T and Inui K (2005) Metformin is a superior substrate for renal organic cation transporter OCT2 rather than hepatic OCT1. *Drug Metab Pharmacokinet* **20**:379-386.
- Knipp GT, Ho NF, Barsuhn CL and Borchardt RT (1997) Paracellular diffusion in Caco-2 cell monolayers: effect of perturbation on the transport of hydrophilic compounds that vary in charge and size. *J Pharm Sci* **86**:1105-1110.
- Kong J, Zhang Z, Musch MW, Ning G, Sun J, Hart J, Bissonnette M and Li YC (2008) Novel role of the vitamin D receptor in maintaining the integrity of the intestinal mucosal barrier. *Am J Physiol Gastrointest Liver Physiol* **294**:G208-216.
- Lee K and Thakker DR (1999) Saturable transport of H<sub>2</sub>-antagonists ranitidine and famotidine across Caco-2 cell monolayers. *J Pharm Sci* **88**:680-687.
- Li Q, Sai Y, Kato Y, Muraoka H, Tamai I and Tsuji A (2004) Transporter-mediated renal handling of nafamostat mesilate. *J Pharm Sci* **93**:262-272.
- McLean AD and Chandler GS (1980) Contracted Gaussian basis sets for molecular calculations. I. Second row atoms, Z=11--18. *The Journal of Chemical Physics* **72**:5639-5648.
- Petitjean M (1994) On the analytical calculation of van der Waals surfaces and volumes: Some numerical aspects. *Journal of Computational Chemistry* **15**:507-523.
- Proctor WR, Bourdet DL and Thakker DR (2008) Mechanisms underlying saturable intestinal absorption of metformin. *Drug Metab Dispos* **36**:1650-1658.
- Raghavachari K, Binkley JS, Seeger R and Pople JA (1980) Self-consistent molecular orbital methods. 20. A basis set for correlated wave functions. *The Journal of Chemical Physics* **72**:650-654.
- Rahner C, Mitic LL and Anderson JM (2001) Heterogeneity in expression and subcellular localization of claudins 2, 3, 4, and 5 in the rat liver, pancreas, and gut. *Gastroenterology* **120**:411-422.

- Ruddy SB and Hadzija BW (1992) Iontophoretic permeability of polyethylene glycols through hairless rat skin: application of hydrodynamic theory for hindered transport through liquid-filled pores. *Drug Des Discov* **8**:207-224.
- Saito H, Yamamoto M, Inui K and Hori R (1992) Transcellular transport of organic cation across monolayers of kidney epithelial cell line LLC-PK. *Am J Physiol* **262**:C59-66.
- Schultz SG and Solomon AK (1961) Determination of the effective hydrodynamic radii of small molecules by viscometry. *J Gen Physiol* **44**:1189-1199.
- Seki T, Harada S, Hosoya O, Morimoto K and Juni K (2008) Evaluation of the establishment of a tight junction in Caco-2 cell monolayers using a pore permeation model involving two different sizes. *Biol Pharm Bull* **31**:163-166.
- Song IS, Shin HJ and Shin JG (2008) Genetic variants of organic cation transporter 2 (OCT2) significantly reduce metformin uptake in oocytes. *Xenobiotica* **38**:1252-1262.
- Sparidans RW, Taal BG and Beijnen JH (1999) Bioanalysis of m-iodobenzylguanidine in plasma by high-performance liquid chromatography after derivatization with benzoin. *J Chromatogr B Biomed Sci Appl* **730**:193-199.
- Steward MC (1982) Paracellular non-electrolyte permeation during fluid transport across rabbit gall-bladder epithelium. *J Physiol* **322**:419-439.
- Van Itallie CM and Anderson JM (2004) The molecular physiology of tight junction pores. *Physiology (Bethesda)* **19**:331-338.
- Van Itallie CM and Anderson JM (2006) Claudins and epithelial paracellular transport. *Annu Rev Physiol* **68**:403-429.
- Van Itallie CM, Fanning AS and Anderson JM (2003) Reversal of charge selectivity in cation or anion-selective epithelial lines by expression of different claudins. *Am J Physiol Renal Physiol* **285**:F1078-1084.
- Van Itallie CM, Fanning AS, Bridges A and Anderson JM (2009a) ZO-1 stabilizes the tight junction solute barrier through coupling to the perijunctional cytoskeleton. *Mol Biol Cell* **20**:3930-3940.
- Van Itallie CM, Holmes J, Bridges A and Anderson JM (2009b) Claudin-2-dependent changes in noncharged solute flux are mediated by the extracellular domains and require attachment to the PDZ-scaffold. *Ann N Y Acad Sci* **1165**:82-87.
- Van Itallie CM, Holmes J, Bridges A, Gookin JL, Coccaro MR, Proctor W, Colegio OR and Anderson JM (2008) The density of small tight junction pores varies among cell types and is increased by expression of claudin-2. *J Cell Sci* **121**:298-305.

- Van Itallie CM, Rogan S, Yu A, Vidal LS, Holmes J and Anderson JM (2006) Two splice variants of claudin-10 in the kidney create paracellular pores with different ion selectivities. *Am J Physiol Renal Physiol* **291**:F1288-1299.
- Wang HZ and Veenstra RD (1997) Monovalent ion selectivity sequences of the rat connexin43 gap junction channel. *J Gen Physiol* **109**:491-507.
- Watson CJ, Rowland M and Warhurst G (2001) Functional modeling of tight junctions in intestinal cell monolayers using polyethylene glycol oligomers. *Am J Physiol Cell Physiol* **281**:C388-397.
- Whitley D (1998) Van der Waals surface graphs and molecular shape. *Journal of Mathematical Chemistry* **23**:377-397.
- Yu AS, Cheng MH, Angelow S, Gunzel D, Kanzawa SA, Schneeberger EE, Fromm M and Coalson RD (2009) Molecular basis for cation selectivity in claudin-2-based paracellular pores: identification of an electrostatic interaction site. *J Gen Physiol* **133**:111-127.
- Zeissig S, Burgel N, Gunzel D, Richter J, Mankertz J, Wahnschaffe U, Kroesen AJ, Zeitz M, Fromm M and Schulzke JD (2007) Changes in expression and distribution of claudin 2, 5 and 8 lead to discontinuous tight junctions and barrier dysfunction in active Crohn's disease. *Gut* **56**:61-72.

## **CHAPTER 5**

### **CATION-SELECTIVE TRANSPORTERS INVOLVED IN APICAL UPTAKE AND ACCUMULATION OF METFORMIN IN CACO-2 CELLS AND INTESTINAL EPITHELIUM**



## 5.A. ABSTRACT

In the intestinal cell model, Caco-2, metformin is transported across the apical (AP) membrane by bidirectional transporter(s) that were inhibited by prototypical inhibitors of human organic cation transporters (hOCTs). The goal of this study was to determine the specific transporter(s) involved in AP uptake/efflux in Caco-2 cells and consequently the intestine. This was determined through a novel chemical inhibition approach to systematically rule in or out candidate cation-selective transporters. Metformin substrate specificity towards candidate transporters hOCT1-3, and N2 was assessed in Chinese hamster ovary (CHO) cells expressing these transporters (Ming et al., 2009). Metformin was confirmed to be a substrate for hOCT1-3 and not a substrate for hOCTN2. Potency (e.g.  $IC_{50}$  values) of identified inhibitors on metformin transport was assessed in the hOCT-CHO cells. Inhibition of metformin [10 $\mu$ M] AP uptake in Caco-2 cells by mitoxantrone [80 $\mu$ M], a select inhibitor of hOCT1 in relation to hOCT2 and hOCT3, reduced the saturable carrier-mediated transport by 40%. Inhibitors for the material and toxin extrusion 1 (MATE1) and hOCT2 did not affect AP uptake. Corticosterone [150 $\mu$ M] and desipramine [200 $\mu$ M] were used to inhibit (hOCT1-3) and (hOCT1-3, PMAT), respectively. Corticosterone inhibition was no different than mitoxantrone inhibition, indicating hOCT3 was not involved in AP uptake. Desipramine decreased the saturable AP uptake by 70%, indicating involvement of PMAT. hOCT1 and PMAT were determined to be the major cation-selective transporters involved in AP uptake of metformin in Caco-2 cells. These results provide new insight into the function of cation-selective transporters in Caco-2 cells and pinpoint the transporters most likely responsible for intestinal accumulation and absorption of metformin.

## 5.B. INTRODUCTION

Metformin, an oral anti-hyperglycemic agent, is a hydrophilic drug (calculated logD at pH 7.4 of -6.13) (Saitoh et al., 2004) which exists as a cation at all physiological pH values (pKa 12.4). Consequently, the physiochemical properties of metformin prohibit efficient membrane permeability by passive diffusion and should result in poor intestinal absorption and reduced oral bioavailability. However, the drug is well absorbed across the intestine with approximately 60-80% of the dose absorbed across the intestine (Pentikainen et al., 1979; Tucker et al., 1981). This results in a higher than expected oral bioavailability ranging between 40-60% (Pentikainen, 1986; Sambol et al., 1996). In addition, intestinal absorption of metformin is known to be dose-dependent and variable (Tucker et al., 1981; Sambol et al., 1996). Metformin accumulates significantly in the intestine following oral administration to levels 30-300-fold higher than the plasma concentration (Bailey et al., 2008). The intestine also plays a significant role in the overall glucose-lowering effects of metformin (Stepensky et al., 2002), likely due to its activation of intracellular targets to increase intestinal uptake and metabolism of glucose (Bailey et al., 1994; Walker et al., 2005). The dichotomy between the predicted absorption based on the physiochemical properties and the clinical observations support the involvement of carrier-mediated transport processes in metformin intestinal accumulation, absorption, and pharmacology.

The absorption processes of metformin have been studied extensively in the Caco-2 cell monolayers, an established model of intestinal epithelium derived from human colon carcinoma (Hidalgo et al., 1989). Metformin was shown to be taken up across the apical (AP) membrane of the Caco-2 cells efficiently by bidirectional cation-selective transporter(s) (Chapter 2). Metformin efflux across the basolateral (BL) membrane of Caco-2 cell

monolayers was inefficient and rate limiting to transcellular transport, resulting in accumulation of metformin in the cells. Consequently, the absorptive transport of metformin was predominantly ( $\geq 90\%$ ) via paracellular transport. In order to rectify this observation with the reported high fraction of dose absorbed and dose-dependent absorption, it was hypothesized that the bidirectional cation-selective transport mechanism(s) on the AP membrane mediates efficient absorption by providing a cycling mechanism to increase intestinal transit time and allow for repeated opportunities to be absorbed through the paracellular space. However, the transporter(s) involved in this process in Caco-2 cells and in the intestine remain unknown.

The transport processes that drive metformin distribution in the liver, the major target organ for metformin pharmacology, and elimination in the kidney, which is the major organ for metformin elimination, have been studied extensively (Wang et al., 2002; Kimura et al., 2005a; Kimura et al., 2005b; Shu et al., 2008; Song et al., 2008; Nies et al., 2009; Tsuda et al., 2009b). Human organic cation transporters (hOCTs) and other cation-selective transporters have been implicated in the transport of metformin in the kidney and the liver. In the liver, hOCT1, and to a lesser extent hOCT3, are likely responsible for uptake of metformin into hepatocytes of the liver (Wang et al., 2002; Shu et al., 2008; Nies et al., 2009). In the kidney, metformin is considered to be actively excreted by vectorial transport involving cation-selective transporters. The current hypothesis is that hOCT2 is responsible for taking metformin across the plasma membrane into the proximal tubular cells (Kimura et al., 2005a; Song et al., 2008; Tsuda et al., 2009b), while the material and toxin extrusion transporter 1 (MATE1) and to a lesser extent the kidney specific MATE2-K are responsible for metformin egress across the basolateral membrane into the urine (Tsuda et al., 2009a;

Tsuda et al., 2009b). The role that these proteins and other cation-selective transporters have in facilitating intestinal accumulation and absorption of metformin and other hydrophilic cations remain largely unknown.

The intestine and Caco-2 cell model expresses several cation-selective transporters potentially capable of transporting metformin. The human intestine has detectable expression of the organic cation/carnitine transporter hOCTN2, hOCT1, hOCT2, and hOCT3 (Englund et al., 2006; Seithel et al., 2006; Hilgendorf et al., 2007; Koepsell et al., 2007; Meier et al., 2007). A recent study has shown that the plasma membrane monoamine transporter (PMAT) is expressed in human intestine and capable of transporting metformin (Zhou et al., 2007). The expression of cation transporters in Caco-2 cells is less known and reports in literature are often contradictory. Caco-2 cells have low but detectable levels of hOCT1, hOCT2, hOCT3, and hOCTN2 (Hayer-Zillgen et al., 2002; Hilgendorf et al., 2007; Hayeshi et al., 2008). There are no reports regarding the expression of MATE isoforms in human intestine or in Caco-2 cells, nor are there any published reports on the presence of PMAT expression in Caco-2 cells.

The goal of this work was to determine which of the known cation-selective intestinal transporters play significant role in intestinal accumulation and oral absorption of metformin and to estimate their relative importance in metformin absorption. To achieve this goal, known inhibitors of these transporters were utilized in a novel chemical inhibition scheme to rule in or out candidate transporters and to determine their relative contribution to metformin overall apical uptake in Caco-2 cell monolayers. Identifying the transporter(s) involved in metformin AP uptake will provide insight into the role these proteins have in absorption and the overall disposition of metformin.

## 5.C. MATERIALS AND METHODS

### Materials

Eagle's minimum essential medium (EMEM) with Earle's salts and L-glutamate, F-12 Nutrient Mixture, penicillin-streptomycin-amphotericin B solution (100x), non-essential amino acids (100x), geneticin, Superscript III reverse transcriptase, and HEPES (1M) were obtained from Invitrogen Corporation (Carlsbad, CA, USA). Hank's balanced salt solution (HBSS) with calcium and magnesium was purchased from Mediatech, Inc. (Manassas, VA, USA). Hygromycin B solution was obtained from Roche Applied Science (Indianapolis, IN, USA). Fetal bovine serum (FBS), trypsin-EDTA (1X), metformin hydrochloride, sodium-dodecyl sulfate (SDS), D-(+) glucose, mitoxantrone dihydrochloride, famotidine, cimetidine, corticosterone, desipramine hydrochloride, 1-methyl-4-phenylpyrimidium (MPP<sup>+</sup>) iodide, D-amphetamine hemisulfate salt, 2-[N-Morpholino]ethanesulfonic acid (MES), SYBR Green JumpStartTaq ReadyMix™, and sodium hydroxide (NaOH) were purchased from Sigma-Aldrich (St. Louis, MO, USA). [<sup>14</sup>C]Metformin (54 µCi/µmol) was purchased from Moravsek Biochemicals and Radiochemicals (Brea, CA, USA). [<sup>3</sup>H]MPP<sup>+</sup> acetate (83 Ci/mmol) and [<sup>14</sup>C]TEA (51 µCi/µmol) were purchased from New England Nuclear (PerkinElmer, Waltham, MA, USA). [<sup>3</sup>H]-L-carnitine hydrochloride (85 Ci/mmol) was purchased from Amersham (Buckinghamshire, UK). hOCT1-3, N2, and mock transfected Chinese hamster ovary (CHO) cells were previously generated and characterized active clones were obtained for these studies (Ming et al., 2009). The Caco-2 (HTB-37) cell line was obtained from the American Type Culture Collection (Manassas, VA, USA).

## **Organic Cation Transporter-Overexpressing Chinese Hamster Ovarian (CHO) Cells**

CHO cells were handled and cultured using established methods (Ming et al., 2009), with minor deviations. CHO cells stably expressing hOCT1, hOCT2, hOCT3, hOCTN2, and vector-control cells (Mock) were cultured in F12 Nutrient Mix supplemented with 10% fetal bovine serum, 100 units/ml penicillin, 100 µg/ml streptomycin, and 0.25 µg/ml amphotericin B with additional 500 µg/ml geneticin for hOCT1-3 and Mock-CHO cells or 200 µg/ml hygromycin B for hOCTN2 CHO cells. All cell lines were maintained at 37°C with 5% CO<sub>2</sub> and 90% relative humidity. The cells were passaged following 90% confluency using trypsin-EDTA, and plated at a 1:20 ratio in 75-cm<sup>2</sup> T flasks. All experiments were performed with CHO cells within the 5 passages of each other.

## **CHO Cell Transport Experiments**

All CHO cell lines were treated identically in regards to transport experiments as described previously (Ming et al., 2009). Briefly, CHO cells were seeded at 100,000 cells/cm<sup>2</sup> into sterile 24-well polycarbonate plates (Corning Life Science, Lowell, MA, USA). Cell culture media was changed the first day post seeding and every other day thereafter. Transport experiments were performed between days 5-7 post seeding. CHO cell monolayers were preincubated with transport buffer solution (HBSS with 25 mM D-glucose and 10 mM HEPES, pH 7.2) for 30 min at 37°C. Uptake experiment was initiated by replacing the buffer solution with 300µL of dosing solution. Uptake was terminated at the indicated time points by aspirating the donor solution and washing the monolayer 3x with 1-mL of ice cold (e.g. 4°C) transport buffer. The cell monolayers were allowed to dry and 500 µL of 0.1%SDS in 0.1N NaOH was added to each well. Plates were shaken for 3 hours to ensure total lysis of the cell monolayer. Protein content of the cell lysate was determined by

the bicinchoninic acid (BCA) protein assay (Pierce, Rockford, IL, USA) with bovine serum albumin as a standard. Radiolabeled compound in the cell lysate was analyzed by liquid scintillation spectrometry and the rate of initial uptake of each compound was determined. Function of each hOCT expressing cell line was assessed prior to metformin experiments by measuring uptake of [ $^{14}\text{C}$ ]TEA (0.15  $\mu\text{Ci}/\text{ml}$ , 10  $\mu\text{M}$ ) at 5 min for hOCT1-3 and [ $^3\text{H}$ ]L-carnitine (0.2  $\mu\text{Ci}/\text{ml}$ , 10  $\mu\text{M}$ ) at 5 min for hOCTN2 in relation to the uptake of each substrate in mock transfected CHO cells. Cell lines with at least 5-fold greater uptake than mock transfected cells were used for metformin related uptake. A time-course of [ $^{14}\text{C}$ ]Metformin (0.15  $\mu\text{Ci}/\text{mL}$ , 10  $\mu\text{M}$ ) uptake was performed for each hOCT CHO cell line in addition to mock CHO cells to assess uptake linearity in relation to time. A time-point was selected in the initial linear-range of uptake with respect to time for each cell line and concentration dependent uptake of metformin was examined. The uptake rate (e.g. the mass of metformin transported per minute and milligram of total protein) for the uptake into the mock CHO cells was subtracted from the uptake rates obtained in each hOCT expressing cell line to give a corrected uptake rate accounting for only the carrier-mediated transport of metformin.

Inhibition of metformin by various cation-selective inhibitors outlined in Table 5.1 were performed as described previously (Ming et al., 2009), with minor deviations. CHO cell monolayers were preincubated with transport buffer in the presence of inhibitor or vehicle control for 30 min at 37°C prior to experimentation. Uptake of metformin was initiated by replacing the buffer with 0.3 mL of donor solution of [ $^{14}\text{C}$ ]metformin [10  $\mu\text{M}$ , 0.15  $\mu\text{Ci}/\text{ml}$ ] in the presence of inhibitor or vehicle control. Eight different inhibitor concentrations were evaluated for each inhibitor selected. Uptake was terminated at a time-point at which uptake was in the initial linear phase for each cell line (typically 5 min) by

aspirating dose solution and washing the monolayer 3x with 1mL of ice cold (e.g. 4°C) transport buffer. Protein content and metformin accumulation in the cell lysate was performed as described above. Inhibition of metformin uptake [10μM] by cation-selective inhibitors was reported relative to the vehicle control data. Non-specific cell associated radioactivity was removed from each data point by subtracting the uptake data from the mock CHO experiments from the hOCT expressing uptake data.

### **Caco-2 Cell Culture**

Caco-2 cells were cultured at 37°C in EMEM with 10% FBS, 1% NEAA, and 100 U/ml penicillin, 100 μg/mL streptomycin, and 0.25 μg/mL amphotericin B in an atmosphere of 5% CO<sub>2</sub> and 90% relative humidity. The cells were passaged following 90% confluency using trypsin-EDTA, and plated at a 1:10 ratio in 75-cm<sup>2</sup> T flasks. The cells (passage numbers 30 to 38) were seeded at a density of 60,000 cells/cm<sup>2</sup> on polycarbonate membranes of Transwells™ (12 mm i.d., 0.4 μm pore size, Corning Life Science, Lowell, MA, USA). Medium was changed the day following seeding and every other day thereafter (AP volume 0.5 mL, BL volume 1.5 mL). The Caco-2 cell monolayers were used 21-28 days post seeding. Transepithelial electrical resistance (TEER) was measured to ensure monolayer integrity. Measurements were obtained using an EVOM Epithelial Tissue Voltohmmeter and an Endohm-12 electrode (World Precision Instruments, Sarasota, FL, USA). Cell monolayers with TEER values greater than 300 Ω·cm<sup>2</sup> were used in transport experiments.

### **Inhibition of Metformin Apical Uptake in Caco-2 Cell Monolayers**

Initial AP uptake of metformin was performed using methods outlined previously (Proctor et al., 2008) with minor deviations. Inhibition of initial AP uptake in Caco-2 cells of [<sup>14</sup>C]metformin [0.15μCi/mL, 10μM], [<sup>14</sup>C]TEA [0.15μCi/mL, 10μM], or [<sup>3</sup>H]MPP<sup>+</sup>



[0.15 $\mu$ Ci/mL, 1 $\mu$ M] was performed in the absence (control) or presence of D-amphetamine [50 $\mu$ M], cimetidine [25 $\mu$ M], mitoxantrone [80 $\mu$ M], corticosterone [150 $\mu$ M], desipramine [200 $\mu$ M], and MPP<sup>+</sup> [5mM]. During uptake experiments, cell monolayers were preincubated for 30 min in transport buffer in the presence of inhibitors outlined above or vehicle control (0.5% DMSO) bathing both the AP and BL compartments. Apical uptake experiments were initiated by replacing the buffer solution in the AP donor compartment with transport buffer containing the substrate in the presence of an inhibitor or vehicle control. The experiment was terminated during the initial linear uptake range in Caco-2 cell monolayers at 5 min for metformin and TEA and 3 min for MPP<sup>+</sup>. Uptake was stopped by washing the cell monolayers with 0.75mL of 4°C transport buffer three times in each compartment. The cell monolayers were allowed to dry, excised from the insert, and placed in 500  $\mu$ L of 0.1%SDS in 0.1N NaOH for 3 hours, while shaking. Protein content of the cell lysate was determined by the BCA protein assay with bovine serum albumin as a standard. Metformin in the cell lysate was analyzed by liquid scintillation spectrometry and the rate of initial uptake of metformin was determined.

### **Metformin AP Uptake in Caco-2 Cell Monolayers as a Function of Extracellular pH**

The effect of varying extracellular pH on metformin AP uptake was examined in Caco-2 cell monolayers using methods previously established with minor deviations (Bourdet and Thakker, 2006). Transport solution was buffered with 10 mM MES (pH 5.5, 6.0, 6.5) or 10 mM HEPES (pH 7.0, 7.4, 8.0). All wells were preincubated with transport buffer (pH 7.4) in both AP and BL compartments for 30 min prior to the start of the experiment. The AP buffer was then replaced with 0.4 mL of the appropriate pH transport buffer containing metformin (0.15 $\mu$ Ci/mL, 10 $\mu$ M). Uptake was determined over 5 min after

which the AP solution was aspirated and monolayers washed three times with 4°C transport buffer. Cell monolayers were assayed for metformin and protein content as described above. Four determinations were made for each extracellular pH and statistical differences from that of the control (pH 7.4) were determined using one-way analysis of variance analysis (ANOVA) followed by Bonferroni post-test analysis. Statistical analysis was performed using GraphPad Prism (GraphPad Software, La Jolla, CA, USA).

### **Quantitative Polymerase Chain Reaction (PCR) to Determine the Expression of Cation-selective Transporter Genes in Caco-2 Cells**

The mRNA expression of human hOCT1, hOCT3, hOCTN2, and PMAT, relative to glyceraldehyde 3-phosphate dehydrogenase (GAPDH), in Caco-2 cells and human intestine was determined using quantitative real time-polymerase chain reaction (RT-PCR) analysis. RT-PCR experiments were conducted using established methods (Holmes et al., 2006) with minor deviations. Total RNA was isolated from Caco-2 cell monolayers using RNeasy Mini Prep columns (Qiagen, Valencia CA, USA). RNA samples were subjected to DNA digestion by TURBO DNase (Ambion/Applied Biosystems, Austin, TX, USA) to remove potential genomic DNA contamination. cDNA was synthesized from total Caco-2 RNA (5 µg) using Superscript III reverse transcriptase (Invitrogen Corporation, Carlsbad, CA, USA). An equal amount of RNA was included in a No-RT control for each separate RNA sample. Real-time PCR was performed with 1:20 dilutions of the cDNA (in triplicate). Quantitative PCR reactions (25µL total volume) were performed using SYBR Green JumpStartTaq ReadyMix™ for quantitative PCR (Sigma–Aldrich Co., St. Louis, MO, USA), with primer pairs at 0.75 µM final reaction concentration, and 5 µL of cDNA or No-Template negative control. RT-PCR amplification was performed in a Applied Biosystems 7300 Real-Time

PCR System (Applied Biosystems, Inc. Foster City, CA, USA) thermal cycler at 95°C for 10 min followed by 40 cycles of 95°C for 15 s, 55°C for 60 s, and 72°C for 25 s. Human GAPDH, hOCT1, hOCT3, hOCTN2, and PMAT primer pairs were obtained from Invitrogen (Carlsbad CA, USA). GAPDH forward and reverse primer sequences were 3'-GACCCCTTCATTGACCTCAACTAC-5' and 3'-TTGACGGTGCCATGGAATTT-5', respectively with an amplified product length of 80 base pairs (bp). hOCT1 forward and reverse primer sequences were 3'-GACGCCGAGAACCTTGGG-5' and 3'-GGGTAGGCAAGTATGAGG-5', respectively with an amplified product length of 198 bp. hOCT3 forward and reverse primer sequences were 3'-GGAGTTTCGCTCTGTTCAGG-5' and 3'-GGAATGTGGACTGCCAAGTT-5', respectively with an amplified product of 216 bp. hOCTN2 forward and reverse primer sequences were 3'-AGTGGGCTATTTTGGGCTTT-5' and 3'-GGTCGTAGGCACCAAGGTAA-5', respectively with an amplified product of 398 bp. PMAT forward and reverse primer sequences were 3'-TTCATCACGGACGTGGACTA-5' and 3'-CGTCGCAGATGCTGATAAAA-5', respectively with an amplified product of 202 bp. Amplified products were separated and detected using gel electrophoresis (2% agarose gel with 0.5 µg/mL ethidium bromide) to ensure singular products at the appropriate size (Figure 5.7A). The lowest signal threshold at which all sample amplified were above the background was set and the cycle at which the each sample crossed the threshold, or cycle threshold ( $C_t$ ), was determined for each sample. All gene products were amplified above the fluorescent threshold by cycle 35 in the cDNA sample.

The housekeeping gene GAPDH expression was determined in each RT-PCR run and served as the normalization control. cDNA preparation, fluorescent threshold, and PCR

conditions remained constant in order to calculate the expression of transporter genes in relation to GAPDH. Relative expression values were calculated by  $2^{\Delta C_t}$ , where  $\Delta C_t = (C_{t, \text{GAPDH}} - C_{t, \text{gene}})$ ; therefore, the expression value of GAPDH was set to 1.0. Experimental error was estimated for each gene in each Caco-2 treatment group by comparing the CV (%) of the average  $C_t$  value of that gene,  $\text{error} = [(2^{\%CV})/100] \cdot [\text{relative expression value}]$ . Relative expression values for each target gene were reported if their CV values were less than or equal to 15% for the triplicate values.

### Data Analysis

A Michaelis-Menten equation with one saturable component was fit to the corrected uptake rate data obtained in CHO cell experiments, which represented only the carrier-mediated transport, described by the following expression:

$$V = \frac{(V_{\max} * C)}{(K_m + C)} \quad (5.1)$$

where  $C$  is the metformin concentration,  $V_{\max}$  is the maximal velocity, and  $K_m$  is the Michaelis-Menten constant.

Inhibitory potency (e.g.  $IC_{50}$  value) was determined for each inhibitor across the hOCT expressing cell line. The following equation was fit to the corrected uptake data:

$$V = \frac{V_o}{\left[1 + \left(I/IC_{50}\right)^n\right]} \quad (5.2)$$

where  $V$  is the uptake rate in the presence of inhibitor  $[I]$ ,  $V_o$  is the uptake rate in the absence of inhibitor,  $IC_{50}$  is the inhibitor concentration to achieve 50% inhibition, and  $n$  is the Hill coefficient. Uptake kinetic model and  $IC_{50}$  curve model estimates were obtained by non-linear least squares regression analysis by WinNonlin (Pharsight, Mountain View, CA,

USA).  $IC_{50}$  data for hOCT expressing CHO cells and Caco-2 uptake data were reported relative to control. All data presented are expressed as mean  $\pm$  SD from 3 measurements unless otherwise noted. Statistical significance was evaluated by one-way analysis of variance analysis (ANOVA) followed by Bonferroni post-test analysis unless otherwise noted.

## 5.D. RESULTS

### Metformin is a Substrate for hOCT1-3 and Not a Substrate for hOCTN2

Functional activity of each CHO cell line expressing individual hOCT1-3 or hOCTN2 (Ming et al., 2009) were determined by measuring uptake of probe substrates TEA and L-carnitine for hOCT1-3 and hOCTN2, respectively, in relation to uptake of the probe substrates in the mock transfected cells. TEA uptake was  $7.6 \pm 0.07$ -,  $7.8 \pm 0.06$ -, and  $9.9 \pm 0.4$ -fold greater in hOCT1, hOCT2, and hOCT3 expressing CHO cells, respectively, than mock cells (data not shown). L-Carnitine uptake was  $(57 \pm 3)$ -fold greater in hOCTN2-CHO cells than mock CHO cells (data not shown). Metformin [ $10\mu\text{M}$ ] uptake was evaluated in hOCT1, hOCT2, hOCT3, and hOCTN2 expressing CHO cells (Ming et al., 2009); uptake into the hOCT1-3 expressing cells was linear with time for up to 5 min and several fold greater than that into the mock transfected cells (Figure 5.1A-C). In contrast, metformin uptake into hOCTN2 expressing CHO cells was inefficient and not significantly different from uptake into the mock CHO cells (Figure 5.1D); therefore metformin was determined not to be a substrate for hOCTN2 and further studies with this cell line were omitted.

Uptake (5 min) of metformin into the hOCT1-3 expressing CHO cells as a function of concentration exhibited a hyperbolic relationship (Figure 5.2A-C). In contrast, metformin uptake into mock transfected cells was linear to 10mM donor concentration (data not shown). A Michaelis-Menten equation (Eq. (5.1)) was fit to the concentration dependent uptake of metformin in hOCT1-3 CHO cells to obtain estimates of apparent  $K_m$  and  $V_{max}$  values. The transport kinetic parameters estimated for metformin uptake in hOCT1-3 CHO cells are presented in Figure 5.2 for each hOCT expressing CHO cell line.

### **Inhibition of hOCT1-, hOCT2-, and hOCT3-mediated Metformin Uptake in CHO Cells by a Panel of Cation-Selective Inhibitors**

Inhibition of metformin [10 $\mu$ M] uptake into hOCT expressing CHO cells by a panel of cation-selective inhibitors (see Table 5.1 for chemical structures) was examined for the purpose of identifying inhibitors that would selectively inhibit hOCT1-, hOCT2-, or hOCT3-mediated metformin uptake into cells without inhibiting the other two hOCT transporters.  $IC_{50}$  curves were generated for inhibition of metformin uptake by D-Amphetamine, mitoxantrone, corticosterone, desipramine, and famotidine into hOCT1, hOCT2, and hOCT3 expressing CHO cells (Figure 5.3A-C). Uptake of metformin into the three hOCT expressing cells was inhibited by the five inhibitors in a concentration dependent manner. Mitoxantrone, the target hOCT1-specific inhibitor (Koepsell et al., 2007), was a potent inhibitor of hOCT1 with an  $IC_{50}$  value of  $3.0 \pm 0.8 \mu\text{M}$ , which is 40 to 60-fold lower than its estimated  $IC_{50}$  values for hOCT2 and hOCT3 (Table 5.2). Corticosterone, desipramine, and famotidine were also strong inhibitors of hOCT1-mediated metformin transport at the same relative inhibitory potency (e.g.  $IC_{50}$  values  $< 10\mu\text{M}$ ); however, they were not as selective for hOCT1 as mitoxantrone (Table 5.2). D-Amphetamine, as expected by its reported hOCT2 selectivity (Amphoux et al., 2006), was a potent inhibitor of hOCT2 with an estimated  $IC_{50}$  value of  $5.7 \pm 1.0 \mu\text{M}$ , which is 10 to 20-times lower than its estimated  $IC_{50}$  values for hOCT1 and hOCT3. Corticosterone and desipramine were the most potent hOCT2 inhibitors with  $IC_{50}$  values estimated to be less than  $3\mu\text{M}$ , while famotidine  $IC_{50}$  value for hOCT2 mediated metformin transport was  $\sim 20 \mu\text{M}$  (Table 5.2). Mitoxantrone was the least potent inhibitor of hOCT2 with an  $IC_{50}$  value of  $\sim 140 \mu\text{M}$  which is very similar to the reported  $IC_{50}$

value for cimetidine inhibition of hOCT2 mediated metformin uptake of 147  $\mu$ M (Tsuda et al., 2009b).

The profile of  $IC_{50}$  curves for inhibition of metformin uptake into the hOCT3 expressing CHO cells was the most diverse with  $IC_{50}$  values spanning 3 orders of magnitude (Figure 5.3C). Corticosterone was the most potent inhibitor of hOCT3-mediated metformin uptake with an  $IC_{50}$  value of  $0.15 \pm 0.05$   $\mu$ M, followed by famotidine, desipramine, D-amphetamine, and mitoxantrone (Table 5.2). Famotidine was tested as a selective hOCT3 inhibitor in relation to hOCT1 and hOCT2 based on a previous report of MPP<sup>+</sup> inhibition in hOCT1, hOCT2, and hOCT3 expressing *Xenopus laevis* oocytes (Bourdet et al., 2005). Famotidine was a potent inhibitor of hOCT3 mediated metformin uptake with an  $IC_{50}$  value of  $2.7 \pm 0.2$   $\mu$ M, yet this was only 2- and 7-fold lower than the  $IC_{50}$  values for hOCT1 and hOCT3 mediated metformin uptake, respectively. These data suggest that famotidine inhibition of hOCT3 mediated metformin transport was not specific enough to be used to estimate the contribution of hOCT3 in metformin AP uptake in Caco-2 cells.

#### **hOCT1 and PMAT Mediate Apical Uptake of Metformin into Caco-2 Cell Monolayers**

The experimentally derived inhibition data for hOCT1-3 and previously reported inhibition data for MATE1 and PMAT uptake of metformin, TEA, serotonin, or MPP<sup>+</sup> (as noted) is presented in Table 5.2. This data allowed for selection of inhibitors and the appropriate concentration to selectively rule in or rule out candidate transporters that may mediate AP uptake of metformin in Caco-2 cells. The concentration selected for each inhibitor was at least 4-fold greater than the estimated  $IC_{50}$  value for metformin uptake by the target transporter, but at least 2-fold less than the  $IC_{50}$  values for other metformin transporters that may play a role in cellular uptake, when possible. Figure 5.4 depicts the chemical



inhibition scheme employed in examining specific transporter involvement in AP uptake of metformin in Caco-2 cells with each inhibitor, their respective concentration, and the proposed candidate transporters inhibited.

Metformin initial AP uptake was evaluated in the presence and absence of each inhibitor at the concentration outlined in Figure 5.4. D-amphetamine and cimetidine inhibition had no effect on the AP uptake of metformin in Caco-2 cells (Figure 5.5A). Mitoxantrone [80 $\mu$ M] significantly decreased the AP uptake of metformin to  $74 \pm 8\%$  ( $p < 0.01$ ) of the control. Similarly, corticosterone inhibited AP transport by  $\sim 25\%$ , reducing the AP uptake to  $73 \pm 3\%$  ( $p < 0.01$ ) (Figure 5.5A). The difference between the inhibition by mitoxantrone and corticosterone was insignificant. Inhibition by 200 $\mu$ M desipramine reduced the AP uptake of metformin by  $\sim 50\%$  with only  $49 \pm 5\%$  ( $p < 0.001$ ) of metformin uptake remaining. MPP<sup>+</sup> reduced metformin uptake by  $\sim 75\%$ , indicating that  $26 \pm 1\%$  of metformin AP uptake may be attributed to non-specific binding and/or uptake via passive diffusion.

In addition to metformin, the ability of corticosterone and desipramine to inhibit the carrier-mediated uptake of two additional probe substrates, TEA [10  $\mu$ M] and MPP<sup>+</sup> [1  $\mu$ M], on the AP membrane of Caco-2 cells was examined (Figure 5.5B). Metformin, TEA, and MPP<sup>+</sup> uptake across the AP membrane in Caco-2 cells was corrected to account for only the saturable carrier-mediated transport by subtracting the remaining uptake in the presence of 5mM MPP<sup>+</sup>. Approximately 40% of the saturable carrier-mediated transport of metformin was inhibited by corticosterone, while desipramine inhibited an additional 30% of the carrier-mediated transport can be attributed to PMAT, leaving approximately 30% of the carrier-mediated transport remaining (Figure 5.5B). Similar to metformin, approximately 35% of

the saturable carrier-mediated transport of TEA was inhibited by corticosterone, with desipramine inhibiting an additional 35% of the carrier-mediated transport. Approximately 30% of TEA carrier-mediated uptake was not inhibited by desipramine or corticosterone. MPP<sup>+</sup> carrier-mediated uptake was only inhibited approximately 25% by corticosterone (Figure 5.5B). However, desipramine almost completely abolished the carrier-mediated transport of MPP<sup>+</sup>, leaving only ~10% of the saturable transport remaining. Desipramine inhibition on MPP<sup>+</sup> (~90%) was significantly different ( $p < 0.05$ ) than desipramine inhibition on metformin and TEA (~70%).

### **Metformin AP Uptake is Not Enhanced with a Decrease in Extracellular pH**

The pH dependence on AP uptake of metformin was examined to determine if particular cation-selective transporters were involved. For example, PMAT is the only cation-selective candidate transporter explored here to have been shown to increase function with an inward proton gradient (Xia et al., 2007; Zhou et al., 2007), where hOCT1-3 function was not changed (Koepsell et al., 2007) or decreased in the presence of an inward proton gradient (Martel et al., 2001). Therefore, metformin [10 $\mu$ M] AP uptake in Caco-2 cells was examined in transport buffer with pH values ranging from 5.5 to 8.0 (Figure 5.6). Reducing the extracellular pH decreased the initial AP uptake of metformin. There was a significant decrease in AP uptake of metformin at pH 6.0 (73% of the pH 7.4 value,  $p < 0.05$ ) in relation to the uptake at pH 7.4. Although not significantly different, the mean metformin uptake rate at pH 8.0 increased to ~120% of that at pH 7.4.

## **PMAT mRNA is Highly Expressed in Caco-2 Cells in Relation to hOCT1 and hOCT3 mRNA**

The expression of hOCT1, hOCT3, hOCTN2, and PMAT mRNA relative to GAPDH mRNA were examined in the parental Caco-2 cells (HTB-37) using quantitative RT-PCR (Figure 5.7B). The PCR primer pairs were produced singular gene products at the appropriate amplified lengths from RNA isolated from Caco-2 cells (HTB-37), where no gene products were detected in the No-RT negative control samples (Figure 5.7A). Although metformin was shown not to be a substrate for hOCTN2 (Figure 5.1D), the relative expression of this cation-selective transporter was determined. hOCTN2 is reported to be one of the most highly expressed cation-selective transporter in Caco-2 cells and in the human intestine (Englund et al., 2006; Kim et al., 2007; Maubon et al., 2007; Meier et al., 2007), thus, providing a basis for comparison for the other cation-selective transporters in Caco-2 cells. hOCT1 relative expression was the lowest in Caco-2 cells of the cation-selective transporters examined in this study. The relative expression of hOCT1 mRNA was approximately 4-, 11-, and 8-fold lower than hOCT3, hOCTN2, and PMAT relative expression, respectively. PMAT relative expression was approximately 25% lower than hOCTN2. These results support the relative expression data for these cation-selective transporters in the Caco-2 P27.7 clone (Chapter 3).

## 5.E. DISCUSSION

Previous studies showed that one or more AP uptake transporter(s) played a significant role in the intestinal absorption of metformin despite the fact that this drug was predominantly absorbed via the paracellular route (Proctor et al., 2008; Chapter 2). Based on the chemical structure of metformin with net positive charge at all physiological pH values, and based on the previously published reports (Kimura et al., 2005a; Koepsell et al., 2007; Tanihara et al., 2007; Zhou et al., 2007; Nies et al., 2009; Tsuda et al., 2009b) it is a reasonable assumption that organic cation transporters, hOCT1-3 and hOCTN1-2, as well as other cation-selective transporters such as PMAT and MATE1 may play an important role in the intestinal absorption of metformin. The data presented here confirm previous reports that metformin was a superior substrate for hOCT2 than for hOCT1 or hOCT3 (Kimura et al., 2005a; Nies et al., 2009), and for the first time clearly demonstrated that metformin was not a substrate for hOCTN2. The latter finding is highly significant in that it rules out metformin transport by one of the most highly expressed cation-selective transporters present in both Caco-2 cells and human intestine (Englund et al., 2006; Kim et al., 2007; Maubon et al., 2007; Meier et al., 2007), as well as the heart, liver, and kidney (Tamai et al., 1998; Wu et al., 1999; Hilgendorf et al., 2007). The substrate affinity of hOCTN1 for metformin and further functional studies were omitted from this report due to hOCTN1 substrate specificity towards predominantly zwitterionic compounds, in particular ergothioneine (Grundemann et al., 2005). Unlike hOCTN2 which has been localized to the AP membrane of Caco-2 cells (Elimrani et al., 2003) and intestine (Kato et al., 2006), localization of hOCTN1 in Caco-2 cells was found to be exclusively intracellular (Lamhonwah et al., 2005). A later report revealed hOCTN1 was localized to the mitochondria in Caco-2 cells (Lamhonwah and Tein,

2006); therefore making this transporter a very unlikely candidate in mediating metformin AP uptake in Caco-2 cells and consequently the intestine.

In this report and in literature reports, metformin was shown to be a substrate for hOCT1-3 (Figure 5.2. (Kimura et al., 2005a; Nies et al., 2009)), MATE1 (Tanihara et al., 2007), and PMAT (Zhou et al., 2007); however protein expression, function, and localization for these candidate transporters in Caco-2 cells is unknown. The wide substrate specificity of cation-selective transporters towards metformin and the potential for multiple transporters expressed on the AP membrane in Caco-2 cells presented a challenge to elucidate the specific transporter(s) responsible for AP uptake of metformin. To address this problem, a novel chemical inhibition approach was implemented to estimate the contribution of each candidate transporter on the apical membrane in Caco-2 cells (Figure 5.4). The chemical inhibitors for a particular transporter were selected if their  $IC_{50}$  values were at least 4-fold lower than the respective values for other candidate transporters. The inhibitor concentrations were maximized to a point where they were 50% or less of the concentration of the  $IC_{50}$  values for the other candidate transporters. This ensured 100% inhibition of the target transporter with only modestly affecting other candidate transporters. Prior to implementing this inhibition scheme, the selectivity and potency of each compound to inhibit metformin transport by different transporters was evaluated in cell lines stably expressing single hOCT transporters that were available (Figure 5.3 and Table 5.2), so that appropriate inhibitor concentrations could be identified.

The chemical inhibition scheme (Figure 5.4) employed systematically estimated or eliminated the contribution of the five candidate transporters from mediating AP uptake of metformin in Caco-2 cells. For example, mitoxantrone was determined to be a selective

inhibitor of hOCT1-mediated metformin transport in relation to hOCT2 and hOCT3 at concentrations  $\leq 80\mu\text{M}$ ; therefore  $80\mu\text{M}$  of mitoxantrone was used to determine the role of hOCT1 in metformin Caco-2 AP uptake. The contribution of hOCT2-mediated metformin uptake in relation to hOCT1 and hOCT3 was determined by inhibiting uptake with D-amphetamine at  $50\mu\text{M}$ . Cimetidine at  $25\mu\text{M}$  should completely inhibit any contribution of MATE1 transport, while inhibiting  $\sim 50\%$  of hOCT3-mediated metformin transport. Cimetidine at that concentration likely will not affect hOCT1-, hOCT2-, and PMAT-mediated metformin transport (Table 5.2). Therefore, metformin AP uptake was examined in the presence of  $25\mu\text{M}$  cimetidine to evaluate the contribution of MATE1 and to a lesser extent hOCT3. Corticosterone at  $150\mu\text{M}$  should sufficiently inhibit hOCT1-3, while not significantly inhibiting PMAT; hence corticosterone at this concentration was used to determine the hOCT1-3 contribution to overall metformin AP uptake. The difference between inhibition by corticosterone [ $150\mu\text{M}$ ] and that by D-amphetamine [ $50\mu\text{M}$ ] and mitoxantrone [ $80\mu\text{M}$ ] represents the contribution of hOCT3-mediated metformin transport. Desipramine at  $200\mu\text{M}$  will adequately inhibit hOCT1-3, MATE1, and PMAT; therefore this concentration was selected to achieve complete inhibition of metformin AP uptake by all cation-selective transporters. Thus, the difference in the extent of inhibition by desipramine and that by corticosterone will represent the contribution of MATE1 and PMAT mediated metformin uptake. High concentrations of pan-cation-selective substrate/inhibitor  $\text{MPP}^+$  (e.g.  $\geq 5\text{ mM}$ ) have been shown to completely inhibit cation-selective carrier-mediated transport (Sato et al., 2008), where any remaining uptake represented the contributions of non-specific binding and/or passive diffusion. Therefore,  $\text{MPP}^+$  [ $5\text{mM}$ ] was used to

completely inhibit carrier-mediated transport and to account for potential contributions of carrier-mediated transport not inhibited by the “select” inhibitors.

By this approach, the contribution of hOCT1 in mediating the overall AP uptake in Caco-2 cells was determined to be approximately 25% (Figure 5.5A). When accounting for only the carrier-mediated saturable transport, hOCT1 contributed approximately 40% of metformin uptake. hOCT2 did not contribute to metformin initial AP uptake in Caco-2 cells, due to the lack of inhibition by D-amphetamine. This was further confirmed by inhibition by corticosterone, which should have completely inhibited hOCT1-3; yet the percent inhibited was no different than the value observed when only hOCT1 was inhibited (Figure 5.5A). Furthermore, the lack of a significant additive effect between inhibiting only hOCT1 and inhibiting hOCT1-3 indicated that hOCT3 also played an insignificant role in the AP uptake of metformin in Caco-2 cells. Additionally, MATE1 was not involved in the AP uptake in Caco-2 cells, for cimetidine did not inhibit metformin uptake. Finally, inhibition by desipramine, which should have inhibited hOCT1-3, MATE1, and PMAT, resulted in an approximately 50% reduction in the overall AP uptake of metformin in Caco-2 cells. This reduction accounted for approximately 70% of the saturable carrier-mediated transport of metformin (Figure 5.5B). By subtracting the hOCT1 component from this, it appeared that PMAT contributed at least 30% of the saturable carrier-mediated transport. These observations together indicated that hOCT1 and PMAT are the two major cation-selective transporters responsible for AP uptake of metformin in Caco-2 cells.

PMAT is localized on the AP membrane of human intestine enterocytes and is known to transport metformin with an apparent  $K_m$  of  $1.32 \pm 0.11$  mM (Zhou et al., 2007). Protein expression and localization in Caco-2 cells is unknown. There is limited evidence for the

localization of hOCT1 in the intestine and in Caco-2 cells. Lateral and cytosolic staining of hOCT1 was observed in sections of human intestine when staining with a rat Oct1 polyclonal antibody, while protein staining was not detected with this antibody in Caco-2 cells (Muller et al., 2005). Another study using a rat Oct1 antibody demonstrated AP localization of hOCT1 in Caco-2 cells (Ng, 2002). Based on these results, it appears that both hOCT1 and PMAT are expressed on the AP membrane of Caco-2 cells. The gene expression of both hOCT1 and PMAT were detected in the Caco-2 cells (Figure 5.7). The relative mRNA expression for hOCT1 was approximately 8-fold lower than PMAT mRNA expression (Figure 5.7B). PMAT mRNA expression in Caco-2 cells was a novel finding, although protein expression and membrane localization remains unknown.

The difference in relative mRNA expression between PMAT and hOCT1 suggest that PMAT may be the major transporter mediating metformin uptake on the AP membrane in Caco-2 cells and ultimately in the human intestine; yet the inhibition data supported that both transporters contributed almost equally to the carrier-mediated saturable transport of metformin. There is a possibility that mRNA expression did not correlate with functional PMAT protein in Caco-2 cells. Another possible explanation was that the function of PMAT on the AP membrane in Caco-2 cells may be underestimated when using this chemical inhibition approach. For example, it is possible that the mitoxantrone inhibition data in Caco-2 cells may actually represent mitoxantrone inhibition of PMAT and not exclusively hOCT1. The inhibitory potency of mitoxantrone on PMAT-mediated metformin transport is unknown. Furthermore, the inhibition of AP uptake by corticosterone at 150  $\mu\text{M}$ , which was concluded to be due to inhibition of hOCT1-3, may be, in part, due to inhibition of PMAT. The reported  $IC_{50}$  value of  $450 \pm 77 \mu\text{M}$  for corticosterone was for inhibiting serotonin uptake



(Engel et al., 2004), not metformin transport. It is conceivable that metformin mediated transport by PMAT may be more susceptible to corticosterone inhibition and thus confound the interpretation of the data.

Desipramine inhibited ~70% of the carrier-mediated saturable transport of metformin, of which at least 30% was attributed to PMAT. Desipramine was shown here to be a potent inhibitor of hOCT1-3-mediated metformin transport with  $IC_{50}$  values  $< 5 \mu\text{M}$  and has been reported to be a sufficient inhibitor PMAT mediated transport of serotonin ( $IC_{50} 32.6 \pm 2.7 \mu\text{M}$ ) (Table 5.2) (Engel et al., 2004). The potency of desipramine to inhibit PMAT-mediated metformin transport is unknown. These uncertainties potentially limit the accuracy of the estimates made through this novel chemical inhibition scheme. Regardless, the approach employed here implicated two cation-selective transporters in facilitating the AP uptake of metformin in Caco-2 cells, while ruling out an additional three candidate transporters. Further studies are underway to confirm these results and to more accurately estimate the contributions of both hOCT1 and PMAT in Caco-2 cells by using siRNA knock-down approaches to selectively target each transporter.

Another significant finding of this work involved the similarities between the inhibition profile for metformin and TEA (Figure 5.5B). Both metformin and TEA were inhibited to an identical extent by both corticosterone and desipramine, supporting the notion that these compounds share similar uptake and inhibition properties in Caco-2 cells. Interestingly, desipramine did not abolish the carrier-mediated transport of both compounds, leaving ~30% of the transport uninhibited. During  $\text{MPP}^+$  uptake experiments, only 10% of the AP uptake was not inhibited by desipramine. An explanation to account for the difference between  $\text{MPP}^+$  and metformin inhibition by desipramine is that there was an

unknown or unidentified transporter, not subject to desipramine inhibition, that could transport metformin and TEA efficiently and not MPP<sup>+</sup>. The possibility of an unidentified cation-selective transporter on the AP membrane in Caco-2 cells cannot be ruled out until more definitive studies addressing metformin uptake are performed (e.g. siRNA knockdown of hOCT1 and PMAT expression).

PMAT has been shown to function as a proton-symporter, in which transport activity was enhanced in the presence of an inward proton gradient (Barnes et al., 2006; Xia et al., 2007). For example, metformin uptake was enhanced ~4-fold in PMAT expressing MDCK cells when the extracellular pH was reduced from 7.4 to 6.6 (Zhou et al., 2007). To examine if metformin uptake in Caco-2 displayed similar pH dependence, AP uptake of metformin was examined at extracellular pH ranging from 5.5 to 8.0 (Figure 5.6). Surprisingly AP uptake was not enhanced with decreasing pH, but actually significantly decreased at pH 6.0 and appeared to increase at pH 8.0, albeit not significantly, in relation to pH 7.4. Similar pH dependence on AP uptake in Caco-2 cells was observed with MPP<sup>+</sup> uptake by Martel et al. in 2001. They reported almost identical results in which MPP<sup>+</sup> uptake was reduced to 86% at pH 6.2 and increased to 116% at pH 8.2 in relation to control (pH 7.4) (Martel et al., 2001). They observed similar pH dependency for AP uptake of MPP<sup>+</sup> into HEK293 cells expressing hOCT3. Currently the proton-symporter functionality of PMAT has been demonstrated only in renal cells (e.g. MDCK) transfected with exogenous PMAT and *Xenopus laevis* oocytes expressing PMAT (Barnes et al., 2006; Xia et al., 2007). It remains unknown whether PMAT expressed in the human intestine or Caco-2 cells possesses the same driving force for PMAT mediated transport. Regardless of the discrepancy between reported PMAT pH dependence and the metformin uptake in Caco-2 cells, high relative expression of PMAT

mRNA in Caco-2 cells, its AP localization in human intestine, and the metformin inhibition data support PMAT function and localization on the AP membrane of Caco-2 cells. Future studies are necessary to more accurately measure PMAT function and protein expression in Caco-2 cells.

Due to the various cation-selective transporter capable of transporting metformin that share similar affinities, the inhibition data provides functional data supporting overall localization and function of these transporters in Caco-2 cells and possible in the intestine. For example, the expression and localization of hOCT2 in Caco-2 cells has been controversial. Although not expressed in human intestine, there are contradictory reports regarding expression of hOCT2 in Caco-2 cells (Muller et al., 2005; Hilgendorf et al., 2007; Maubon et al., 2007; Hayeshi et al., 2008). There is only one report of the presence of hOCT2 protein in Caco-2 cells, demonstrated using immunofluorescent staining with an antibody grown against hOCT2 (Muller et al., 2005). Faint staining on the lateral membrane and cytosolic compartment was observed, and the staining was partially ablated when the antibody was preabsorbed with the hOCT2 antigenic peptides. Regardless of membrane localization, the data presented here indicates that hOCT2 is not active on the AP membrane and if present on the BL membrane it does not appear to be active due to the inefficient BL uptake of metformin observed previously in Caco-2 cells with an apparent  $K_m$  of  $12.3 \pm 0.4$  mM (Chapter 2).

The results here indicated that MATE1 protein was not active on the AP membrane in Caco-2 cells. MATE1 protein expression has been shown to be predominantly in the liver, spleen, kidney, and to a lesser extent the heart (Otsuka et al., 2005); however the expression and role of this transporter in the intestine and in Caco-2 cells remains unknown. It has been

shown to be localized in humans on the brush-boarder membranes of the proximal and distal convoluted tubules of the kidney and bile canaliculi in the liver (Otsuka et al., 2005), therefore it was conceivable that if present it would be localized on AP membrane in Caco-2 cells. MATE1 functions as proton antiporter to efflux compounds from the proximal tubular cells and hepatocytes into the urine and bile, respectively (Otsuka et al., 2005). Considering the low pH of the intestinal lumen and inward pH gradient, MATE1 if present in the intestine will most likely function as a secretory efflux pump. Nevertheless, the similarity between the reported affinity of metformin for MATE1 and the apparent  $K_m$  for saturable AP uptake in Caco-2 cells (apparent  $K_m$   $0.9 \pm 0.2$  mM) (Chapter 2) warranted consideration as a candidate AP transporter. In summary, MATE1 expression and localization in Caco-2 cells has yet to be fully examined, although functional data supports the absence of MATE1 on the AP membrane in Caco-2 cells.

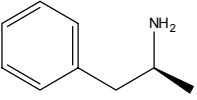
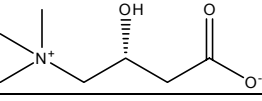
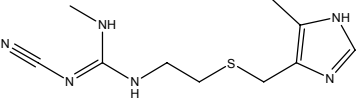
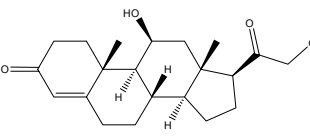
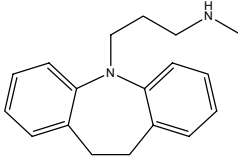
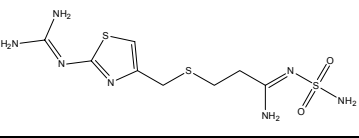
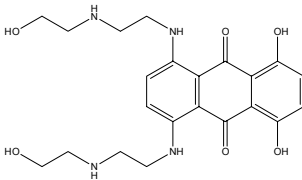
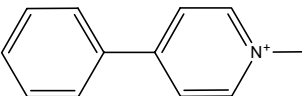
In conclusion, the data presented in this report support the involvement of hOCT1 and PMAT in AP transport of metformin in Caco-2 cells. Explicit data regarding protein expression, function, and localization of these two cation-selective transporters in Caco-2 cells are still lacking. Future work is underway to definitively assess the role of these transporters in Caco-2 cells and ultimately to extend this knowledge in understanding the metformin transport mechanisms in the human intestine. Potential differences between the cation-transporter function in Caco-2 cells and human intestine that may arise from this work will have implications in how the Caco-2 cell model is used to assess absorption of similar compounds and will refine interpretation of existing data in the literature. Identification of the intestinal transporters that facilitates metformin uptake will provide insight into the mechanisms responsible for the dose-dependent and variable absorption of metformin (Noel,

1979; Tucker et al., 1981) and intestinal accumulation and associated pharmacology (Stepensky et al., 2002; Bailey et al., 2008). Lastly, the novel chemical inhibition scheme outlined here could be used to elucidate the contributions of cation-selective transporters involved in metformin or other promiscuous substrates in other cell lines, tissues, or organs.

## **5.F. ACKNOWLEDGMENTS**

We gratefully acknowledge Dr. Xin Ming for his guidance and assistance in the hOCT CHO studies. We also would like to acknowledge Dr. Craig Lee (UNC Eshelman School of Pharmacy) for providing resources to perform the quantitative RT-PCR studies. Finally, funding for this work was generously provided by the Amgen, Inc. and the PhRMA Foundation in the form of pre-doctoral fellowships awarded to William R. Proctor.

**Table 5.1. Chemical Inhibitors of Cation-Selective Candidate Transporters**

Inhibitor	Structure	Target Transporter(s)	Ref.	Not Evaluated
D-Amphetamine		hOCT2	(1)	hOCTN2 MATE1 PMAT
L-Carnitine		hOCTN2	(2-4)	PMAT
Cimetidine		MATE1	(5-9)	
Corticosterone		hOCT1-3 MATE1	(3, 7, 10-12)	
Desipramine		hOCT1-3 MATE1 PMAT	(6, 7, 13, 14)	hOCTN2
Famotidine		hOCT3 MATE1	(5, 15)	hOCTN2 PMAT
Mitoxantrone		hOCT1	(3)	MATE1 PMAT
MPP <sup>+</sup>		All Cation-Selective Transporters	(4, 6, 7, 10, 13, 16)	

References: (1) (Amphoux et al., 2006) (2) (Wagner et al., 2000) (3) (Koepsell et al., 2007) (4) (Tanihara et al., 2007) (5) (Tsuda et al., 2009b) (6) (Zhang et al., 1998) (7) (Engel and Wang, 2005) (8) (Suhre et al., 2005) (9) (Tahara et al., 2005) (10) (Grundemann et al., 1998) (11) (Hayer-Zillgen et al., 2002) (12) (Otsuka et al., 2005) (13) (Gorboulev et al., 1997) (14) (Wu et al., 2000) (15) (Bourdet et al., 2005) (16) (Ohashi et al., 1999)

**Table 5.2. Experimental  $IC_{50}$  Values for Chemical Inhibitors on Metformin Uptake into CHO Cells Expressing hOCT1-3 and Literature PMAT and MATE1  $IC_{50}$  Values**

Inhibitor	Target Transporters	Experimental $IC_{50}$ Values			Literature $IC_{50}$ Values	
		hOCT1	hOCT2	hOCT3	PMAT	MATE1
Mitoxantrone	hOCT1	<b>3.0 ± 0.8</b>	135 ± 12	174 ± 19	NA	NA
D-Amphetamine	hOCT2	106 ± 2	<b>5.7 ± 1</b>	70 ± 5	NA	NA
Famotidine	hOCT3	6.4 ± 1.0	20 ± 2	2.7 ± 0.2	NA	0.6 ± 0.2 <sup>[2]†</sup>
Corticosterone	hOCT1-3	<b>3.2 ± 0.5</b>	<b>1.3 ± 0.1</b>	<b>0.15 ± 0.05</b>	450 ± 77 <sup>[1]*</sup>	NA
Desipramine	hOCT1-3, PMAT, MATE1	<b>2.2 ± 0.4</b>	<b>2.4 ± 0.2</b>	<b>3.8 ± 0.3</b>	<b>33 ± 3</b> <sup>[1]*</sup>	<b>55.7 ± 14</b> <sup>[2]†</sup>
Cimetidine	MATE1	166 <sup>[3]†</sup>	147 ± 11 <sup>[2]</sup>	17 <sup>[3]†</sup>	>500 <sup>[1]*</sup>	<b>1.1 ± 0.3</b> <sup>[2]</sup>

\*  $IC_{50}$  values were reported for inhibiting serotonin or MPP<sup>+</sup> uptake, not metformin. <sup>†</sup> Reported  $IC_{50}$  values were for inhibition of TEA. Boxes highlighted (grey) represent the target transporter(s) for each inhibitor based on the criteria specified in “Materials and Methods” section. NA: Not available

References: <sup>[1]</sup> (Engel and Wang, 2005) <sup>[2]</sup> (Tsuda et al., 2009b) <sup>[3]</sup> (Koepsell et al., 2007)



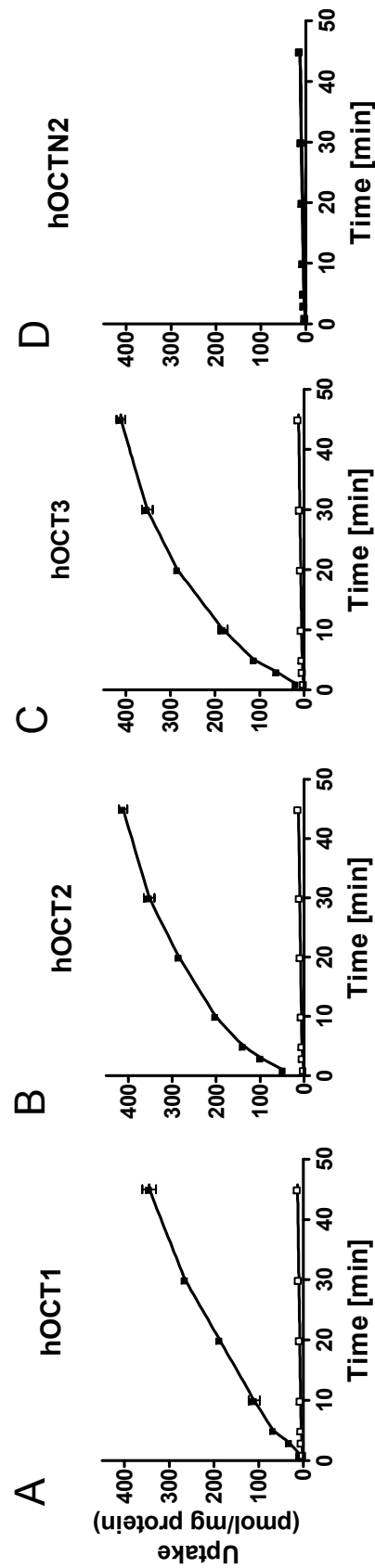


**Figure 5.1. Time-course for Uptake of Metformin in CHO-hOCT1, CHO-hOCT2, CHO-hOCT3, CHO-hOCTN2, and Mock CHO Cells.** Uptake of  $[^{14}\text{C}]$ metformin [10  $\mu\text{M}$ ] was determined over the indicated time-points up to 45 minutes in OCT expressing CHO cells (closed symbols ■) and mock cells (open symbols □). Metformin uptake in hOCT1 expressing (A), hOCT2 expressing (B), hOCT3 expressing (C), and hOCTN2 expressing CHO cells (D) as a function of time is shown in relation to metformin uptake into mock cells. Uptake data are represented as total mass of metformin taken up into the cells per milligram of total protein. Data represent mean  $\pm$  S.D. with N=3 measurements.

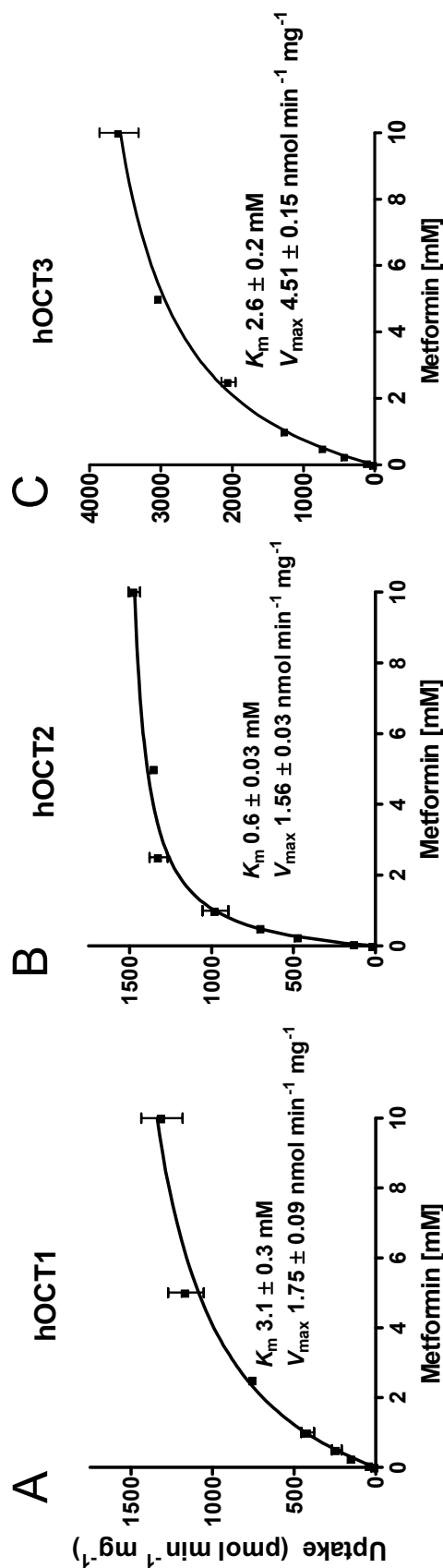


**Figure 5.2. Concentration Dependent Uptake of Metformin into CHO Cells Expressing hOCT1, hOCT2, and hOCT3.** Uptake of  $[^{14}\text{C}]$  metformin at the indicated concentrations was determined in the CHO-hOCT1 (A), CHO-hOCT2 (B), and CHO-OCT3 (C) cells for 5 minutes. Nonspecific cell-associated radioactivity was determined by measuring the compound uptake in the mock cells at each metformin concentration. These values were then subtracted from the values in the each of the hOCT expressing CHO cells to obtain the final OCT related kinetic curves. Apparent  $K_m$  and  $V_{\max}$  parameters were estimated by fitting a Michaelis-Menten equation to the data using non-linear least squares regression analysis. The solid line in each graph represents the model fits. Data represent mean  $\pm$  S.D. with  $N=3$  measurements.

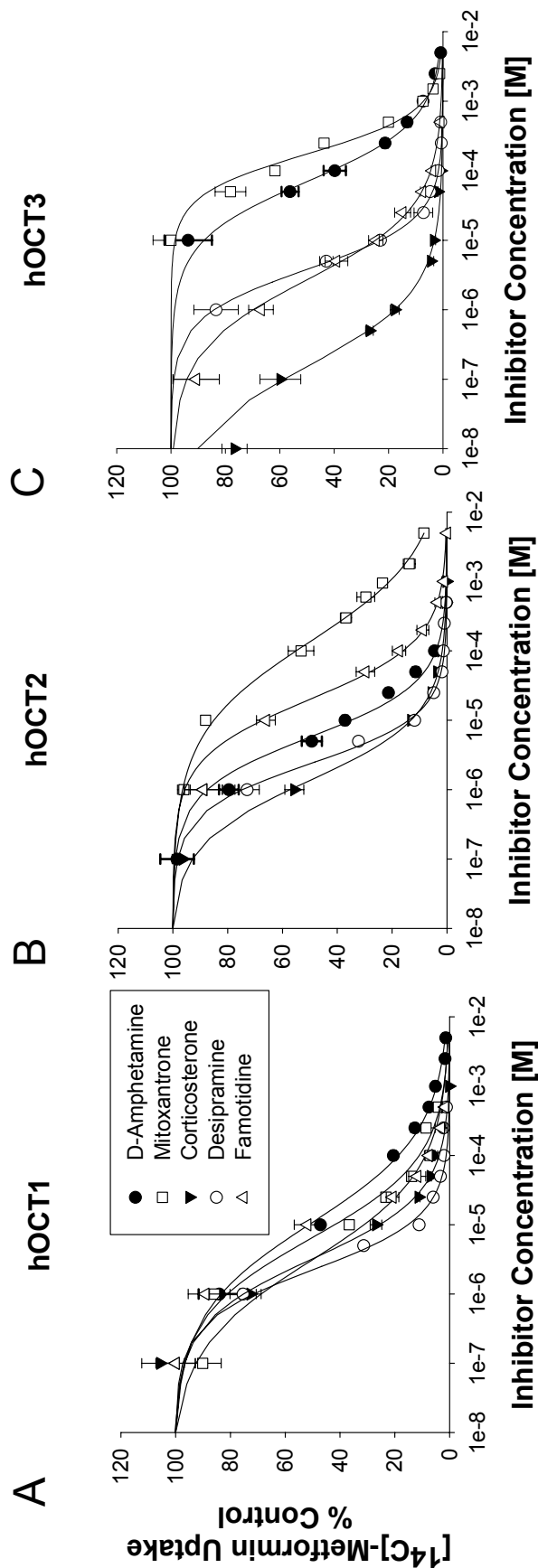


**Figure 5.3. Concentration-dependent Inhibition of hOCT1-, hOCT2-, and hOCT3-mediated Metformin Uptake by Cation-selective Inhibitors.** Uptake of [ $^{14}$ C]metformin [10 $\mu$ M] in CHO-hOCT1 (A), CHO-hOCT2 (B), CHO-hOCT3 (C), and mock cells was determined in the absence or presence of increasing concentrations of D-amphetamine ( $\bullet$ ), mitoxantrone ( $\square$ ), corticosterone ( $\blacktriangledown$ ), desipramine ( $\circ$ ), and famotidine ( $\Delta$ ) for 5 minutes. Nonspecific cell-associated radioactivity was determined by measuring substrate uptake in the mock cells at each inhibitor concentration. These values were then subtracted from the values in hOCT-transfected cells to give corrected data that were used for generation of the inhibition curves. The data represent inhibition of the transporter-mediated metformin uptake only and are reported as a percent of the uninhibited control. Solid lines are model fits obtained following fitting the inhibition curves to a Hill equation using non-linear least square regression analysis. Data represent mean  $\pm$  S.D. with N=3 measurements

## AP Membrane of Caco-2 Cells

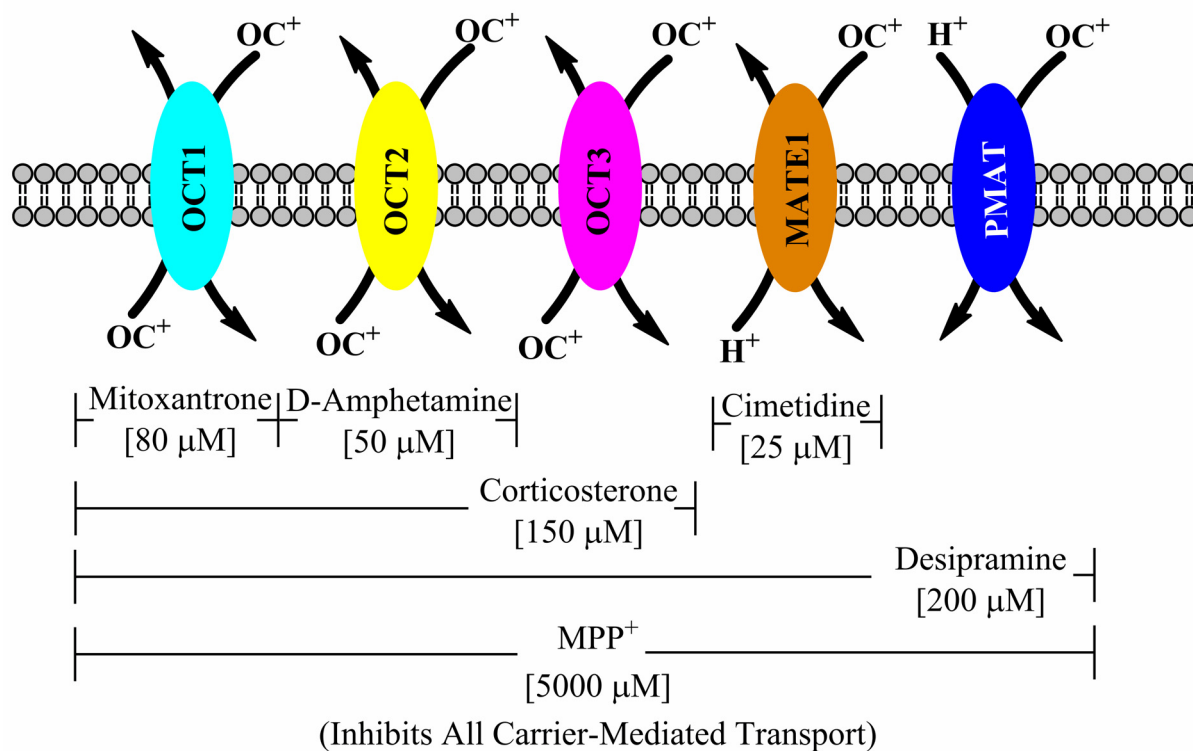


**Figure 5.4. A Novel Chemical Inhibition Scheme to Elucidate the Contribution of Candidate Cation-Selective Transporters Involved in Metformin Initial AP Uptake in Caco-2 Cells.** The chemical inhibition scheme employed to inhibit initial AP metformin uptake in Caco-2 cells are depicted with the concentrations selected and the candidate transporters targeted for each inhibitor.

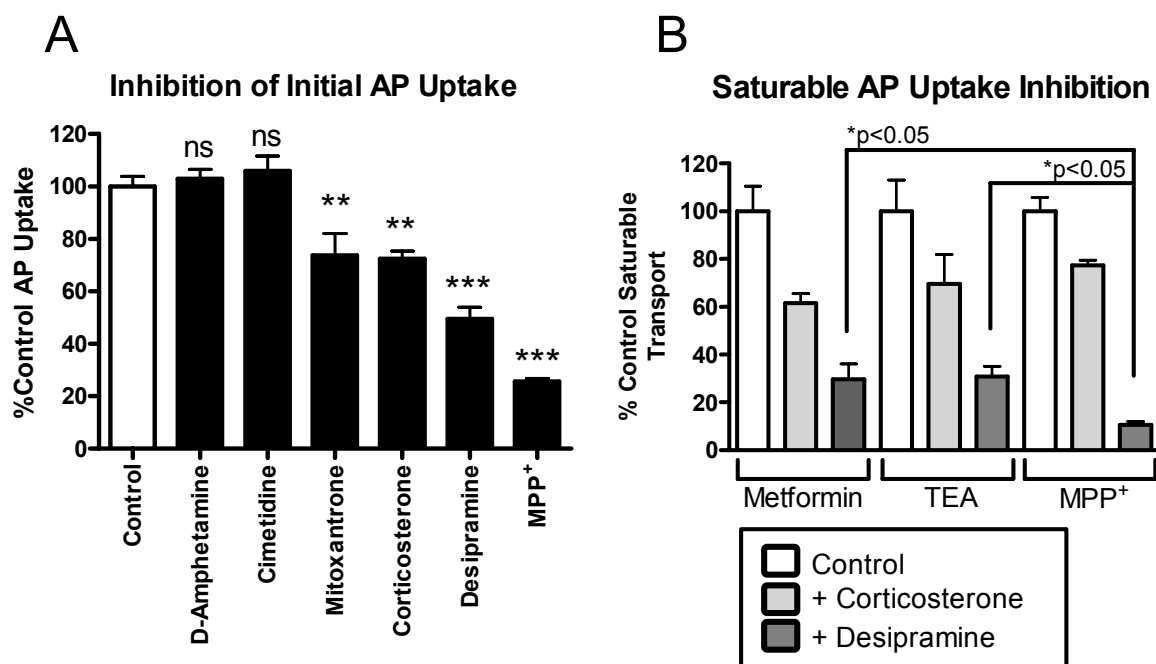


**Figure 5.5. The Contribution of Candidate Cation-Selective Transporters Involved in Metformin Initial AP Uptake in Caco-2 Cells.** (A). Inhibition of [ $^{14}\text{C}$ ]metformin [ $10\mu\text{M}$ ] AP uptake in Caco-2 cells in the absence (Control) or presence of D-amphetamine [ $50\mu\text{M}$ ], cimetidine [ $25\mu\text{M}$ ], mitoxantrone [ $80\mu\text{M}$ ], corticosterone [ $150\mu\text{M}$ ], desipramine [ $200\mu\text{M}$ ], and MPP<sup>+</sup> [ $5\text{mM}$ ] for 5 min. (B). Saturable transport of [ $^{14}\text{C}$ ]metformin [ $10\mu\text{M}$ ], [ $^{14}\text{C}$ ]TEA [ $10\mu\text{M}$ ], and [ $^3\text{H}$ ]MPP<sup>+</sup> [ $1\mu\text{M}$ ] in the absence (Control) or presence of corticosterone [ $150\mu\text{M}$ ] or desipramine [ $200\mu\text{M}$ ] for 5-min (metformin, TEA) and 3-min (MPP<sup>+</sup>). Saturable carrier-mediated transport for each substrate was determined by subtracting the uptake rate obtained in the presence of MPP<sup>+</sup> [ $5\text{mM}$ ] from each value. Statistical differences were determined between uptake rates and control uptake rates by one-way ANOVA analysis with Bonferroni post-test comparisons (A) or two-way ANOVA with Bonferroni post-test comparisons (B). Data are reported as percent relative to control values. Data are expressed as mean  $\pm$  S.D. with N=3. \* $p<0.05$ , \*\* $p<0.01$ , \*\*\* $p<0.001$ , and NS: not significant.

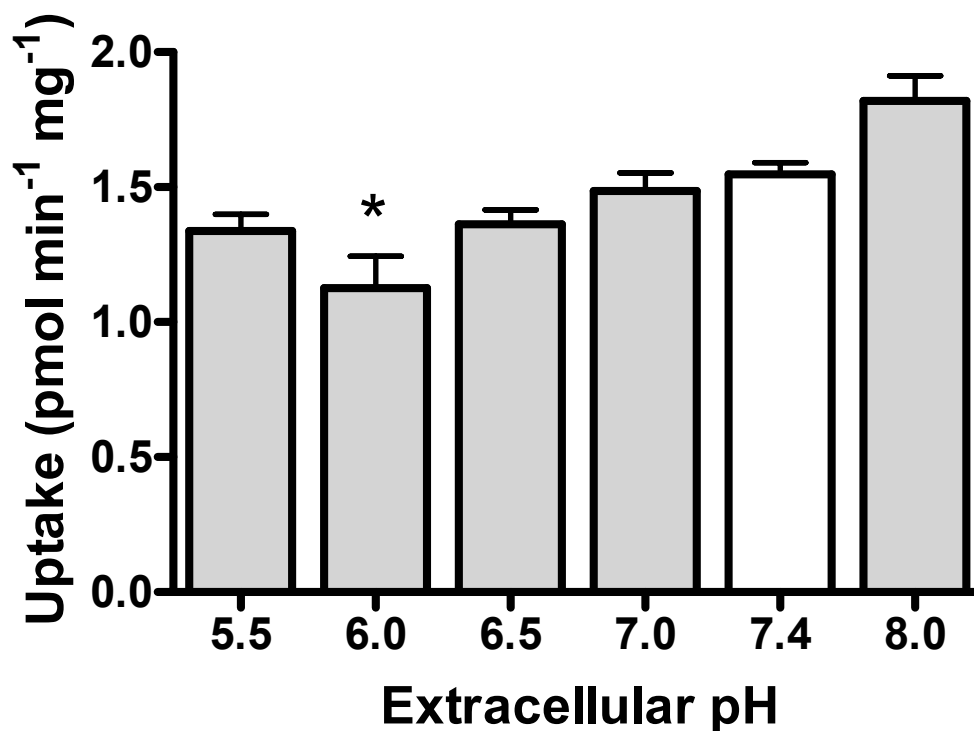


**Figure 5.6. Effect of Extracellular pH on Metformin AP Uptake in Caco-2 Cells.** [<sup>14</sup>C]Metformin [10μM] AP uptake in Caco-2 cells was determined at varying pH values for 5 min. Cells were pre-incubated for 30min at pH 7.4 prior to uptake experiments. Uptake was initiated by replacing only the buffer in the AP compartment with metformin in transport buffer at varying pH. Data are reported as uptake rate per milligram of total protein in the Caco-2 monolayer. Statistical differences were determined between uptake rates at pH values in relation to control (pH 7.4) uptake rates by one-way ANOVA analysis with Bonferroni post-test comparisons. Data represent mean ± S.D, with N=4 measurements. \*p<0.05.

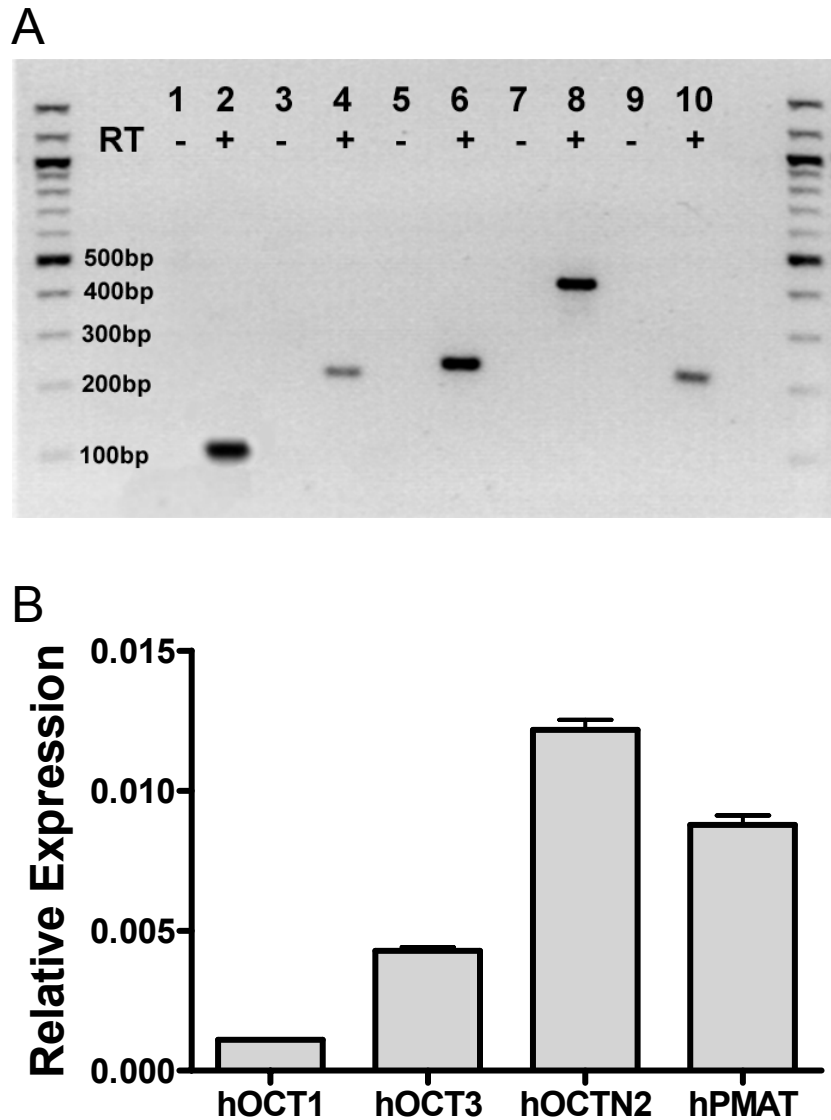


**Figure 5.7. Relative mRNA Expression of hOCT1, hOCT3, hOCTN2, and PMAT in Caco-2 (HTB-37) Cells Relative to GAPDH Expression.** A. Amplified RT-PCR products for GAPDH (lanes 1-2), hOCT1 (lanes 3-4), hOCT3 (lanes 5-6), hOCTN2 (lanes 7-8), and PMAT (lanes 9-10) for Caco-2 cDNA RT samples (+) or No-RT (-) negative controls were separated by electrophoresis in 2% agarose with ethidium bromide (0.5 $\mu$ g/mL). Band intensities are not representative of relative expression levels. B. The relative expression of hOCT1, hOCT3, hOCTN2, and PMAT mRNA relative to GAPDH mRNA determined by quantitative RT-PCR analysis. Data represent mean  $\pm$  S.D. N=3.

## 5.G. REFERENCES

- Amphoux A, Vialou V, Drescher E, Bruss M, Mannoury La Cour C, Rochat C, Millan MJ, Giros B, Bonisch H and Gautron S (2006) Differential pharmacological in vitro properties of organic cation transporters and regional distribution in rat brain. *Neuropharmacology* **50**:941-952.
- Bailey CJ, Mynett KJ and Page T (1994) Importance of the intestine as a site of metformin-stimulated glucose utilization. *Br J Pharmacol* **112**:671-675.
- Bailey CJ, Wilcock C and Scarpello JH (2008) Metformin and the intestine. *Diabetologia* **51**:1552-1553.
- Barnes K, Dobrzynski H, Foppolo S, Beal PR, Ismat F, Scullion ER, Sun L, Tellez J, Ritzel MW, Claycomb WC, Cass CE, Young JD, Billeter-Clark R, Boyett MR and Baldwin SA (2006) Distribution and functional characterization of equilibrative nucleoside transporter-4, a novel cardiac adenosine transporter activated at acidic pH. *Circ Res* **99**:510-519.
- Bourdet DL, Pritchard JB and Thakker DR (2005) Differential substrate and inhibitory activities of ranitidine and famotidine toward human organic cation transporter 1 (hOCT1; SLC22A1), hOCT2 (SLC22A2), and hOCT3 (SLC22A3). *J Pharmacol Exp Ther* **315**:1288-1297.
- Bourdet DL and Thakker DR (2006) Saturable absorptive transport of the hydrophilic organic cation ranitidine in Caco-2 cells: role of pH-dependent organic cation uptake system and P-glycoprotein. *Pharm Res* **23**:1165-1177.
- Elimrani I, Lahjouji K, Seidman E, Roy MJ, Mitchell GA and Qureshi I (2003) Expression and localization of organic cation/carnitine transporter OCTN2 in Caco-2 cells. *Am J Physiol Gastrointest Liver Physiol* **284**:G863-871.
- Engel K and Wang J (2005) Interaction of organic cations with a newly identified plasma membrane monoamine transporter. *Mol Pharmacol* **68**:1397-1407.
- Engel K, Zhou M and Wang J (2004) Identification and characterization of a novel monoamine transporter in the human brain. *J Biol Chem* **279**:50042-50049.
- Englund G, Rorsman F, Ronnblom A, Karlbom U, Lazorova L, Grasjo J, Kindmark A and Artursson P (2006) Regional levels of drug transporters along the human intestinal tract: co-expression of ABC and SLC transporters and comparison with Caco-2 cells. *Eur J Pharm Sci* **29**:269-277.
- Gorboulev V, Ulzheimer JC, Akhoundova A, Ulzheimer-Teuber I, Karbach U, Quester S, Baumann C, Lang F, Busch AE and Koepsell H (1997) Cloning and characterization of two human polyspecific organic cation transporters. *DNA Cell Biol* **16**:871-881.



- Grundemann D, Harlfinger S, Golz S, Geerts A, Lazar A, Berkels R, Jung N, Rubbert A and Schomig E (2005) Discovery of the ergothioneine transporter. *Proc Natl Acad Sci U S A* **102**:5256-5261.
- Grundemann D, Schechinger B, Rappold GA and Schomig E (1998) Molecular identification of the corticosterone-sensitive extraneuronal catecholamine transporter. *Nat Neurosci* **1**:349-351.
- Hayer-Zillgen M, Bruss M and Bonisch H (2002) Expression and pharmacological profile of the human organic cation transporters hOCT1, hOCT2 and hOCT3. *Br J Pharmacol* **136**:829-836.
- Hayeshi R, Hilgendorf C, Artursson P, Augustijns P, Brodin B, Dehertogh P, Fisher K, Fossati L, Hovenkamp E, Korjamo T, Masungi C, Maubon N, Mols R, Mullertz A, Monkkonen J, O'Driscoll C, Oppers-Tiemissen HM, Ragnarsson EG, Rooseboom M and Ungell AL (2008) Comparison of drug transporter gene expression and functionality in Caco-2 cells from 10 different laboratories. *Eur J Pharm Sci* **35**:383-396.
- Hidalgo IJ, Raub TJ and Borchardt RT (1989) Characterization of the human colon carcinoma cell line (Caco-2) as a model system for intestinal epithelial permeability. *Gastroenterology* **96**:736-749.
- Hilgendorf C, Ahlin G, Seithel A, Artursson P, Ungell AL and Karlsson J (2007) Expression of thirty-six drug transporter genes in human intestine, liver, kidney, and organotypic cell lines. *Drug Metab Dispos* **35**:1333-1340.
- Holmes JL, Van Itallie CM, Rasmussen JE and Anderson JM (2006) Claudin profiling in the mouse during postnatal intestinal development and along the gastrointestinal tract reveals complex expression patterns. *Gene Expr Patterns* **6**:581-588.
- Kato Y, Mikihiro S, Sugiura T, Wakayama T, Kubo Y, Kobayashi D, Sai Y, Tamai I, Iseki S and Tsuji A (2006) Organic cation/carnitine transporter OCTN2 (Slc22a5) is responsible for carnitine transport across the apical membranes of small intestinal epithelial cells in mouse. *Mol Pharmacol* **70**:829-837.
- Kim HR, Park SW, Cho HJ, Chae KA, Sung JM, Kim JS, Landowski CP, Sun D, Abd El-Aty AM, Amidon GL and Shin HC (2007) Comparative gene expression profiles of intestinal transporters in mice, rats and humans. *Pharmacol Res* **56**:224-236.
- Kimura N, Masuda S, Tanihara Y, Ueo H, Okuda M, Katsura T and Inui K (2005a) Metformin is a superior substrate for renal organic cation transporter OCT2 rather than hepatic OCT1. *Drug Metab Pharmacokinet* **20**:379-386.
- Kimura N, Okuda M and Inui K (2005b) Metformin Transport by Renal Basolateral Organic Cation Transporter hOCT2. *Pharm Res* **22**:255-259.

- Koepsell H, Lips K and Volk C (2007) Polyspecific organic cation transporters: structure, function, physiological roles, and biopharmaceutical implications. *Pharm Res* **24**:1227-1251.
- Lamhonwah AM, Ackerley C, Onizuka R, Tilups A, Lamhonwah D, Chung C, Tao KS, Tellier R and Tein I (2005) Epitope shared by functional variant of organic cation/carnitine transporter, OCTN1, *Campylobacter jejuni* and *Mycobacterium paratuberculosis* may underlie susceptibility to Crohn's disease at 5q31. *Biochem Biophys Res Commun* **337**:1165-1175.
- Lamhonwah AM and Tein I (2006) Novel localization of OCTN1, an organic cation/carnitine transporter, to mammalian mitochondria. *Biochem Biophys Res Commun* **345**:1315-1325.
- Martel F, Grundemann D, Calhau C and Schomig E (2001) Apical uptake of organic cations by human intestinal Caco-2 cells: putative involvement of ASF transporters. *Naunyn Schmiedeberg's Arch Pharmacol* **363**:40-49.
- Maubon N, Le Vee M, Fossati L, Audry M, Le Ferrec E, Bolze S and Fardel O (2007) Analysis of drug transporter expression in human intestinal Caco-2 cells by real-time PCR. *Fundam Clin Pharmacol* **21**:659-663.
- Meier Y, Eloranta JJ, Darimont J, Ismail MG, Hiller C, Fried M, Kullak-Ublick GA and Vavricka SR (2007) Regional distribution of solute carrier (SLC) mRNA expression along the human intestinal tract. *Drug Metab Dispos*.
- Ming X, Ju W, Wu H, Tidwell RR, Hall JE and Thakker DR (2009) Transport of dicationic drugs pentamidine and furamidine by human organic cation transporters. *Drug Metab Dispos* **37**:424-430.
- Muller J, Lips KS, Metzner L, Neubert RH, Koepsell H and Brandsch M (2005) Drug specificity and intestinal membrane localization of human organic cation transporters (OCT). *Biochem Pharmacol* **70**:1851-1860.
- Ng C (2002) Novel Cation-Sensitive Mechanisms for Intestinal Absorption and Secretion of Famotidine and Ranitidine: Potential Clinical Implications, in: *Pharmacy*, pp 186, University of North Carolina at Chapel Hill, Chapel Hill.
- Nies AT, Koepsell H, Winter S, Burk O, Klein K, Kerb R, Zanger UM, Keppler D, Schwab M and Schaeffeler E (2009) Expression of organic cation transporters OCT1 (SLC22A1) and OCT3 (SLC22A3) is affected by genetic factors and cholestasis in human liver. *Hepatology* **50**:1227-1240.
- Noel M (1979) Kinetic study of normal and sustained release dosage forms of metformin in normal subjects. *Res Clin Pharmacol* **1**:33-44.

- Ohashi R, Tamai I, Yabuuchi H, Nezu JJ, Oku A, Sai Y, Shimane M and Tsuji A (1999) Na(+)-dependent carnitine transport by organic cation transporter (OCTN2): its pharmacological and toxicological relevance. *J Pharmacol Exp Ther* **291**:778-784.
- Otsuka M, Matsumoto T, Morimoto R, Arioka S, Omote H and Moriyama Y (2005) A human transporter protein that mediates the final excretion step for toxic organic cations. *Proc Natl Acad Sci U S A* **102**:17923-17928.
- Pentikainen PJ (1986) Bioavailability of metformin. Comparison of solution, rapidly dissolving tablet, and three sustained release products. *Int J Clin Pharmacol Ther Toxicol* **24**:213-220.
- Pentikainen PJ, Neuvonen PJ and Penttila A (1979) Pharmacokinetics of metformin after intravenous and oral administration to man. *Eur J Clin Pharmacol* **16**:195-202.
- Proctor WR, Bourdet DL and Thakker DR (2008) Mechanisms underlying saturable intestinal absorption of metformin. *Drug Metab Dispos* **36**:1650-1658.
- Saitoh R, Sugano K, Takata N, Tachibana T, Higashida A, Nabuchi Y and Aso Y (2004) Correction of permeability with pore radius of tight junctions in Caco-2 monolayers improves the prediction of the dose fraction of hydrophilic drugs absorbed by humans. *Pharm Res* **21**:749-755.
- Sambol NC, Chiang J, O'Conner M, Liu CY, Lin ET, Goodman AM, Benet LZ and Haram JH (1996) Pharmacokinetics and pharmacodynamics of metformin in healthy subjects and patients with noninsulin-dependent diabetes mellitus. *J Clin Pharmacol* **36**:1012-1021.
- Sato T, Masuda S, Yonezawa A, Tanihara Y, Katsura T and Inui K (2008) Transcellular transport of organic cations in double-transfected MDCK cells expressing human organic cation transporters hOCT1/hMATE1 and hOCT2/hMATE1. *Biochem Pharmacol* **76**:894-903.
- Seithel A, Karlsson J, Hilgendorf C, Bjorquist A and Ungell A (2006) Variability in mRNA expression of ABC- and SLC-transporters in human intestinal cells: comparison between human segments and Caco-2 cells. *Eur J Pharm Sci* **28**:291-299.
- Shu Y, Brown C, Castro RA, Shi RJ, Lin ET, Owen RP, Sheardown SA, Yue L, Burchard EG, Brett CM and Giacomini KM (2008) Effect of genetic variation in the organic cation transporter 1, OCT1, on metformin pharmacokinetics. *Clin Pharmacol Ther* **83**:273-280.
- Song IS, Shin HJ and Shin JG (2008) Genetic variants of organic cation transporter 2 (OCT2) significantly reduce metformin uptake in oocytes. *Xenobiotica* **38**:1252-1262.
- Stepensky D, Friedman M, Raz I and Hoffman A (2002) Pharmacokinetic-pharmacodynamic analysis of the glucose-lowering effect of metformin in diabetic rats reveals first-pass pharmacodynamic effect. *Drug Metab Dispos* **30**:861-868.

- Suhre WM, Ekins S, Chang C, Swaan PW and Wright SH (2005) Molecular determinants of substrate/inhibitor binding to the human and rabbit renal organic cation transporters hOCT2 and rbOCT2. *Mol Pharmacol* **67**:1067-1077.
- Tahara H, Kusuhara H, Endou H, Koepsell H, Imaoka T, Fuse E and Sugiyama Y (2005) A species difference in the transport activities of H<sub>2</sub> receptor antagonists by rat and human renal organic anion and cation transporters. *J Pharmacol Exp Ther* **315**:337-345.
- Tamai I, Ohashi R, Nezu J, Yabuuchi H, Oku A, Shimane M, Sai Y and Tsuji A (1998) Molecular and functional identification of sodium ion-dependent, high affinity human carnitine transporter OCTN2. *J Biol Chem* **273**:20378-20382.
- Tanihara Y, Masuda S, Sato T, Katsura T, Ogawa O and Inui K (2007) Substrate specificity of MATE1 and MATE2-K, human multidrug and toxin extrusions/H(+)-organic cation antiporters. *Biochem Pharmacol* **74**:359-371.
- Tsuda M, Terada T, Mizuno T, Katsura T, Shimakura J and Inui K (2009a) Targeted disruption of the multidrug and toxin extrusion 1 (mate1) gene in mice reduces renal secretion of metformin. *Mol Pharmacol* **75**:1280-1286.
- Tsuda M, Terada T, Ueba M, Sato T, Masuda S, Katsura T and Inui K (2009b) Involvement of human multidrug and toxin extrusion 1 in the drug interaction between cimetidine and metformin in renal epithelial cells. *J Pharmacol Exp Ther* **329**:185-191.
- Tucker GT, Casay C, Phillips PJ, Connor H, Ward JD and Woods HF (1981) Metformin kinetics in healthy subjects and in patients with diabetes mellitus. *J Clin. Pharmac.* **12**:235-246.
- Wagner CA, Lukewille U, Kaltenbach S, Moschen I, Broer A, Risler T, Broer S and Lang F (2000) Functional and pharmacological characterization of human Na(+)-carnitine cotransporter hOCTN2. *Am J Physiol Renal Physiol* **279**:F584-591.
- Walker J, Jijon HB, Diaz H, Salehi P, Churchill T and Madsen KL (2005) 5-aminoimidazole-4-carboxamide riboside (AICAR) enhances GLUT2-dependent jejunal glucose transport: a possible role for AMPK. *Biochem J* **385**:485-491.
- Wang DS, Jonker JW, Kato Y, Kusuhara H, Schinkel AH and Sugiyama Y (2002) Involvement of organic cation transporter 1 in hepatic and intestinal distribution of metformin. *J Pharmacol Exp Ther* **302**:510-515.
- Wu X, Huang W, Ganapathy ME, Wang H, Kekuda R, Conway SJ, Leibach FH and Ganapathy V (2000) Structure, function, and regional distribution of the organic cation transporter OCT3 in the kidney. *Am J Physiol Renal Physiol* **279**:F449-458.
- Wu X, Huang W, Prasad PD, Seth P, Rajan DP, Leibach FH, Chen J, Conway SJ and Ganapathy V (1999) Functional characteristics and tissue distribution pattern of

- organic cation transporter 2 (OCTN2), an organic cation/carnitine transporter. *J Pharmacol Exp Ther* **290**:1482-1492.
- Xia L, Engel K, Zhou M and Wang J (2007) Membrane localization and pH-dependent transport of a newly cloned organic cation transporter (PMAT) in kidney cells. *Am J Physiol Renal Physiol* **292**:F682-690.
- Zhang L, Schaner ME and Giacomini KM (1998) Functional characterization of an organic cation transporter (hOCT1) in a transiently transfected human cell line (HeLa). *J Pharmacol Exp Ther* **286**:354-361.
- Zhou M, Xia L and Wang J (2007) Metformin transport by a newly cloned proton-stimulated organic cation transporter (plasma membrane monoamine transporter) expressed in human intestine. *Drug Metab Dispos* **35**:1956-1962.

## **CHAPTER 6**

## **CONCLUSIONS**

The studies undertaken for this dissertation project has focused on elucidating the mechanisms by which metformin is absorbed across intestinal epithelium. Metformin is a water soluble hydrophilic drug with a pKa of 12.4 and a calculated log D value of -6.13 at pH 7.4 (Saitoh et al., 2004). Despite its very hydrophilic nature, multiple hydrogen donor/acceptor sites, and net charge at all physiologic pH values, all of which typically contributing to poor oral absorption, metformin is highly absorbed in humans with fraction of dose absorbed ranging between 60-80% (Pentikainen et al., 1979; Tucker et al., 1981). The dichotomy between the predicted and observed absorption of metformin suggests the involvement of carrier-mediated transport processes. This is supported by clinical evidence for intestinal accumulation (Bailey et al., 2008) and dose-dependent absorption of metformin (Sambol et al., 1996). Therefore, intestinal transport processes may drive the pharmacokinetics of metformin; yet the transporter(s) involved in the intestinal absorption remain unknown. This dissertation work describes a novel mechanism by which metformin is absorbed across intestinal epithelium. At the heart of this mechanism lie two interconnected processes of carrier-mediated transport and paracellular transport. These processes are traditionally considered to be independent routes of absorption, with compounds favoring one or the other route for their absorption, but appear to work in concert yielding high and sustained absorption of this very hydrophilic drug.

To investigate the intestinal absorption processes of metformin, Caco-2 cell monolayers, an established model for human intestinal epithelium, were used so that cellular mechanisms of metformin transport could be examined. Initial work on metformin transport across Caco-2 cell monolayers revealed that the absorptive transport was saturable and dose-dependent (Chapter 2). This was the first report of saturable absorptive transport of

metformin across an *in vitro* cell model that corresponded to the dose-dependent intestinal absorption observed *in vivo* (Tucker et al., 1981; Sambol et al., 1996). Interestingly, the saturable component of absorptive transport across Caco-2 cell monolayers appeared to be a high affinity and low capacity system with an apparent  $K_m$  and  $V_{max}$  values of 0.06 mM and 5 pmol min<sup>-1</sup> mg protein<sup>-1</sup>, respectively. These transport kinetic estimates were striking due to the reported affinities of known organic cation transporters (hOCTs) for metformin, with  $K_m$  values in the millimolar range (Kimura et al., 2005; Nies et al., 2009). Thus, dose-dependent absorption of metformin across Caco-2 cell monolayers likely involved an unknown transporter with high affinity towards metformin or involved a saturable process distinct from classic carrier-mediated transcellular transport. Additionally, metformin is administered orally with doses ranging between 250 mg and 1g tablets, which would produce millimolar concentrations of drug in the gut lumen. Therefore, the saturable component of absorptive transport would potentially be saturated across the dose range administered and undergo linear absorption pharmacokinetics. Nonetheless, these results provided first *in vitro* evidence of a saturable intestinal transport of metformin, consistent with the clinically observed dose-dependent saturable absorption observed for this drug in the clinic, although the exact mechanism responsible for this dose-dependency in Caco-2 cells was unclear.

The results of this study showed that metformin was taken up across the apical (AP) membrane by a carrier-mediated transport process with  $K_m$  and  $V_{max}$  values of 0.9 mM and 330 pmol min<sup>-1</sup> mg of protein<sup>-1</sup>, respectively (Chapter 2). The discrepancy between the  $K_m$  value for metformin AP uptake and overall absorptive transport indicated that AP uptake likely did not contribute significantly to the dose-dependent transport across Caco-2 cell monolayers. This conclusion was in contrast to the transport kinetics of the H<sub>2</sub>-receptor



antagonist, ranitidine. Ranitidine, like metformin, possesses a net positive charge at gut lumen pH with a pKa of 8.2 and is hydrophilic with a calculated log D value of 0.7 at pH 7.4 (Matsson et al., 2007), and is also highly absorbed with an oral bioavailability in humans ranging from 40-70% (Lin, 1991). Ranitidine has similar  $K_m$  values for absorptive transport and initial AP uptake of approximately 0.5 and 0.3 mM, respectively (Bourdet and Thakker, 2006), indicating that AP uptake is likely defining absorptive transport of this drug.

Elucidating the role of transporters in the AP uptake of metformin in Caco-2 cells was a focus of initial investigation. The AP uptake was significantly inhibited by prototypical hOCT substrates and/or inhibitors (Chapter 2). Furthermore, AP efflux was efficient and capable of trans-stimulation and trans-inhibition by metformin and hOCT inhibitors, respectively. These results supported the presence of bidirectional uptake / efflux “OCT-like” mechanism(s) on the AP membrane of Caco-2 cells capable of efficiently transporting metformin. Moreover, the  $K_m$  for AP uptake was within the range of reported affinities of hOCTs for metformin. Caco-2 cells were reported to have detectable levels of hOCT1, hOCT2, hOCT3, and hOCTN2 mRNA (Muller et al., 2005; Englund et al., 2006). MATE1 expression in Caco-2 cells and in the human intestine remains unknown. PMAT mRNA was detected in the Caco-2 cells and was shown to be highly expressed relative to hOCT1 or hOCT3 (Chapters 4 and 5). This is the first evidence of PMAT expression in Caco-2 cells, which has been shown to be expressed on the AP membrane of epithelial cells of the villus tips of the intestine (Zhou et al., 2007).

Metformin is a substrate for cation-selective transporters hOCT1, hOCT2, hOCT3, MATE1, and PMAT with apparent  $K_m$  values ranging from 0.6 to 3 mM [Chapter 5 and (Tanihara et al., 2007; Zhou et al., 2007; Nies et al., 2009)]. Additionally, metformin was

determined not to be a substrate for hOCTN2 (Chapter 5), ruling out the contributions of this highly expressed cation-selective transporter in AP uptake in Caco-2 cells and in the intestine, in addition to metformin transport in the liver, kidney, heart, and skeletal muscle where hOCTN2 is expressed (Tamai et al., 1998). As a result, putative cation-selective transporters responsible for AP uptake in Caco-2 cells were limited to hOCT1, hOCT2, hOCT3, MATE1, and PMAT.

A novel chemical inhibition scheme was implemented to elucidate the contributions of putative cation-selective transporters in facilitating metformin uptake across the AP membrane (Chapter 5). These results implicated both hOCT1 and PMAT in facilitating AP uptake of metformin into Caco-2 cells with almost equal contributions. Furthermore, the contributions of MATE1, hOCT2, and hOCT3 were determined to be insignificant in the AP uptake of metformin in Caco-2 cells. Similar studies employing this chemical inhibition scheme in human intestinal tissue should be performed to confirm the role hOCT1 and PMAT in mediating metformin AP uptake and to validate the Caco-2 cell model to study the intestinal transport processes for cationic compounds. Additionally, this approach, which employed easily obtained chemical inhibitors, can be used to estimate the contribution of these transporters in facilitating transport of metformin and other organic cations in other tissues or organs. This approach also could be used to functionally implicate transporters at specific membranes, where cellular localization of specific transporters is unknown.

hOCT1 localization in Caco-2 cells and consequently in the intestine has been controversial. Human monoclonal antibodies for hOCT1 are not readily available; however rat Oct1 antibody has been used to examine hOCT1 localization in human cells and tissues. hOCT1 was localized to the AP membrane of Caco-2 (Ng, 2002). Another report failed to

observe hOCT1 staining in Caco-2 cells, but did detect punctated and diffused staining on the lateral membrane and cytosolic compartment of fixed human intestinal slices (Muller et al., 2005). Mouse Oct1 appeared to be localized to the basolateral (BL) membrane of the intestine based on *in vivo* accumulation studies with metformin in Oct1 competent or deficient mice (Wang et al., 2002), although direct evidence for localization of Oct1 in the mouse intestine is lacking. The two latter studies and hOCT1 localization to the BL membrane in hepatocytes (Nies et al., 2009) have presented a case for BL localization of this transporter in the human intestine and consequently in Caco-2 cells. The data presented in this dissertation provide functional evidence supporting AP localization of hOCT1 in Caco-2 cells, consistent with the previous evidence of AP localization of hOCT1 based on ranitidine AP uptake in Caco-2 cells (Bourdet and Thakker, 2006). In summary, the results presented here and previous reports support hOCT1 AP localization in Caco-2 cells.

Although protein expression and localization was detected in human intestine (Zhou et al., 2007), PMAT function in the intestine and its role in facilitating intestinal accumulation of metformin was unknown. The chemical inhibition studies implicated PMAT in mediating at least 30% of the carrier-mediated AP uptake of metformin (Chapter 5). PMAT functions as a proton symporter, where an inward proton gradient enhanced metformin uptake in MDCKII cells that stably expressed PMAT (Zhou et al., 2007). Conversely, metformin AP uptake in Caco-2 cells was inhibited in the presence of an inward proton gradient (Chapter 5). It remains unclear whether PMAT functions as a proton symporter in all cell lines and tissues. Regardless, high relative PMAT expression in Caco-2 cells (Chapter 4), AP localization of PMAT in human intestine (Zhou et al., 2007), and the chemical inhibition data (Chapter 5) support PMAT function and localization on the AP

membrane of Caco-2 cells and a role of this transporter in AP uptake of metformin. Of course, it is difficult to rule out the possibility that the chemical inhibitors, which identified hOCT1- and PMAT-mediated metformin AP uptake, may have inhibited an unidentified transporter. For that reason, further studies are underway using siRNA to specifically knock down both hOCT1 and PMAT separately to obtain unequivocal evidence on whether AP uptake of metformin is mediated by these two transporters in Caco-2 cells.

Interestingly, the chemical inhibitors that were used to estimate the contributions of hOCT1 and PMAT in AP metformin uptake did not abolish all of the carrier-mediated metformin transport across the AP membrane (Chapter 5). Approximately 35% of the carrier-mediated transport of both metformin and the hydrophilic hOCT substrate tetraethylammonium (TEA) remained intact after inhibiting hOCT1-3 and PMAT. However, inhibition of hOCT1-3 and PMAT almost completely inhibited the carrier-mediated transport of 1-methyl-4-phenylpyrimidinium (MPP<sup>+</sup>), leaving only 10% remaining. An explanation for this observation is the presence of a yet unknown AP transporter of TEA and metformin in Caco-2 cells that was not inhibited by hOCT1-3, MATE1, and PMAT inhibitors. Further studies are warranted to account for the remaining uptake of metformin and TEA not subject to desipramine inhibition and to identify unknown cation-selective transporter(s) present in Caco-2 cells. Additionally, PMAT was shown to have greater expression relative to hOCT1 (Chapters 4 and 5) and has similar transport affinity towards metformin as hOCT1; therefore, PMAT likely mediates a majority of metformin AP uptake in Caco-2 cells. These results have implications for not only metformin absorption and intestinal accumulation, but other hydrophilic cationic drugs and nutrients that share similar substrate specificity towards these transporters.

The basolateral membrane in Caco-2 cells presents a major barrier for metformin transcellular transport. Metformin efflux across the BL membrane was inefficient and appeared to be a passive process over the concentration range employed (Chapter 2). This was not surprising for there does not appear to be efficient transport of hydrophilic organic cations across the basolateral membrane of Caco-2 cells. BL efflux of both metformin and ranitidine was not subject to *trans*-stimulation or *trans*-inhibition by hOCT substrates and/or inhibitors, and the BL efflux clearance did not change with increased loaded concentrations (Chapter 2 and (Bourdet and Thakker, 2006)). In addition, metformin and ranitidine BL uptake was also inefficient in Caco-2 cells, even though this process was saturable with apparent  $K_m$  values of approximately 13 and 67 mM, respectively (Chapter 2 and (Lee et al., 2002)). The mechanisms of the BL transport of metformin and ranitidine remain unknown; although this pathway likely plays an insignificant part in overall absorption of metformin.

The efficient uptake of metformin across the AP membrane and inefficient BL efflux resulted in significant accumulation of metformin in Caco-2 cells relative to the amount of drug absorbed across the monolayer. This result is the first cell-based evidence supporting metformin accumulation in intestinal epithelial cells that was observed *in vivo* in both humans and animal models (Wilcock and Bailey, 1994; Bailey et al., 2008). Intestinal accumulation likely accounts for the slow rate of metformin absorption that is rate limiting to its overall disposition (Tucker et al., 1981). Additionally, inefficient BL efflux limited transcellular transport, forcing the absorptive transport through the paracellular space. Both rate comparison and cellular kinetic analysis approaches indicated that  $\geq 90\%$  of the overall transport occurred via paracellular transport (Chapter 2). The apparent permeability ( $P_{app}$ ) of metformin decreased 3 fold over 0.05 to 10 mM donor concentrations; yet  $\leq 10\%$  could be

attributed to transcellular transport processes. In other words, the absorptive transport of metformin was predominantly paracellular, which clearly contained a significant saturable component.

The phenomenon of saturable paracellular transport was previously reported for ranitidine absorptive transport across Caco-2 cells (Gan et al., 1998; Lee and Thakker, 1999; Bourdet et al., 2006). Ranitidine was shown to increase the trans-epithelial electrical resistance (TEER) across Caco-2 monolayers, which was attributed to a saturable paracellular transport mechanism mediated by electrostatic interactions between the cationic amine group of ranitidine and anionic residues of the lateral space and/or tight-junction (TJ) (Gan et al., 1998; Lee and Thakker, 1999). Similarly, metformin significantly increased the TEER at high donor concentrations (e.g.  $\geq 5\text{mM}$ ) (Chapter 2; data not shown). Kinetic compartmental modeling of transport and cellular accumulation data revealed that absorptive transport of ranitidine comprised approximately equal contributions of carrier-mediated transcellular transport and paracellular transport, both containing saturable processes (Bourdet et al., 2006). The studies in Caco-2 cells on the mechanism of absorptive transport of ranitidine and metformin provided irrefutable evidence supporting the presence of a novel saturable paracellular transport mechanism for small hydrophilic organic cations.

The molecular mechanism responsible for the concentration-dependent paracellular transport was unknown prior to the findings of this dissertation research, although potential involvement of the TJ proteins claudins was speculated (Bourdet et al., 2006). Claudins are transmembrane proteins believed to form pores in the TJ that regulate flux of ions and small neutral molecules across epithelial tissue (Van Itallie and Anderson, 2006). Specific claudin isoforms are known to confer charge selectivity to inorganic ions that traverse across the

epithelial monolayer; this charge selectivity is conferred via electrostatic interactions between the ions and certain charged amino acid residues in the extracellular loops of claudins that make up the pores in the TJ (Colegio et al., 2002). Claudin-2, in particular, has been shown to confer cation-selectivity, and preferentially facilitating metal ion diffusion driven by electrostatic interactions between the positive charge on the metal ions and negative charge on anionic residues of its extracellular loops (Yu et al., 2009). In addition, claudin-2 pores appear to have an approximate radius of 4 Å that permit flux of small organic non-charged molecules of molecular radii  $\leq 4$  Å in a size-dependent manner (Van Itallie et al., 2008), albeit to a lesser extent than its ability to facilitate cation flux. Accordingly, claudin-2 presented an ideal candidate to examine the role of cation-selective claudins in facilitating paracellular transport of a small organic cation like metformin across Caco-2 cell monolayers.

Short term treatment with the active metabolite of vitamin D<sub>3</sub>, 1 $\alpha$ ,25-dihydroxyvitamin D<sub>3</sub> (1,25-(OH)<sub>2</sub>D<sub>3</sub>), was reported to induce claudin-2 expression in Caco-2 cells (Fujita et al., 2008); hence this model was selected to evaluate the effects of claudin-2 expression on paracellular transport of metformin. Claudin-2 mRNA and protein were induced by 4 fold following 1,25-(OH)<sub>2</sub>D<sub>3</sub>-treatment. Surprisingly of the 30 genes that encode proteins responsible for TJ structure and for regulation of TJ function, only claudin-2 expression increased greater than 2 fold following 1,25-(OH)<sub>2</sub>D<sub>3</sub>-treatment (Chapter 3). Claudin-12, -15, and -16 expression has been shown to increase cation paracellular transport (Van Itallie et al., 2003; Hou et al., 2005; Fujita et al., 2008), yet the relative gene expression for each of these proteins was either unchanged (claudin-12) or decreased (claudin-15, and -16) as a result of vitamin D<sub>3</sub>-treatment (Chapter 3). Therefore, it appeared that 1,25-(OH)<sub>2</sub>D<sub>3</sub>-

treatment selectively induced claudin-2 expression. Accompanied with the induction of claudin-2, there was a significant increase (e.g. 25%) in metformin transport, without any change in the AP uptake, AP efflux, or BL efflux. Transport of a related but smaller organic cation, guanidine, increased even more (2 fold) upon the induction of claudin-2 by 1,25-(OH)<sub>2</sub>D<sub>3</sub>-treatment (Chapter 3). In addition, 1,25-(OH)<sub>2</sub>D<sub>3</sub>-treatment increased the overall barrier integrity of the monolayer by reducing the transport of the paracellular probe mannitol, perhaps by reducing the number of pores capable of permitting flux of small non-charged species. These observations highlighted three significant findings: 1) Claudin-2 pores were capable of facilitating paracellular transport of metformin and other small organic cations in a size-dependent manner. 2) 1,25-(OH)<sub>2</sub>D<sub>3</sub>-treatment increased the barrier integrity of the monolayer, decreasing the flux of small neutral molecules while increasing the flux of small organic cations. 3) 1,25-(OH)<sub>2</sub>D<sub>3</sub>-treatment increased the population of cation-selective pores while decreasing the overall porosity of the monolayer.

Paracellular transport of metformin increased across Caco-2 monolayers treated with 1,25-(OH)<sub>2</sub>D<sub>3</sub>. This novel finding was the first direct evidence that physiologically relevant TJ modulation can enhance the transport of charged organic solutes. Overwhelming circumstantial evidence implicated claudin-2 in facilitating metformin paracellular transport; thus, providing a molecular mechanism behind the observed saturable paracellular transport. Transport kinetics for the saturable component of metformin absorptive transport across Caco-2 cells described a high affinity and low capacity system (Chapter 2), which was most likely representative of the electrostatic interaction within claudin-2 pores rather than transport processes involving hOCT1 or PMAT. Currently, claudin-2 is the only pore forming TJ protein known to confer both cation-selectivity that is also capable of regulating



flux of small neutral molecules with radii less than 4 Å in a size-dependent manner (Van Itallie et al., 2008; Van Itallie et al., 2009). Characterization of the pore properties for other cation-selective claudin isoforms (e.g. claudin-10a, claudin-12, claudin-15, and claudin-16) have yet to be determined; however these isoforms were either not detected in Caco-2 cells or 1,25-(OH)<sub>2</sub>D<sub>3</sub>-treatment did not increase their expression (Chapter 3).

1,25-(OH)<sub>2</sub>D<sub>3</sub>-treatment in Caco-2 cells affected the expression of numerous TJ proteins examined (Chapter 3) and potentially could have affected the expression and function of other proteins not evaluated in this study. Although 1,25-(OH)<sub>2</sub>D<sub>3</sub>-treatment provided ample evidence implicating claudin-2 in paracellular transport of organic cations, direct evidence for claudin-2 mediated metformin paracellular transport was lacking. LLC-PK<sub>1</sub> cells that stably expressed exogenous claudin-2 under the control of an inducible promoter (Van Itallie et al., 2003) were employed to evaluate claudin-2 expression on the paracellular transport of metformin and similar guanidine containing cations. Claudin-2 expression was modulated in the monolayer to a maximum level at which overall monolayer integrity was not significantly altered. Surprisingly, paracellular transport of metformin was not affected by claudin-2 expression in this cell model; although guanidine and 1-methylguanidine paracellular transport increased with increasing claudin-2 expression (Chapter 4). The inability of claudin-2 to facilitate metformin paracellular transport in LLC-PK<sub>1</sub> monolayers could be due to a slightly smaller claudin-2 pore radius in this cell model in relation to the claudin-2 pore radius of the 1,25-(OH)<sub>2</sub>D<sub>3</sub>-induced Caco-2 monolayers. Using the ratios of paracellular  $P_{app}$  values for guanidine and 1-methylguanidine, the claudin-2 pore radius was estimated to be approximately 4 Å, which was not significantly different from the estimated radius of the claudin-2 pores in 1,25-(OH)<sub>2</sub>D<sub>3</sub>-induced Caco-2 cell monolayers.

Due to the limited number of organic cations assessed in this work, it is possible that the estimates were not precise enough to pick up subtle changes in the claudin-2 pore radius between the two systems, which could have resulted in the differential ability of induced claudin-2 to stimulate metformin transport in Caco-2 cells. Further studies are required to examine potential differences between the claudin-2 pore in these systems to explain the discrepancy between the LLC-PK<sub>1</sub> and Caco-2 data.

Regardless of the LLC-PK<sub>1</sub> metformin results, this work provided the first direct measurement of claudin-2 facilitated transport of organic cations at physiological relevant concentrations. Previous work demonstrated claudin-2 facilitated diffusion of organic cations (Yu et al., 2009); yet the permeability of the organic cations was measured indirectly by electrophysiological measurements (e.g. dilution potentials) and at concentrations that are supra-physiological (75 mM donor solutions). The study also employed inducible promoters to account for the endogenous claudins that may alter paracellular transport of the ions studied, but they failed to account for the effect of additional claudin-2 expression on the monolayer integrity by monitoring the flux of neutral paracellular probe (e.g. mannitol or PEG). Therefore, alterations to the monolayer may have confounded the data and produced effects not directly attributed to claudin-2 electrostatics. The data presented in this work clearly demonstrated the ability of claudin-2 to mediate paracellular transport of organic cations.

Facilitated diffusion of metformin by claudin-2 pores and/or other cation-selective claudin pores in the intestine would be expected to enhance the paracellular transport of metformin and modestly increase its overall oral absorption. However, paracellular transport alone could not account for the high fraction of dose absorbed of metformin in humans.

Metformin and mannitol had equivalent paracellular  $P_{app}$  across Caco-2 cell monolayers (Chapter 2); though the fraction of dose absorbed in humans for metformin and mannitol were significantly different with values of 80% (Tucker et al., 1981) and 16% (Artursson and Karlsson, 1991), respectively. Therefore, a novel “sponge” hypothesis was formulated to explain how metformin could be highly absorbed across human intestine through a predominantly paracellular mechanism. At the heart of this hypothesis are the cation-selective bidirectional transport mechanisms acting on the apical (AP) membrane of intestinal enterocytes (e.g. hOCT1 and PMAT). These transporters work in an inward direction at high metformin lumen concentrations and function to sequester metformin in the intestine as the dose transits down the intestine. The accumulated drug is then effluxed back into the lumen by the bidirectional cation-selective transporters, which allows for subsequent re-uptake into distal enterocytes or to be absorbed via a combination of passive and facilitated paracellular diffusion. At higher doses, less percent of the dose is capable of being accumulated in the intestine and more of the drug passes through the intestine unabsorbed and collects in the feces, resulting in saturable dose-dependent absorption.

Although claudin-2-mediated metformin transport may explain a slight increase in metformin bioavailability over mannitol, it is intestinal accumulation and repeating cycling by AP bidirectional transporters that truly explains the high bioavailability of metformin. This novel absorption mechanism accounts for how efficient absorption of metformin can occur through a presumably inefficient pathway (e.g. paracellular transport). Therefore, genetic, hormonal, chemical, and pathological modulations to these transport processes likely account for a portion of the intra- and inter-individual variability observed in metformin disposition and efficacy.

Clinical observations of metformin intestinal accumulation (Bailey et al., 2008), slow rate and dose-dependency of absorption (Tucker et al., 1981), and the reliance of the entire length of the small intestine for complete absorption (Vidon et al., 1988) support the sponge hypothesis absorption mechanism. Only approximately 20% of the dose is absorbed from the duodenum (Vidon et al., 1988), leaving the remaining to be absorbed slowly; thus controlling portal exposure and reducing the likelihood of saturating hepatic uptake transporters (e.g. hOCT1). Metformin accumulates in the liver at concentrations over 4 fold higher than the plasma concentrations (Wang et al., 2003) and liver accumulation likely accounts for a significant portion of the overall volume of distribution (Shu et al., 2008). Therefore, the slow rate of absorption observed clinically and explained by this novel absorption mechanism enables efficient accumulation into the organ responsible for the majority of metformin glucose-lowering effects.

This novel absorption mechanism can account for the intestine related pharmacology of metformin. Intestinal administration of metformin was shown to be necessary for metformin to elicit a significant portion of its glucose-lowering effect (Stepensky et al., 2002). Metformin induces glucose utilization in the intestine by increasing glucose uptake (Bailey et al., 1994; Walker et al., 2005) and stimulated anaerobic glucose metabolism to produce lactate (Bailey et al., 2008). Metformin requires entry into the cell to indirectly activate its main pharmacological target, the AMP-activated protein kinase (AMPK), via inhibition of complex I of the mitochondrial respiratory chain (Zou et al., 2004). Furthermore, accumulation of metformin in the cytosol is necessary to achieve adequate concentrations at the mitochondrial membrane to efficiently inhibit complex I (El-Mir et al., 2000). Prolonged absorption, likely mediated by the repeated cycling from the enterocytes

and inefficient BL efflux, would maintain sufficient intracellular concentrations required to generate an intestine-related pharmacologic response. In summary, the data presented here provides the first direct evidence linking discrete transport processes at each membrane to account for bioaccumulation in intestinal epithelial cells. Furthermore, the proposed absorption mechanism for metformin accounts for its efficient absorption and accumulation necessary for the pharmacologic response in the intestine and liver.

This dissertation project began with the initial goal of examining the role of cation-selective transporters in the absorptive transport of metformin in relation to the transport processes of another hydrophilic cationic drug, ranitidine. Both metformin and ranitidine AP uptake were mediated by hOCTs, most likely by PMAT and hOCT1, while ranitidine also was effluxed across the AP membrane by P-glycoprotein (P-gp) (Bourdet and Thakker, 2006). Efflux across the BL membrane was rate limiting to the transcellular transport of both compounds; yet the contributions of transcellular transport for metformin and ranitidine were significantly different with estimates of 10% and 50%, respectively. Ranitidine and metformin have pKa values of 8.2 and 12.4, respectively. Most biologically relevant cations are similar to ranitidine that contain primary or secondary amine functionalities, with pKa values ranging between 7 and 9; therefore at lumen pH they exist primarily as cations. It is hypothesized that cation-selective AP transporters facilitate uptake of cationic compounds into intestinal enterocytes to create a concentration gradient forcing the neutral unionized species in the cytosol to diffuse across the BL membrane into the blood. Therefore, adequate absorption would be achieved without vectorial transport; thus reducing the evolutionary pressure for cation-selective BL efflux transporters. In the case of metformin, drug accumulated in the enterocytes due the absence of neutral species capable of diffusing across

the BL membrane. This novel hypothesis accurately describes the transcellular transport processes for ranitidine and metformin across Caco-2 cell monolayers. Furthermore, this explanation accounts for the discrepancy between why there are several known cation-selective transporters on the AP membrane and no apparent mechanisms for cation-selective BL efflux in the intestine. Future work with compounds containing similar hydrophilicity with ionizable groups that have varying pKa values could be used to confirm this absorption mechanism *in vitro* and *in vivo*.

## 6. REFERENCES

- Artursson P and Karlsson J (1991) Correlation between oral drug absorption in humans and apparent drug permeability coefficients in human intestinal epithelial (Caco-2) cells. *Biochem Biophys Res Commun* **175**:880-885.
- Bailey CJ, Mynett KJ and Page T (1994) Importance of the intestine as a site of metformin-stimulated glucose utilization. *Br J Pharmacol* **112**:671-675.
- Bailey CJ, Wilcock C and Scarpello JH (2008) Metformin and the intestine. *Diabetologia* **51**:1552-1553.
- Bourdet DL, Pollack GM and Thakker DR (2006) Intestinal absorptive transport of the hydrophilic cation ranitidine: a kinetic modeling approach to elucidate the role of uptake and efflux transporters and paracellular vs. transcellular transport in Caco-2 cells. *Pharm Res* **23**:1178-1187.
- Bourdet DL and Thakker DR (2006) Saturable absorptive transport of the hydrophilic organic cation ranitidine in Caco-2 cells: role of pH-dependent organic cation uptake system and P-glycoprotein. *Pharm Res* **23**:1165-1177.
- Colegio OR, Van Itallie CM, McCrea HJ, Rahner C and Anderson JM (2002) Claudins create charge-selective channels in the paracellular pathway between epithelial cells. *Am J Physiol Cell Physiol* **283**:C142-147.
- El-Mir MY, Nogueira V, Fontaine E, Averet N, Rigoulet M and Leverve X (2000) Dimethylbiguanide inhibits cell respiration via an indirect effect targeted on the respiratory chain complex I. *J Biol Chem* **275**:223-228.
- Englund G, Rorsman F, Ronnblom A, Karlbom U, Lazorova L, Grasjo J, Kindmark A and Artursson P (2006) Regional levels of drug transporters along the human intestinal tract: co-expression of ABC and SLC transporters and comparison with Caco-2 cells. *Eur J Pharm Sci* **29**:269-277.
- Fujita H, Sugimoto K, Inatomi S, Maeda T, Osanai M, Uchiyama Y, Yamamoto Y, Wada T, Kojima T, Yokozaki H, Yamashita T, Kato S, Sawada N and Chiba H (2008) Tight junction proteins claudin-2 and -12 are critical for vitamin D-dependent Ca<sup>2+</sup> absorption between enterocytes. *Mol Biol Cell* **19**:1912-1921.
- Gan LS, Yanni S and Thakker DR (1998) Modulation of the tight junctions of the Caco-2 cell monolayers by H<sub>2</sub>-antagonists. *Pharm Res* **15**:53-57.
- Hou J, Paul DL and Goodenough DA (2005) Paracellin-1 and the modulation of ion selectivity of tight junctions. *J Cell Sci* **118**:5109-5118.
- Kimura N, Masuda S, Tanihara Y, Ueo H, Okuda M, Katsura T and Inui K (2005) Metformin is a superior substrate for renal organic cation transporter OCT2 rather than hepatic OCT1. *Drug Metab Pharmacokinet* **20**:379-386.

- Lee K, Ng C, Brouwer KL and Thakker DR (2002) Secretory transport of ranitidine and famotidine across Caco-2 cell monolayers. *J Pharmacol Exp Ther* **303**:574-580.
- Lee K and Thakker DR (1999) Saturable transport of H<sub>2</sub>-antagonists ranitidine and famotidine across Caco-2 cell monolayers. *J Pharm Sci* **88**:680-687.
- Lin JH (1991) Pharmacokinetic and pharmacodynamic properties of histamine H<sub>2</sub>-receptor antagonists. Relationship between intrinsic potency and effective plasma concentrations. *Clin Pharmacokinet* **20**:218-236.
- Matsson P, Englund G, Ahlin G, Bergstrom CA, Norinder U and Artursson P (2007) A global drug inhibition pattern for the human ATP-binding cassette transporter breast cancer resistance protein (ABCG2). *J Pharmacol Exp Ther* **323**:19-30.
- Muller J, Lips KS, Metzner L, Neubert RH, Koepsell H and Brandsch M (2005) Drug specificity and intestinal membrane localization of human organic cation transporters (OCT). *Biochem Pharmacol* **70**:1851-1860.
- Ng C (2002) Novel Cation-Sensitive Mechanisms for Intestinal Absorption and Secretion of Famotidine and Ranitidine: Potential Clinical Implications, in: *Pharmacy*, pp 186, University of North Carolina at Chapel Hill, Chapel Hill.
- Nies AT, Koepsell H, Winter S, Burk O, Klein K, Kerb R, Zanger UM, Keppler D, Schwab M and Schaeffeler E (2009) Expression of organic cation transporters OCT1 (SLC22A1) and OCT3 (SLC22A3) is affected by genetic factors and cholestasis in human liver. *Hepatology* **50**:1227-1240.
- Pentikainen PJ, Neuvonen PJ and Penttila A (1979) Pharmacokinetics of metformin after intravenous and oral administration to man. *Eur J Clin Pharmacol* **16**:195-202.
- Saitoh R, Sugano K, Takata N, Tachibana T, Higashida A, Nabuchi Y and Aso Y (2004) Correction of permeability with pore radius of tight junctions in Caco-2 monolayers improves the prediction of the dose fraction of hydrophilic drugs absorbed by humans. *Pharm Res* **21**:749-755.
- Sambol NC, Chiang J, O'Conner M, Liu CY, Lin ET, Goodman AM, Benet LZ and Haram JH (1996) Pharmacokinetics and pharmacodynamics of metformin in healthy subjects and patients with noninsulin-dependent diabetes mellitus. *J Clin Pharmacol* **36**:1012-1021.
- Shu Y, Brown C, Castro RA, Shi RJ, Lin ET, Owen RP, Sheardown SA, Yue L, Burchard EG, Brett CM and Giacomini KM (2008) Effect of genetic variation in the organic cation transporter 1, OCT1, on metformin pharmacokinetics. *Clin Pharmacol Ther* **83**:273-280.
- Stepensky D, Friedman M, Raz I and Hoffman A (2002) Pharmacokinetic-pharmacodynamic analysis of the glucose-lowering effect of metformin in diabetic rats reveals first-pass pharmacodynamic effect. *Drug Metab Dispos* **30**:861-868.



- Tamai I, Ohashi R, Nezu J, Yabuuchi H, Oku A, Shimane M, Sai Y and Tsuji A (1998) Molecular and functional identification of sodium ion-dependent, high affinity human carnitine transporter OCTN2. *J Biol Chem* **273**:20378-20382.
- Tanihara Y, Masuda S, Sato T, Katsura T, Ogawa O and Inui K (2007) Substrate specificity of MATE1 and MATE2-K, human multidrug and toxin extrusions/H(+)-organic cation antiporters. *Biochem Pharmacol* **74**:359-371.
- Tucker GT, Casay C, Phillips PJ, Connor H, Ward JD and Woods HF (1981) Metformin kinetics in healthy subjects and in patients with diabetes mellitus. *J Clin. Pharmac.* **12**:235-246.
- Van Itallie CM and Anderson JM (2006) Claudins and epithelial paracellular transport. *Annu Rev Physiol* **68**:403-429.
- Van Itallie CM, Fanning AS and Anderson JM (2003) Reversal of charge selectivity in cation or anion-selective epithelial lines by expression of different claudins. *Am J Physiol Renal Physiol* **285**:F1078-1084.
- Van Itallie CM, Holmes J, Bridges A and Anderson JM (2009) Claudin-2-dependent changes in noncharged solute flux are mediated by the extracellular domains and require attachment to the PDZ-scaffold. *Ann N Y Acad Sci* **1165**:82-87.
- Van Itallie CM, Holmes J, Bridges A, Gookin JL, Coccaro MR, Proctor W, Colegio OR and Anderson JM (2008) The density of small tight junction pores varies among cell types and is increased by expression of claudin-2. *J Cell Sci* **121**:298-305.
- Vidon N, Chaussade S, Noel M, Franchisseur C, Huchet B and Bernier JJ (1988) Metformin in the digestive tract. *Diabetes Res Clin Pract* **4**:223-229.
- Walker J, Jijon HB, Diaz H, Salehi P, Churchill T and Madsen KL (2005) 5-aminoimidazole-4-carboxamide riboside (AICAR) enhances GLUT2-dependent jejunal glucose transport: a possible role for AMPK. *Biochem J* **385**:485-491.
- Wang DS, Jonker JW, Kato Y, Kusuhara H, Schinkel AH and Sugiyama Y (2002) Involvement of organic cation transporter 1 in hepatic and intestinal distribution of metformin. *J Pharmacol Exp Ther* **302**:510-515.
- Wang DS, Kusuhara H, Kato Y, Jonker JW, Schinkel AH and Sugiyama Y (2003) Involvement of organic cation transporter 1 in the lactic acidosis caused by metformin. *Mol Pharmacol* **63**:844-848.
- Wilcock C and Bailey CJ (1994) Accumulation of metformin by tissues of the normal and diabetic mouse. *Xenobiotica* **24**:49-57.
- Yu AS, Cheng MH, Angelow S, Gunzel D, Kanzawa SA, Schneeberger EE, Fromm M and Coalson RD (2009) Molecular basis for cation selectivity in claudin-2-based

- paracellular pores: identification of an electrostatic interaction site. *J Gen Physiol* **133**:111-127.
- Zhou M, Xia L and Wang J (2007) Metformin transport by a newly cloned proton-stimulated organic cation transporter (plasma membrane monoamine transporter) expressed in human intestine. *Drug Metab Dispos* **35**:1956-1962.
- Zou MH, Kirkpatrick SS, Davis BJ, Nelson JS, Wiles WG, Schlattner U, Neumann D, Brownlee M, Freeman MB and Goldman MH (2004) Activation of the AMP-activated protein kinase by the anti-diabetic drug metformin in vivo. Role of mitochondrial reactive nitrogen species. *J Biol Chem* **279**:43940-43951.